

# Theorie des Quantentransports

Theory of quantum transport

Vorlesung  
winter semester 2019/2020  
Technische Universität Berlin



Dr. Gernot Schaller

March 18, 2021



# Contents

<b>1</b>	<b>Open quantum systems</b>	<b>11</b>
1.1	Kraus map . . . . .	11
1.2	Lindblad master equation . . . . .	13
1.2.1	General properties . . . . .	13
1.2.2	Example: Master Equation for a cavity in a thermal bath . . . . .	16
1.3	Microscopic Lindblad Derivation . . . . .	18
1.3.1	Mathematical Prerequisites . . . . .	18
1.3.2	General Standard Quantum-Optical Derivation . . . . .	21
1.3.3	Example: Harmonic oscillator in a thermal bath . . . . .	30
1.3.4	Equilibrium Thermodynamics . . . . .	33
1.3.5	Coarse-Graining . . . . .	37
1.3.6	Example: Spin-Boson Model . . . . .	42
1.3.7	Fermions . . . . .	47
1.3.8	Example: Single resonant level . . . . .	48
1.4	Superoperator Notation . . . . .	51
1.4.1	Energy eigenbasis representation . . . . .	51
1.4.2	General vectorization . . . . .	52
<b>2</b>	<b>Stationary Quantum transport</b>	<b>55</b>
2.1	Example: Single-Electron-Transistor . . . . .	56
2.2	Phenomenologic definition of currents . . . . .	58
2.3	Nonequilibrium thermodynamics . . . . .	60
2.4	Steady-State Dynamics . . . . .	61
2.5	Example: The single-electron transistor . . . . .	63
2.6	Example: The double quantum dot . . . . .	64
2.7	Example: Phonon-Assisted Tunneling . . . . .	68
2.8	Example: Attainability of cooling . . . . .	72
<b>3</b>	<b>Full Counting Statistics</b>	<b>77</b>
3.1	Phenomenologic Introduction of counting fields . . . . .	77
3.1.1	Single jump type . . . . .	77
3.1.2	Different jump types . . . . .	81
3.1.3	Net particle transfers . . . . .	81
3.1.4	Long-term dynamics of cumulants . . . . .	82
3.1.5	Dynamics of current and noise . . . . .	83
3.1.6	Example: The single-electron transistor . . . . .	84
3.1.7	Example: Absorbtion refrigerator . . . . .	86

3.2	Energy-resolved Counting Statistics . . . . .	87
3.3	Waiting times and Full Counting Statistics . . . . .	88
3.4	Microscopic derivation of counting fields . . . . .	91
3.4.1	Example: transient SRL energy current . . . . .	94
3.4.2	Example: SET monitored by a quantum point contact . . . . .	94
3.4.3	Example: pure dephasing model . . . . .	100
3.4.4	Example: spin current . . . . .	102
3.5	Symmetries in Full Counting Statistics . . . . .	104
3.5.1	Mathematical Motivation . . . . .	104
3.5.2	Microscopic discussion for multiple counting fields . . . . .	106
<b>4</b>	<b>Transport in the strong coupling limit</b>	<b>109</b>
4.1	Exactly solvable models: The Fano-Anderson model . . . . .	109
4.1.1	Heisenberg Picture Dynamics . . . . .	110
4.1.2	Asymptotic evolution . . . . .	110
4.1.3	Time-dependent and stationary occupation . . . . .	112
4.1.4	Stationary Current . . . . .	113
4.2	Polaron master equation . . . . .	116
4.2.1	Single bosonic reservoir . . . . .	116
4.2.2	Multiple reservoir example: Phonon-coupled single electron transistor . . . . .	117
4.3	Bosonic reaction-coordinate mappings . . . . .	127
4.3.1	Bosonic Bogoliubov transforms . . . . .	128
4.3.2	Two-mode example . . . . .	129
4.3.3	Derivation of the mapping . . . . .	131
4.3.4	Application: Spin-boson model . . . . .	136
4.4	Fermionic reaction-coordinate mappings . . . . .	139
4.4.1	Fermionic Bogoliubov transforms . . . . .	139
4.4.2	Two-mode example . . . . .	140
4.4.3	Derivation of the mapping . . . . .	140
4.4.4	Application: Single-electron transistor . . . . .	143
4.5	Reduced stationary state . . . . .	145
<b>5</b>	<b>Periodically driven systems</b>	<b>147</b>
5.1	Closed systems . . . . .	147
5.1.1	Floquet theory . . . . .	147
5.1.2	Example: Circularly driven two-level system . . . . .	148
5.1.3	Extended space decomposition . . . . .	150
5.1.4	Example: Driven two-level system . . . . .	151
5.2	Open systems . . . . .	153
5.2.1	Secular and Nonsecular master equation . . . . .	153
5.2.2	Example: open two-level system for circular driving . . . . .	158
5.2.3	Upgrade: Two-terminal driven Two-Level system . . . . .	159

<b>6</b>	<b>Feedback control</b>	<b>161</b>
6.1	Measurement . . . . .	161
6.1.1	Projective measurements . . . . .	161
6.1.2	Weak measurements . . . . .	162
6.2	External piecewise-constant feedback . . . . .	165
6.2.1	Repeated feedback operations . . . . .	165
6.2.2	Continuous feedback limit . . . . .	166
6.2.3	Example: Feedback control of the SET . . . . .	166
6.3	Wiseman-Milburn feedback . . . . .	167
6.3.1	Dissipative control loops . . . . .	167
6.3.2	Application: Stabilization of Fock states . . . . .	170
<b>7</b>	<b>Selected applications</b>	<b>173</b>
7.1	An electronic Maxwell demon: External feedback . . . . .	173
7.1.1	Phenomenology of an electronic setup . . . . .	173
7.1.2	Conventional entropy production in rate equations . . . . .	178
7.1.3	Entropic analysis of rate equations with feedback . . . . .	182
7.1.4	Our example: Maxwell's demon . . . . .	185
7.2	An electronic Maxwell demon: Autonomous feedback . . . . .	189
7.3	Charge detectors . . . . .	197
7.3.1	Single quantum dot . . . . .	199
7.3.2	Double quantum dot:Least-invasive measurement . . . . .	203
7.3.3	Triple quantum dot:Least invasive measurement . . . . .	207
7.3.4	Projective QPC limit . . . . .	210
7.4	A non-perturbative form for entropy production . . . . .	215
7.4.1	Example: Two coupled qubits . . . . .	219
7.4.2	Example: Transient entropy production for pure-dephasing . . . . .	219
7.4.3	Conclusion: Entropy production for periodic driving . . . . .	220

Die Veranstaltung mit Vorlesung und Übung gilt als Vertiefungsfach (10 LP). Die Vorlesung wird Donnerstags und Freitags von 10:00-12:00 im EW 203 stattfinden, die dazugehörige Übung wird von Sebastian Restrepo gehalten wird Donnerstags von 16:00-18:00 im EW 733 stattfinden. Die Veranstaltung ist erweiterbar zu einem vollen Wahlpflichtfach (12 LP), indem zusätzlich an einem Seminar oder einer Spezialvorlesung aus der Theoretischen Physik teilgenommen wird (in Absprache mit dem Dozenten).

Voraussetzungen für die Teilnahme: Quantenmechanik, Quantenmechanik II, Konzept der Dichtematrix und von bosonischen wie fermionischen Erzeugern und Vernichtern.

Ein Vorlesungsskript (Englisch) wird online verfügbar sein unter

<http://www1.itp.tu-berlin.de/schaller/lectures.html>.

Korrekturen und Vorschläge sollten an folgende email-Adresse gesendet werden:

[gernot.schaller@tu-berlin.de](mailto:gernot.schaller@tu-berlin.de).

Hierfür danke ich bereits Javier Cerrillo, Felix Mende und Sebastian Restrepo.

Zuletzt noch ein Hinweis: Dieses Skript wird während der Vorlesung ausgebaut und verbessert werden. Es wird nach jeder Vorlesung in aktualisierter Fassung online gestellt, es empfiehlt sich daher, nicht gleich zu Anfang alles auszudrucken.

Literaturhinweise:

- H.-P. Breuer and F. Petruccione, *The Theory of Open Quantum Systems*, Oxford University Press, Oxford (2002). [1]
- M. O. Scully and M. S. Zubairy, *Quantum Optics*, Cambridge University Press (1997). [2]
- L. Mandel and E. Wolf, *Optical coherence and quantum optics*, Cambridge University Press (1995). [3]
- N. G. van Kampen, *Stochastic processes in physics and chemistry*, Elsevier (1981). [4]
- M. Schlosshauer, *Decoherence and the quantum-to-classical transition*, Springer (2007). [5]
- H. M. Wiseman and G. J. Milburn, *Quantum Measurement and Control*, Cambridge University Press, Cambridge (2010). [6]
- G. Schaller, *Open Quantum Systems Far from Equilibrium* Springer Lecture Notes in Physics **881**, Springer (2014). [7]

Wir werden folgende Inhalte behandeln

- mikroskopische Ableitungen von Mastergleichungen
- Entropie-Produktion in Lindblad-Mastergleichungen
- Thermodynamik von Nichtgleichgewichtsreservoirern
- stark gekoppelte Systeme
- Fluktuationstheoreme und zweiter Hauptsatz
- getriebene Systeme (externes Treiben und Rückkopplung)

# Prerequisites

Throughout the lecture, we will use units where  $\hbar = 1$  and  $k_B = 1$ . In these units, energy has units of inverse time, for example the argument  $Ht$  of the time evolution operator is manifestly dimensionless. As far as the Boltzmann constant is concerned, we will rather work with the inverse temperature  $\beta$ , which has dimension of inverse energy (or time).

Treating quantum transport requires to go beyond the treatment of isolated quantum systems, which are merely governed by a Schrödinger equation. We will therefore make use of some more advanced concepts:

- General quantum systems can be conveniently described by a **density matrix**

$$\rho = \sum_n P_n |\Psi_n\rangle \langle \Psi_n| ,$$

where  $|\Psi_n\rangle$  denote normalized  $\langle \Psi_n | \Psi_n \rangle = 1$  states and  $0 \leq P_n \leq 1$  with  $\sum_n P_n = 1$  the corresponding probabilities. In this representation, the states need not necessarily be orthogonal, i.e., in general  $\langle \Psi_n | \Psi_m \rangle \neq \delta_{nm}$ . Density matrices fulfil the mathematical properties

$$\text{Tr} \{ \rho \} = 1, \quad \rho = \rho^\dagger, \quad \langle \Psi | \rho | \Psi \rangle \geq 0 \quad \forall \quad | \Psi \rangle .$$

The first condition imposes the normalization of probabilities, the second ensures that all eigenvalues of the density matrix are real, and the third preserves enables the probabilistic interpretation of the density matrix by enforcing that all probabilities  $P_n$  are non-negative. Thus, density matrices are positive semidefinite. Denoting the eigenvalues of a density matrix with  $\lambda_n$ , we see that  $0 \leq \lambda_n \leq 1$  with  $\sum_n \lambda_n = 1$ , and the **spectral representation** of a density matrix

$$\rho = \sum_n \lambda_n |\Phi_n\rangle \langle \Phi_n| \quad : \quad \langle \Phi_n | \Phi_m \rangle = \delta_{nm}$$

provides in general another decomposition of a density matrix. The eigenvectors  $|\Phi_n\rangle$  are not necessarily the same as the states  $|\Psi_n\rangle$  and consequently the eigenvalues  $\lambda_n$  can be different from the probabilities  $P_n$ .

- A density matrix is called **pure**, if and only if

$$\rho_p = \rho_p^2 ,$$

i.e.,  $\rho_p = |\Psi\rangle \langle \Psi|$  for some state  $|\Psi\rangle$ . Other density matrices are called **mixed**.

- While a solution of the Schrödinger equation obeys (we use units with  $\hbar = 1$  throughout)  $i\dot{|\Psi\rangle} = -H(t)|\Psi\rangle$ , the density matrix obeys the **von-Neumann** evolution equation

$$\dot{\rho} = -i[H(t), \rho] ,$$

where the indicated time-dependence in the Hamiltonian may arise either from externally driving a parameter or the use of a different picture such as the interaction picture.

As such, the solution of the von-Neumann equation can be formally written as

$$\rho(t) = U(t)\rho_0U^\dagger(t) ,$$

where  $U(t)$  is the **time evolution operator**, in general governed by the differential equation

$$\dot{U} = -iH(t)U(t) .$$

Only if  $H(t) \rightarrow H$  is constant, we can solve this differential equation by a **matrix exponential**

$$U(t) \rightarrow e^{-iHt} = \sum_{n=0}^{\infty} \frac{(-i)^n t^n}{n!} H^n .$$

- The expectation value of an operator can be obtained by performing the trace

$$\langle A \rangle = \text{Tr} \{A\rho\} = \text{Tr} \{\rho A\} = \sum_m P_m \langle n| A |\Psi_m\rangle \langle \Psi_m|n\rangle = \sum_m P_m \langle \Psi_m| A |\Psi_m\rangle .$$

- Under a **projective measurement** of an observable  $O$  with spectral decomposition  $O = O^\dagger = \sum_m O_m |m\rangle \langle m|$  with outcome  $m$ , the density matrix transforms as

$$\rho \rightarrow \rho^{(m)} = \frac{|m\rangle \langle m| \rho |m\rangle \langle m|}{P_m} \quad : \quad P_m = \text{Tr} \{|m\rangle \langle m| \rho\} ,$$

where  $P_m$  is the probability for this measurement outcome.

- Of particular importance are the **canonical equilibrium state**

$$\rho_c = \frac{e^{-\beta H}}{\text{Tr} \{e^{-\beta H}\}}$$

with given inverse temperature  $\beta = 1/(k_B T)$  and Hamiltonian  $H$ , and the **grand-canonical equilibrium state**

$$\rho_{gc} = \frac{e^{-\beta(H-\mu N)}}{\text{Tr} \{e^{-\beta(H-\mu N)}\}} ,$$

with particle number operator  $N$  and chemical potential  $\mu$ .

- At given average energy and particle number, the grand-canonical equilibrium state maximizes the **von-Neumann entropy**

$$S(\rho) \equiv -\text{Tr} \{\rho \ln \rho\} = -\sum_n \lambda_n \ln \lambda_n ,$$

$$S_{gc} = \beta [\langle H \rangle - \mu \langle N \rangle] + \ln \text{Tr} \{e^{-\beta(H-\mu N)}\} .$$

- Matrix exponentials can be easily made explicit at the example of **Pauli matrices**

$$\sigma^x = \begin{pmatrix} 0 & 1 \\ 1 & 0 \end{pmatrix}, \quad \sigma^y = \begin{pmatrix} 0 & -i \\ +i & 0 \end{pmatrix}, \quad \sigma^z = \begin{pmatrix} +1 & 0 \\ 0 & -1 \end{pmatrix}.$$

Any two-level system (qubit) for example can be conveniently described by Pauli matrices. From the properties of the Pauli matrices  $\sigma^\alpha \sigma^\beta + \sigma^\beta \sigma^\alpha = 2\delta_{\alpha\beta} \mathbf{1}$  one can for example conclude that for  $n_x^2 + n_y^2 + n_z^2 = 1$  one has

$$e^{-i\alpha[n_x\sigma^x + n_y\sigma^y + n_z\sigma^z]} = \cos(\alpha)\mathbf{1} - i\sin(\alpha)[n_x\sigma^x + n_y\sigma^y + n_z\sigma^z],$$

which can be useful to compute the time evolution operator of an undriven qubit.

- When two quantum systems with Hilbert spaces  $V$  and  $W$  interact, one can construct a basis of the joint Hilbert space  $C$  by **tensor products** of the basis vectors of the individual Hilbert spaces

$$|c_{ij}\rangle = |v_i\rangle \otimes |w_j\rangle,$$

and the dimension of the composite system is the product of the individual dimensions  $N_c = N_v N_w$ . With the two-dimensional Hilbert space of a two-level system, the Hilbert space of two qubits is then four-dimensional. For  $N$  qubits, we thus find a  $2^N$ -dimensional Hilbert space necessary to describe the system.

- The problems we are aiming at are most conveniently treated within the language of second quantization. Thus, we represent operators mostly in terms of creation and annihilation (ladder) operators.

The **bosonic ladder operators** obey commutation relations

$$[b_k, b_q^\dagger] = \delta_{kq}, \quad [b_k, b_q] = 0,$$

where  $k$  and  $q$  denote modes. The total particle number operator is then given by

$$N = \sum_k b_k^\dagger b_k.$$

A convenient basis choice are then the **Fock states** defined as the eigenstates of the particle number operator. For a system with  $N$  modes we can label them by  $N$  integer numbers with

$$|n_1, n_2, \dots, n_N\rangle = |n_1\rangle \otimes |n_2\rangle \otimes \dots \otimes |n_N\rangle \quad n_i \in \{0, 1, 2, 3, \dots\}.$$

One can show that

$$\begin{aligned} b_k^\dagger |n_1, \dots, n_k, \dots, n_N\rangle &= \sqrt{n_k + 1} |n_1, \dots, n_k + 1, \dots, n_N\rangle, \\ b_k |n_1, \dots, n_k, \dots, n_N\rangle &= \sqrt{n_k} |n_1, \dots, n_k - 1, \dots, n_N\rangle. \end{aligned}$$

Consequently, we can represent all Fock states by acting with creation operators on the **vacuum state**

$$|n_1, \dots, n_N\rangle = \prod_k \frac{(b_k^\dagger)^{n_k}}{\sqrt{n_k!}} |0, \dots, 0\rangle.$$

In contrast, **fermionic ladder operators** obey anticommutation relations

$$\{f_k, f_q^\dagger\} = \delta_{kq}, \quad \{f_k, f_q\} = 0,$$

where  $\{A, B\} = AB + BA$ . The total particle number operator is again given by

$$N = \sum_k f_k^\dagger f_k,$$

and the Fock states are labeled by

$$|n_1, n_2, \dots, n_N\rangle \quad n_i \in \{0, 1\}.$$

The creation and annihilation operators act similarly as in the bosonic case, and likewise one can construct the Fock states by acting with creation (raising) operators on the vacuum state. However, note that there is an ambiguity in the sign of the Fock states, since the different creation operators anti-commute.

- For a bosonic Hamiltonian

$$H = \sum_k \omega_k b_k^\dagger b_k$$

with single-particle energies  $\omega_k$  one can for the grand-canonical equilibrium state show for  $\mu < \omega_k : \forall k$  that

$$\begin{aligned} \langle a_k \rangle &= \text{Tr} \left\{ a_k \frac{e^{-\beta(H-\mu N)}}{\text{Tr} \{e^{-\beta(H-\mu N)}\}} \right\} = 0, \\ \langle a_k^\dagger a_q \rangle &= \text{Tr} \left\{ a_k^\dagger a_q \frac{e^{-\beta(H-\mu N)}}{\text{Tr} \{e^{-\beta(H-\mu N)}\}} \right\} = \delta_{kq} \frac{1}{e^{\beta(\omega_k - \mu)} - 1} \equiv \delta_{kq} n_B(\omega_k), \end{aligned}$$

where  $n_B(\omega)$  is the **Bose-Einstein distribution** (often used with  $\mu = 0$ ).

- For a fermionic Hamiltonian

$$H = \sum_k \epsilon_k f_k^\dagger f_k$$

with single-particle energies  $\epsilon_k$  one can for the grand-canonical equilibrium state generally ( $\mu \in \mathbb{R}$ ) show that

$$\begin{aligned} \langle f_k \rangle &= \text{Tr} \left\{ f_k \frac{e^{-\beta(H-\mu N)}}{\text{Tr} \{e^{-\beta(H-\mu N)}\}} \right\} = 0, \\ \langle f_k^\dagger f_q \rangle &= \text{Tr} \left\{ f_k^\dagger f_q \frac{e^{-\beta(H-\mu N)}}{\text{Tr} \{e^{-\beta(H-\mu N)}\}} \right\} = \delta_{kq} \frac{1}{e^{\beta(\epsilon_k - \mu)} + 1} \equiv \delta_{kq} n_F(\epsilon_k), \end{aligned}$$

where  $n_F(\omega)$  is the **Fermi-Dirac distribution** (also Fermi function).

# Chapter 1

## Open quantum systems

We typically imagine an open quantum system as part of a larger, closed, quantum system as shown in Fig. 1.1. One could in principle tackle such problems by just solving the dynamics of the von-Neumann equation for the complete system, described by the full Hamiltonian

$$\dot{\rho}_{\text{tot}} = -i[H_S + H_I + H_B, \rho_{\text{tot}}] . \quad (1.1)$$

If it was possible to obtain the global solution  $\rho_{\text{tot}}(t)$ , one could obtain any observable of the system via  $\langle A \rangle_t = \text{Tr} \{A\rho_{\text{tot}}(t)\}$ . Unfortunately, a typical reservoir has an enormously large number of degrees of freedom, and the dimension of the Hilbert space scales even worse. Therefore, apart from some particular examples (some of which we will discuss), this path is typically not taken. Instead, since we are typically only interested in the dynamics of a small part (that we call system) of the whole universe, and we are interested in finding a time-dependent solution for the density matrix of that local part  $\rho_S(t)$ . In general, this cannot be a von-Neumann equation

$$\dot{\rho}_S \neq -i[H_{\text{eff}}(t), \rho_S(t)] , \quad (1.2)$$

since the solution to these equations is always unitary, preserving information on the initial state. However, realistic reservoirs exchange information, energy and possibly also matter with a quantum system. Thus, we are looking for a general evolution equation for the local system density matrix.

### 1.1 Kraus map

One approach to this is based on formal requirements: Any evolution equation should preserve all properties (trace, hermiticity, and positivity) of the density matrix.

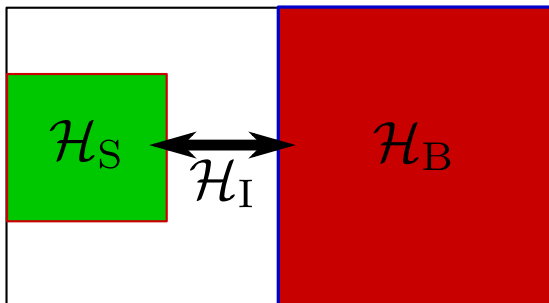


Figure 1.1: An open quantum system can be conceived as being part of a larger closed quantum system, where the system part ( $\mathcal{H}_S$ ) is coupled to the bath or reservoir ( $\mathcal{H}_B$ ) via the interaction Hamiltonian  $\mathcal{H}_I$ .

The most general evolution preserving all the nice properties of a density matrix is the so-called **Kraus map**. A density matrix  $\rho$  (Hermitian, positive definite, and with trace one) can be mapped to another density matrix  $\rho'$  via

$$\rho' = \sum_{\alpha\beta} \gamma_{\alpha\beta} A_\alpha \rho A_\beta^\dagger, \quad \text{with} \quad \sum_{\alpha\beta} \gamma_{\alpha\beta} A_\beta^\dagger A_\alpha = \mathbf{1}, \quad (1.3)$$

where the prefactors  $\gamma_{\alpha\beta}$  form a Hermitian ( $\gamma_{\alpha\beta} = \gamma_{\beta\alpha}^*$ ) and positive definite ( $\sum_{\alpha\beta} x_\alpha^* \gamma_{\alpha\beta} x_\beta \geq 0$  or equivalently all eigenvalues of  $(\gamma_{\alpha\beta})$  are non-negative) matrix. It is straightforward to see that the above map preserves trace and Hermiticity of the density matrix.

We first rewrite the map in a simpler way. Since the matrix  $\gamma_{\alpha\beta}$  is Hermitian, it can be diagonalized by a suitable unitary transformation, and we introduce the new operators  $A_\alpha = \sum_{\alpha'} U_{\alpha\alpha'} \bar{K}_{\alpha'}$

$$\begin{aligned} \rho' &= \sum_{\alpha\beta} \sum_{\alpha'\beta'} \gamma_{\alpha\beta} U_{\alpha\alpha'} \bar{K}_{\alpha'} \rho U_{\beta\beta'}^* K_{\beta'}^\dagger = \sum_{\alpha'\beta'} \bar{K}_{\alpha'} \rho \bar{K}_{\beta'}^\dagger \underbrace{\sum_{\alpha\beta} U_{\alpha\alpha'} \gamma_{\alpha\beta} U_{\beta\beta'}^*}_{\gamma_{\alpha'} \delta_{\alpha'\beta'}} \\ &= \sum_{\alpha} \gamma_{\alpha} \bar{K}_{\alpha} \rho \bar{K}_{\alpha}^\dagger, \end{aligned} \quad (1.4)$$

where  $\gamma_{\alpha} \geq 0$  represent the eigenvalues of the matrix  $(\gamma_{\alpha\beta})$ . Since these are by construction positive, we introduce further new operators  $K_{\alpha} = \sqrt{\gamma_{\alpha}} \bar{K}_{\alpha}$  to obtain the simplest representation of a Kraus map.

$$\rho' = \sum_{\alpha} K_{\alpha}^\dagger \rho K_{\alpha} \quad : \quad \sum_{\alpha} K_{\alpha}^\dagger K_{\alpha} = \mathbf{1}. \quad (1.5)$$

Here, it is very simple to see that  $\rho'$  inherits the positivity from  $\rho$ . We simply insert the spectral representation of  $\rho = \sum_n \lambda_n |n\rangle \langle n|$

$$\begin{aligned} \langle \Psi | \rho' | \Psi \rangle &= \sum_{\alpha} \langle \Psi | K_{\alpha} \rho K_{\alpha}^\dagger | \Psi \rangle = \sum_n \lambda_n \sum_{\alpha} \langle \Psi | K_{\alpha} | n \rangle \langle n | K_{\alpha}^\dagger | \Psi \rangle \\ &= \sum_n \underbrace{\lambda_n}_{\geq 0} \underbrace{\sum_{\alpha} |\langle n | K_{\alpha}^\dagger | \Psi \rangle|^2}_{\geq 0} \geq 0. \end{aligned} \quad (1.6)$$

That means, a positive definite matrix  $\rho$  (with  $\lambda_n \geq 0$ ) will map to a positive definite matrix  $\rho'$ .

**Def. 1** (Kraus map). *The map*

$$\rho(t + \Delta t) = \sum_{\alpha} K_{\alpha}(t, \Delta t) \rho(t) K_{\alpha}^\dagger(t, \Delta t) \quad (1.7)$$

*with Kraus operators  $K_{\alpha}(t, \Delta t)$  obeying the relation  $\sum_{\alpha} K_{\alpha}^\dagger(t, \Delta t) K_{\alpha}(t, \Delta t) = \mathbf{1}$  preserves Hermiticity, trace, and positivity of the density matrix.*

Obviously, both unitary evolution and the average evolution under measurement are just special cases of a Kraus map. Though Kraus maps are heavily used in quantum information, they are not often very easy to interpret. For example, it is not straightforward to identify the unitary and the non-unitary part induced by the Kraus map.

## 1.2 Lindblad master equation

Any dynamical evolution equation for the density matrix should (at least in some approximate sense) preserve its interpretation as density matrix, i.e., trace, Hermiticity, and positivity must be preserved. By construction, the measurement postulate and unitary evolution preserve these properties. However, more general evolutions are conceivable.

It is convenient to use a differential equation for the density matrix as the desired evolution equation. The most general first order differential equation that is time-local, linear in  $\rho$ , and has time-independent coefficients that preserves the density matrix properties is known as **Lindblad form** (sometimes also Lindblad-Gorini-Kossakowski-Sudarshan – LGKS generator).

### 1.2.1 General properties

**Def. 2** (Lindblad form). *In an  $N$ -dimensional system Hilbert space, a master equation of Lindblad form [8, 9] has the structure*

$$\dot{\rho} = -i[H, \rho] + \sum_{\alpha, \beta=1}^{N^2-1} \gamma_{\alpha\beta} \left( A_{\alpha}\rho A_{\beta}^{\dagger} - \frac{1}{2} \{A_{\beta}^{\dagger}A_{\alpha}, \rho\} \right) \equiv \mathcal{L}\rho, \quad (1.8)$$

where the Hermitian operator  $H = H^{\dagger}$  can be interpreted as an effective Hamiltonian and  $\gamma_{\alpha\beta} = \gamma_{\beta\alpha}^*$  is a positive semidefinite matrix, i.e., it fulfills  $\sum_{\alpha\beta} x_{\alpha}^* \gamma_{\alpha\beta} x_{\beta} \geq 0$  for all vectors  $x$  (or, equivalently that all eigenvalues of  $(\gamma_{\alpha\beta})$  are non-negative  $\gamma_i \geq 0$ ). After suitable transformations, this can be written as

$$\dot{\rho} = -i[H, \rho] + \sum_{\alpha}^{N^2-1} \left( L_{\alpha}\rho L_{\alpha}^{\dagger} - \frac{1}{2} \{L_{\alpha}^{\dagger}L_{\alpha}, \rho\} \right) \equiv \mathcal{L}\rho. \quad (1.9)$$

First, we show that the Lindblad master equation can be written in simpler form: As the dampening matrix  $\gamma$  is Hermitian, it can be diagonalized by a suitable unitary transformation  $U$ , such that  $\sum_{\alpha\beta} U_{\alpha'\alpha} \gamma_{\alpha\beta} (U^{\dagger})_{\beta\beta'} = \delta_{\alpha'\beta'} \gamma_{\alpha'}$  with  $\gamma_{\alpha} \geq 0$  representing its non-negative eigenvalues. Using this unitary operation, a new set of operators can be defined via  $A_{\alpha} = \sum_{\alpha'} U_{\alpha'\alpha} \bar{L}_{\alpha'}$ . Inserting this decomposition in the master equation, we obtain

$$\begin{aligned} \dot{\rho} &= -i[H, \rho] + \sum_{\alpha, \beta=1}^{N^2-1} \gamma_{\alpha\beta} \left( A_{\alpha}\rho A_{\beta}^{\dagger} - \frac{1}{2} \{A_{\beta}^{\dagger}A_{\alpha}, \rho\} \right) \\ &= -i[H, \rho] + \sum_{\alpha', \beta'} \left[ \sum_{\alpha\beta} \gamma_{\alpha\beta} U_{\alpha'\alpha} U_{\beta'\beta}^* \right] \left( \bar{L}_{\alpha'}\rho \bar{L}_{\beta'}^{\dagger} - \frac{1}{2} \{ \bar{L}_{\beta'}^{\dagger} \bar{L}_{\alpha'}, \rho \} \right) \\ &= -i[H, \rho] + \sum_{\alpha} \gamma_{\alpha} \left( \bar{L}_{\alpha}\rho \bar{L}_{\alpha}^{\dagger} - \frac{1}{2} \{ \bar{L}_{\alpha}^{\dagger} \bar{L}_{\alpha}, \rho \} \right), \end{aligned} \quad (1.10)$$

where  $\gamma_{\alpha} \geq 0$  denote the  $N^2 - 1$  non-negative eigenvalues of the dampening matrix. Furthermore, we can absorb the  $\gamma_{\alpha}$  in the Lindblad operators  $L_{\alpha} = \sqrt{\gamma_{\alpha}} \bar{L}_{\alpha}$ , such that another form of a Lindblad

master equation is indeed

$$\dot{\rho} = -i[H, \rho] + \sum_{\alpha} \left( L_{\alpha} \rho L_{\alpha}^{\dagger} - \frac{1}{2} \{L_{\alpha}^{\dagger} L_{\alpha}, \rho\} \right). \quad (1.11)$$

**Exercise 1** (Trace and Hermiticity preservation by Lindblad forms). *Show that the Lindblad form master equation preserves trace and Hermiticity of the density matrix.*

Evidently, the representation of a master equation is not unique. Any other unitary operation would lead to a different non-diagonal form of  $\gamma_{\alpha\beta}$  which however describes the same master equation. In addition, we note here that the master equation is not only invariant to unitary transformations of the operators  $A_{\alpha}$ , but in the diagonal representation also to inhomogeneous transformations of the form

$$\begin{aligned} L_{\alpha} &\rightarrow L'_{\alpha} = L_{\alpha} + a_{\alpha} \mathbf{1} \\ H &\rightarrow H' = H + \frac{1}{2i} \sum_{\alpha} \gamma_{\alpha} (a_{\alpha}^* L_{\alpha} - a_{\alpha} L_{\alpha}^{\dagger}) + b \mathbf{1}, \end{aligned} \quad (1.12)$$

with  $a_{\alpha} \in \mathbb{C}$  and a real number  $b \in \mathbb{R}$ . The numbers  $a_{\alpha}$  can be chosen such that the Lindblad operators are traceless  $\text{Tr} \{L_{\alpha}\} = 0$ , which is a popular convention. Choosing  $b$  simply corresponds to gauging the energy of the system.

**Exercise 2** (Shift invariance). *Show the invariance of the diagonal representation of a Lindblad form master equation (1.10) with respect to the transformation (1.12).*

We would like to demonstrate the preservation of positivity here. Since preservation of Hermiticity follows directly from the Lindblad form, we can – since at any time we know that  $\rho = \rho^{\dagger}$  – formally write the density matrix in its spectral representation

$$\rho(t) = \sum_j \lambda_j(t) |\Psi_j(t)\rangle \langle \Psi_j(t)| \quad (1.13)$$

with eigenvalues  $\lambda_j(t) \in \mathbb{R}$  (we still have to show that these remain positive) and time-dependent orthonormal eigenstates. The eigenvectors themselves are normalized at all times  $\langle \Psi_i(t) | \Psi_j(t) \rangle = \delta_{ij}$ , and by acting on this expression with a time derivative we see that  $\langle \dot{\Psi}_i | \Psi_i \rangle + \langle \Psi_i | \dot{\Psi}_i \rangle = 0$ .

Therefore, the time-derivative of the density matrix becomes

$$\dot{\rho} = \sum_j \left[ \dot{\lambda}_j |\Psi_j\rangle \langle \Psi_j| + \lambda_j \left[ \dot{\Psi}_j \right] \langle \Psi_j| + \lambda_j |\Psi_j\rangle \left[ \dot{\Psi}_j \right] \right], \quad (1.14)$$

and sandwiching the time-derivative above with the eigenvector  $|\Psi_i\rangle$  leads to the cancellation of two terms, such that  $\langle \Psi_i(t) | \dot{\rho} | \Psi_i(t) \rangle = \dot{\lambda}_i(t)$ . On the other hand, we can also sandwich the right-hand

side of the Lindblad equation to obtain

$$\begin{aligned}
\dot{\lambda}_i &= -i \langle \Psi_i | H | \Psi_i \rangle \lambda_i + i \lambda_i \langle \Psi_i | H | \Psi_i \rangle \\
&\quad + \sum_{\alpha} \left[ \langle \Psi_i | L_{\alpha} \left( \sum_j \lambda_j | \Psi_j \rangle \langle \Psi_j | \right) L_{\alpha}^{\dagger} | \Psi_i \rangle - \langle \Psi_i | L_{\alpha}^{\dagger} L_{\alpha} | \Psi_i \rangle \lambda_i \right] \\
&= \sum_j \left( \sum_{\alpha} |\langle \Psi_i | L_{\alpha} | \Psi_j \rangle|^2 \right) \lambda_j - \sum_j \left( \sum_{\alpha} |\langle \Psi_j | L_{\alpha} | \Psi_i \rangle|^2 \right) \lambda_i.
\end{aligned} \tag{1.15}$$

This is nothing but a rate equation

$$\dot{\lambda}_i = \sum_j R_{j \rightarrow i}(t) \lambda_j(t) - \sum_j R_{i \rightarrow j} \lambda_i(t) = \sum_j R_{ij}(t) \lambda_j(t) \tag{1.16}$$

with positive but time-dependent transition rates

$$R_{j \rightarrow i}(t) = \sum_{\alpha} |\langle \Psi_i(t) | L_{\alpha} | \Psi_j(t) \rangle|^2 \geq 0. \tag{1.17}$$

The rate matrix in the rate equation  $\dot{\boldsymbol{\lambda}} = R(t)\boldsymbol{\lambda}(t)$  contains the rates as

$$(R(t))_{ij} = \begin{cases} R_{j \rightarrow i}(t) & : j \neq i \\ -\sum_{j \neq i} R_{i \rightarrow j} & : j = i \end{cases}. \tag{1.18}$$

Therefore, only the diagonal entries of the rate matrix are negative. From this, it follows first that the sum of all eigenvalues (i.e., the trace of  $\rho$ ) is conserved and second, that all eigenvalues remain positive. To see this, assume that one eigenvalue approaches zero  $\lambda_{\bar{n}} \rightarrow 0$  while all others are still positive. Then, the time derivative of  $\lambda_{\bar{n}}$  is always positive, i.e., it can never become negative. From this, it follows that the positivity of the eigenvalues  $\lambda_j(t)$  (and thereby that of the density matrix) is granted for all times, a valid initialization provided. This can be seen by considering the time derivative of an eigenvalue  $\bar{n}$  that vanishes at a certain time  $\lambda_{\bar{n}}(t^*) = 0$  while all other eigenvalues are non-negative  $\lambda_{n \neq \bar{n}}(t^*) \geq 0$ . From this, it follows that the time derivative of the monitored critical eigenvalue is

$$\dot{\lambda}_{\bar{n}}|_{t=t^*} = \sum_n R_{\bar{n}n}(t^*) \lambda_n(t^*) = \sum_{n \neq \bar{n}} R_{n \rightarrow \bar{n}}(t^*) \lambda_n(t^*) \geq 0, \tag{1.19}$$

i.e., the eigenvalue will increase again, if it ever reaches zero. Thereby, it can never become negative (and we can repeat the argument for the other eigenvalues), such that the density matrix remains positive at all times. The argument fails, of course, if some eigenvalues are already negative (i.e., for an invalid initial condition), such that the Lindblad evolution can only preserve the density matrix properties, but not cure them.

Unfortunately, the basis within which this simple rate equation holds is time-dependent and also only known after solving the master equation and diagonalizing the solution. The rate equation representation is therefore not very practical, unless the eigenbasis is constant in time.

### 1.2.2 Example: Master Equation for a cavity in a thermal bath

Consider the Lindblad form master equation

$$\begin{aligned} \dot{\rho} = & -i [\Omega a^\dagger a, \rho] + \Gamma(1 + n_B) \left[ a\rho a^\dagger - \frac{1}{2}a^\dagger a\rho - \frac{1}{2}\rho a^\dagger a \right] \\ & + \Gamma n_B \left[ a^\dagger \rho a - \frac{1}{2}aa^\dagger \rho - \frac{1}{2}\rho aa^\dagger \right], \end{aligned} \quad (1.20)$$

with bosonic operators  $[a, a^\dagger] = \mathbf{1}$  and Bose-Einstein bath occupation  $n_B = [e^{\beta\Omega} - 1]^{-1}$  (we consider  $\mu = 0$ ) and cavity frequency  $\Omega > 0$ . Finally,  $\Gamma > 0$  is a constant (spontaneous emission rate).

#### Steady state solution

In Fock-space representation, these operators act as  $a^\dagger |n\rangle = \sqrt{n+1} |n+1\rangle$  (where  $0 \leq n < \infty$ ), such that the above master equation couples only the diagonals of the density matrix  $\rho_n = \langle n | \rho | n \rangle$  to each other. This is directly visible by sandwiching the master equation with  $\langle n | \dots | n \rangle$

$$\begin{aligned} \dot{\rho}_n = & \Gamma(1 + n_B) [(n+1)\rho_{n+1} - n\rho_n] + \Gamma n_B [n\rho_{n-1} - (n+1)\rho_n] \\ = & \Gamma n_B n \rho_{n-1} - \Gamma [n + (2n+1)n_B] \rho_n + \Gamma(1 + n_B)(n+1)\rho_{n+1}, \end{aligned} \quad (1.21)$$

which shows that the rate equation arising for the diagonals even has a simple tri-diagonal form. That makes it particularly easy to calculate its stationary state recursively, since the boundary solution  $n_B \bar{\rho}_0 = (1 + n_B) \bar{\rho}_1$  implies for all  $n$  the relation

$$\frac{\bar{\rho}_{n+1}}{\bar{\rho}_n} = \frac{n_B}{1 + n_B} = e^{-\beta\Omega}, \quad (1.22)$$

i.e., the stationary state is a thermalized Gibbs state with the same temperature as the reservoir.

**Exercise 3** (Moments). *Calculate the expectation value of the number operator  $\hat{n} = a^\dagger a$  and its square  $\hat{n}^2 = a^\dagger a a^\dagger a$  in the stationary state of the master equation (1.20).*

In general, the matrix elements of the density matrix  $\rho_{nm} = \langle n | \rho | m \rangle$  will obey

$$\begin{aligned} \dot{\rho}_{nm} = & -i\Omega(n-m)\rho_{nm} + \Gamma(1 + n_B) \left[ \sqrt{(n+1)(m+1)}\rho_{n+1,m+1} - \frac{n+m}{2}\rho_{nm} \right] \\ & + \Gamma n_B \left[ \sqrt{nm}\rho_{n-1,m-1} - \frac{n+1+m+1}{2}\rho_{nm} \right] \\ = & \left[ -i\Omega(n-m) - \Gamma \frac{(1+n_B)(n+m) + n_B(n+1+m+1)}{2} \right] \rho_{nm} \\ & + \Gamma(1 + n_B)\sqrt{(n+1)(m+1)}\rho_{n+1,m+1} + \Gamma n_B\sqrt{nm}\rho_{n-1,m-1}, \end{aligned} \quad (1.23)$$

and it is straightforward to see that vanishing coherences (off-diagonal matrix elements)  $\bar{\rho}_{n \neq m} = 0$  are a valid steady-state solution. Not being aware of the Lindblad form we may nevertheless ask whether there are other solutions. The above equation shows that among the coherences, only few

couple, and by arranging them in a favorable form we can write these equations in matrix form with infinite-dimensional tri-diagonal matrices (for brevity we use  $\gamma = \Gamma n_B$  and  $\bar{\gamma} = \Gamma(1 + n_B)$ )

$$W = \begin{pmatrix} & & & \vdots & & & \\ & & & & & & \\ & \ddots & & +\bar{\gamma}\sqrt{nm} & & & \\ \dots & +\gamma\sqrt{nm} & [-i\Omega(n-m) - \bar{\gamma}\frac{n+m}{2} - \gamma\frac{n+1+m+1}{2}] & +\bar{\gamma}\sqrt{(n+1)(m+1)} & \dots & & \\ & 0 & +\gamma\sqrt{(n+1)(m+1)} & & \ddots & & \\ & & & \vdots & & & \end{pmatrix}. \quad (1.24)$$

By examining every column in detail, we see that the real part of the diagonal entries has always larger magnitude than the sum of the off-diagonal entries, since

$$\bar{\gamma}\frac{n+m}{2} + \gamma\frac{n+1+m+1}{2} \geq +\bar{\gamma}\sqrt{nm} + \gamma\sqrt{(n+1)(m+1)}. \quad (1.25)$$

The above equation naturally follows from  $(x-y)^2 = x^2 + y^2 - 2xy \geq 0$ , with  $x^2 \rightarrow \bar{\gamma}n$  and  $y^2 \rightarrow \bar{\gamma}m$  or  $x^2 \rightarrow \gamma(n+1)$  and  $y^2 \rightarrow \gamma(m+1)$ , respectively. Furthermore, we see that equality actually only holds for the diagonal elements ( $n = m$ ). From Gershgorins circle theorem, we can therefore conclude that all the eigenvalues of the matrix  $W$  have for  $n \neq m$  a negative real part. Consequently, the coherences must decay and the stationary state only contains populations in the Fock space representation.

### Transient dynamics

A simpler way to solve the particular master equation at hand is by using it to calculate the expectation value  $\langle n \rangle = \text{Tr} \{ a^\dagger a \rho \}$  of the particle number operator

$$\begin{aligned} \frac{d}{dt} \langle n \rangle &= \langle a^\dagger a \dot{\rho} \rangle \\ &= +\Gamma(1 + n_B) \text{Tr} \left\{ \left[ a^\dagger a^\dagger a a - (a^\dagger a)^2 \right] \rho \right\} \\ &\quad + \Gamma n_B \text{Tr} \left\{ \left[ a a^\dagger a a^\dagger - \frac{1}{2} a^\dagger a a a^\dagger - \frac{1}{2} a a^\dagger a^\dagger a \right] \rho \right\}, \end{aligned} \quad (1.26)$$

where we have used the invariance of the trace under cyclic permutations to move the density matrix to the right. Further using the bosonic commutation relations we get the very simple equation

$$\frac{d}{dt} \langle n \rangle = -\Gamma(1 + n_B) \langle n \rangle + \Gamma n_B (1 + \langle n \rangle), \quad (1.27)$$

which yields the same steady state solution

$$\frac{\bar{n}}{1 + \bar{n}} = \frac{n_B}{1 + n_B} = e^{-\beta\Omega}, \quad (1.28)$$

which we had before in Eq. (1.22). Likewise, the dynamics of the creation and annihilation operators becomes

$$\begin{aligned} \frac{d}{dt} \langle a \rangle &= \left[ -i\Omega - \frac{\Gamma(1 + n_B) + \Gamma n_B}{2} \right] \langle a \rangle, \\ \frac{d}{dt} \langle a^\dagger \rangle &= \left[ +i\Omega - \frac{\Gamma(1 + n_B) + \Gamma n_B}{2} \right] \langle a^\dagger \rangle, \end{aligned} \quad (1.29)$$

such that these expectation values will in the long run approach the origin. Considering observables like

$$\langle x \rangle = \frac{1}{\sqrt{2m\Omega}} \langle a^\dagger + a \rangle, \quad \langle p \rangle = i\sqrt{\frac{m\Omega}{2}} \langle a^\dagger - a \rangle, \quad (1.30)$$

we see that position and momentum are damped to the origin, since they obey the coupled equations

$$\frac{d}{dt} \langle x \rangle = \frac{1}{m} \langle p \rangle - \frac{\Gamma(1 + 2n_B)}{2} \langle x \rangle, \quad \frac{d}{dt} \langle p \rangle = -m\Omega^2 \langle x \rangle - \frac{\Gamma(1 + 2n_B)}{2} \langle p \rangle. \quad (1.31)$$

Mostly, one is not as fortunate as in this case, where the resulting evolution equations close with just a few variables, but deriving and solving equations of motion for observables from master equations is a popular tool for solving them.

## 1.3 Microscopic Lindblad Derivation

### 1.3.1 Mathematical Prerequisites

Master equations are often used to describe the dynamics of systems interacting with one or many large reservoirs (baths). To derive them from microscopic models – including the Hamiltonian of the full system – requires to review some basic mathematical concepts.

#### Tensor Product

The greatest advantage of the density matrix formalism is visible when quantum systems composed of several subsystems are considered. Roughly speaking, the tensor product represents a way to construct a larger vector space from two (or more) smaller vector spaces.

**Def. 3** (Tensor Product). *Let  $V$  and  $W$  be Hilbert spaces (vector spaces with scalar product) of dimension  $m$  and  $n$  with basis vectors  $\{|v\rangle\}$  and  $\{|w\rangle\}$ , respectively. Then  $V \otimes W$  is a Hilbert space of dimension  $m \cdot n$ , and a basis is spanned by  $\{|v\rangle \otimes |w\rangle\}$ , which is a set combining every basis vector of  $V$  with every basis vector of  $W$ .*

*Mathematical properties*

- *Bilinearity*  $(z_1 |v_1\rangle + z_2 |v_2\rangle) \otimes |w\rangle = z_1 |v_1\rangle \otimes |w\rangle + z_2 |v_2\rangle \otimes |w\rangle$  as well as  $|v\rangle \otimes (z_1 |w_1\rangle + z_2 |w_2\rangle) = z_1 |v\rangle \otimes |w_1\rangle + z_2 |v\rangle \otimes |w_2\rangle$
- *operators acting on the combined Hilbert space  $A \otimes B$  act on the basis states as  $(A \otimes B)(|v\rangle \otimes |w\rangle) = (A|v\rangle) \otimes (B|w\rangle)$*
- *any linear operator on  $V \otimes W$  can be decomposed as  $C = \sum_i c_i A_i \otimes B_i$*
- *the scalar product is inherited in the natural way, i.e., one has for  $|a\rangle = \sum_{ij} a_{ij} |v_i\rangle \otimes |w_j\rangle$  and  $|b\rangle = \sum_{k\ell} b_{k\ell} |v_k\rangle \otimes |w_\ell\rangle$  the scalar product  $\langle a|b\rangle = \sum_{ijk\ell} a_{ij}^* b_{k\ell} \langle v_i|v_k\rangle \langle w_j|w_\ell\rangle = \sum_{ij} a_{ij}^* b_{ij}$*

If more than just two vector spaces are combined to form a larger vector space, the dimension of the joint vector space grows rapidly, as e.g. exemplified by the case of a qubit: Its Hilbert space is just spanned by two vectors  $|0\rangle$  and  $|1\rangle$ . The joint Hilbert space of two qubits is four-dimensional, of three qubits 8-dimensional, and of  $n$  qubits  $2^n$ -dimensional. Eventually, this exponential growth of the Hilbert space dimension for composite quantum systems is at the heart of quantum computing.

**Exercise 4** (Tensor Products of Operators). *Let  $\sigma$  denote the Pauli matrices, i.e.,*

$$\sigma^1 = \begin{pmatrix} 0 & +1 \\ +1 & 0 \end{pmatrix} \quad \sigma^2 = \begin{pmatrix} 0 & -i \\ +i & 0 \end{pmatrix} \quad \sigma^3 = \begin{pmatrix} +1 & 0 \\ 0 & -1 \end{pmatrix}$$

*Compute the trace of the operator*

$$\begin{aligned} \Sigma &= a\mathbf{1} \otimes \mathbf{1} + \sum_{i=1}^3 \alpha_i \sigma^i \otimes \mathbf{1} + \sum_{j=1}^3 \beta_j \mathbf{1} \otimes \sigma^j + \sum_{i,j=1}^3 a_{ij} \sigma^i \otimes \sigma^j \\ &\equiv a + \sum_{i=1}^3 \alpha_i \sigma_1^i + \sum_{j=1}^3 \beta_j \sigma_2^j + \sum_{i,j=1}^3 a_{ij} \sigma_1^i \sigma_2^j. \end{aligned}$$

Since the scalar product is inherited, this typically enables a convenient calculation of the trace in case of a few operator decomposition, e.g., for just two operators

$$\begin{aligned} \text{Tr} \{A \otimes B\} &= \sum_{n_A, n_B} \langle n_A, n_B | A \otimes B | n_A, n_B \rangle \\ &= \left[ \sum_{n_A} \langle n_A | A | n_A \rangle \right] \left[ \sum_{n_B} \langle n_B | B | n_B \rangle \right] \\ &= \text{Tr}_A \{A\} \text{Tr}_B \{B\}, \end{aligned} \tag{1.31}$$

where  $\text{Tr}_{A/B}$  denote the trace in the Hilbert space of  $A$  and  $B$ , respectively.

### The partial trace

Whereas the full trace maps a matrix to a number, one could also imagine a **partial trace** to reduce a full density matrix (or statistical operator) to a matrix acting only on a subspace. This is done with the partial trace.

**Def. 4** (Partial Trace). *Let  $|a_1\rangle$  and  $|a_2\rangle$  be vectors of state space  $A$  and  $|b_1\rangle$  and  $|b_2\rangle$  vectors of state space  $B$ . Then, the partial trace over state space  $B$  is defined via*

$$\text{Tr}_B \{|a_1\rangle \langle a_2| \otimes |b_1\rangle \langle b_2|\} = |a_1\rangle \langle a_2| \text{Tr} \{|b_1\rangle \langle b_2|\}. \tag{1.32}$$

Notation-wise, we note that an index can be suppressed when the normal trace is considered, such that the dimension is clear from the operator.

The partial trace is linear, such that the partial trace of arbitrary operators is calculated similarly. One may therefore calculate the most general partial trace via

$$\mathrm{Tr}_B \{C\} = \sum_{\alpha} c_{\alpha} \mathrm{Tr}_B \{A_{\alpha} \otimes B_{\alpha}\} = \sum_{\alpha} c_{\alpha} A_{\alpha} \mathrm{Tr} \{B_{\alpha}\}. \quad (1.33)$$

**Exercise 5 (Partial Trace).** *Compute the partial trace of a pure density matrix  $\rho = |\Psi\rangle\langle\Psi|$  in the bipartite state*

$$|\Psi\rangle = \frac{1}{\sqrt{2}} (|01\rangle + |10\rangle) \equiv \frac{1}{\sqrt{2}} (|0\rangle \otimes |1\rangle + |1\rangle \otimes |0\rangle)$$

### The reduced density matrix

For composite systems, it is usually not necessary to keep all information of the complete system in the density matrix. Rather, one would like to have a density matrix that encodes all the information on a particular subsystem only. Obviously, the map  $\rho \rightarrow \mathrm{Tr}_B \{\rho\}$  to such a reduced density matrix should leave all expectation values of observables  $A$  acting only on the considered subsystem invariant.

**Def. 5 (Reduced density matrix).** *Let  $\rho_{AB}$  be a density matrix in the composite Hilbert space  $A \otimes B$  with dimension  $N_A \cdot N_B$*

$$\rho_{AB} = \sum_{n_A, m_A=1}^{N_A} \sum_{n_B, m_B=1}^{N_B} \rho_{(n_A, n_B), (m_A, m_B)} |n_A\rangle \langle m_A| \otimes |n_B\rangle \langle m_B|. \quad (1.34)$$

*Then, the reduced density matrix*

$$\rho_A = \sum_{n_A, m_A=1}^{N_A} \left[ \sum_{n_B}^{N_B} \rho_{(n_A, n_B), (m_A, n_B)} \right] |n_A\rangle \langle m_A| = \sum_{n_A, m_A=1}^{N_A} \rho_{n_A, m_A}^{(A)} |n_A\rangle \langle m_A| \quad (1.35)$$

*is a valid density matrix in  $A$ , and for all local observables we have  $\mathrm{Tr} \{A\rho_A\} = \mathrm{Tr} \{A \otimes \mathbf{1}\rho_{AB}\}$ .*

This definition is the only linear map that respects the invariance of expectation values while mapping a large density matrix  $\rho_{AB}$  to a reduced one  $\rho_A$ . Its analog in the classical context is the computation of a marginal probability distribution via  $P_i = \sum_j P_{ij}$ .

We check these statements explicitly by using the density matrix properties of  $\rho_{AB}$

- The trace of the reduced density matrix is one

$$\mathrm{Tr} \{\rho_A\} = \sum_{n_A} \rho_{n_A, n_A}^{(A)} = \sum_{n_A} \sum_{n_B} \rho_{(n_A, n_B), (n_A, n_B)} = \mathrm{Tr} \{\rho_{AB}\} = 1. \quad (1.36)$$

- The reduced density matrix is hermitian

$$\rho_A^{\dagger} = \sum_{n_A, m_A} \sum_{n_B} \rho_{(n_A, n_B), (m_A, n_B)}^* |m_A\rangle \langle n_A| = \sum_{n_A, m_A} \sum_{n_B} \rho_{(m_A, n_B), (n_A, n_B)} |m_A\rangle \langle n_A| = \rho_A, \quad (1.37)$$

which we can see by exchanging  $n_A \leftrightarrow m_A$  in the last line.

- The reduced density matrix is positive

$$\langle \Psi_A | \rho_A | \Psi_A \rangle = \sum_{n_A, m_A} \sum_{n_B} \rho_{(n_A n_B), (m_A n_B)} \langle \Psi_A | n_A \rangle \langle m_A | \Psi_A \rangle = \sum_{n_B} \langle \Psi_A, n_B | \rho_{AB} | \Psi_A, n_B \rangle \geq 0. \quad (1.38)$$

- Finally, expectation values of local observables, i.e., those that act trivially on Hilbert space  $B$ , only depend on the reduced density matrix

$$\begin{aligned} \text{Tr} \{ (A \otimes \mathbf{1}) \rho_{AB} \} &= \sum_{n_A, n_B} \langle n_A, n_B | A \otimes \mathbf{1} \rho_{AB} | n_A, n_B \rangle = \sum_{n_A, \bar{n}_A} \langle n_A | A | \bar{n}_A \rangle \left[ \sum_{n_B} \rho_{(\bar{n}_A n_B), (n_A n_B)} \right] \\ &= \text{Tr} \{ A \rho_A \}, \end{aligned} \quad (1.39)$$

i.e., the object defined in this way makes sense.

### 1.3.2 General Standard Quantum-Optical Derivation

In many cases, it is possible to derive a master equation rigorously based only on a few assumptions. Open quantum systems for example are mostly treated as part of a much larger closed quantum system (the union of system and bath), where the partial trace is used to eliminate the unwanted (typically many) degrees of freedom of the bath, see Fig. 1.1. Technically speaking, we will consider Hamiltonians of the form

$$H = H_S \otimes \mathbf{1} + \mathbf{1} \otimes H_B + H_I, \quad (1.40)$$

where the system and bath Hamiltonians act only on the system and bath Hilbert space, respectively. Since the index clearly defines on which space the respective Hamiltonian is acting, we write only

$$H = H_S + H_B + H_I. \quad (1.41)$$

It is important to note that the interaction Hamiltonian acts nontrivially on both Hilbert spaces

$$H_I = \sum_{\alpha} A_{\alpha} \otimes B_{\alpha}, \quad (1.42)$$

where the summation over  $\alpha$  just labels the possible coupling operators (limited in the worst case by the dimension of the system Hilbert space  $\alpha < N^2 - 1$ ). As we consider physical observables here, it is in general required that all Hamiltonians of system, bath, and interaction are self-adjoint. However, we can use this to demand even stronger that

$$A_{\alpha} = A_{\alpha}^{\dagger}, \quad B_{\alpha} = B_{\alpha}^{\dagger} \quad (1.43)$$

for all  $\alpha$ .

**Exercise 6** (Hermiticity of Couplings). *Show that it is always possible to choose Hermitian coupling operators  $A_\alpha = A_\alpha^\dagger$  and  $B_\alpha = B_\alpha^\dagger$  using that  $H_I = H_I^\dagger$ .*

Based on these assumptions, we will derive the master equation generally, for an arbitrary quantum system coupled to a single thermal environment [1]. This generality will at first appear a bit technical but may prove useful later-on, since it also allows us to show general properties for later reference.

### Interaction Picture

When the interaction  $H_I$  is small, it is justified to apply perturbation theory. The von-Neumann equation in the joint total quantum system

$$\dot{\rho} = -i[H_S + H_B + H_I, \rho] \quad (1.44)$$

describes the full evolution of the combined density matrix. This equation can be formally solved by the unitary evolution  $\rho(t) = e^{-iHt} \rho_0 e^{+iHt}$ , which however is impractical to compute as  $H$  involves too many degrees of freedom.

Transforming to the interaction picture

$$\boldsymbol{\rho}(t) = e^{+i(H_S+H_B)t} \rho(t) e^{-i(H_S+H_B)t}, \quad (1.45)$$

which will be denoted by bold symbols throughout, the von-Neumann equation transforms into

$$\dot{\boldsymbol{\rho}} = -i[\mathbf{H}_I(t), \boldsymbol{\rho}], \quad (1.46)$$

where the in general time-dependent interaction Hamiltonian

$$\begin{aligned} \mathbf{H}_I(t) &= e^{+i(H_S+H_B)t} H_I e^{-i(H_S+H_B)t} = \sum_{\alpha} e^{+iH_S t} A_{\alpha} e^{-iH_S t} \otimes e^{+iH_B t} B_{\alpha} e^{-iH_B t} \\ &= \sum_{\alpha} \mathbf{A}_{\alpha}(t) \otimes \mathbf{B}_{\alpha}(t) \end{aligned} \quad (1.47)$$

allows to perform perturbation theory.

Without loss of generality we will for simplicity assume here the case of Hermitian coupling operators  $A_\alpha = A_\alpha^\dagger$  and  $B_\alpha = B_\alpha^\dagger$ . One heuristic way to perform perturbation theory is to formally integrate Eq. (1.46) and to re-insert the result in the r.h.s. of Eq. (1.46). The time-derivative of the system density matrix is obtained by performing the partial trace

$$\dot{\rho}_S = -i \text{Tr}_B \{[\mathbf{H}_I(t), \rho_0]\} - \int_0^t \text{Tr}_B \{[\mathbf{H}_I(t), [\mathbf{H}_I(t'), \boldsymbol{\rho}(t')]]\} dt'. \quad (1.48)$$

This integro-differential equation is still exact but unfortunately not closed as the r.h.s. does not depend on  $\rho_S$  but the full density matrix at all previous times.

### Born approximation

To close the above equation, we employ factorization of the initial density matrix

$$\rho_0 = \rho_S^0 \otimes \bar{\rho}_B \quad (1.49)$$

together with perturbative considerations: Assuming that  $\mathbf{H}_I(t) = \mathcal{O}\{\lambda\}$  with  $\lambda$  being a small dimensionless perturbation parameter (solely used for bookkeeping purposes here) and that the environment is so large such that it is hardly affected by the presence of the system, we may formally expand the full density matrix

$$\rho(t) = \rho_S(t) \otimes \bar{\rho}_B + \mathcal{O}\{\lambda\}, \quad (1.50)$$

where the neglect of all higher orders is known as **Born approximation**. Eq. (1.48) demonstrates that the Born approximation is equivalent to a perturbation theory in the interaction Hamiltonian

$$\dot{\rho}_S = -i\text{Tr}_B \{[\mathbf{H}_I(t), \rho_0]\} - \int_0^t \text{Tr}_B \{[\mathbf{H}_I(t), [\mathbf{H}_I(t'), \rho_S(t') \otimes \bar{\rho}_B]]\} dt' + \mathcal{O}\{\lambda^3\}. \quad (1.51)$$

Using the decomposition of the interaction Hamiltonian (1.42), this obviously yields a closed equation for the system density matrix

$$\begin{aligned} \dot{\rho}_S = & -i \sum_{\alpha} [\mathbf{A}_{\alpha}(t) \rho_S^0 \text{Tr} \{ \mathbf{B}_{\alpha}(t) \bar{\rho}_B \} - \rho_S^0 \mathbf{A}_{\alpha}(t) \text{Tr} \{ \bar{\rho}_B \mathbf{B}_{\alpha}(t) \}] \\ & - \sum_{\alpha\beta} \int_0^t \left[ \mathbf{A}_{\alpha}(t) \mathbf{A}_{\beta}(t') \rho_S(t') \text{Tr} \{ \mathbf{B}_{\alpha}(t) \mathbf{B}_{\beta}(t') \bar{\rho}_B \} \right. \\ & \quad - \mathbf{A}_{\alpha}(t) \rho_S(t') \mathbf{A}_{\beta}(t') \text{Tr} \{ \mathbf{B}_{\alpha}(t) \bar{\rho}_B \mathbf{B}_{\beta}(t') \} \\ & \quad - \mathbf{A}_{\beta}(t') \rho_S(t') \mathbf{A}_{\alpha}(t) \text{Tr} \{ \mathbf{B}_{\beta}(t') \bar{\rho}_B \mathbf{B}_{\alpha}(t) \} \\ & \quad \left. + \rho_S(t') \mathbf{A}_{\beta}(t') \mathbf{A}_{\alpha}(t) \text{Tr} \{ \bar{\rho}_B \mathbf{B}_{\beta}(t') \mathbf{B}_{\alpha}(t) \} \right] dt'. \end{aligned} \quad (1.52)$$

The Born approximation also requires that the reservoir is in an equilibrium state, i.e.,

$$[H_B, \bar{\rho}_B] = 0, \quad (1.53)$$

such that it cannot change on its own. Then, we can without loss of generality proceed by assuming that the single coupling operator expectation value vanishes

$$\text{Tr} \{ \mathbf{B}_{\alpha}(t) \bar{\rho}_B \} = 0. \quad (1.54)$$

This situation can always be constructed by simultaneously modifying system Hamiltonian  $H_S$  and coupling operators  $A_{\alpha}$ , see exercise 7.

**Exercise 7** (Vanishing single-operator expectation values). *Show for  $[H_B, \bar{\rho}_B] = 0$  that by modifying system and interaction Hamiltonian*

$$H_S \rightarrow H_S + \sum_{\alpha} g_{\alpha} A_{\alpha}, \quad B_{\alpha} \rightarrow B_{\alpha} - g_{\alpha} \mathbf{1}$$

*one can construct a situation where  $\text{Tr} \{ \mathbf{B}_{\alpha}(t) \bar{\rho}_B \} = 0$ . Determine  $g_{\alpha}$ .*

Using the cyclic property of the trace, we simplify further

$$\dot{\rho}_S = - \sum_{\alpha\beta} \int_0^t dt' \left[ C_{\alpha\beta}(t, t') [\mathbf{A}_\alpha(t), \mathbf{A}_\beta(t') \rho_S(t')] + C_{\beta\alpha}(t', t) [\rho_S(t') \mathbf{A}_\beta(t'), \mathbf{A}_\alpha(t)] \right] \quad (1.55)$$

with the **bath correlation function**

$$C_{\alpha\beta}(t_1, t_2) = \text{Tr} \{ \mathbf{B}_\alpha(t_1) \mathbf{B}_\beta(t_2) \bar{\rho}_B \} . \quad (1.56)$$

The integro-differential equation (1.55) is often termed **non-Markovian master equation**, as the r.h.s. depends on the value of the dynamical variable (the density matrix) at all previous times – weighted by the bath correlation functions. We will see later that non-Markovianity can also be defined more rigorously based on violation of contractivity. It does preserve trace and Hermiticity of the system density matrix, but not necessarily its positivity. Such integro-differential equations can only be solved in very specific cases, e.g., when the correlation functions have a very simple decay law. Therefore, we motivate further approximations, for which we need to discuss the analytic properties of the bath correlation functions.

### Markov approximation

It is quite straightforward to see that when the bath Hamiltonian commutes with the bath density matrix  $[H_B, \bar{\rho}_B] = 0$ , the bath correlation functions actually only depend on the difference of their time arguments

$$C_{\alpha\beta}(t_1, t_2) = C_{\alpha\beta}(t_1 - t_2) = \text{Tr} \{ e^{+iH_B(t_1-t_2)} B_\alpha e^{-iH_B(t_1-t_2)} B_\beta \bar{\rho}_B \} . \quad (1.57)$$

Since we chose our coupling operators Hermitian, we have the additional symmetry that

$$C_{\alpha\beta}(\tau) = C_{\beta\alpha}^*(-\tau) . \quad (1.58)$$

One can now evaluate several system-bath models and when the bath has a dense spectrum, the bath correlation functions are typically found to be strongly peaked around zero, see exercise 8.

**Exercise 8** (Bath Correlation Function). *Evaluate the Fourier transform  $\gamma_{11}(\omega) = \int C_{11}(\tau) e^{+i\omega\tau} d\tau$  of the bath correlation functions for the coupling operators  $B_1 = \sum_k [h_k b_k + h_k^* b_k^\dagger]$  and for a bosonic bath  $H_B = \sum_k \omega_k b_k^\dagger b_k$  in the canonical thermal equilibrium state  $\bar{\rho}_B^0 = \frac{e^{-\beta H_B}}{\text{Tr} \{ e^{-\beta H_B} \}}$ . You may use the continuous representation  $J(\omega) = 2\pi \sum_k |h_k|^2 \delta(\omega - \omega_k)$ .*

In superoperator notation, one can also write the integro-differential equation (1.55) as

$$\dot{\rho}_S = \int_0^t \mathcal{W}(t-t') \rho_S(t') dt' , \quad (1.59)$$

where the kernel  $\mathcal{W}(\tau)$  assigns a much smaller weight to density matrices far in the past than to the density matrix just an instant ago. In the most extreme case, we would approximate

$C_{\alpha\beta}(t_1, t_2) \approx \Gamma_{\alpha\beta}\delta(t_1 - t_2)$ , but we will be cautious here and assume that only the density matrix varies slower than the decay time of the bath correlation functions. Therefore, we replace in the r.h.s.  $\rho_S(t') \rightarrow \rho_S(t)$  (**first Markov approximation**), which yields in Eq. (1.51)

$$\dot{\rho}_S = - \int_0^t \text{Tr}_B \{ [\mathbf{H}_I(t), [\mathbf{H}_I(t'), \rho_S(t) \otimes \bar{\rho}_B]] \} dt' \quad (1.60)$$

This equation is often called **Born-Redfield equation**. It is time-local and preserves trace and Hermiticity, but still has time-dependent coefficients (also when transforming back from the interaction picture). We substitute  $\tau = t - t'$

$$\begin{aligned} \dot{\rho}_S &= - \int_0^t \text{Tr}_B \{ [\mathbf{H}_I(t), [\mathbf{H}_I(t - \tau), \rho_S(t) \otimes \bar{\rho}_B]] \} d\tau \quad (1.61) \\ &= - \sum_{\alpha\beta} \int_0^t \{ C_{\alpha\beta}(\tau) [\mathbf{A}_\alpha(t), \mathbf{A}_\beta(t - \tau) \rho_S(t)] + C_{\beta\alpha}(-\tau) [\rho_S(t) \mathbf{A}_\beta(t - \tau), \mathbf{A}_\alpha(t)] \} d\tau \end{aligned}$$

The problem that the r.h.s. still depends on time is removed by extending the integration bounds to infinity (**second Markov approximation**) – by the same reasoning that the bath correlation functions decay rapidly

$$\dot{\rho}_S = - \int_0^\infty \text{Tr}_B \{ [\mathbf{H}_I(t), [\mathbf{H}_I(t - \tau), \rho_S(t) \otimes \bar{\rho}_B]] \} d\tau. \quad (1.62)$$

This equation is called **Redfield equation** (sometimes also Markovian master equation), which in the original Schrödinger picture

$$\begin{aligned} \dot{\rho}_S &= -i [H_S, \rho_S(t)] - \sum_{\alpha\beta} \int_0^\infty C_{\alpha\beta}(\tau) [A_\alpha, e^{-iH_S\tau} A_\beta e^{+iH_S\tau} \rho_S(t)] d\tau \\ &\quad - \sum_{\alpha\beta} \int_0^\infty C_{\beta\alpha}(-\tau) [\rho_S(t) e^{-iH_S\tau} A_\beta e^{+iH_S\tau}, A_\alpha] d\tau \quad (1.63) \end{aligned}$$

is time-local, preserves trace and Hermiticity, and has constant coefficients – best prerequisites for treatment with established solution methods.

**Exercise 9** (Properties of the Markovian Master Equation). *Show that the Markovian Master equation (1.63) preserves trace and Hermiticity of the density matrix.*

In addition, it can be obtained easily from the coupling Hamiltonian: We have so far not used that the coupling operators should be Hermitian, and the above form is therefore also valid for non-Hermitian coupling operators.

There is just one problem left: In the general case, it is not of Lindblad form. Note that there are specific cases where the Markovian master equation is of Lindblad form, but these rather include simple limits. Though this is sometimes considered a rather cosmetic drawback, it may lead to unphysical results such as negative probabilities.

### Secular Approximation

To generally obtain a Lindblad type master equation, a further approximation is required. The secular approximation involves an averaging in the interaction picture over fast oscillating terms in time  $t$ . In general, we can write the master equation so far as

$$\dot{\rho}_{\mathbf{S}} = \sum_{\omega\omega'} \mathcal{L}_{\omega\omega'} e^{i(\omega-\omega')t} \rho_{\mathbf{S}}(t) = \sum_{\omega} \mathcal{L}_{\omega\omega} \rho_{\mathbf{S}}(t) + \sum_{\omega \neq \omega'} \mathcal{L}_{\omega\omega'} e^{i(\omega-\omega')t} \rho_{\mathbf{S}}(t). \quad (1.64)$$

Here, the  $\omega$  are energy differences (**Bohr-frequencies**) of the system, and  $\mathcal{L}_{\omega\omega'}$  are the associated superoperators. When we integrate over both sides of the equation, we see that when  $\rho_{\mathbf{S}}(t)$  varies only slowly, the terms with  $\omega \neq \omega'$  are suppressed in comparison to terms with  $\omega = \omega'$ , since they are multiplied by the rapidly oscillating phase factor (Riemann-Lebesgue theorem). Completely neglecting them is known as **secular approximation**

$$\dot{\rho}_{\mathbf{S}} \approx \sum_{\omega} \mathcal{L}_{\omega\omega} \rho_{\mathbf{S}}(t). \quad (1.65)$$

In order to identify the oscillation frequencies in the interaction picture, it is necessary to at least formally calculate the interaction picture dynamics of the system coupling operators. We begin by writing Eq. (1.62) in the interaction picture again explicitly – now using the Hermiticity of the coupling operators

$$\begin{aligned} \dot{\rho}_{\mathbf{S}} &= - \int_0^{\infty} \sum_{\alpha\beta} \{ C_{\alpha\beta}(\tau) [\mathbf{A}_{\alpha}(t), \mathbf{A}_{\beta}(t-\tau) \rho_{\mathbf{S}}(t)] + \text{h.c.} \} d\tau \\ &= + \int_0^{\infty} \sum_{\alpha\beta} C_{\alpha\beta}(\tau) \sum_{a,b,c,d} \left\{ |a\rangle \langle a| \mathbf{A}_{\beta}(t-\tau) |b\rangle \langle b| \rho_{\mathbf{S}}(t) |d\rangle \langle d| \mathbf{A}_{\alpha}(t) |c\rangle \langle c| \right. \\ &\quad \left. - |d\rangle \langle d| \mathbf{A}_{\alpha}(t) |c\rangle \langle c| |a\rangle \langle a| \mathbf{A}_{\beta}(t-\tau) |b\rangle \langle b| \rho_{\mathbf{S}}(t) \right\} d\tau + \text{h.c.}, \end{aligned} \quad (1.66)$$

where we have introduced the system energy eigenbasis

$$H_S |a\rangle = E_a |a\rangle. \quad (1.67)$$

We can use this eigenbasis to make the time-dependence of the coupling operators in the interaction picture explicit. To reduce the notational effort, we abbreviate  $A_{\alpha}^{ab} = \langle a| A_{\alpha} |b\rangle$  and  $L_{ab} = |a\rangle \langle b|$ . Then, the density matrix becomes

$$\begin{aligned} \dot{\rho}_{\mathbf{S}} &= + \int_0^{\infty} \sum_{\alpha\beta} C_{\alpha\beta}(\tau) \sum_{a,b,c,d} \left\{ e^{+i(E_a-E_b)(t-\tau)} e^{+i(E_d-E_c)t} A_{\beta}^{ab} A_{\alpha}^{dc} L_{ab} \rho_{\mathbf{S}}(t) L_{cd}^{\dagger} \right. \\ &\quad \left. - e^{+i(E_a-E_b)(t-\tau)} e^{+i(E_d-E_c)t} A_{\beta}^{ab} A_{\alpha}^{dc} L_{cd}^{\dagger} L_{ab} \rho_{\mathbf{S}}(t) \right\} d\tau + \text{h.c.}, \\ &= \sum_{\alpha\beta} \sum_{a,b,c,d} \int_0^{\infty} C_{\alpha\beta}(\tau) e^{+i(E_b-E_a)\tau} d\tau e^{-i(E_b-E_a-(E_d-E_c)t)} A_{\beta}^{ab} (A_{\alpha}^{cd})^* \left\{ L_{ab} \rho_{\mathbf{S}}(t) L_{cd}^{\dagger} - L_{cd}^{\dagger} L_{ab} \rho_{\mathbf{S}}(t) \right\} \\ &\quad + \text{h.c.} \end{aligned} \quad (1.68)$$

The secular approximation now involves neglecting all terms that are oscillatory in time  $t$  (long-time average), i.e., we have

$$\begin{aligned} \dot{\rho}\mathbf{s} = & \sum_{\alpha\beta} \sum_{a,b,c,d} \Gamma_{\alpha\beta}(E_b - E_a) \delta_{E_b-E_a, E_d-E_c} A_{\beta}^{ab} (A_{\alpha}^{cd})^* \left\{ +L_{ab}\rho\mathbf{s}(t)L_{cd}^{\dagger} - L_{cd}^{\dagger}L_{ab}\rho\mathbf{s}(t) \right\} \\ & + \sum_{\alpha\beta} \sum_{a,b,c,d} \Gamma_{\alpha\beta}^*(E_b - E_a) \delta_{E_b-E_a, E_d-E_c} (A_{\beta}^{ab})^* A_{\alpha}^{cd} \left\{ +L_{cd}\rho\mathbf{s}(t)L_{ab}^{\dagger} - \rho\mathbf{s}(t)L_{ab}^{\dagger}L_{cd} \right\}, \end{aligned} \quad (1.69)$$

where we have introduced the half-sided Fourier transform of the bath correlation functions

$$\Gamma_{\alpha\beta}(\omega) = \int_0^{\infty} C_{\alpha\beta}(\tau) e^{+i\omega\tau} d\tau. \quad (1.70)$$

This equation preserves trace, Hermiticity, and positivity of the density matrix and hence all desired properties, since it is of Lindblad form (which will be shown later). Unfortunately, it is in general not so easy to obtain as it requires diagonalization of the system Hamiltonian first – simple limits arise when the system Hamiltonian is given in a diagonal form. By using the transformations  $\alpha \leftrightarrow \beta$ ,  $a \leftrightarrow c$ , and  $b \leftrightarrow d$  in the second line and also using that the  $\delta$ -function is symmetric, we may rewrite the master equation as

$$\begin{aligned} \dot{\rho}\mathbf{s} = & \sum_{\alpha\beta} \sum_{a,b,c,d} [\Gamma_{\alpha\beta}(E_b - E_a) + \Gamma_{\beta\alpha}^*(E_b - E_a)] \delta_{E_b-E_a, E_d-E_c} A_{\beta}^{ab} (A_{\alpha}^{cd})^* L_{ab}\rho\mathbf{s}(t)L_{cd}^{\dagger} \\ & - \sum_{\alpha\beta} \sum_{a,b,c,d} \Gamma_{\alpha\beta}(E_b - E_a) \delta_{E_b-E_a, E_d-E_c} A_{\beta}^{ab} (A_{\alpha}^{cd})^* L_{cd}^{\dagger}L_{ab}\rho\mathbf{s}(t) \\ & - \sum_{\alpha\beta} \sum_{a,b,c,d} \Gamma_{\beta\alpha}^*(E_b - E_a) \delta_{E_b-E_a, E_d-E_c} A_{\beta}^{ab} (A_{\alpha}^{cd})^* \rho\mathbf{s}(t)L_{cd}^{\dagger}L_{ab}. \end{aligned} \quad (1.71)$$

In order to separate the unitary and dissipative contributions, we split the matrix-valued function  $\Gamma_{\alpha\beta}(\omega)$  into Hermitian and anti-Hermitian parts

$$\begin{aligned} \Gamma_{\alpha\beta}(\omega) &= \frac{1}{2}\gamma_{\alpha\beta}(\omega) + \frac{1}{2}\sigma_{\alpha\beta}(\omega), \\ \Gamma_{\beta\alpha}^*(\omega) &= \frac{1}{2}\gamma_{\alpha\beta}(\omega) - \frac{1}{2}\sigma_{\alpha\beta}(\omega), \end{aligned} \quad (1.72)$$

with Hermitian  $\gamma_{\alpha\beta}(\omega) = \gamma_{\beta\alpha}^*(\omega)$  and anti-Hermitian  $\sigma_{\alpha\beta}(\omega) = -\sigma_{\beta\alpha}^*(\omega)$ . These new functions can be interpreted as full even and odd Fourier transforms of the bath correlation functions

$$\begin{aligned} \gamma_{\alpha\beta}(\omega) &= \Gamma_{\alpha\beta}(\omega) + \Gamma_{\beta\alpha}^*(\omega) = \int_{-\infty}^{+\infty} C_{\alpha\beta}(\tau) e^{+i\omega\tau} d\tau, \\ \sigma_{\alpha\beta}(\omega) &= \Gamma_{\alpha\beta}(\omega) - \Gamma_{\beta\alpha}^*(\omega) = \int_{-\infty}^{+\infty} C_{\alpha\beta}(\tau) \text{sgn}(\tau) e^{+i\omega\tau} d\tau. \end{aligned} \quad (1.73)$$

**Exercise 10** (Odd Fourier Transform). *Show that the odd Fourier transform  $\sigma_{\alpha\beta}(\omega)$  may be obtained from the even Fourier transform  $\gamma_{\alpha\beta}(\omega)$  by a Cauchy principal value integral*

$$\sigma_{\alpha\beta}(\omega) = \frac{i}{\pi} \mathcal{P} \int_{-\infty}^{+\infty} \frac{\gamma_{\alpha\beta}(\Omega)}{\omega - \Omega} d\Omega.$$

In the master equation, these replacements lead to

$$\begin{aligned} \dot{\rho}_{\mathbf{S}} &= \sum_{\alpha\beta} \sum_{a,b,c,d} \gamma_{\alpha\beta}(E_b - E_a) \delta_{E_b - E_a, E_d - E_c} A_{\beta}^{ab} (A_{\alpha}^{cd})^* \left[ L_{ab} \rho_{\mathbf{S}}(t) L_{cd}^{\dagger} - \frac{1}{2} \left\{ L_{cd}^{\dagger} L_{ab}, \rho_{\mathbf{S}}(t) \right\} \right] \\ &\quad - i \sum_{\alpha\beta} \sum_{a,b,c,d} \frac{1}{2i} \sigma_{\alpha\beta}(E_b - E_a) \delta_{E_b - E_a, E_d - E_c} A_{\beta}^{ab} (A_{\alpha}^{cd})^* \left[ L_{cd}^{\dagger} L_{ab}, \rho_{\mathbf{S}}(t) \right] \\ &= \sum_{\alpha\beta} \sum_{a,b,c,d} \gamma_{\alpha\beta}(E_b - E_a) \delta_{E_b - E_a, E_d - E_c} A_{\beta}^{ab} (A_{\alpha}^{cd})^* \left[ L_{ab} \rho_{\mathbf{S}}(t) L_{cd}^{\dagger} - \frac{1}{2} \left\{ L_{cd}^{\dagger} L_{ab}, \rho_{\mathbf{S}}(t) \right\} \right] \\ &\quad - i \left[ \sum_{\alpha\beta} \sum_{a,b,c} \frac{1}{2i} \sigma_{\alpha\beta}(E_b - E_c) \delta_{E_b, E_a} A_{\beta}^{cb} (A_{\alpha}^{ca})^* L_{ab}, \rho_{\mathbf{S}}(t) \right]. \end{aligned} \quad (1.74)$$

To prove that we have a Lindblad form, it is easy to see first that the term in the commutator

$$H_{\text{LS}} = \sum_{\alpha\beta} \sum_{a,b,c} \frac{1}{2i} \sigma_{\alpha\beta}(E_b - E_c) \delta_{E_b, E_a} A_{\beta}^{cb} (A_{\alpha}^{ca})^* |a\rangle \langle b| \quad (1.75)$$

is an effective Hamiltonian. This Hamiltonian is often called Lamb-shift Hamiltonian, since it renormalizes the system Hamiltonian due to the interaction with the reservoir. Note that we have  $[H_S, H_{\text{LS}}] = 0$ .

**Exercise 11** (Lamb-shift). *Show that  $H_{\text{LS}} = H_{\text{LS}}^{\dagger}$  and  $[H_{\text{LS}}, H_S] = 0$ .*

To show the Lindblad-form of the non-unitary evolution, we identify the Lindblad jump operator  $L_{\alpha} = |a\rangle \langle b| = L_{(a,b)}$ . For an  $N$ -dimensional system Hilbert space with  $N$  eigenvectors of  $H_S$  we would have  $N^2$  such jump operators, but the identity matrix  $\mathbf{1} = \sum_a |a\rangle \langle a|$  has trivial action, which can be used to eliminate one jump operator. It remains to be shown that the matrix

$$\gamma_{(ab),(cd)} = \sum_{\alpha\beta} \gamma_{\alpha\beta}(E_b - E_a) \delta_{E_b - E_a, E_d - E_c} A_{\beta}^{ab} (A_{\alpha}^{cd})^* \quad (1.76)$$

is non-negative, i.e.,  $\sum_{a,b,c,d} x_{ab}^* \gamma_{(ab),(cd)} x_{cd} \geq 0$  for all  $x_{ab}$ . We first note that for Hermitian coupling operators the Fourier transform matrix at fixed  $\omega$  is positive (recall that  $B_{\alpha} = B_{\alpha}^{\dagger}$  and  $[\bar{\rho}_B, H_B] = 0$ ,

such that  $\bar{\rho}_B = \sum_\ell \rho_\ell |\ell\rangle \langle \ell|$  with  $\rho_\ell \geq 0$  and  $H_B = \sum_\ell E_\ell |\ell\rangle \langle \ell|$

$$\begin{aligned}
\sum_{\alpha\beta} x_\alpha^* \gamma_{\alpha\beta}(\omega) x_\beta &= \int_{-\infty}^{+\infty} d\tau e^{+i\omega\tau} \text{Tr} \left\{ e^{iH_B\tau} \left[ \sum_\alpha x_\alpha^* B_\alpha \right] e^{-iH_B\tau} \left[ \sum_\beta x_\beta B_\beta \right] \bar{\rho}_B \right\} \\
&= \int_{-\infty}^{+\infty} d\tau e^{+i\omega\tau} \sum_{nm} e^{+i(E_n - E_m)\tau} \langle n| B^\dagger |m\rangle \langle m| B \bar{\rho}_B |n\rangle \\
&= \sum_{nm} 2\pi\delta(\omega + E_n - E_m) |\langle m| B |n\rangle|^2 \rho_n \geq 0.
\end{aligned} \tag{1.77}$$

Alternatively, Bochner's theorem can be used to confirm this argument. To show from this the positivity of the dampening matrix, we replace the Kronecker symbol in the dampening coefficients an auxiliary summation

$$\begin{aligned}
\sum_{abcd} x_{ab}^* \gamma_{(ab),(cd)} x_{cd} &= \sum_\omega \sum_{\alpha\beta} \sum_{abcd} \gamma_{\alpha\beta}(\omega) \delta_{E_b - E_a, \omega} \delta_{E_d - E_c, \omega} x_{ab}^* \langle a| A_\beta |b\rangle x_{cd} \langle c| A_\alpha |d\rangle^* \\
&= \sum_\omega \sum_{\alpha\beta} \left[ \sum_{cd} x_{cd} \langle c| A_\alpha |d\rangle^* \delta_{E_d - E_c, \omega} \right] \gamma_{\alpha\beta}(\omega) \left[ \sum_{ab} x_{ab}^* \langle a| A_\beta |b\rangle \delta_{E_b - E_a, \omega} \right] \\
&= \sum_\omega \sum_{\alpha\beta} y_\alpha^*(\omega) \gamma_{\alpha\beta}(\omega) y_\beta(\omega) \geq 0.
\end{aligned} \tag{1.78}$$

Transforming Eq. (1.74) back to the Schrödinger picture (note that the  $\delta$ -functions prohibit the occurrence of oscillatory factors), we finally obtain the Born-Markov-Secular (BMS) master equation.

**Def. 6** (BMS master equation). *In the weak coupling limit, an interaction Hamiltonian of the form  $H_I = \sum_\alpha A_\alpha \otimes B_\alpha$  with  $A_\alpha = A_\alpha^\dagger$  and  $B_\alpha = B_\alpha^\dagger$  as well as  $[H_B, \bar{\rho}_B] = 0$  and  $\text{Tr} \{B_\alpha \bar{\rho}_B\} = 0$  leads in the system energy eigenbasis  $H_S |a\rangle = E_a |a\rangle$  to the Lindblad-form master equation ( $L_{ab} \equiv |a\rangle \langle b|$ )*

$$\begin{aligned}
\dot{\rho}_S &= -i \left[ H_S + \sum_{ab} \sigma_{ab} L_{ab}, \rho_S(t) \right] + \sum_{a,b,c,d} \gamma_{ab,cd} \left[ L_{ab} \rho_S(t) L_{cd}^\dagger - \frac{1}{2} \left\{ L_{cd}^\dagger L_{ab}, \rho_S(t) \right\} \right], \\
\gamma_{ab,cd} &= \sum_{\alpha\beta} \gamma_{\alpha\beta}(E_b - E_a) \delta_{E_b - E_a, E_d - E_c} \langle a| A_\beta |b\rangle \langle c| A_\alpha |d\rangle^*, \\
\sigma_{ab} &= \sum_{\alpha\beta} \sum_c \frac{1}{2i} \sigma_{\alpha\beta}(E_b - E_c) \delta_{E_b, E_a} \langle c| A_\beta |b\rangle \langle c| A_\alpha |a\rangle^*.
\end{aligned} \tag{1.79}$$

where the constants are given by even and odd Fourier transforms

$$\gamma_{\alpha\beta}(\omega) = \int_{-\infty}^{+\infty} C_{\alpha\beta}(\tau) e^{+i\omega\tau} d\tau, \quad \sigma_{\alpha\beta}(\omega) = \int_{-\infty}^{+\infty} C_{\alpha\beta}(\tau) \text{sgn}(\tau) e^{+i\omega\tau} d\tau = \frac{i}{\pi} \mathcal{P} \int_{-\infty}^{+\infty} \frac{\gamma_{\alpha\beta}(\omega')}{\omega - \omega'} d\omega' \tag{1.80}$$

of the bath correlation functions

$$C_{\alpha\beta}(\tau) = \text{Tr} \left\{ e^{+iH_B\tau} B_\alpha e^{-iH_B\tau} B_\beta \bar{\rho}_B \right\}. \tag{1.81}$$

This definition provides a generic recipe for a Lindblad type master equation in the weak-coupling limit:

- It requires to rewrite the coupling operators in Hermitian form, the calculation of the bath correlation function Fourier transforms, and the diagonalization of the system Hamiltonian. It is expected to yield good results in the weak coupling and Markovian limit (nearly flat FTs  $\gamma_{\alpha\beta}(\omega)$  for the Markov approximation) and large system energy splittings (for the secular approximation).
- The operators  $L_{ab} = |a\rangle\langle b|$  are in general non-local, as e.g. for bipartite systems, the energy eigenstates of the system are usually entangled.
- The **Lamb-shift** terms  $\sigma_{\alpha\beta}(\omega)$  are often neglected in the weak-coupling limit, as the modification of the system Hamiltonian will be negligible in comparison to the original system. In particular in presence of degeneracies, this is not applicable.
- In the case that the spectrum of the system Hamiltonian is non-degenerate, we have further simplifications, e.g.  $\delta_{E_b, E_a} \rightarrow \delta_{ab}$ . By taking matrix elements of Eq. (1.79) in the energy eigenbasis  $\rho_{aa} = \langle a | \rho_S | a \rangle$ , we obtain an effective **rate equation** for the populations only

$$\dot{\rho}_{aa} = + \sum_b \gamma_{ab,ab} \rho_{bb} - \left[ \sum_b \gamma_{ba,ba} \right] \rho_{aa}, \quad (1.82)$$

i.e., in the system energy eigenbasis, the coherences decouple from the evolution of the populations, see Fig. 1.2. The transition rates from state  $b$  to state  $a$  reduce in this case to

$$\gamma_{ab,ab} = \sum_{\alpha\beta} \gamma_{\alpha\beta}(E_b - E_a) \langle a | A_\beta | b \rangle \langle a | A_\alpha | b \rangle^* \geq 0, \quad (1.83)$$

which – after inserting all definitions – condenses basically to **Fermis Golden Rule**. Therefore, with such a rate equation description, open quantum systems can be described with the same complexity as closed quantum systems, since only  $N$  dynamical variables have to be evolved.

The BMS master equation is problematic for near-degenerate systems: For exact degeneracies, couplings to coherences between energetically degenerate states have to be kept, but for lifted degeneracies, they are neglected. This discontinuous behaviour may map to observables and poses the question which of the two resulting equations is correct, in particular for near degeneracies. Despite such problems, the BMS master equation is heavily used since beyond the Lindblad form it has many favorable properties. For example, we will see later that if coupled to a single thermal bath, the quantum system generally relaxes to the Gibbs equilibrium, i.e., we obtain simply equilibration of the system temperature with the temperature of the bath.

### 1.3.3 Example: Harmonic oscillator in a thermal bath

In this section, we will use the example

$$H = \Omega a^\dagger a + (a + a^\dagger) \otimes \sum_k \left( h_k b_k + h_k^* b_k^\dagger \right) + \sum_k \omega_k b_k^\dagger b_k, \quad (1.84)$$

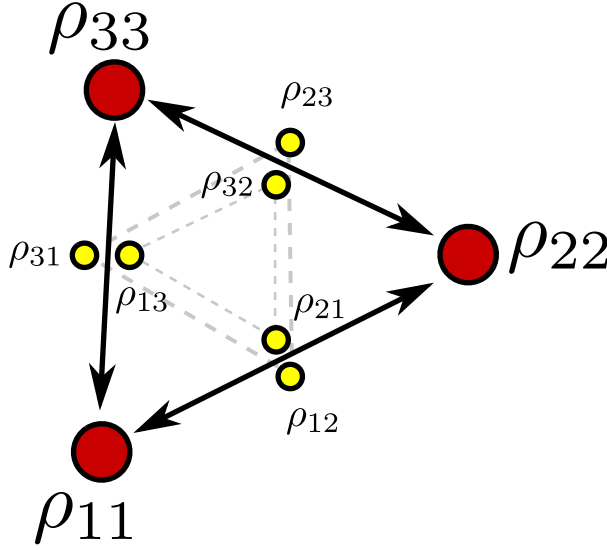


Figure 1.2: Sketch of the topology of matrix element couplings in a BMS master equation for just three levels. For any pair of populations (red), there exist two coherences (yellow). For a non-degenerate system, the populations and coherences in the system energy eigenbasis evolve formally separately. The transition rates between populations (solid arrows) are positive, whereas the couplings between coherences (dashed) are complex-valued.

which describes a harmonic oscillator of frequency  $\Omega$  (system) coupled to many other oscillator modes  $\omega_k$  (bath) via their  $x$ -coordinates.

Transforming into the interaction picture (bold symbols), the von-Neumann equation reads

$$\dot{\boldsymbol{\rho}} = -i \left[ (ae^{-i\Omega t} + a^\dagger e^{+i\Omega t}) \sum_k (h_k b_k e^{-i\omega_k t} + h_k^* b_k^\dagger e^{+i\omega_k t}), \boldsymbol{\rho} \right]. \quad (1.85)$$

We see that there is just one system and bath coupling operator, respectively, and that therefore these operators are already Hermitian by construction. We see that the time-dependent interaction Hamiltonian has many oscillatory terms, and evaluating all these terms seems challenging at first.

One fundamental requirement is immediately fulfilled, since for a thermal bath we have

$$\text{Tr} \left\{ b_k e^{-\beta\omega_k} b_k^\dagger b_k \right\} = 0, \quad (1.86)$$

i.e., no further transformations are necessary. Furthermore, since in our example we have only a single system coupling operator  $\mathbf{A}(t) = (ae^{-i\Omega t} + a^\dagger e^{+i\Omega t})$ , there is consequently also only a single correlation function, which we can readily compute for a thermal bath  $\bar{\rho}_B = e^{-\beta \sum_k \omega_k b_k^\dagger b_k} / Z_B$

$$\begin{aligned} C(t_1, t_2) &= \sum_{kk'} \text{Tr} \left\{ \left( h_k b_k e^{-i\omega_k t_1} + h_k^* b_k^\dagger e^{+i\omega_k t_1} \right) \left( h_{k'} b_{k'} e^{-i\omega_{k'} t_2} + h_{k'}^* b_{k'}^\dagger e^{+i\omega_{k'} t_2} \right) \bar{\rho}_B \right\} \\ &= \sum_k |h_k|^2 \left[ e^{-i\omega_k(t_1-t_2)} \langle b_k b_k^\dagger \rangle + e^{+i\omega_k(t_1-t_2)} \langle b_k^\dagger b_k \rangle \right] \\ &= \sum_k |h_k|^2 \left[ e^{-i\omega_k(t_1-t_2)} (1 + n_B(\omega_k)) + e^{+i\omega_k(t_1-t_2)} n_B(\omega_k) \right] \\ &= \frac{1}{2\pi} \int_0^\infty J(\omega) \left[ e^{-i\omega(t_1-t_2)} (1 + n_B(\omega)) + e^{+i\omega(t_1-t_2)} n_B(\omega) \right] d\omega, \end{aligned} \quad (1.87)$$

where we have introduced the **spectral density** (also spectral coupling density)

$$J(\omega) = 2\pi \sum_k |t_k|^2 \delta(\omega - \omega_k) \quad (1.88)$$

and the Bose distribution  $n_B(\omega) = [e^{\beta\omega} - 1]^{-1}$ . For bosons, the frequencies of the reservoir oscillators must be positive  $\omega_k > 0$ , which explains the boundaries of the integrals. However, by analytically continuing the spectral density as an odd function such that  $\tilde{J}(|\omega|) = J(|\omega|)$  and  $\tilde{J}(-\omega) = -\tilde{J}(+\omega)$  and using the identity  $n_B(-\omega) = -[1 + n_B(+\omega)]$ , we can write this as a single term

$$C(t_1 - t_2) = \frac{1}{2\pi} \int_{-\infty}^{+\infty} \tilde{J}(\omega)[1 + n_B(\omega)]e^{-i\omega(t_1-t_2)}d\omega, \quad (1.89)$$

from which we can – without calculation – identify the Fourier transform of the correlation function  $\gamma(\omega) = \int C(\tau)e^{+i\omega\tau}d\tau = \tilde{J}(\omega)[1 + n_B(\omega)]$ . As shown before generally, we note that it is positive  $\gamma(\omega) \geq 0$ .

Coming back to our example, we would get

$$\begin{aligned} \dot{\rho} &= -i[\Omega a^\dagger a, \rho] - \int_0^\infty C(+\tau)[(a + a^\dagger), e^{-i\Omega a^\dagger a\tau}(a + a^\dagger)e^{+i\Omega a^\dagger a\tau}\rho]d\tau \\ &\quad - \int_0^\infty C^*(+\tau)\left[\rho e^{-i\Omega a^\dagger a\tau}(a + a^\dagger)e^{+i\Omega a^\dagger a\tau}, (a + a^\dagger)\right] \\ &= -i[\Omega a^\dagger a, \rho] - \left\{ \int_0^\infty C(+\tau)[(a + a^\dagger), (ae^{+i\Omega\tau} + a^\dagger e^{-i\Omega\tau})\rho]d\tau + \text{h.c.} \right\} \\ &= -i[\Omega a^\dagger a, \rho] - \left\{ \Gamma(+\Omega)[(a + a^\dagger), a\rho] + \Gamma(-\Omega)[(a + a^\dagger), a^\dagger\rho] + \text{h.c.} \right\}, \end{aligned} \quad (1.90)$$

where we have used the conjugation property (1.58) valid for Hermitian coupling operators and defined the half-sided FT  $\Gamma(\omega) = \int_0^\infty C(\tau)e^{+i\omega\tau}d\tau$ .

We make this explicit for our example. In the interaction picture, we have

$$\begin{aligned} \dot{\rho} &= - \int_0^\infty C(\tau) [(ae^{-i\Omega t} + a^\dagger e^{+i\Omega t}), (ae^{-i\Omega(t-\tau)} + a^\dagger e^{+i\Omega(t-\tau)})\rho] + \text{h.c.} \\ &\approx - \int_0^\infty C(\tau)e^{-i\Omega\tau}d\tau[a, a^\dagger\rho] - \int_0^\infty C(\tau)e^{+i\Omega\tau}d\tau[a^\dagger, a\rho] + \text{h.c.} \\ &= -\Gamma(-\Omega)(aa^\dagger\rho - a^\dagger\rho a) - \Gamma(+\Omega)(a^\dagger a\rho - a\rho a^\dagger) \\ &\quad - \Gamma^*(-\Omega)(\rho a a^\dagger - a^\dagger\rho a) - \Gamma^*(+\Omega)(\rho a^\dagger a - a\rho a^\dagger). \end{aligned} \quad (1.91)$$

Here, the secular approximation amounts to neglecting all terms that oscillate with  $e^{\pm 2i\Omega t}$ . Splitting into hermitian and anti-hermitian parts for a  $1 \times 1$  matrix just means separating real and imaginary parts  $\Gamma(+\Omega) = \frac{1}{2}\gamma + \frac{1}{2}\sigma$  and  $\Gamma(-\Omega) = \frac{1}{2}\bar{\gamma} + \frac{1}{2}\bar{\sigma}$

$$\dot{\rho} = \gamma \left[ a\rho a^\dagger - \frac{1}{2} \{a^\dagger a, \rho\} \right] + \bar{\gamma} \left[ a^\dagger \rho a - \frac{1}{2} \{aa^\dagger, \rho\} \right] - i \left[ \frac{\sigma}{2} a^\dagger a + \frac{\bar{\sigma}}{2} aa^\dagger, \rho \right]. \quad (1.92)$$

This is a Lindblad form master equation when  $\gamma > 0$  and  $\bar{\gamma} > 0$ . Indeed, we have already computed the Fourier transform of the full correlation function, which we showed to be non-negative. The real part of the half-sided Fourier transforms of the correlation function

$$\begin{aligned} \Gamma(\omega) + \Gamma^*(\omega) &= \int_0^\infty C(\tau)e^{+i\omega\tau}d\tau + \int_0^\infty C^*(\tau)e^{-i\omega\tau}d\tau \\ &= \int_0^\infty C(\tau)e^{+i\omega\tau}d\tau + \int_0^\infty C(-\tau)e^{-i\omega\tau}d\tau = \int_0^\infty C(\tau)e^{+i\omega\tau}d\tau + \int_{-\infty}^0 C(\tau)e^{+i\omega\tau}d\tau \\ &= \int_{-\infty}^{+\infty} C(\tau)e^{+i\omega\tau}d\tau = \gamma(\omega) = \tilde{J}(\omega)[1 + n_B(\omega)] \end{aligned} \quad (1.93)$$

is given by the full Fourier transform of the correlation function, which we have shown to be positive. From  $\omega = +\Omega$  we conclude  $\gamma = J(\Omega)[1 + n_B(\Omega)]$  and from  $\omega = -\Omega$  we obtain  $\bar{\gamma} = J(\Omega)n_B(\Omega)$ , such that by transforming back to the Schrödinger picture, we get

$$\begin{aligned} \dot{\rho} = & -i \left[ \left( \Omega + \frac{\sigma}{2} + \frac{\bar{\sigma}}{2} \right) a^\dagger a, \rho \right] + J(\Omega)(1 + n_B) \left[ a \rho a^\dagger - \frac{1}{2} a^\dagger a \rho - \frac{1}{2} \rho a^\dagger a \right] \\ & + J(\Omega)n_B \left[ a^\dagger \rho a - \frac{1}{2} a a^\dagger \rho - \frac{1}{2} \rho a a^\dagger \right], \end{aligned} \quad (1.94)$$

This is very similar to what we used in Eq. (1.20), it only differs in the neglect of **Lamb-shift** terms  $\sigma$  and  $\bar{\sigma}$ , which would merely correspond to a re-interpretation of the cavity frequency  $\Omega$ . To see that this is the same as Def. 6, we insert  $a^\dagger a = \sum_{n=0}^{\infty} n |n\rangle \langle n|$  and  $a = \sum_{n=1}^{\infty} \sqrt{n} |n-1\rangle \langle n|$  as well as the hermitian conjugate. So, this simple master equation only admits transitions between neighboring energy eigenstates, which is enforced by the matrix elements of the system coupling operator.

### 1.3.4 Equilibrium Thermodynamics

The BMS limit has beyond its relatively compact Lindblad form further appealing properties in the case of a bath that is in thermal equilibrium

$$\bar{\rho}_B = \frac{e^{-\beta H_B}}{\text{Tr}\{e^{-\beta H_B}\}} \quad (1.95)$$

with inverse temperature  $\beta$ . These root in further analytic properties of the bath correlation functions such as the Kubo-Martin-Schwinger (KMS) condition

$$C_{\alpha\bar{\alpha}}(\tau) = C_{\bar{\alpha}\alpha}(-\tau - i\beta). \quad (1.96)$$

**Exercise 12** (KMS condition). *Show the validity of the KMS condition for a thermal bath with  $\bar{\rho}_B = \frac{e^{-\beta H_B}}{\text{Tr}\{e^{-\beta H_B}\}}$ .*

For the Fourier transform, this shift property implies

$$\begin{aligned} \gamma_{\alpha\bar{\alpha}}(-\omega) &= \int_{-\infty}^{+\infty} C_{\alpha\bar{\alpha}}(\tau) e^{-i\omega\tau} d\tau = \int_{-\infty}^{+\infty} C_{\bar{\alpha}\alpha}(-\tau - i\beta) e^{-i\omega\tau} d\tau \\ &= \int_{+\infty-i\beta}^{-\infty-i\beta} C_{\bar{\alpha}\alpha}(\tau') e^{+i\omega(\tau'+i\beta)} (-d\tau)' = \int_{-\infty-i\beta}^{+\infty-i\beta} C_{\bar{\alpha}\alpha}(\tau') e^{+i\omega\tau'} d\tau' e^{-\beta\omega} \\ &= \int_{-\infty}^{+\infty} C_{\bar{\alpha}\alpha}(\tau') e^{+i\omega\tau'} d\tau' e^{-\beta\omega} = \gamma_{\bar{\alpha}\alpha}(+\omega) e^{-\beta\omega}, \end{aligned} \quad (1.97)$$

where in the last line we have used that the bath correlation functions are analytic in  $\tau$  in the complex plane and vanish at infinity, such that we may safely deform the integration contour. Finally,

the KMS condition can thereby be used to prove that for a reservoir with inverse temperature  $\beta$ , the density matrix

$$\bar{\rho}_S = \frac{e^{-\beta H_S}}{\text{Tr} \{e^{-\beta H_S}\}} \quad (1.98)$$

is one stationary state of the BMS master equation.

**Exercise 13** (Thermalization). *Show that  $\bar{\rho}_S = \frac{e^{-\beta H_S}}{\text{Tr} \{e^{-\beta H_S}\}}$  is a stationary state of the BMS master equation, when  $\gamma_{\alpha\bar{\alpha}}(-\omega) = \gamma_{\bar{\alpha}\alpha}(+\omega)e^{-\beta\omega}$ .*

Things become a bit more complicated when the reservoir is in the grand-canonical equilibrium state

$$\bar{\rho}_B = \frac{e^{-\beta(H_B - \mu N_B)}}{\text{Tr} \{e^{-\beta(H_B - \mu N_B)}\}}, \quad (1.99)$$

with the chemical potential  $\mu$  and the particle number operator  $N_B$  of the bath. Then, the normal KMS condition is not fulfilled anymore by the correlation function. Chemical potentials become relevant for models discussing particle transport. To talk about transport, it is natural to assume that the total particle number  $N = N_S + N_B$  is a conserved quantity  $[H_S, N_S] = [H_B, N_B] = [H_I, N_S + N_B] = 0$ . In this case one can show that [10] the KMS relation is generalized according to

$$\sum_{\bar{\alpha}} A_{\bar{\alpha}} C_{\alpha\bar{\alpha}}(\tau) = \sum_{\bar{\alpha}} e^{+\beta\mu N_S} A_{\bar{\alpha}} e^{-\beta\mu N_S} C_{\bar{\alpha}\alpha}(-\tau - i\beta). \quad (1.100)$$

This modifies the detailed-balance relation of the master equation coefficients to

$$\frac{\gamma_{ab,cd}}{\gamma_{dc,ba}} = e^{\beta[(E_b - E_a) - \mu(N_b - N_a)]}. \quad (1.101)$$

In the end, these modified relations can be used to show that a stationary state of the BMS master equation is given by

$$\bar{\rho}_S = \frac{e^{-\beta(H_S - \mu N_S)}}{\text{Tr} \{e^{-\beta(H_S - \mu N_S)}\}}, \quad (1.102)$$

i.e., both temperature  $\beta$  and chemical potential  $\mu$  must equilibrate with the reservoir.

**Exercise 14** (Equilibration). *Show that Eqns. (1.100) and (1.101) hold. It will be useful to use conservation of the total particle number and Eq. (1.80).*

Finally, we consider the evolution of the system entropy. We first recall an early result by Lindblad [11] stating that completely-positive trace-preserving maps (Kraus maps) are contractive. To this end, we first start with some definitions. First, we define the von-Neumann entropy of the system

**Def. 7** (von-Neumann entropy). *The von-Neumann entropy of a system described by density matrix  $\rho$  is defined as*

$$S(\rho) = -\text{Tr} \{ \rho \ln \rho \} . \quad (1.103)$$

*We have  $0 \leq S(\rho) \leq \ln N$  and for an  $N \times N$  density matrix  $\rho$ .*

The von-Neumann entropy can serve as an entanglement measure for states that are globally pure. It is sometimes used synonymously with the Shannon entropy  $S_{\text{Sh}} = -\sum_i P_i \ln P_i$  but is strictly speaking not the same. They only coincide in the basis where the density matrix is diagonal. The Shannon entropy is formally basis-dependent whereas the von-Neumann entropy is not.

**Exercise 15** (von-Neumann entropy). *Compute the von-Neumann entropy of the reduced density matrix  $\rho_1$  of  $\rho_{12}^{a/b} = |\Psi^{a/b}\rangle \langle \Psi^{a/b}|$  for*

$$|\Psi^a\rangle = \frac{1}{\sqrt{2}} [|01\rangle + |10\rangle] , \quad |\Psi^b\rangle = \frac{1}{2} [|01\rangle + |00\rangle + |10\rangle + |11\rangle] .$$

Furthermore, we introduce a pseudo-distance between density matrices

**Def. 8** (Quantum Relative Entropy). *The quantum relative entropy between two density matrices  $\rho$  and  $\sigma$  is defined as*

$$D(\rho||\sigma) = \text{Tr} \{ \rho (\ln \rho - \ln \sigma) \} . \quad (1.104)$$

Obviously, the relative entropy vanishes when the two density matrices are equal  $D(\rho||\rho) = 0$ . Furthermore, the relative entropy can be shown to be non-negative  $D(\rho||\sigma) \geq 0$ . It is also not a real distance, since it is not symmetric. Lindblads result states that Kraus maps  $\mathcal{K}\rho = \rho'$  are contractive, i.e., that

$$D(\mathcal{K}\rho||\mathcal{K}\sigma) \leq D(\rho||\sigma) , \quad (1.105)$$

i.e., with each application of the Kraus map, the two states  $\rho$  and  $\sigma$  are closer together.

This can be exploited for Lindblad generators in the following way: Taking the Kraus map  $\mathcal{K} = e^{\mathcal{L}\Delta t}$  and choosing the distance to the steady state  $\sigma = \bar{\rho}$ , which fulfils  $\mathcal{L}\bar{\rho} = 0$ , we can expand the inequality

$$D(\rho||\bar{\rho}) - D(e^{\mathcal{L}\Delta t}\rho||\bar{\rho}) \geq 0 \quad (1.106)$$

for small  $\Delta t$  to obtain Spohn's inequality.

**Def. 9** (Spohn's inequality [12]). *Let  $\mathcal{L}$  be a Lindblad-type generator and  $\bar{\rho}$  its stationary state fulfilling  $\mathcal{L}\bar{\rho} = 0$ . Then the physical evolution obeys at all times the inequality*

$$-\text{Tr} \{[\mathcal{L}\rho][\ln \rho - \ln \bar{\rho}]\} \geq 0. \quad (1.107)$$

What is the meaning of this inequality, apart from its formal meaning as some contraction rate?

One can see that the first term in Spohn's inequality is just the time derivative of the von-Neumann entropy

$$\dot{S}(\rho) = -\text{Tr} \{ \dot{\rho} \ln \rho \} - \text{Tr} \left\{ \rho \frac{d}{dt} \ln \rho \right\} = -\text{Tr} \{ (\mathcal{L}\rho) \ln \rho \}. \quad (1.108)$$

Here, we have used that the density matrix is always diagonalizable  $\rho = U \rho_D U^\dagger$ , leading to

$$\begin{aligned} \text{Tr} \left\{ \rho \frac{d}{dt} \ln \rho \right\} &= \text{Tr} \left\{ U \rho_D U^\dagger \dot{U} (\ln \rho_D) U^\dagger + U \rho_D U^\dagger U (\ln \rho_D) \dot{U}^\dagger + U \rho_D U^\dagger U \rho_D^{-1} \dot{\rho}_D U^\dagger \right\} \\ &= \text{Tr} \left\{ \rho_D U^\dagger \dot{U} (\ln \rho_D) + \rho_D (\ln \rho_D) \dot{U}^\dagger U + \dot{\rho}_D \right\} \\ &= \text{Tr} \left\{ \rho_D (\ln \rho_D) (\dot{U}^\dagger U + U^\dagger \dot{U}) + \dot{\rho}_D \right\} = 0, \end{aligned} \quad (1.109)$$

where we have used that  $U^\dagger U = \mathbf{1}$ , correspondingly  $\dot{U}^\dagger U + U^\dagger \dot{U} = \mathbf{0}$ , and  $\text{Tr} \{ \dot{\rho}_D \} = 0$  (conservation of probabilities).

The interpretation of the second term in Spohn's inequality is different. When the stationary state of the system is a thermal Gibbs state  $\bar{\rho} = e^{-\beta(H_S - \mu N_S)} / Z_S$  with inverse temperature  $\beta$ , chemical potential  $\mu$ , system Hamiltonian  $H_S$ , and system particle number operator  $N_S$ , we would get

$$\text{Tr} \{ (\mathcal{L}\rho) (\ln \bar{\rho}) \} = -\beta \text{Tr} \{ (\mathcal{L}\rho) (H_S - \mu N_S) \} - \ln(Z_S) \text{Tr} \{ \mathcal{L}\rho \} = -\beta \text{Tr} \{ (H_S - \mu N_S) \mathcal{L}\rho \} = -\beta \dot{Q}, \quad (1.110)$$

where  $\dot{Q} = I_E - \mu I_M = \text{Tr} \{ (H_S - \mu N_S) \dot{\rho} \}$  denotes the heat current entering the system from the reservoir. This terminology also implies that it counts positive when entering the system. Therefore, Spohn's inequality can be written as

$$\dot{S} - \beta \dot{Q} \geq 0, \quad (1.111)$$

which bounds the rate at which heat enters the system by the change of its entropy. For a reservoir kept at equilibrium with temperature  $T$  and potential  $\mu$  throughout, we have

$$dU_{\text{res}} = T dS_{\text{res}} + \mu dN_{\text{res}}. \quad (1.112)$$

This implies for the change of the reservoir entropy (we work in units with  $k_B = 1$ )

$$\frac{dS_{\text{res}}}{dt} = \beta \left[ \frac{dU_{\text{res}}}{dt} - \mu \frac{dN_{\text{res}}}{dt} \right] \approx -\beta [I_E - \mu I_M] = -\beta \dot{Q}. \quad (1.113)$$

Here, we have neglected the contribution of the interaction energy between system and reservoir – consistent with the use of the weak-coupling assumption in the derivation of such master equations. Eventually, Spohn’s inequality can be read as

$$\dot{S} + \dot{S}_{\text{res}} \geq 0. \quad (1.114)$$

This is the second law of thermodynamics formulated for both system and reservoir (neglecting higher-order interaction effects)! Clearly, the system entropy may decrease (e.g. when a system relaxes down to its ground state), but at the same time, entropy is generated in the reservoirs. Since our master equation treatment is so far incomplete, we can up to now not track this contribution.

### 1.3.5 Coarse-Graining

#### Perturbation Theory in the Interaction Picture

Although the BMS approximation respects of course the exact initial condition, we have in the derivation made several long-term approximations. For example, the Markov approximation implied that we consider timescales much larger than the decay time of the bath correlation functions. Similarly, the secular approximation implied timescales larger than the inverse minimal splitting of the system energy eigenvalues. Therefore, we can only expect the solution originating from the BMS master equation to be an asymptotically valid long-term approximation.

Coarse-graining in contrast provides a possibility to obtain valid short-time approximations of the density matrix with a generator that is of Lindblad form. We start with the von-Neumann equation in the interaction picture (1.46). For factorizing initial density matrices, it is formally solved by  $\mathbf{U}(t)\rho_S^0 \otimes \bar{\rho}_B \mathbf{U}^\dagger(t)$ , where the time evolution operator

$$\mathbf{U}(t) = \hat{\mathcal{T}} \exp \left\{ -i \int_0^t \mathbf{H}_I(t') dt' \right\} \quad (1.115)$$

obeys the evolution equation

$$\dot{\mathbf{U}} = -i\mathbf{H}_I(t)\mathbf{U}(t), \quad (1.116)$$

which defines the time-ordering operator  $\hat{\mathcal{T}}$ . Formally integrating this equation with the evident initial condition  $\mathbf{U}(0) = \mathbf{1}$  yields

$$\begin{aligned} \mathbf{U}(t) &= \mathbf{1} - i \int_0^t \mathbf{H}_I(t') \mathbf{U}(t') dt' \\ &= \mathbf{1} - i \int_0^t \mathbf{H}_I(t') dt' - \int_0^t dt' \mathbf{H}_I(t') \left[ \int_0^{t'} dt'' \mathbf{H}_I(t'') \mathbf{U}(t'') \right] \\ &= \sum_{n=0}^{\infty} (-i)^n \int_0^t dt_1 \int_0^{t_1} dt_2 \dots \int_0^{t_{n-1}} dt_n \mathbf{H}_I(t_1) \dots \mathbf{H}_I(t_n). \end{aligned} \quad (1.117)$$

In particular, we can define the truncated operator to second order

$$\mathbf{U}_2(t) = \mathbf{1} - i \int_0^t \mathbf{H}_I(t_1) dt_1 - \int_0^t dt_1 dt_2 \mathbf{H}_I(t_1) \mathbf{H}_I(t_2) \Theta(t_1 - t_2), \quad (1.118)$$

where we have introduced the Heaviside function to account for the ordering of the integral bounds. For the Hermitian conjugate operator we obtain

$$\mathbf{U}_2^\dagger(t) = \mathbf{1} + i \int_0^t \mathbf{H}_I(t_1) dt_1 - \int_0^t dt_1 dt_2 \mathbf{H}_I(t_1) \mathbf{H}_I(t_2) \Theta(t_2 - t_1). \quad (1.119)$$

To keep the discussion at a moderate level, we assume  $\text{Tr}_B \{ \mathbf{H}_I \bar{\rho}_B \} = 0$  from the beginning. For a reservoir of independent modes put in a thermal state  $\bar{\rho}_B$  and an interaction  $H_I$  that is linear in creation and annihilation operators of the reservoir, this is always automatically fulfilled. In other cases, this situation can be reached after transforming both  $H_S$  and  $H_I$ , see exercise 7. The exact solution  $\rho_S(t) = \text{Tr}_B \{ \mathbf{U}(t) \rho_S^0 \otimes \bar{\rho}_B \mathbf{U}^\dagger(t) \}$  is then approximated by

$$\begin{aligned} \rho_S^{(2)}(t) \approx & \rho_S^0 + \text{Tr}_B \left\{ \int_0^t dt_1 \int_0^t dt_2 \mathbf{H}_I(t_1) \rho_S^0 \otimes \bar{\rho}_B \mathbf{H}_I(t_2) \right\} \\ & - \int_0^t dt_1 dt_2 \text{Tr}_B \left\{ \Theta(t_1 - t_2) \mathbf{H}_I(t_1) \mathbf{H}_I(t_2) \rho_S^0 \otimes \bar{\rho}_B + \Theta(t_2 - t_1) \rho_S^0 \otimes \bar{\rho}_B \mathbf{H}_I(t_1) \mathbf{H}_I(t_2) \right\}. \end{aligned} \quad (1.120)$$

Again, we introduce the bath correlation functions with two time arguments as in Eq. (1.56)

$$C_{\alpha\beta}(t_1, t_2) = \text{Tr} \{ \mathbf{B}_\alpha(t_1) \mathbf{B}_\beta(t_2) \bar{\rho}_B \}, \quad (1.121)$$

such that we have

$$\begin{aligned} \rho_S^{(2)}(t) = & \rho_S^0 + \sum_{\alpha\beta} \int_0^t dt_1 \int_0^t dt_2 C_{\alpha\beta}(t_1, t_2) \left[ \mathbf{A}_\beta(t_2) \rho_S^0 \mathbf{A}_\alpha(t_1) \right. \\ & \left. - \Theta(t_1 - t_2) \mathbf{A}_\alpha(t_1) \mathbf{A}_\beta(t_2) \rho_S^0 - \Theta(t_2 - t_1) \rho_S^0 \mathbf{A}_\alpha(t_1) \mathbf{A}_\beta(t_2) \right]. \end{aligned} \quad (1.122)$$

Typically, in the interaction picture, the system coupling operators  $\mathbf{A}_\alpha(t)$  will simply carry some oscillatory time dependence. In the worst case, they may remain time-independent. Therefore, the decay of the correlation function is essential for the convergence of the above integrals as  $t \rightarrow \infty$ . In this way, Markovian approximation and weak-coupling assumptions are related. In particular, we note that the truncated density matrix may remain finite even when  $t \rightarrow \infty$ , rendering the expansion convergent also in the long-term limit.

## Coarse-Graining

The basic idea of **coarse-graining** is to match this approximate expression for the system density matrix at time  $t = \tau$  with one resulting from a Markovian generator

$$\rho_S^{\text{CG}}(\tau) = e^{\mathcal{L}_\tau^{\text{CG}} \cdot \tau} \rho_S^0 \approx \rho_S^0 + \tau \mathcal{L}_\tau^{\text{CG}} \rho_S^0, \quad (1.123)$$

such that we can infer the action of the generator on an arbitrary density matrix

$$\begin{aligned}
\mathcal{L}_\tau^{\text{CG}} \rho_{\mathbf{S}} &= \frac{1}{\tau} \sum_{\alpha\beta} \int_0^\tau dt_1 \int_0^\tau dt_2 C_{\alpha\beta}(t_1, t_2) \left[ \mathbf{A}_\beta(t_2) \rho_{\mathbf{S}} \mathbf{A}_\alpha(t_1) \right. \\
&\quad \left. - \Theta(t_1 - t_2) \mathbf{A}_\alpha(t_1) \mathbf{A}_\beta(t_2) \rho_{\mathbf{S}} - \Theta(t_2 - t_1) \rho_{\mathbf{S}} \mathbf{A}_\alpha(t_1) \mathbf{A}_\beta(t_2) \right] \\
&= -i \left[ \frac{1}{2i\tau} \int_0^\tau dt_1 \int_0^\tau dt_2 \sum_{\alpha\beta} C_{\alpha\beta}(t_1, t_2) \text{sgn}(t_1 - t_2) \mathbf{A}_\alpha(t_1) \mathbf{A}_\beta(t_2), \rho_{\mathbf{S}} \right] \\
&\quad + \frac{1}{\tau} \int_0^\tau dt_1 \int_0^\tau dt_2 \sum_{\alpha\beta} C_{\alpha\beta}(t_1, t_2) \left[ \mathbf{A}_\beta(t_2) \rho_{\mathbf{S}} \mathbf{A}_\alpha(t_1) - \frac{1}{2} \{ \mathbf{A}_\alpha(t_1) \mathbf{A}_\beta(t_2), \rho_{\mathbf{S}} \} \right], \quad (1.124)
\end{aligned}$$

where we have inserted  $\Theta(x) = \frac{1}{2} [1 + \text{sgn}(x)]$  – in order to separate unitary and dissipative effects of the system-reservoir interaction.

**Def. 10** (CG Master Equation). *In the weak coupling limit, an interaction Hamiltonian of the form  $H_I = \sum_{\alpha} A_{\alpha} \otimes B_{\alpha}$  leads to the Lindblad-form master equation in the interaction picture*

$$\begin{aligned}
\dot{\rho}_{\mathbf{S}} &= -i \left[ \frac{1}{2i\tau} \int_0^\tau dt_1 \int_0^\tau dt_2 \sum_{\alpha\beta} C_{\alpha\beta}(t_1, t_2) \text{sgn}(t_1 - t_2) \mathbf{A}_\alpha(t_1) \mathbf{A}_\beta(t_2), \rho_{\mathbf{S}} \right] \\
&\quad + \frac{1}{\tau} \int_0^\tau dt_1 \int_0^\tau dt_2 \sum_{\alpha\beta} C_{\alpha\beta}(t_1, t_2) \left[ \mathbf{A}_\beta(t_2) \rho_{\mathbf{S}} \mathbf{A}_\alpha(t_1) - \frac{1}{2} \{ \mathbf{A}_\alpha(t_1) \mathbf{A}_\beta(t_2), \rho_{\mathbf{S}} \} \right],
\end{aligned}$$

where the bath correlation functions are given by

$$C_{\alpha\beta}(t_1, t_2) = \text{Tr} \left\{ e^{+iH_B t_1} B_{\alpha} e^{-iH_B t_1} e^{+iH_B t_2} B_{\beta} e^{-iH_B t_2} \bar{\rho}_B \right\}. \quad (1.125)$$

We have not used Hermiticity of the coupling operators nor that the bath correlation functions do typically only depend on a single argument. However, if the coupling operators were chosen Hermitian, it is easy to show the Lindblad form, but it actually is in Lindblad form also for non-Hermitian couplings. Obtaining the master equation requires the calculation of bath correlation functions and the evolution of the coupling operators in the interaction picture. As for reservoirs in equilibrium we have  $[H_B, \bar{\rho}_B] = 0$ , we can use that the correlation functions depend only on the difference of the arguments and insert the Fourier transform

$$\begin{aligned}
C_{\alpha\beta}(t_1 - t_2) &= \frac{1}{2\pi} \int d\omega \gamma_{\alpha\beta}(\omega) e^{-i\omega(t_1 - t_2)} d\omega, \\
C_{\alpha\beta}(t_1 - t_2) \text{sgn}(t_1 - t_2) &= \frac{1}{2\pi} \int d\omega \sigma_{\alpha\beta}(\omega) e^{-i\omega(t_1 - t_2)} d\omega. \quad (1.126)
\end{aligned}$$

Then, we can perform the integration by defining

$$A_{\alpha}^{\omega, \tau} = \int_0^\tau \mathbf{A}_{\alpha}(t) e^{-i\omega t} dt, \quad (1.127)$$

where the main observation is that we can calculate this whenever one has the spectral representation of the system Hamiltonian. Insertion leads to

$$\begin{aligned} \dot{\rho}_{\mathbf{S}} = & -i \left[ \frac{1}{2i\tau} \sum_{\alpha\beta} \frac{1}{2\pi} \int d\omega \sigma_{\alpha\beta}(\omega) A_{\alpha}^{+\omega,\tau} A_{\beta}^{-\omega,\tau}, \rho_{\mathbf{S}} \right] \\ & + \frac{1}{\tau} \sum_{\alpha\beta} \frac{1}{2\pi} \int d\omega \gamma_{\alpha\beta}(\omega) \left[ A_{\beta}^{-\omega,\tau} \rho_{\mathbf{S}} A_{\alpha}^{+\omega,\tau} - \frac{1}{2} \{ A_{\alpha}^{+\omega,\tau} A_{\beta}^{-\omega,\tau}, \rho_{\mathbf{S}} \} \right]. \end{aligned} \quad (1.128)$$

**Exercise 16** (Lindblad form). *By assuming Hermitian coupling operators  $A_{\alpha} = A_{\alpha}^{\dagger}$ , show that the CG master equation is of Lindblad form for all coarse-graining times  $\tau$ .*

Thus, we have found that the best approximation to the exact solution at time  $t$  can be written as  $\rho_S(t) \approx e^{\mathcal{L}_t^{\text{CG}}} \rho_0$ . Since  $\mathcal{L}_t^{\text{CG}}$  is of Lindblad form, it preserves the density matrix properties. Unfortunately, this is not the solution to a (single) master equation only. By acting with a time-derivative, we can see that

$$\frac{d}{dt} \rho_S(t) = \left[ \left( \frac{d}{dt} e^{\mathcal{L}_t^{\text{CG}}} \right) e^{-\mathcal{L}_t^{\text{CG}}} \right] e^{+\mathcal{L}_t^{\text{CG}}} \rho_0 = \underbrace{\left[ \left( \frac{d}{dt} e^{\mathcal{L}_t^{\text{CG}}} \right) e^{-\mathcal{L}_t^{\text{CG}}} \right]}_{\neq \mathcal{L}_t^{\text{CG}}} \rho_S(t), \quad (1.129)$$

where the term in brackets defines the time-dependent generator of dynamical coarse-graining.

### Correspondence to the quantum-optical master equation

Let us make once more the time-dependence of the coupling operators explicit, which is most conveniently done in the system energy eigenbasis. Now, we also assume that the bath correlation functions only depend on the difference of their time arguments  $C_{\alpha\beta}(t_1, t_2) = C_{\alpha\beta}(t_1 - t_2)$ , such that we may use the Fourier transform definitions in Eq. (1.73) to obtain

$$\begin{aligned} \dot{\rho}_{\mathbf{S}} = & -i \left[ \frac{1}{2i\tau} \sum_{abc} \int_0^{\tau} dt_1 \int_0^{\tau} dt_2 \sum_{\alpha\beta} C_{\alpha\beta}(t_1 - t_2) \text{sgn}(t_1 - t_2) |a\rangle \langle a| \mathbf{A}_{\alpha}(t_1) |c\rangle \langle c| \mathbf{A}_{\beta}(t_2) |b\rangle \langle b|, \rho_{\mathbf{S}} \right] \\ & + \frac{1}{\tau} \int_0^{\tau} dt_1 \int_0^{\tau} dt_2 \sum_{\alpha\beta} \sum_{abcd} C_{\alpha\beta}(t_1 - t_2) \left[ |a\rangle \langle a| \mathbf{A}_{\beta}(t_2) |b\rangle \langle b| \rho_{\mathbf{S}} |d\rangle \langle d| \mathbf{A}_{\alpha}(t_1) |c\rangle \langle c| \right. \\ & \left. - \frac{1}{2} \{ |d\rangle \langle d| \mathbf{A}_{\alpha}(t_1) |c\rangle \langle c| \cdot |a\rangle \langle a| \mathbf{A}_{\beta}(t_2) |b\rangle \langle b|, \rho_{\mathbf{S}} \} \right] \\ = & -i \frac{1}{4i\pi\tau} \int d\omega \sum_{abc} \int_0^{\tau} dt_1 \int_0^{\tau} dt_2 \sum_{\alpha\beta} \sigma_{\alpha\beta}(\omega) e^{-i\omega(t_1-t_2)} e^{+i(E_a-E_c)t_1} e^{+i(E_c-E_b)t_2} A_{\beta}^{cb} A_{\alpha}^{ac} [L_{ab}, \rho_{\mathbf{S}}] \\ & + \frac{1}{2\pi\tau} \int d\omega \int_0^{\tau} dt_1 \int_0^{\tau} dt_2 \sum_{\alpha\beta} \sum_{abcd} \gamma_{\alpha\beta}(\omega) e^{-i\omega(t_1-t_2)} e^{+i(E_a-E_b)t_2} e^{+i(E_d-E_c)t_1} A_{\beta}^{ab} A_{\alpha}^{dc} \times \\ & \times \left[ L_{ab} \rho_{\mathbf{S}} L_{cd}^{\dagger} - \frac{1}{2} \{ L_{cd}^{\dagger} L_{ab}, \rho_{\mathbf{S}} \} \right]. \end{aligned} \quad (1.130)$$

We perform the temporal integrations by invoking

$$\int_0^\tau e^{i\alpha_k t_k} dt_k = \tau e^{i\alpha_k \tau/2} \text{sinc} \left[ \frac{\alpha_k \tau}{2} \right] \quad (1.131)$$

with  $\text{sinc}(x) = \sin(x)/x$  to obtain

$$\begin{aligned} \dot{\rho}_{\mathbf{S}} &= -i \frac{\tau}{4i\pi} \int d\omega \sum_{abc} \sum_{\alpha\beta} \sigma_{\alpha\beta}(\omega) e^{i\tau(E_a - E_b)/2} \text{sinc} \left[ \frac{\tau}{2}(E_a - E_c - \omega) \right] \text{sinc} \left[ \frac{\tau}{2}(E_c - E_b + \omega) \right] \times \\ &\quad \times \langle c | A_\beta | b \rangle \langle c | A_\alpha^\dagger | a \rangle^* [ |a\rangle \langle b|, \rho_{\mathbf{S}} ] \\ &\quad + \frac{\tau}{2\pi} \int d\omega \sum_{\alpha\beta} \sum_{abcd} \gamma_{\alpha\beta}(\omega) e^{i\tau(E_a - E_b + E_d - E_c)/2} \text{sinc} \left[ \frac{\tau}{2}(E_d - E_c - \omega) \right] \text{sinc} \left[ \frac{\tau}{2}(\omega + E_a - E_b) \right] \times \\ &\quad \times \langle a | A_\beta | b \rangle \langle c | A_\alpha^\dagger | d \rangle^* \left[ |a\rangle \langle b| \rho_{\mathbf{S}} (|c\rangle \langle d|)^\dagger - \frac{1}{2} \left\{ (|c\rangle \langle d|)^\dagger |a\rangle \langle b|, \rho_{\mathbf{S}} \right\} \right]. \end{aligned} \quad (1.132)$$

Therefore, we have the same structure as before, but now with dampening and Lamb-shift coefficients that explicitly depend on the coarse-graining time

$$\begin{aligned} \dot{\rho}_{\mathbf{S}} &= -i \left[ \sum_{ab} \sigma_{ab}^\tau |a\rangle \langle b|, \rho_{\mathbf{S}} \right] \\ &\quad + \sum_{abcd} \gamma_{ab,cd}^\tau \left[ |a\rangle \langle b| \rho_{\mathbf{S}} (|c\rangle \langle d|)^\dagger - \frac{1}{2} \left\{ (|c\rangle \langle d|)^\dagger |a\rangle \langle b|, \rho_{\mathbf{S}} \right\} \right]. \end{aligned} \quad (1.133)$$

These coefficients can be determined by an integral over all frequencies

$$\begin{aligned} \sigma_{ab}^\tau &= \frac{1}{2i} \int d\omega \sum_c e^{i\tau(E_a - E_b)/2} \frac{\tau}{2\pi} \text{sinc} \left[ \frac{\tau}{2}(E_a - E_c - \omega) \right] \text{sinc} \left[ \frac{\tau}{2}(E_b - E_c - \omega) \right] \times \\ &\quad \times \left[ \sum_{\alpha\beta} \sigma_{\alpha\beta}(\omega) \langle c | A_\beta | b \rangle \langle c | A_\alpha^\dagger | a \rangle^* \right], \\ \gamma_{ab,cd}^\tau &= \int d\omega e^{i\tau(E_a - E_b + E_d - E_c)/2} \frac{\tau}{2\pi} \text{sinc} \left[ \frac{\tau}{2}(E_d - E_c - \omega) \right] \text{sinc} \left[ \frac{\tau}{2}(E_b - E_a - \omega) \right] \times \\ &\quad \times \left[ \sum_{\alpha\beta} \gamma_{\alpha\beta}(\omega) \langle a | A_\beta | b \rangle \langle c | A_\alpha^\dagger | d \rangle^* \right]. \end{aligned} \quad (1.134)$$

Finally, we note that in the limit of large coarse-graining times  $\tau \rightarrow \infty$  and assuming Hermitian coupling operators  $A_\alpha = A_\alpha^\dagger$ , these dampening coefficients converge to the ones in definition 6, i.e., formally

$$\begin{aligned} \lim_{\tau \rightarrow \infty} \sigma_{ab}^\tau &= \sigma_{ab}, \\ \lim_{\tau \rightarrow \infty} \gamma_{ab,cd}^\tau &= \gamma_{ab,cd}. \end{aligned} \quad (1.135)$$

**Exercise 17** (CG-BMS correspondence). *Show for Hermitian coupling operators that when  $\tau \rightarrow \infty$ , CG and BMS approximation are equivalent. You may use the identity*

$$\lim_{\tau \rightarrow \infty} \tau \operatorname{sinc} \left[ \frac{\tau}{2} (\Omega_a - \omega) \right] \operatorname{sinc} \left[ \frac{\tau}{2} (\Omega_b - \omega) \right] = 2\pi \delta_{\Omega_a, \Omega_b} \delta(\Omega_a - \omega).$$

This shows that coarse-graining provides an alternative derivation of the quantum-optical master equation, replacing three subsequent approximations (Born-, Markov- and secular) by just one (perturbative expansion in the interaction).

### 1.3.6 Example: Spin-Boson Model

The spin-boson model describes the interaction of a spin with a bosonic environment

$$\begin{aligned} H_S &= \Omega \sigma^z + T \sigma^x, & H_B &= \sum_k \omega_k b_k^\dagger b_k, \\ H_I &= \sigma^z \otimes \sum_k \left[ h_k b_k + h_k^* b_k^\dagger \right], \end{aligned} \quad (1.136)$$

where  $\Omega$  and  $T$  denote parameters of the system Hamiltonian,  $\sigma^\alpha$  the Pauli matrices, and  $b^\dagger$  creates a boson with frequency  $\omega_k$  in the reservoir. The coupling to the reservoir and the distribution of reservoir energies is in summary described by the spectral coupling density

$$\Gamma(\omega) = 2\pi \sum_k |h_k|^2 \delta(\omega - \omega_k). \quad (1.137)$$

The model can be motivated by a variety of setups, e.g. a charge qubit (singly-charged double quantum dot) that is coupled to vibrations. We note the a priori Hermitian coupling operators

$$A_1 = \sigma^z, \quad B_1 = \sum_k \left[ h_k b_k + h_k^* b_k^\dagger \right]. \quad (1.138)$$

For completeness, we state these operators in the interaction picture

$$\begin{aligned} \mathbf{A}_1(\mathbf{t}) &= \frac{2\Omega T}{T^2 + \Omega^2} \sin^2 \left[ 2t\sqrt{T^2 + \Omega^2} \right] \sigma^x + \frac{T}{\sqrt{T^2 + \Omega^2}} \sin \left[ 2t\sqrt{T^2 + \Omega^2} \right] \sigma^y \\ &\quad + \left[ \frac{\Omega^2}{T^2 + \Omega^2} + \frac{T^2}{T^2 + \Omega^2} \cos \left( 2t\sqrt{T^2 + \Omega^2} \right) \right] \sigma^z \\ \mathbf{B}_1(\mathbf{t}) &= \sum_k \left[ h_k b_k e^{-i\omega_k t} + h_k^* b_k^\dagger e^{+i\omega_k t} \right]. \end{aligned} \quad (1.139)$$

In particular, in the so-called pure dephasing limit ( $T = 0$ ), the system coupling operator remains constant in the interaction picture.

**Exact solution: pure-dephasing limit**

The limit when  $T = 0$  can be solved exactly. Then, we can apply the so-called **polaron transformation** (also: Lang-Firsov) to the whole Hamiltonian

$$U = \exp \left\{ -\sigma^z \sum_k \left( \frac{h_k}{\omega_k} b_k - \frac{h_k^*}{\omega_k} b_k^\dagger \right) \right\}. \quad (1.140)$$

We note the following relations

$$\begin{aligned} U \sigma^z U^\dagger &= \sigma^z, \\ U \sigma^\pm U^\dagger &= e^{\pm 2 \sum_k \left( \frac{h_k^*}{\omega_k} b_k^\dagger - \frac{h_k}{\omega_k} b_k \right)} \sigma^\pm, \\ U b_k U^\dagger &= b_k - \frac{h_k^*}{\omega_k} \sigma^z. \end{aligned} \quad (1.141)$$

**Exercise 18** (Polaron transform). *Find a way to derive these relations.*

From this we conclude that in the Schrödinger picture (recall that  $T = 0$ )

$$\begin{aligned} U H U^\dagger &= \Omega \sigma^z + \sigma^z \sum_k \left( h_k b_k + h_k^* b_k^\dagger - 2 \frac{|h_k|^2}{\omega_k} \sigma^z \right) + \sum_k \omega_k \left( b_k^\dagger - \frac{h_k}{\omega_k} \sigma^z \right) \left( b_k - \frac{h_k^*}{\omega_k} \sigma^z \right) \\ &= \Omega \sigma^z - \sum_k \frac{|h_k|^2}{\omega_k} + \sum_k \omega_k b_k^\dagger b_k. \end{aligned} \quad (1.142)$$

This means that in this frame, the evolution of spin and boson are completely decoupled. Consequently, we can e.g. compute the expectation value of  $\sigma^\alpha$  via

$$\begin{aligned} \langle \sigma^\alpha \rangle &= \text{Tr} \left\{ e^{+iHt} \sigma^\alpha e^{-iHt} \rho_0 \right\} = \text{Tr} \left\{ U^\dagger U e^{+iHt} U^\dagger U \sigma^\alpha U^\dagger U e^{-iHt} U^\dagger U \rho_0 \right\} \\ &= \text{Tr} \left\{ U^\dagger e^{+iU H U^\dagger t} U \sigma^\alpha U^\dagger e^{-iU H U^\dagger t} U \rho_0 \right\} \\ &= \text{Tr} \left\{ U^\dagger e^{+i\Omega t \sigma^z} e^{+i \sum_k \omega_k t b_k^\dagger b_k} U \sigma^\alpha U^\dagger e^{-i \sum_k \omega_k t b_k^\dagger b_k} e^{-i\Omega t \sigma^z} U \rho_0 \right\}. \end{aligned} \quad (1.143)$$

For  $\alpha = +$  we further calculate

$$\begin{aligned} \langle \sigma^+ \rangle &= \text{Tr} \left\{ U^\dagger e^{+i \sum_k \omega_k t b_k^\dagger b_k} e^{2 \sum_k \left( \frac{h_k^*}{\omega_k} b_k^\dagger - \frac{h_k}{\omega_k} b_k \right)} e^{-i \sum_k \omega_k t b_k^\dagger b_k} e^{+i\Omega t \sigma^z} \sigma^+ e^{-i\Omega t \sigma^z} U \rho_0 \right\} \\ &= e^{+2i\Omega t} \text{Tr} \left\{ U^\dagger e^{2 \sum_k \left( \frac{h_k^*}{\omega_k} b_k^\dagger e^{+i\omega_k t} - \frac{h_k}{\omega_k} b_k e^{-i\omega_k t} \right)} U U^\dagger \sigma^+ U \rho_0 \right\} \\ &= e^{+2i\Omega t} \text{Tr} \left\{ e^{2 \sum_k \left( \frac{h_k^*}{\omega_k} (b_k^\dagger + \frac{h_k}{\omega_k} \sigma^z) e^{+i\omega_k t} - \frac{h_k}{\omega_k} (b_k + \frac{h_k^*}{\omega_k} \sigma^z) e^{-i\omega_k t} \right)} e^{-2 \sum_k \left( \frac{h_k^*}{\omega_k} b_k^\dagger - \frac{h_k}{\omega_k} b_k \right)} \sigma^+ \rho_0 \right\} \\ &= e^{+2i\Omega t} \text{Tr} \left\{ e^{4i \sum_k \frac{|h_k|^2}{\omega_k^2} \sin(\omega_k t) \sigma^z} \sigma^+ \rho_S^0 \right\} \text{Tr} \left\{ e^{2 \sum_k \left( \frac{h_k^*}{\omega_k} b_k^\dagger e^{+i\omega_k t} - \frac{h_k}{\omega_k} b_k e^{-i\omega_k t} \right)} e^{-2 \sum_k \left( \frac{h_k^*}{\omega_k} b_k^\dagger - \frac{h_k}{\omega_k} b_k \right)} \bar{\rho}_B \right\} \\ &= e^{+2i\Omega t} \text{Tr} \left\{ e^{4i \sum_k \frac{|h_k|^2}{\omega_k^2} \sin(\omega_k t) \sigma^z} \sigma^+ \rho_S^0 \right\} B(t), \end{aligned} \quad (1.144)$$

where we have used initial factorization  $\rho_0 = \rho_S^0 \otimes \bar{\rho}_B$ . Using that  $e^X e^Y = e^{X+Y+[X,Y]/2}$  when  $[X, [X, Y]] = [Y, [X, Y]] = 0$ , we can further evaluate the decoherence factor resulting from the reservoir

$$\begin{aligned}
B(t) &= \text{Tr} \left\{ \exp \left\{ 2 \sum_k \left[ \frac{h_k^* b_k^\dagger}{\omega_k} (e^{+i\omega_k t} - 1) - \frac{h_k b_k}{\omega_k} (e^{-i\omega_k t} - 1) \right] \right\} \bar{\rho}_B \right\} e^{-4i \sum_k \frac{|h_k|^2}{\omega_k^2} \sin(\omega_k t)} \\
&= \text{Tr} \left\{ \exp \left\{ +2 \sum_k \frac{h_k^* b_k^\dagger}{\omega_k} (e^{+i\omega_k t} - 1) \right\} \exp \left\{ -2 \sum_k \frac{h_k b_k}{\omega_k} (e^{-i\omega_k t} - 1) \right\} \bar{\rho}_B \right\} \times \\
&\quad \times e^{-4 \sum_k \frac{|h_k|^2}{\omega_k^2} [1 - \cos(\omega_k t) + i \sin(\omega_k t)]}.
\end{aligned} \tag{1.145}$$

Now, we can use that

$$\begin{aligned}
\text{Tr} \left\{ e^{+\alpha_k b_k^\dagger} e^{-\alpha_k^* b_k} \frac{e^{-\beta \omega_k b_k^\dagger b_k}}{Z_k} \right\} &= \sum_{n,m=0}^{\infty} \frac{(+\alpha_k)^n (-\alpha_k^*)^m}{n!m!} \text{Tr} \left\{ (b_k^\dagger)^n b_k^m \frac{e^{-\beta \omega_k b_k^\dagger b_k}}{Z_k} \right\} \\
&= \sum_{q=0}^{\infty} \sum_{n=0}^q \frac{(-|\alpha_k|^2)^n}{(n!)^2} (1 - e^{-\beta \omega_k}) e^{-\beta \omega_k q} \frac{q!}{(q-n)!} \\
&= e^{-|\alpha_k|^2 n_B(\omega_k)}
\end{aligned} \tag{1.146}$$

with  $|\alpha_k|^2 = 8|h_k|^2/\omega_k^2[1 - \cos(\omega_k t)]$ . This then implies for the decoherence factor

$$B(t) = \exp \left\{ -\frac{2}{\pi} \int_0^\infty \frac{\Gamma(\omega)}{\omega^2} [1 - \cos(\omega t)] [1 + 2n_B(\omega)] d\omega \right\} \exp \left\{ -\frac{2i}{\pi} \int_0^\infty \frac{\Gamma(\omega)}{\omega^2} \sin(\omega t) d\omega \right\}. \tag{1.147}$$

Eventually, it follows that the populations remain unaffected and that in the interaction picture the coherences decay according to [7]

$$\begin{aligned}
\rho_{01}(t) &= \exp \left\{ -8 \sum_k |h_k|^2 \frac{\sin^2(\omega_k t/2)}{\omega_k^2} \coth \left( \frac{\beta \omega_k}{2} \right) \right\} \rho_{01}^0 \\
&= \exp \left\{ -\frac{4}{\pi} \int_0^\infty \Gamma(\omega) \frac{\sin^2(\omega t/2)}{\omega^2} \coth \left( \frac{\beta \omega}{2} \right) d\omega \right\} \rho_{01}^0.
\end{aligned} \tag{1.148}$$

### BMS master equation: general

We first diagonalize the system part of the Hamiltonian to obtain the eigenbasis  $H_S |n\rangle = E_n |n\rangle$ , where

$$E_\pm = \pm \sqrt{\Omega^2 + T^2}, \quad |\pm\rangle = \frac{1}{\sqrt{T^2 + (\Omega \pm \sqrt{\Omega^2 + T^2})^2}} \left[ (\Omega \pm \sqrt{\Omega^2 + T^2}) |0\rangle + T |1\rangle \right], \tag{1.149}$$

where  $|0/1\rangle$  denote the eigenvectors of the  $\sigma^z$  Pauli matrix with  $\sigma^z |i\rangle = (-1)^i |i\rangle$ .

**Exercise 19** (Eigenbasis). *Confirm the validity of Eq. (1.149).*

Second, we calculate the correlation function (in this case, there is just one). Since the bath coupling operator is the same as in Sec. 1.3.3, we can readily deduce

$$\gamma(\omega) = \Gamma(+\omega)\Theta(+\omega)[1 + n_B(+\omega)] + \Gamma(-\omega)\Theta(-\omega)n_B(-\omega) = J(\omega)[1 + n_B(\omega)], \quad (1.150)$$

where  $J(-\omega) = -J(+\omega)$  and  $J(|\omega|) = \Gamma(|\omega|)$ . We compute some relevant dampening coefficients from Def. 6

$$\begin{aligned} \gamma_{-+,-+} &= \Gamma(+2\sqrt{\Omega^2 + T^2})[1 + n_B(+2\sqrt{\Omega^2 + T^2})]|\langle -|\sigma^z|+\rangle|^2, \\ \gamma_{+-,+ -} &= \Gamma(+2\sqrt{\Omega^2 + T^2})n_B(+2\sqrt{\Omega^2 + T^2})|\langle -|\sigma^z|+\rangle|^2, \\ \gamma_{--,++} &= \gamma(0)\langle -|\sigma^z|-\rangle\langle +|\sigma^z|+\rangle = \gamma_{++,--}. \end{aligned} \quad (1.151)$$

We have to say that finite  $\gamma(0) = \lim_{\omega \rightarrow 0} \Gamma(\omega)[1 + n_B(\omega)]$  requires that for small frequencies the spectral coupling density should grow linearly (a so-called ohmic spectral density).

The explicit calculation of the non-vanishing Lamb-shift terms  $\sigma_{--}$  and  $\sigma_{++}$  is possible but more involved. Fortunately, it can be omitted for many applications. Since the system Hamiltonian is non-degenerate, the populations evolve according to

$$\dot{\rho}_{--} = +\gamma_{-+,-+}\rho_{++} - \gamma_{+-,+ -}\rho_{--}, \quad \dot{\rho}_{++} = +\gamma_{+-,+ -}\rho_{--} - \gamma_{-+,-+}\rho_{++}, \quad (1.152)$$

which is independent from the coherences

$$\dot{\rho}_{-+} = -i(E_- - E_+ + \sigma_{--} - \sigma_{++})\rho_{-+} + \left[ \gamma_{--,++} - \frac{\gamma_{-+,-+} + \gamma_{+-,+ -}}{2} \right] \rho_{-+} \equiv \eta\rho_{-+}. \quad (1.153)$$

Altogether, we can write this as a superoperator

$$\mathcal{L} \begin{pmatrix} \rho_{--} \\ \rho_{++} \\ \rho_{-+} \\ \rho_{+-} \end{pmatrix} = \begin{pmatrix} -\gamma_{+-,+ -} & +\gamma_{-+,-+} & 0 & 0 \\ +\gamma_{+-,+ -} & -\gamma_{-+,-+} & 0 & 0 \\ 0 & 0 & \eta & 0 \\ 0 & 0 & 0 & \eta^* \end{pmatrix} \begin{pmatrix} \rho_{--} \\ \rho_{++} \\ \rho_{-+} \\ \rho_{+-} \end{pmatrix}, \quad (1.154)$$

which has the block structure in the system energy eigenbasis. Since the Lamb-shift terms  $\sigma_{ii}$  are purely imaginary, the quantities at hand already allow us to deduce that the coherences will decay since  $\Re\eta \leq 0$ . More precisely, we have  $|\rho_{-+}|^2 = e^{-(2\gamma_{--,++} + \gamma_{-+,-+} + \gamma_{+-,+ -})t} |\rho_{-+}^0|^2$ , which shows that the decoherence rate increases with temperature (finite  $n_B$ ) but can also at zero temperature not be suppressed below a minimum value. A special (exactly solvable) case arises when the system parameter  $T$  vanishes: Then, the interaction commutes with the system Hamiltonian leaving the energy of the system invariant. Consistently, the eigenbasis is in this case that of  $\sigma^z$  and the coefficients  $\gamma_{-+,-+}$  and  $\gamma_{+-,+ -}$  do vanish. In contrast, the coefficient  $\gamma_{--,++} \rightarrow -\gamma(0)$  may remain finite. Such models are called pure dephasing models (since only their coherences decay). However, for finite  $T$  the steady state of the master equation is given by (we assume here  $\mu = 0$ )

$$\frac{\bar{\rho}_{++}}{\bar{\rho}_{--}} = \frac{\gamma_{+-,+ -}}{\gamma_{-+,-+}} = \frac{n_B(+2\sqrt{\Omega^2 + T^2})}{1 + n_B(+2\sqrt{\Omega^2 + T^2})} = e^{-2\beta\sqrt{\Omega^2 + T^2}}, \quad (1.155)$$

i.e., the stationary state is given by the thermalized one.

### Coarse-Graining master equation: pure dephasing

In a completely analogous way, we can set up the coarse-graining master equation. However, we also see that computation of the involved integrals becomes a bit tedious. Therefore, we constrain ourselves here only to the trivial pure-dephasing limit  $T = 0$ . Then, the system coupling operator becomes time-independent  $e^{+iH_S t} \sigma^z e^{-iH_S t} = \sigma^z$ , and with using that  $\sigma^z \sigma^z = \mathbf{1}$ , such that the Lamb-shift vanishes, the coarse-graining master equation in the interaction picture from Def. 10 reads

$$\begin{aligned}
\dot{\rho} &= \frac{1}{\tau} \int_0^\tau dt_1 \int_0^\tau dt_2 C(t_1 - t_2) [\sigma^z \rho \sigma^z - \rho] \\
&= \frac{1}{2\pi\tau} \int_0^\tau dt_1 \int_0^\tau dt_2 \int d\omega \Gamma(\omega) [1 + n_B(\omega)] e^{-i\omega(t_1 - t_2)} [\sigma^z \rho \sigma^z - \rho] \\
&= \frac{1}{2\pi} \int d\omega \Gamma(\omega) [1 + n_B(\omega)] \tau \text{sinc}^2\left(\frac{\omega\tau}{2}\right) [\sigma^z \rho \sigma^z - \rho] \\
&\equiv \Sigma(\tau) [\sigma^z \rho \sigma^z - \rho],
\end{aligned} \tag{1.156}$$

where we have used that

$$\int_0^\tau dt_1 \int_0^\tau dt_2 e^{-i\omega(t_1 - t_2)} = 4 \frac{\sin^2(\omega\tau/2)}{\omega^2} = \tau^2 \text{sinc}^2\left(\frac{\omega\tau}{2}\right) \tag{1.157}$$

with the band-filter function  $\text{sinc}(x) = \sin(x)/x$ . We note that this dynamics can be solved exactly, and that coarse-graining readily provides the exact solution. In the limit of infinite coarse-graining times  $\tau \rightarrow \infty$ , this would yield

$$\dot{\rho} = \gamma(0) [\sigma^z \rho \sigma^z - \rho], \tag{1.158}$$

where we have used that  $\gamma(0) = \lim_{\omega \rightarrow 0} \Gamma(\omega) [1 + n_B(\omega)]$ . Generally, the evolution equation  $\dot{\rho} = \Sigma(\tau) [\sigma^z \rho \sigma^z - \rho]$  leads to dual equation for the expectation values

$$\frac{d}{dt} \langle \sigma^\pm \rangle = -2\Sigma(\tau) \langle \sigma^\pm \rangle, \quad \langle \sigma^\pm \rangle_t = e^{-2\Sigma(\tau)t} \langle \sigma^\pm \rangle_0. \tag{1.159}$$

Therefore, for a time-dependent dynamical coarse-graining time  $\Sigma(\tau) = \Sigma(t)$  we obtain a time-dependent coherence decay rate exponent, which can also be written as

$$\rho_{01}(t) = e^{-2\Sigma(t)t} \rho_{01}^0. \tag{1.160}$$

With

$$\begin{aligned}
2\Sigma(t)t &= \frac{1}{\pi} \int d\omega J(\omega) [1 + n_B(\omega)] \frac{4 \sin^2(\omega t/2)}{\omega^2} \\
&= \frac{4}{\pi} \int_0^\infty d\omega \Gamma(\omega) [1 + 2n_B(\omega)] \frac{4 \sin^2(\omega t/2)}{\omega^2} \\
&= \frac{4}{\pi} \int_0^\infty d\omega \Gamma(\omega) \coth\left(\frac{\beta\omega}{2}\right) \frac{\sin^2(\omega t/2)}{\omega^2}.
\end{aligned} \tag{1.161}$$

This is precisely the same as the decay predicted in Eq. (1.148)

### 1.3.7 Fermions

With fermionic tunneling terms, the tensor product decomposition between system and reservoir operators is not obvious, as exemplified by a typical coupling between system ( $d$ ) and reservoir ( $c_k$ )

$$H_I = \sum_k t_k d^\dagger c_k + \sum_k t_k^* c_k^\dagger d = d^\dagger \sum_k t_k c_k - d \sum_k t_k^* c_k^\dagger. \quad (1.162)$$

This is manifest in the fact that system and bath operators do not commute but anticommute. One can however also represent fermions in a tensor-product form, which is achieved by the **Jordan-Wigner-transform**.

**Def. 11** (Jordan-Wigner transform). *For fermions distributed on  $N$  sites, the decomposition*

$$c_i = \underbrace{\sigma^z \otimes \dots \otimes \sigma^z}_{i-1} \otimes \sigma^- \otimes \underbrace{\mathbf{1} \otimes \dots \otimes \mathbf{1}}_{N-i} \quad (1.163)$$

obeys the fermionic anti-commutation relations

$$\{c_i, c_j\} = \mathbf{0} = \{c_i^\dagger, c_j^\dagger\}, \quad \{c_i, c_j^\dagger\} = \delta_{ij} \mathbf{1}. \quad (1.164)$$

We may use this Jordan-Wigner transform to represent the fermionic tunneling Hamiltonians in a tensor product form. Of  $N$  sites in total, we identify the first  $N_S$  sites with fermions on the system and the remaining  $N - N_S$  sites with fermions in the reservoir, e.g. for one system fermion ( $N_S = 1$ ) and  $N - 1$  reservoir fermions labeled by  $1 \leq k \leq N - 1$

$$\begin{aligned} d &= \sigma^- \otimes \underbrace{\mathbf{1} \otimes \dots \otimes \mathbf{1}}_{N-1}, \\ c_k &= \sigma^z \otimes \underbrace{\sigma^z \otimes \dots \otimes \sigma^z}_{(k-1)\times} \otimes \sigma^- \otimes \underbrace{\mathbf{1} \otimes \dots \otimes \mathbf{1}}_{N-1-k}. \end{aligned} \quad (1.165)$$

This immediately leads to a tensor product decomposition of the tunneling Hamiltonian

$$H_I = \sigma^+ \sigma^z \otimes \sum_k t_k \tilde{c}_k - \sigma^- \sigma^z \otimes \sum_k t_k^* \tilde{c}_k^\dagger, \quad (1.166)$$

where we have defined

$$\tilde{c}_k = \underbrace{\sigma^z \otimes \dots \otimes \sigma^z}_{(k-1)\times} \otimes \sigma^- \otimes \mathbf{1} \otimes \dots \otimes \mathbf{1}. \quad (1.167)$$

We can use

$$\sigma^- \sigma^z = \sigma^- \equiv \tilde{d}, \quad -\sigma^+ \sigma^z = +\sigma^+ \equiv \tilde{d}^\dagger \quad (1.168)$$

to write the tunnel Hamiltonian as

$$H_I = -\tilde{d}^\dagger \otimes \sum_k t_k \tilde{c}_k - \tilde{d} \otimes \sum_k t_k^* \tilde{c}_k^\dagger, \quad (1.169)$$

where the new operators obviously also obey fermionic anticommutation relations in their respective Hilbert space, but do now commute with each other. In particular, in grand-canonical reservoir states one only has expressions of the form

$$c_k^\dagger c_k = \mathbf{1} \otimes \tilde{c}_k^\dagger \tilde{c}_k, \quad (1.170)$$

and likewise for the Hamiltonian, such that the previously introduced theory applies. A similar reasoning applies for more general systems.

### 1.3.8 Example: Single resonant level

We consider a single quantum dot coupled to a reservoir, where

$$H = \epsilon d^\dagger d + d^\dagger \sum_k t_k c_k - d \sum_k t_k^* c_k^\dagger + \sum_k \epsilon_k c_k^\dagger c_k. \quad (1.171)$$

Insertion of the previously mentioned Jordan-Wigner transform allows to write the Hamiltonian alternatively as

$$H = \epsilon \tilde{d}^\dagger \tilde{d} - \tilde{d}^\dagger \otimes \sum_k t_k \tilde{c}_k - \tilde{d} \otimes \sum_k t_k^* \tilde{c}_k^\dagger + \sum_k \epsilon_k \tilde{c}_k^\dagger \tilde{c}_k. \quad (1.172)$$

In this representation, the operators with a tilde act only on the reduced Hilbert space of system and reservoir, respectively.

#### Exact solution

One way for the exact solution proceeds along the Heisenberg equations of motion based on (1.171) for the individual fermionic operators (bold symbols denote the Heisenberg picture in this section)

$$\begin{aligned} \dot{\mathbf{d}} &= -i\epsilon \mathbf{d}(t) - i \sum_k t_k \mathbf{c}_k(t), \\ \dot{\mathbf{c}}_k &= -i\epsilon_k \mathbf{c}_k(t) - i t_k^* \mathbf{d}(t). \end{aligned} \quad (1.173)$$

Laplace-transforming via  $D(s) = \int_0^\infty \mathbf{d}(t) e^{-st} dt$  and  $C_k(s) = \int_0^\infty \mathbf{c}_k(t) e^{-st} dt$  yields algebraic equations

$$\begin{aligned} sD(s) - d &= -i\epsilon D(s) - i \sum_k t_k C_k(s), \\ sC_k(s) - c_k &= -i\epsilon_k C_k(s) - i t_k^* D(s). \end{aligned} \quad (1.174)$$

Here, we can eliminate

$$C_k(s) = \frac{c_k - i t_k^* D(s)}{s + i\epsilon_k} \quad (1.175)$$

and insert this in the first equation

$$\left[ s + i\epsilon + \sum_k |t_k|^2 \frac{1}{s + i\epsilon_k} \right] D(s) = d - i \sum_k t_k \frac{1}{s + i\epsilon_k} c_k. \quad (1.176)$$

We can directly solve this

$$D(s) = \frac{d - i \sum_k t_k \frac{1}{s+i\epsilon_k} c_k}{s + i\epsilon + \sum_k |t_k|^2 \frac{1}{s+i\epsilon_k}}. \quad (1.177)$$

Assuming a continuum of reservoir modes, we can introduce the spectral coupling density

$$\sum_k |t_k|^2 \frac{1}{s \pm i\epsilon_k} = \frac{1}{2\pi} \int \frac{\Gamma(\omega)}{s \pm i\omega} d\omega \quad : \quad \Gamma(\omega) = 2\pi \sum_k |t_k|^2 \delta(\omega - \epsilon_k). \quad (1.178)$$

In the limit where  $\Gamma(\omega)$  is constant (wideband limit), this becomes simple, as can be seen by considering the wideband limit of a Lorentzian spectral density  $\Gamma(\omega) = \Gamma \frac{\delta^2}{\omega^2 + \delta^2}$

$$\lim_{\delta \rightarrow \infty} \int \frac{\Gamma \delta^2}{\omega^2 + \delta^2} \frac{1}{s \pm i\omega} d\omega = \lim_{\delta \rightarrow \infty} \frac{\pi \Gamma \delta}{\delta + s} = \pi \Gamma, \quad (1.179)$$

which leads to the solution

$$D(s) = \frac{d - i \sum_k t_k \frac{1}{s+i\epsilon_k} c_k}{s + i\epsilon + \Gamma/2}, \quad (1.180)$$

and similar for the Laplace transform of the creation operator

$$\bar{D}(s) = \int_0^\infty \mathbf{d}^\dagger(\mathbf{t}) e^{-st} dt = \frac{d^\dagger + i \sum_k t_k^* \frac{1}{s-i\epsilon_k} c_k^\dagger}{s - i\epsilon + \Gamma/2}. \quad (1.181)$$

To compute the occupation of the dot we have to evaluate

$$\begin{aligned} n_d(t) &= \text{Tr} \{ \mathbf{d}^\dagger(\mathbf{t}) \mathbf{d}(\mathbf{t}) \rho_0 \} = \left( \frac{1}{2\pi i} \right)^2 \int_{\gamma_1 - i\infty}^{\gamma_1 + i\infty} ds_1 \int_{\gamma_2 - i\infty}^{\gamma_2 + i\infty} ds_2 \text{Tr} \{ \bar{D}(s_1) D(s_2) \rho_0 \} e^{+(s_1 + s_2)t} \\ &= n_0 e^{-\Gamma t} + \sum_k |t_k|^2 [1 + e^{-\Gamma t} - 2 \cos[(\epsilon_k - \epsilon)t] e^{-\Gamma t/2}] \frac{4f(\epsilon_k)}{\Gamma^2 + 4(\epsilon_k - \epsilon)^2} \\ &= n_0 e^{-\Gamma t} + \frac{1}{2\pi} \int d\omega [1 + e^{-\Gamma t} - 2 \cos[(\omega - \epsilon)t] e^{-\Gamma t/2}] \frac{4\Gamma}{\Gamma^2 + 4(\omega - \epsilon)^2} f(\omega) \end{aligned} \quad (1.182)$$

Here, we have used that  $\text{Tr} \{ d^\dagger d \rho_0 \} = n_0$  and  $\text{Tr} \{ c_k^\dagger c_k \bar{\rho}_B \} = f(\epsilon_k) = [e^{\beta(\epsilon_k - \mu)} + 1]^{-1}$  yields the Fermi function of the reservoir. This solution also obviously respects the initial condition  $n_d(0) = n_0$ . We see that the initial dot occupation relaxes with damped oscillations towards a stationary value

$$\bar{n}_d = \frac{1}{2\pi} \int d\omega \frac{4\Gamma f(\omega)}{\Gamma^2 + 4(\omega - \epsilon)^2}. \quad (1.183)$$

Furthermore, in the weak-coupling limit, we can use

$$\begin{aligned} \lim_{\Gamma \rightarrow 0} \frac{4\Gamma}{\Gamma^2 + 4(\omega - \epsilon)^2} &= 2\pi \delta(\omega - \epsilon), \\ \lim_{\Gamma \rightarrow 0} \frac{4\Gamma}{\Gamma^2 + 4(\omega - \epsilon)^2} \cos((\omega - \epsilon)t) &= 2\pi e^{-\Gamma t/2} \delta(\omega - \epsilon), \end{aligned} \quad (1.184)$$

to obtain a simplified exact solution in the weak-coupling limit

$$n_d(t) \approx e^{-\Gamma t} n_0 + (1 - e^{-\Gamma t}) f(\epsilon). \quad (1.185)$$

We will see later that this does exactly correspond to the master equation solution. Thermodynamically, it just means that the dot equilibrates with the reservoir.

### Coarse-graining dissipator

To derive the corresponding master equation, we take (1.172) as the starting point and evaluate the dissipator in Def. 10. Identifying the non-hermitian coupling operators as

$$\begin{aligned} A_1 &= \tilde{d}^\dagger, & B_1 &= -\sum_k t_k \tilde{c}_k, \\ A_2 &= \tilde{d}, & B_2 &= -\sum_k t_k^* \tilde{c}_k^\dagger, \end{aligned} \quad (1.186)$$

and putting the reservoir in an initial grand-canonical equilibrium state  $\bar{\rho}_B = e^{-\beta(H_B - \mu N_B)} / Z_B$ , we first compute the two reservoir correlation functions

$$\begin{aligned} C_{12}(\tau) &= \sum_k |t_k|^2 e^{-i\epsilon_k \tau} [1 - f(\epsilon_k)] = \frac{1}{2\pi} \int \Gamma(\omega) [1 - f(\omega)] e^{-i\omega \tau} d\omega, \\ C_{21}(\tau) &= \sum_k |t_k|^2 e^{+i\epsilon_k \tau} f(\epsilon_k) = \frac{1}{2\pi} \int \Gamma(\omega) f(\omega) e^{+i\omega \tau} d\omega. \end{aligned} \quad (1.187)$$

We can read off the FTs of the reservoir correlation function

$$\gamma_{12}(\omega) = \Gamma(\omega) [1 - f(\omega)], \quad \gamma_{21}(\omega) = \Gamma(-\omega) f(-\omega), \quad (1.188)$$

which obey the KMS relation for  $\mu = 0$  and from which one can derive the  $\sigma_{12}(\omega)$  and  $\sigma_{21}(\omega)$ . The system coupling operator becomes

$$\begin{aligned} A_1^{+\omega, \tau} &= \int_0^\tau \mathbf{A}_1(\mathbf{t}) e^{-i\omega t} dt = d^\dagger \int_0^\tau e^{i(\epsilon - \omega)t} dt = \tau e^{i(\epsilon - \omega)\tau/2} \text{sinc} \left[ (\epsilon - \omega) \frac{\tau}{2} \right] d^\dagger, \\ A_2^{+\omega, \tau} &= \int_0^\tau \mathbf{A}_2(\mathbf{t}) e^{-i\omega t} dt = d \int_0^\tau e^{i(-\epsilon - \omega)t} dt = \tau e^{i(-\epsilon - \omega)\tau/2} \text{sinc} \left[ (\epsilon + \omega) \frac{\tau}{2} \right] d, \end{aligned} \quad (1.189)$$

and the coarse-graining master equation (1.128) becomes

$$\begin{aligned} \dot{\rho}_S &= -i \left[ \frac{1}{4\pi i} \int d\omega \sigma_{12}(\omega) \tau \text{sinc}^2[(\epsilon - \omega)\tau/2] d^\dagger d + \frac{1}{4\pi i} \int d\omega \sigma_{21}(\omega) \tau \text{sinc}^2[(\epsilon + \omega)\tau/2] d d^\dagger, \rho_S \right] \\ &+ \frac{1}{2\pi} \int d\omega \gamma_{12}(\omega) \tau \text{sinc}^2[(\epsilon - \omega)\tau/2] \left[ d \rho_S d^\dagger - \frac{1}{2} \{d^\dagger d, \rho_S\} \right] \\ &+ \frac{1}{2\pi} \int d\omega \gamma_{21}(\omega) \tau \text{sinc}^2[(\epsilon + \omega)\tau/2] \left[ d^\dagger \rho_S d - \frac{1}{2} \{d d^\dagger, \rho_S\} \right]. \end{aligned} \quad (1.190)$$

For the populations in the system energy eigenbasis (the model does not support coherences), this generates a rate equation

$$\begin{aligned} \dot{\rho}_{00} &= \gamma_{1 \rightarrow 0}(\tau) \rho_{11} - \gamma_{0 \rightarrow 1}(\tau) \rho_{00}, & \dot{\rho}_{11} &= \gamma_{0 \rightarrow 1}(\tau) \rho_{00} - \gamma_{1 \rightarrow 0}(\tau) \rho_{11}, \\ \gamma_{0 \rightarrow 1}(\tau) &= \frac{\tau}{2\pi} \int d\omega \Gamma(\omega) f(\omega) \text{sinc}^2[(\epsilon - \omega)\tau/2], \\ \gamma_{1 \rightarrow 0}(\tau) &= \frac{\tau}{2\pi} \int d\omega \Gamma(\omega) [1 - f(\omega)] \text{sinc}^2[(\epsilon - \omega)\tau/2]. \end{aligned} \quad (1.191)$$

In the wideband limit  $\Gamma(\omega) \rightarrow \Gamma$ , we have  $\gamma_{1 \rightarrow 0}(\tau) + \gamma_{0 \rightarrow 1}(\tau) = \Gamma$ , such that the time-dependent occupation becomes

$$n_d(t) = e^{-\Gamma t} n_0 + \frac{\tau}{2\pi} \int d\omega f(\omega) \text{sinc}^2[(\epsilon - \omega)\tau/2] [1 - e^{-\Gamma t}]. \quad (1.192)$$

When  $\tau = t$ , the time-dependent solution is approximated best. When  $\tau \rightarrow \infty$ , this reduces to

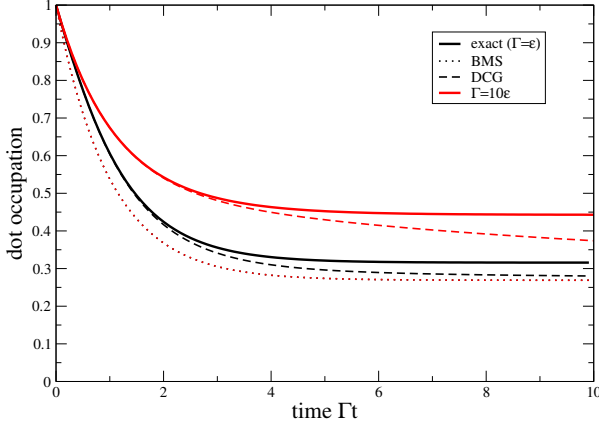


Figure 1.3: Plot of the dot occupation versus time. The BMS solutions (dotted) correspond to the weak-coupling solution (1.185) and are only a function of  $\Gamma t$  such that they lie on top of each other. As the coupling strength is increased, the difference between BMS (dotted) and exact (solid) solutions – compare Eq. (1.182) – increases also at steady state. Dashed curves denote the dynamical coarse-graining solution – Eq. (1.192) – with  $\tau = t$  – which is always good at small times. Other parameters:  $\beta\mu = 0$ ,  $\beta\epsilon = 1$ .

### BMS limit

The BMS limit is obtained for  $\tau \rightarrow \infty$ , which implies with

$$\lim_{\tau \rightarrow \infty} \tau \text{sinc}^2[(\epsilon - \omega)\tau/2] = 2\pi\delta(\epsilon - \omega) \quad (1.193)$$

that the rate equation becomes

$$\dot{\rho}_{00} = \Gamma(\epsilon)[1 - f(\epsilon)]\rho_{11} - \Gamma(\epsilon)f(\epsilon)\rho_{00}, \quad \dot{\rho}_{11} = \Gamma(\epsilon)f(\epsilon)\rho_{00} - \Gamma(\epsilon)[1 - f(\epsilon)]\rho_{11}, \quad (1.194)$$

and the steady state of this is just given by  $\bar{\rho}_{11} = 1 - \bar{\rho}_{00} = f(\epsilon)$ .

The results are summarized in Fig. 1.3.

## 1.4 Superoperator Notation

As a Lindblad master equation is linear in the density matrix  $\rho$ , we can arrange the matrix elements of  $\rho$  in a vector (in arbitrary order) and represent the action of the master equation by a **Liouvillian superoperator**

$$\dot{\rho} = \mathcal{L}\rho. \quad (1.195)$$

If  $\rho$  is an  $N \times N$  matrix, it becomes an  $N^2$ -dimensional vector, and consequently  $\mathcal{L}$  is an  $N^2 \times N^2$  matrix.

### 1.4.1 Energy eigenbasis representation

Mostly however we can further simplify this equation, as for example for a non-degenerate system Hamiltonian, the BMS Liouvillian from Def. 6 has block structure in the populations and coherences of the system's energy eigenbasis

$$\frac{d}{dt} \begin{pmatrix} \rho_{\text{pop}} \\ \rho_{\text{coh}} \end{pmatrix} = \begin{pmatrix} \mathcal{L}_{\text{pop}} & \mathbf{0} \\ \mathbf{0} & \mathcal{L}_{\text{coh}} \end{pmatrix} \begin{pmatrix} \rho_{\text{pop}} \\ \rho_{\text{coh}} \end{pmatrix}. \quad (1.196)$$

When the coherences decay in the long-term limit, or can never be formed due to some superselection rule, it suffices to consider the populations separately  $\dot{\rho}_{\text{pop}} = \mathcal{L}_{\text{pop}}\rho_{\text{pop}}$ , which form a much simpler rate equation. We have tacitly done this in the previous section when discussing the single resonant level.

### 1.4.2 General vectorization

Such a simple block structure does not hold when the secular approximation is not applied or e.g. when the master equation is obtained via coarse-graining with a fixed coarse-graining time. Still, a superoperator representation of master equations can be very helpful, since the treatment of first order differential equations of the form  $\dot{\rho} = \mathcal{L}\rho$  is standard. We can always introduce an extended space by generating the tensor product of the Hilbert space with itself. Then, a matrix can in an arbitrary basis be vectorized by the mapping

$$\rho = \sum_{ij} \rho_{ij} |i\rangle \langle j| \quad \Leftrightarrow \quad \text{vec}(\rho) = \sum_{ij} \rho_{ij} |i\rangle \otimes |j\rangle, \quad (1.197)$$

which evidently preserves all the information. To actually compute such a representation, it is helpful to represent the tensor product by matrices, which is known as **Kronecker product**[13]. For an  $N_A \times M_A$  matrix  $A$  and  $N_B \times M_B$  matrix  $B$ , the Kronecker product yields a matrix representation of the tensor product for a special ordering of the basis

$$A \otimes B = \begin{pmatrix} A_{1,1}B & \dots & A_{1,N_A}B \\ \vdots & & \vdots \\ A_{M_A,1}B & \dots & A_{M_A,N_A}B \end{pmatrix}, \quad (1.198)$$

where  $A_{ij}$  denotes the matrix elements of  $A$ . Therby,  $A \otimes B$  is represented by an  $N_A N_B \times M_A M_B$  matrix. Practically, this just means to write the rows of the matrix  $\rho$  row-by-row into a vector, e.g.

$$\rho = \begin{pmatrix} \rho_{00} & \rho_{01} \\ \rho_{10} & \rho_{11} \end{pmatrix} \quad \Leftrightarrow \quad \text{vec}(\rho) = \begin{pmatrix} \rho_{00} \\ \rho_{01} \\ \rho_{10} \\ \rho_{11} \end{pmatrix}. \quad (1.199)$$

Then, the vectorization of  $A\rho B$  can also be expressed with the tensor product

$$\text{vec}(A\rho B) = A \otimes B^T \text{vec}(\rho), \quad (1.200)$$

where  $B^T$  denotes the transpose of  $B$  (which is in general not the hermitian conjugate). We evidently get

$$\text{vec}(A\rho) = \sum_{ijk} A_{ik} \rho_{kj} |i\rangle \otimes |j\rangle. \quad (1.201)$$

Likewise, we have

$$A \otimes \mathbf{1} \text{vec}(\rho) = \sum_{ij} \rho_{ij} \left( \sum_{kl} A_{kl} |k\rangle \langle l| \right) \otimes |j\rangle = \sum_{ijk} \rho_{ij} A_{ki} |k\rangle \otimes |j\rangle = \sum_{ijk} \rho_{kj} A_{ik} |i\rangle \otimes |j\rangle, \quad (1.202)$$

which shows the equivalence. However, when multiplying from the right we get

$$\text{vec}(\rho B) = \sum_{ijk} \rho_{ik} B_{kj} |i\rangle \otimes |j\rangle. \quad (1.203)$$

Now, we see that

$$\mathbf{1} \otimes B^T \text{vec}(\rho) = \sum_{ij} \rho_{ij} |i\rangle \otimes \left( \sum_{kl} B_{lk} |k\rangle \langle l|j\rangle \right) = \sum_{ijk} \rho_{ij} B_{jk} |i\rangle \otimes |k\rangle = \sum_{ijk} \rho_{ik} B_{kj} |i\rangle \otimes |j\rangle . \quad (1.204)$$

Since we can understand this as successive operations, we get

$$\text{vec}(A\rho B) = (A \otimes \mathbf{1})(\mathbf{1} \otimes B^T)\text{vec}(\rho) = A \otimes B^T \text{vec}(\rho) . \quad (1.205)$$

Accordingly, the vectorized representation of a Lindblad form can be readily written down. Since  $A$  and  $B$  can also be the identity operations, this enables to write a generic Lindblad form by tensor products in an extended space.

Notationally, we will not distinguish between  $\rho$  and  $\text{vec}(\rho)$ . Whether  $\rho$  is interpreted as a matrix or a vector, follows from the action of the operator or superoperator applied to it. Finally, we also note that the trace maps under the vectorization operation to a multiplication with a row vector

$$\text{Tr} \{\rho\} = \text{vec}(\mathbf{1})^T \text{vec}(\rho) , \quad (1.206)$$

where  $\text{vec}(\mathbf{1})^T$  is a row vector with ones only at places of the populations and zeroes elsewhere. For the above example, we would have  $\text{vec}(\mathbf{1})^T = (1, 0, 0, 1)$ .



# Chapter 2

## Stationary Quantum transport

The most obvious way to achieve non-equilibrium quantum dynamics even at steady state is to use a reservoir that is itself in a non-equilibrium state, i.e., a state that cannot simply be characterized by just one temperature and one chemical potential. Since the derivation of the master equation only requires  $[\bar{\rho}_B, H_B] = 0$ , this would still allow for many nontrivial models,  $\langle n | \bar{\rho}_B | n \rangle$  could e.g. follow multi-modal distributions. Such a non-equilibrium situation may be established when a system is coupled to many different baths  $\nu$

$$H_B = \sum_{\nu=1}^K H_B^\nu \quad (2.1)$$

with commuting individual parts  $[H_B^\ell, H_B^k] = 0$ . The reservoirs are kept in local equilibrium states

$$\bar{\rho}_B = \bigotimes_{\nu=1}^K \bar{\rho}_B^\nu \quad : \quad \bar{\rho}_B^\nu = \frac{e^{-\beta_\nu(H_B^\nu - \mu_\nu N_B^\nu)}}{Z_B^\nu}, \quad (2.2)$$

characterized by inverse temperature  $\beta_\nu$  and chemical potential  $\mu_\nu$  and with  $N_B^\nu$  denoting the particle number operator of reservoir  $\nu$ , respectively. The **partition function**  $Z_B^\nu = \text{Tr} \{ e^{-\beta_\nu(H_B^\nu - \mu_\nu N_B^\nu)} \}$  normalizes each reservoir density matrix.

Here, we will consider the case of such multiple reservoirs at different thermal equilibria that are only indirectly coupled via the system: Without the system, they would be completely independent and thus remain at their local equilibrium state. When coupled via the system, the reservoirs will exchange energy and thereby also their state will change in reality, as a battery is discharged in time. Within a master equation treatment, the change of the reservoirs however is not captured, which implies that there is already some assumption of the size difference between the system and the reservoirs. On the other hand, stationary heat and matter currents can be experimentally maintained over very large time scales, such that the assumption of a stationary reservoir can be very well justified in many setups.

Since these are chosen at different equilibria, they drag the system towards different thermal states, and the resulting stationary state is in general a non-thermal one. Since the different compartments interact only indirectly via the system, we have the case of a multi-terminal system, where one can most easily derive the corresponding master equation, since for weak couplings, each contact may be treated separately, as we shall see later.

To each of the reservoirs, the system is coupled via different coupling operators

$$H_I = \sum_{\alpha} A_{\alpha} \otimes B_{\alpha} = \sum_{\alpha} A_{\alpha} \otimes \sum_{\nu=1}^K B_{\alpha}^{\nu}. \quad (2.3)$$

Here, the index  $\nu$  labels the sub-reservoir  $\nu$  and  $B_{\alpha}^{\nu}$  acts non-trivially only on the Hilbert space of this sub-reservoir. Different coupling strengths are encoded in the  $B_{\alpha}^{\nu}$ : If for example one reservoir does not couple to the system operator  $A_{\alpha}$ , we simply have  $B_{\alpha}^{\nu} = 0$ . Since we assume the setting that the first order bath correlation functions vanish  $\langle B_{\alpha}^{\nu} \bar{\rho}_B \rangle = 0$ , the second-order bath correlation functions may be computed additively. In particular, we get from the tensor structure of the reservoir density matrix

$$\text{Tr} \{ \mathbf{B}_{\alpha}^{\nu}(\tau) B_{\beta}^{\mu} \bar{\rho}_B \} = \delta_{\mu\nu} \text{Tr} \{ \mathbf{B}_{\alpha}^{\nu}(\tau) B_{\beta}^{\nu} \bar{\rho}_B \}. \quad (2.4)$$

In other words, there is no correlation function between different reservoirs, and all relevant correlation functions can be computed by just considering the reservoirs separately. One should note that this is a weak-coupling statement: Going to higher than second order in the system-reservoir interaction strength will surely induce correlations between the reservoirs. We can thus write

$$C_{\alpha\beta}(\tau) = \sum_{\nu=1}^K \text{Tr} \{ \mathbf{B}_{\alpha}^{\nu}(\tau) B_{\beta}^{\nu} \bar{\rho}_B \} \equiv \sum_{\nu=1}^K C_{\alpha\beta}^{(\nu)}(\tau). \quad (2.5)$$

This additive decomposition obviously transfers to their Fourier transforms and thus, also to the final Liouvillian (to second order in the coupling)

$$\mathcal{L} = \mathcal{L}^{(0)} + \sum_{\nu=1}^K \mathcal{L}^{(\nu)}. \quad (2.6)$$

Here,  $\mathcal{L}^{(0)}\rho \hat{=} -i[H_S, \rho]$  describes the action of the system Hamiltonian on the system density matrix  $\rho$  and  $\mathcal{L}^{(\nu)}$  denotes the Liouvillian resulting only from the  $\nu$ -th reservoir. The resulting stationary state is in general a non-equilibrium one. Furthermore, the system will in general support a stationary heat current between the two reservoirs.

## 2.1 Example: Single-Electron-Transistor

The simplest example of two-terminal transport is a single quantum dot that is tunnel-coupled to two leads. For a single lead, we have already derived the Liouvillian for a single resonant level coupled to a single junction (we only consider populations  $\rho_{00}$  and  $\rho_{11}$  corresponding to an empty or filled dot) in Eq. (1.194). Writing this in matrix form  $\dot{\rho} = \mathcal{L}\rho$ , one has

$$\mathcal{L} = \begin{pmatrix} -\Gamma f & +\Gamma(1-f) \\ +\Gamma f & -\Gamma(1-f) \end{pmatrix}, \quad (2.7)$$

where the Fermi function  $f = [e^{\beta(\epsilon-\mu)} + 1]^{-1}$  of the contact is evaluated at the dot level  $\epsilon$ , and likewise the tunnel rate is the spectral density evaluated at the dot level  $\Gamma = \Gamma(\epsilon)$ . By additively upgrading it to two (left and right) reservoirs we obtain the Liouvillian for a single-electron transistor (SET) coupled to two (left and right) junctions

$$\mathcal{L} = \begin{pmatrix} -\Gamma_L f_L - \Gamma_R f_R & +\Gamma_L(1-f_L) + \Gamma_R(1-f_R) \\ +\Gamma_L f_L + \Gamma_R f_R & -\Gamma_L(1-f_L) - \Gamma_R(1-f_R) \end{pmatrix}. \quad (2.8)$$

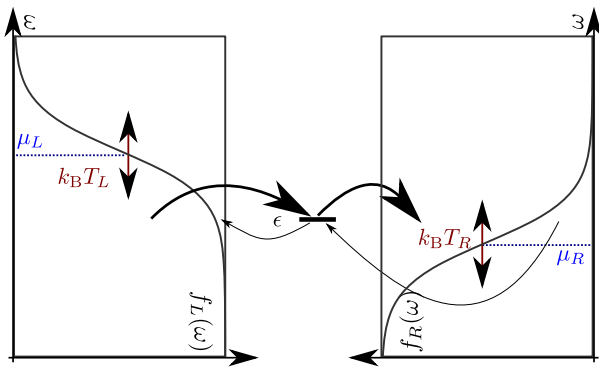


Figure 2.1: Sketch of a single resonant level (QD at energy level  $\epsilon$ ) coupled to two junctions with different Fermi distributions (e.g. with different chemical potentials or different temperatures). If the dot level  $\epsilon$  is changed with a third gate, the device functions as a transistor, since the current through the system is exponentially suppressed when the the dot level  $\epsilon$  is not within the transport window.

Here, the coupling strengths  $\Gamma_\nu = \Gamma_\nu(\epsilon)$  depend on the spectral densities of the reservoirs, and the respective Fermi functions  $f_\nu = [e^{\beta_\nu(\epsilon - \mu_\nu)} + 1]^{-1}$  encode the thermal properties.

One can see that in order to support a current, the dot must be loaded preferentially from one reservoir and be unloaded by the other. This implies that at least at low temperatures, the dot level  $\epsilon$  must be within the **transport window**  $\epsilon \in [\min(\mu_L, \mu_R), \max(\mu_L, \mu_R)]$ , see Fig. 2.1 for an illustration with  $\mu_L > \mu_R$ . If  $\epsilon \gg \mu_L, \mu_R$ , both Fermi functions will vanish  $f_L, f_R \rightarrow 0$ , such that the dot can only be depleted to either reservoir. Once it is empty, it will hardly be refilled, thus inhibiting transport. In contrast, when  $\epsilon \ll \mu_L, \mu_R$ , both Fermi functions will be maximal  $f_L, f_R \rightarrow 1$ , such that the dot can only be filled from either reservoir. Once it is filled, it will remain so, thus also inhibiting transport. The only case where transport becomes relevant is (at small temperatures) when the dot level is inside the transport window, which can be illustrated with the extreme case of infinite bias  $\mu_L \rightarrow +\infty$  and  $\mu_R \rightarrow -\infty$  such that  $f_L \rightarrow 1$  and  $f_R \rightarrow 0$ . Then, the dot can only be loaded from the left and unload to the right, generating a transport scenario. This behaviour also explains the name single-electron transistor, since the dot level  $\epsilon$  may be tuned by a third gate, which thereby controls the current.

We notice that the steady state of the SET could also have been generated by a single reservoir at an average thermal state. This special property holds for some non-equilibrium setups and allows to determine the non-equilibrium steady state analytically. It happens when the coupling structure of all Liouvillians is identical for different reservoirs, such that we may write

$$\mathcal{L}^{(\nu)} = \Gamma^{(\nu)} [\mathcal{L}_A + n^{(\nu)} \mathcal{L}_B] \quad : \quad \forall \nu, \quad (2.9)$$

i.e., the different reservoirs trigger exactly the same transitions within the system, as we saw for the SET. Here,  $n^{(\nu)}$  is a parameter encoding the thermal properties of the respective bath  $\nu$  (e.g. a Fermi-Dirac or a Bose-Einstein distribution evaluated at one of the systems transition frequencies), and  $\mathcal{L}_{A/B}$  simply label parts of the Liouvillian that are proportional to thermal characteristics (B) or not (A). Finally,  $\Gamma^{(\nu)}$  represent coupling constants to the different reservoirs. For coupling to a single reservoir, the stationary state is then defined via the equation

$$\mathcal{L}^{(\nu)} \bar{\rho}^{(\nu)} = \Gamma^{(\nu)} [\mathcal{L}_A + n^{(\nu)} \mathcal{L}_B] \bar{\rho}^{(\nu)} = 0 \quad (2.10)$$

and thus it depends on the thermal parameter  $\bar{\rho}^{(\nu)} = \bar{\rho}(n^{(\nu)})$ . Obviously, the steady state for a single reservoir will be independent of the coupling strength  $\Gamma^{(\ell)}$ , which only affects the speed of relaxation. For the total Liouvillian, it follows that the dependence of the full stationary state on

all thermal parameters simply given by the same dependence on an average thermal parameter

$$\begin{aligned}\mathcal{L}\bar{\rho} &= \sum_{\nu} \mathcal{L}^{(\nu)}\bar{\rho} = \sum_{\nu} \Gamma^{(\nu)} [\mathcal{L}_A + n^{(\nu)}\mathcal{L}_B] \bar{\rho} = \left[ \sum_{\nu} \Gamma^{(\nu)} \right] \left[ \mathcal{L}_A + \frac{\sum_{\nu} \Gamma^{(\nu)} n^{(\nu)}}{\sum_{\nu'} \Gamma^{(\nu')}} \mathcal{L}_B \right] \bar{\rho}, \\ &= \left[ \sum_{\nu} \Gamma^{(\nu)} \right] [\mathcal{L}_A + \bar{n}\mathcal{L}_B] \bar{\rho},\end{aligned}\tag{2.11}$$

where the convex average

$$\bar{n} = \frac{\sum_{\nu} \Gamma^{(\nu)} n^{(\nu)}}{\sum_{\nu} \Gamma^{(\nu)}}\tag{2.12}$$

represents an average thermal parameter (e.g. the average occupation). Formally, this is the same equation that determines the steady state for a single reservoir, which may now however be non-thermal.

**Exercise 20** (Pseudo-Nonequilibrium). *Show that the stationary state of Eq.(2.8) is a thermal one, i.e., that*

$$\frac{\bar{\rho}_{11}}{\bar{\rho}_{00}} = \frac{\bar{f}}{1 - \bar{f}}.$$

*Determine  $\bar{f}$  in dependence of  $\Gamma_{\alpha}$  and  $f_{\alpha}$ .*

## 2.2 Phenomenologic definition of currents

Strictly speaking, a conventional master equation only tells us about the state of the system and not about the changes in the reservoir. For a system that is coupled to a single reservoir, we might from total conservation laws and the dynamics of the system conclude how much energy or how many particles have passed into the reservoir. This is different however for multiple reservoirs, which at non-equilibrium may give rise to steady-state currents. However, the additive decomposition of the Liouville superoperators allows us to phenomenologically identify contributions to the currents from individual reservoirs.

From Eq. (2.6) we can conclude for the energy of the system

$$\frac{d}{dt} \langle E \rangle = \text{Tr} \{ H_S \dot{\rho} \} = -i \text{Tr} \{ H_S [H_S, \rho] \} + \sum_{\nu} \text{Tr} \{ H_S (\mathcal{L}^{(\nu)} \rho) \} .\tag{2.13}$$

We immediately see that the first term vanishes under the trace, and that the contributions of the individual reservoirs is additive. This gives rise to the definition of the energy current entering the system from reservoir  $\nu$

$$I_E^{(\nu)} = \text{Tr} \{ H_S (\mathcal{L}^{(\nu)} \rho) \} = \text{Tr} \{ \mathcal{H}_S \mathcal{L}^{(\nu)} \rho \} .\tag{2.14}$$

Similarly, we can define a particle current. This only makes sense if the system Hamiltonian conserves the total particle number  $[N_S, H_S] = 0$ , which leads to

$$\frac{d}{dt} \langle N \rangle = \text{Tr} \{ N_S \dot{\rho} \} = -i \text{Tr} \{ N_S [H_S, \rho] \} + \sum_{\nu} \text{Tr} \{ N_S (\mathcal{L}^{(\nu)} \rho) \}. \quad (2.15)$$

Again, the commutator term vanishes and the particle (or matter) current entering the system from reservoir  $\nu$  becomes

$$I_M^{(\nu)} = \text{Tr} \{ N_S (\mathcal{L}^{(\nu)} \rho) \} = \text{Tr} \{ \mathcal{N}_S \mathcal{L}^{(\nu)} \rho \}. \quad (2.16)$$

We note that in these definitions we have mixed superoperator (calligraphic) and operator notations, which explains why we have put some brackets in the expressions. Let us first consider the simple case where each Liouvillian  $\mathcal{L}^{(\nu)}$  has block structure in the system energy eigenbasis separating populations and diagonals, with the evolution of the diagonals being given by the usual rate equation

$$\dot{\rho}_{aa} = \sum_{\nu} \sum_b \gamma_{ab,ab}^{(\nu)} \rho_{bb} - \sum_{\nu} \sum_b \gamma_{ba,ba}^{(\nu)} \rho_{aa}. \quad (2.17)$$

Representing the density matrix, particle number operator, and Hamiltonian in the time-independent energy eigenbasis as

$$\rho = \sum_a \rho_{aa} |a\rangle \langle a| + \sum_{a \neq b} \rho_{ab} |a\rangle \langle b|, \quad N_S = \sum_a N_a |a\rangle \langle a|, \quad H_S = \sum_a H_a |a\rangle \langle a|, \quad (2.18)$$

we see that

$$I_M^{(\nu)} = \sum_a N_a \left[ \sum_b \gamma_{ab,ab}^{(\nu)} \rho_{bb} - \sum_b \gamma_{ba,ba}^{(\nu)} \rho_{aa} \right] = \sum_{ab} (N_a - N_b) \gamma_{ab,ab}^{(\nu)} \rho_{bb}. \quad (2.19)$$

At steady state  $\rho_{bb} \rightarrow \bar{\rho}_{bb}$ , this corresponds to the traditional definition of the **matter current for rate equations**, given by the steady state occupation multiplied by the transition rate  $\gamma_{ab,ab}^{(\nu)}$  and the particle number difference between the new state  $a$  and the old state  $b$ . In a completely analogous fashion, we obtain for the energy current entering the system from reservoir  $\nu$

$$I_E^{(\nu)} = \sum_a E_a \left[ \sum_b \gamma_{ab,ab}^{(\nu)} \rho_{bb} - \sum_b \gamma_{ba,ba}^{(\nu)} \rho_{aa} \right] = \sum_{ab} (E_a - E_b) \gamma_{ab,ab}^{(\nu)} \rho_{bb}, \quad (2.20)$$

which is the traditional **energy current for rate equations**. One could alternatively have derived these currents as follows: When the system follows transitions between different energy eigenstates from state  $b$  to state  $a$ , it gains or loses the energy  $E_a - E_b$ . The probability for such a process to happen in the time interval  $\Delta t$  triggered by the reservoir  $\nu$  is just  $\Delta t \gamma_{ab,ab}^{(\nu)} \rho_{bb}$ . Summing over all initial states  $b$  and over all final states  $a$  while multiplying the probabilities with the energy difference per time  $(E_a - E_b)/\Delta t$  then yields the above phenomenological energy current.

We have defined these currents from the perspective of the system. These definitions just require an additive decomposition of the Liouville superoperator, it does actually not need to be of Lindblad form. But can they really be associated with the corresponding change of energy and particle number in the reservoir? Where does e.g. in case of energy balances the energy contained in the interaction Hamiltonian enter? This requires a more careful analysis to be provided later. Below, we will discuss the phenomenologic thermodynamics arising from these definitions.

## 2.3 Nonequilibrium thermodynamics

We first phrase the necessary prerequisites. Let us assume that we have a system coupled to many reservoirs and subject to slow driving  $H_S \rightarrow H_S(t)$ . The slow-driving assumption is necessary to ensure that all previous approximations are applicable, such that only the parameters in the dissipators become time-dependent, eventually leading to a master equation of the form

$$\dot{\rho} = -i[H_S(t), \rho] + \sum_{\nu} \mathcal{L}^{(\nu)}(t)\rho \quad (2.21)$$

for the system density matrix  $\rho$  (we often drop the index  $S$  for brevity).

Denoting the system energy as  $E = \text{Tr} \{H_S(t)\rho(t)\}$ , we can state the first law of thermodynamics for the system as a balance equation

$$\begin{aligned} \dot{E} &= \frac{d}{dt} \text{Tr} \{H_S(t)\rho(t)\} \\ &= \text{Tr} \left\{ \dot{H}_S \rho_S \right\} + \sum_{\nu} \mu_{\nu} \text{Tr} \left\{ N_S(\mathcal{L}^{(\nu)}\rho) \right\} + \sum_{\nu} \text{Tr} \left\{ (H_S - \mu_{\nu} N_S)(\mathcal{L}^{(\nu)}\rho) \right\} . \end{aligned} \quad (2.22)$$

Here, the first term can be interpreted as **mechanical work rate**

$$\dot{W} = \text{Tr} \left\{ \dot{H}_S \rho \right\} , \quad (2.23)$$

the second as **chemical work rate** injected by reservoir  $\nu$

$$\dot{W}^{(\nu)} = \mu_{\nu} \text{Tr} \left\{ N_S(\mathcal{L}^{(\nu)}\rho) \right\} , \quad (2.24)$$

and the third as a **heat current** entering the system from reservoir  $\nu$

$$\dot{Q}^{(\nu)} = \text{Tr} \left\{ (H_S - \mu_{\nu} N_S)(\mathcal{L}^{(\nu)}\rho) \right\} . \quad (2.25)$$

We note that this is not a derivation of the first law. Rather, we have postulated it and used it to classify the individual currents. These definitions remain sensible when  $H_S$  is time-dependent.

Furthermore, we assume that also in case of slow time-dependent driving one has that the dissipators  $\mathcal{L}^{(\nu)}(t)$  drag towards the time-local Gibbs state

$$\mathcal{L}^{(\nu)}(t) \frac{e^{-\beta_{\nu}(H_S(t) - \mu_{\nu} N_S)}}{Z} \equiv \mathcal{L}^{(\nu)}(t) \bar{\rho}^{(\nu)}(t) = 0 . \quad (2.26)$$

In particular, this implies that we can write

$$\ln \bar{\rho}^{(\nu)}(t) = -\beta_{\nu}(H_S(t) - \mu_{\nu} N_S) - \ln Z , \quad (2.27)$$

where  $\ln Z$  is just a number, such that  $\text{Tr} \{(\mathcal{L}^{(\nu)}\rho) \ln Z\} = 0$ . Then, we can show the second law in non-equilibrium as follows

$$\begin{aligned} \dot{S}_i &= \dot{S} - \sum_{\nu} \beta_{\nu} \dot{Q}^{(\nu)} \\ &= -\text{Tr} \{ \dot{\rho} \ln \rho \} + \sum_{\nu} \text{Tr} \{ [\mathcal{L}^{(\nu)}(t)\rho(t)] \ln \bar{\rho}^{(\nu)}(t) \} \\ &= -\sum_{\nu} \text{Tr} \{ [\mathcal{L}^{(\nu)}(t)\rho(t)] [\ln \rho(t) - \ln \bar{\rho}^{(\nu)}(t)] \} , \end{aligned} \quad (2.28)$$

where we have used that  $\dot{S} = -\text{Tr}\{\dot{\rho} \ln \rho\} = -\sum_{\nu} \text{Tr}\{(\mathcal{L}^{(\nu)}\rho) \ln \rho\}$ , since the commutator term does not contribute. With view on Eq. (2.26), we can for each term in the summation use Spohn's inequality to conclude that the **irreversible entropy production rate** is non-negative

$$\dot{S}_i = \dot{S} - \sum_{\nu} \beta_{\nu} \dot{Q}^{(\nu)} = \dot{S} + \sum_{\nu} \dot{S}_{\text{res}}^{(\nu)} \geq 0. \quad (2.29)$$

This denotes the second law in presence of (slow) driving and multiple reservoirs. We stress that we have used very few ingredients to arrive at this result: First, the total Liouvillian is additive in the baths and probability conserving. Second, the stationary state of each Lindblad superoperator is the local thermal equilibrium state, possibly depending on time. Strict positivity of the above entropy production rate in time can also be used to classify a dynamics as Markovian, whereas a dynamics can be considered non-Markovian when the above inequality is violated.

We will now discuss some consequences of this second law.

## 2.4 Steady-State Dynamics

By steady-state we mean that the system density matrix has reached a stationary value, which will in general be a complicated nonequilibrium steady state. The term steady state also means that for the moment we neglect driving  $H_S(t) \rightarrow H_S$ , and the reservoirs only perform chemical work on the system and exchange heat with it – in other words, only matter and energy currents determine the thermodynamics of the model. Given a finite-dimensional Hilbert space and ergodic dynamics, the von-Neumann entropy of the system will saturate at some point  $\dot{S} \rightarrow 0$  and the entropy production rate is given by the heat flows

$$\dot{S}_i \rightarrow -\sum_{\nu} \beta_{\nu} \dot{Q}^{(\nu)} = -\sum_{\nu} \beta_{\nu} \left[ \bar{I}_E^{(\nu)} - \mu_{\nu} \bar{I}_M^{(\nu)} \right] \geq 0, \quad (2.30)$$

where  $\bar{I}_E^{(\nu)}$  and  $\bar{I}_M^{(\nu)}$  are the stationary energy and matter currents entering the system from reservoir  $\nu$ , respectively. Naturally, we see that the entropy production has to vanish when all the average currents vanish (e.g. at a global equilibrium state). Whereas energy and matter conservation imply equalities among the currents at steady state

$$\sum_{\nu} \bar{I}_M^{(\nu)} = 0, \quad \sum_{\nu} \bar{I}_E^{(\nu)} = 0, \quad (2.31)$$

the positivity of entropy production imposes a further constraint among the currents, e.g. for a two-terminal system

$$\begin{aligned} \dot{S}_i &= -\beta_L (\bar{I}_E^{(L)} - \mu_L \bar{I}_M^{(L)}) - \beta_R (\bar{I}_E^{(R)} - \mu_R \bar{I}_M^{(R)}) \\ &= (\beta_R - \beta_L) \bar{I}_E + (\mu_L \beta_L - \mu_R \beta_R) \bar{I}_M \geq 0, \end{aligned} \quad (2.32)$$

where we have introduced the currents from left to right  $\bar{I}_E = +\bar{I}_E^{(L)} = -\bar{I}_E^{(R)}$  and  $\bar{I}_M = +\bar{I}_M^{(L)} = -\bar{I}_M^{(R)}$ .

We first discuss the case of equal temperatures  $\beta = \beta_L = \beta_R$ . The second law implies that

$$(\mu_L - \mu_R) \bar{I}_M \geq 0, \quad (2.33)$$

which is nothing but the trivial statement that the matter current is always directed from a lead with large chemical potential towards the lead with smaller chemical potential.

Next, we consider equal chemical potentials  $\mu_L = \mu_R = \mu$  but different temperatures. Then, our setup has to obey

$$(\beta_R - \beta_L)(\bar{I}_E - \mu\bar{I}_M) \geq 0, \quad (2.34)$$

where  $\bar{I}_E - \mu\bar{I}_M$  is now the heat leaving the left reservoir and entering the right reservoir. When  $\beta_R > \beta_L$  (i.e., the left lead is hotter than the right one  $T_L > T_R$ ), the second law just implies that  $\bar{I}_E - \mu\bar{I}_M \geq 0$ , i.e., the heat has to flow from left to right. Similarly, it has to revert sign when  $\beta_R < \beta_L$ . Altogether, this only tells us that in absence of driving, heat always flows from hot to cold – the Clausius statement of the second law of thermodynamics.

An interesting scenario arises when there are both a temperature and a potential gradient present, dragging to different directions. For a two-terminal system the second law then reads at steady state

$$(\beta_R - \beta_L)\bar{I}_E + (\mu_L\beta_L - \mu_R\beta_R)\bar{I}_M \geq 0. \quad (2.35)$$

With this, it is possible to use a temperature gradient to drive a current against a potential bias, i.e., to perform chemical work. In case of e.g. electrons driven against an electric bias, this would be a **thermoelectric generator**. Without loss of generality we assume  $\mu_L < \mu_R$  and  $\beta_L < \beta_R$  (i.e., the left reservoir is hotter than the right one). The **efficiency** of this generator is then given by the ratio of the generated electric power (or chemical work rate)  $P = -\bar{I}_M(\mu_L - \mu_R)$  divided by the heat entering the system from the hot reservoir

$$\begin{aligned} \eta &= \frac{-\bar{I}_M(\mu_L - \mu_R)}{\bar{I}_E - \mu_L\bar{I}_M} = \frac{-(\beta_R - \beta_L)(\mu_L - \mu_R)\bar{I}_M}{(\beta_R - \beta_L)\bar{I}_E - (\beta_R - \beta_L)\mu_L\bar{I}_M} \\ &= \frac{-(\beta_R - \beta_L)(\mu_L - \mu_R)\bar{I}_M}{(\beta_R - \beta_L)\bar{I}_E + (\mu_L\beta_L - \mu_R\beta_R)\bar{I}_M - (\mu_L\beta_L - \mu_R\beta_R)\bar{I}_M - (\beta_R - \beta_L)\mu_L\bar{I}_M} \\ &\leq \frac{-(\beta_R - \beta_L)(\mu_L - \mu_R)\bar{I}_M}{-(\mu_L\beta_L - \mu_R\beta_R)\bar{I}_M - (\beta_R - \beta_L)\mu_L\bar{I}_M} = \frac{(\beta_R - \beta_L)(\mu_L - \mu_R)}{(\mu_L\beta_L - \mu_R\beta_R) + (\beta_R - \beta_L)\mu_L} \\ &= 1 - \frac{\beta_L}{\beta_R} = 1 - \frac{T_R}{T_L} = 1 - \frac{T_{\text{cold}}}{T_{\text{hot}}} = \eta_{\text{Carnot}}. \end{aligned} \quad (2.36)$$

The efficiency of such a generator is bounded by **Carnot efficiency**, irrespective of the microscopic details. We note that our scenario is different from the classical Carnot or Otto cycles, since our reservoirs are coupled at all times to the system, but it is interesting to see that the same universal law holds.

Conversely, one may apply a potential gradient to a system and use it to let the heat flow against the usual direction. This can be used as a **refrigerator** by cooling a cold reservoir or as a **heat pump** by heating a hot reservoir. Keeping the previous conventions  $\mu_L < \mu_R$  and  $\beta_L < \beta_R$ , let us take a closer look at the performance of such engines. For a refrigerator, we assume that there exists a regime of parameters where the heat entering the system from the cold reservoir is positive  $\dot{Q}_{\text{cold}} = -(\bar{I}_E - \mu_R\bar{I}_M) > 0$ , which can only be driven by chemical or electric work injected into the system  $\dot{W}_{\text{cons}} = +(\mu_L - \mu_R)\bar{I}_M > 0$ . In this regime, we can compare the heat entering the system from the cold reservoir with the chemical work rate injected into the system (alternatively,

the electric power consumed). This is commonly called **coefficient of performance** (COP)

$$\begin{aligned}
\text{COP}_{\text{cooling}} &= \frac{-(\bar{I}_E - \mu_R \bar{I}_M)}{(\mu_L - \mu_R) \bar{I}_M} \\
&= \frac{-[(\beta_R - \beta_L) \bar{I}_E + (\mu_L \beta_L - \mu_R \beta_R) \bar{I}_M] + (\mu_L \beta_L - \mu_R \beta_R) \bar{I}_M + (\beta_R - \beta_L) \mu_R \bar{I}_M}{(\beta_R - \beta_L)(\mu_L - \mu_R) \bar{I}_M} \\
&\leq \frac{+(\mu_L \beta_L - \mu_R \beta_R) \bar{I}_M + (\beta_R - \beta_L) \mu_R \bar{I}_M}{(\beta_R - \beta_L)(\mu_L - \mu_R) \bar{I}_M} \\
&= \frac{\beta_L}{\beta_R - \beta_L} = \frac{T_R}{T_L - T_R} = \frac{T_{\text{cold}}}{T_{\text{hot}} - T_{\text{cold}}}. \tag{2.37}
\end{aligned}$$

A similar calculation holds for the case of heating, where we compare the heat entering the hot reservoir  $\dot{Q}_{\text{hot}} = -(\bar{I}_E - \mu_L \bar{I}_M) > 0$  with the consumed work rate  $\dot{W}_{\text{cons}} = +(\mu_L - \mu_R) \bar{I}_M > 0$

$$\begin{aligned}
\text{COP}_{\text{heating}} &= \frac{-(\bar{I}_E - \mu_L \bar{I}_M)}{(\mu_L - \mu_R) \bar{I}_M} \\
&\leq \frac{\beta_R}{\beta_R - \beta_L} = \frac{T_L}{T_L - T_R} = \frac{T_{\text{hot}}}{T_{\text{hot}} - T_{\text{cold}}}. \tag{2.38}
\end{aligned}$$

**Exercise 21** (Coefficient of Performance). *Calculate the upper bound on the coefficient of performance for heating.*

Conventional heat pumps for houses reach COPs in the order of four, i.e., with each kWh of electric energy one pumps on average four kWh of heat into the house. This explains their commercial use in some occasions despite the relatively high cost of electric energy.

## 2.5 Example: The single-electron transistor

For the previously discussed example of the single-electron transistor with two reservoirs

$$H = \epsilon d^\dagger d + \sum_{\nu \in \{L, R\}} \sum_k \left( t_{k\nu} d c_{k\nu}^\dagger + \text{h.c.} \right) + \sum_{\nu \in \{L, R\}} \sum_k \epsilon_{k\nu} c_{k\nu}^\dagger c_{k\nu} \tag{2.39}$$

we had obtained that the dynamics of the populations  $(P_0, P_1) = (\rho_{00}, \rho_{11})$  followed a simple rate equation, additive in the reservoirs

$$\mathcal{L} = \begin{pmatrix} -\Gamma_L f_L - \Gamma_R f_R & +\Gamma_L(1 - f_L) + \Gamma_R(1 - f_R) \\ +\Gamma_L f_L + \Gamma_R f_R & -\Gamma_L(1 - f_L) - \Gamma_R(1 - f_R) \end{pmatrix}. \tag{2.40}$$

This implies for the currents from left to right

$$\bar{I}_M = \bar{I}_M^{(L)} = \frac{\Gamma_L \Gamma_R}{\Gamma_L + \Gamma_R} (f_L - f_R), \quad \bar{I}_E = \bar{I}_E^{(L)} = \epsilon \bar{I}_M, \tag{2.41}$$

where  $\epsilon$  denotes the dot level, at which the Fermi functions and tunneling rates are evaluated

$$f_\nu = \frac{1}{e^{\beta_\nu(\epsilon - \mu_\nu)} + 1}, \quad \Gamma_\nu = \Gamma_\nu(\epsilon) = 2\pi \sum_k |t_{k\nu}|^2 \delta(\epsilon - \epsilon_{k\nu}). \tag{2.42}$$

We can plot the currents versus the bias voltage at  $\mu_L = +V/2$  and  $\mu_R = -V/2$  to identify the regimes where the device acts as thermoelectric generator or refrigerator, see Fig. 2.2.

Figure 2.2: Plot of the matter current  $\bar{I}_M$  (solid black) and heat currents entering from left ( $\dot{Q}^{(L)}$ , solid red) and right ( $\dot{Q}^{(R)}$ , solid blue) versus bias voltage. The dashed reference is temperatures  $\epsilon\beta_\alpha = 1$ . For large bias voltages, both reservoirs are heated (conventional heater). There is a region where  $-\bar{I}_M(\mu_L - \mu_R) > 0$ , where the system acts as thermoelectric generator, and to the left of it there is a region where the cold right reservoir is cooled while simultaneously the hot left reservoir is heated (blue text). Here, the system acts as a true heat pump.

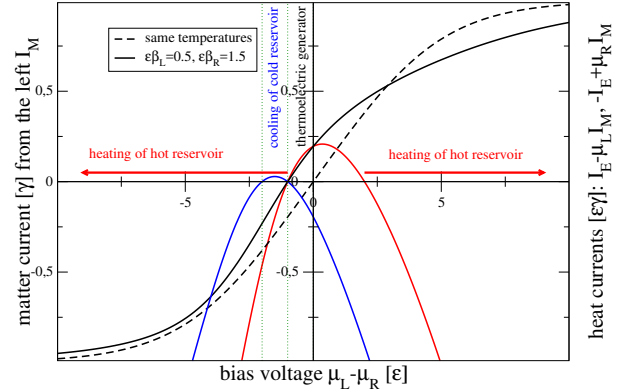
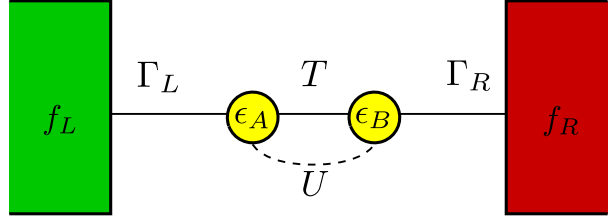


Figure 2.3: A double quantum dot (system) with on-site energies  $\epsilon_{A/B}$  and internal tunneling amplitude  $T$  and Coulomb interaction  $U$  may host at most two electrons. It is weakly tunnel-coupled to two fermionic contacts via the rates  $\Gamma_{L/R}$  at different thermal equilibria described by the Fermi distributions  $f_{L/R}(\omega)$ .



## 2.6 Example: The double quantum dot

### Model definition

We consider a double quantum dot with internal tunnel coupling  $T$  and Coulomb interaction  $U$  that is weakly coupled to two fermionic contacts via the rates  $\Gamma_L$  and  $\Gamma_R$ , see Fig. 2.3. The corresponding Hamiltonian reads

$$\begin{aligned}
 H_S &= \epsilon_A d_A^\dagger d_A + \epsilon_B d_B^\dagger d_B + T (d_A d_B^\dagger + d_B d_A^\dagger) + U d_A^\dagger d_A d_B^\dagger d_B, \\
 H_B &= \sum_k \epsilon_{kL} c_{kL}^\dagger c_{kL} + \sum_k \epsilon_{kR} c_{kR}^\dagger c_{kR}, \\
 H_I &= \sum_k (t_{kL} d_{AC}^\dagger c_{kL} + t_{kL}^* c_{kL} d_A^\dagger) + \sum_k (t_{kR} d_{BC}^\dagger c_{kR} + t_{kR}^* c_{kR} d_B^\dagger). \quad (2.43)
 \end{aligned}$$

In contrast to simple rate equations, the internal tunneling  $T$  is not a transition rate but an amplitude, since it occurs at the level of the Hamiltonian. As noted, for fermions we do not have a tensor product decomposition in the interaction Hamiltonian, as the coupling operators anti-commute. However, we may use a Jordan-Wigner transform and re-introduce local fermions on the system and reservoirs later-on, such that we may derive the master equation in the usual way.

## BMS rate equation

We do now proceed by calculating the Fourier transforms of the bath correlation functions

$$\begin{aligned}\gamma_{12}(\omega) &= \Gamma_L(-\omega)f_L(-\omega), & \gamma_{21}(\omega) &= \Gamma_L(+\omega)[1 - f_L(+\omega)], \\ \gamma_{34}(\omega) &= \Gamma_R(-\omega)f_R(-\omega), & \gamma_{43}(\omega) &= \Gamma_R(+\omega)[1 - f_R(+\omega)]\end{aligned}\quad (2.44)$$

with the continuum tunneling rates  $\Gamma_\alpha(\omega) = 2\pi \sum_k |t_{k\alpha}|^2 \delta(\omega - \epsilon_{k\alpha})$  and Fermi functions  $f_\alpha(\epsilon_{k\alpha}) = \langle c_{k\alpha}^\dagger c_{k\alpha} \rangle = [e^{\beta_\alpha(\epsilon_{k\alpha} - \mu_\alpha)} + 1]^{-1}$ .

**Exercise 22** (DQD bath correlation functions). *Calculate the Fourier transforms (2.44) of the bath correlation functions for the double quantum dot, assuming that the reservoirs are in a thermal equilibrium state with inverse temperatures  $\beta_\alpha$  and chemical potential  $\mu_\alpha$ .*

Next, we diagonalize the system Hamiltonian (in the Fock space basis)

$$\begin{aligned}E_0 &= 0, & |v_0\rangle &= |00\rangle, \\ E_- &= \epsilon - \sqrt{\Delta^2 + T^2}, & |v_-\rangle &\propto \left[ \left( \Delta + \sqrt{\Delta^2 + T^2} \right) |10\rangle + T |01\rangle \right], \\ E_+ &= \epsilon + \sqrt{\Delta^2 + T^2}, & |v_+\rangle &\propto \left[ \left( \Delta - \sqrt{\Delta^2 + T^2} \right) |10\rangle + T |01\rangle \right], \\ E_2 &= 2\epsilon + U, & |v_2\rangle &= |11\rangle,\end{aligned}\quad (2.45)$$

where  $\Delta = (\epsilon_B - \epsilon_A)/2$  and  $\epsilon = (\epsilon_A + \epsilon_B)/2$  and  $|01\rangle = -\tilde{d}_B^\dagger |00\rangle$ ,  $|10\rangle = \tilde{d}_A^\dagger |00\rangle$ , and  $|11\rangle = \tilde{d}_B^\dagger \tilde{d}_A^\dagger |00\rangle$ . We have not symmetrized the coupling operators but to obtain the BMS limit, we may alternatively use Eqns. (1.133) and (1.134) when  $\tau \rightarrow \infty$ . Specifically, when we have no degeneracies in the system Hamiltonian ( $\Delta^2 + T^2 > 0$ ), the master equation in the energy eigenbasis (where  $a, b \in \{0, -, +, 2\}$ ) becomes a rate equation (1.82), where for non-hermitian coupling operators the transition rates from  $b$  to  $a$  are given by

$$\gamma_{ab,ab} = \sum_{\alpha\beta} \gamma_{\alpha\beta}(E_b - E_a) \langle a | A_\beta | b \rangle \langle a | A_\alpha^\dagger | b \rangle^*. \quad (2.46)$$

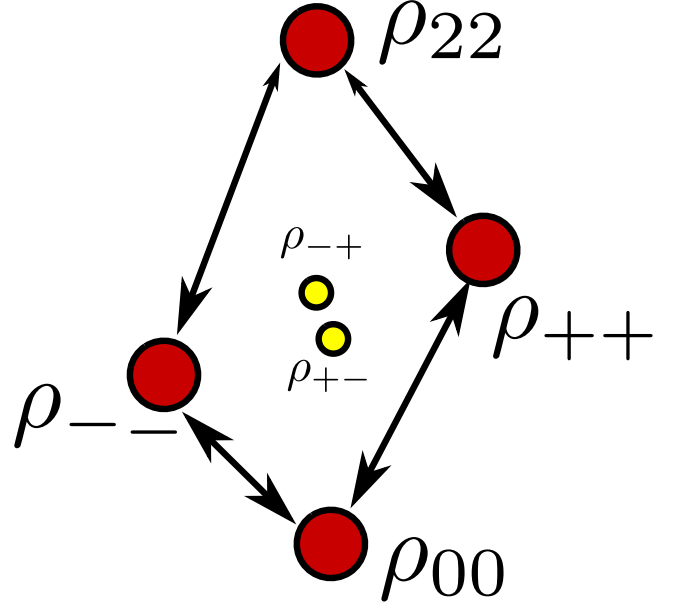
We may calculate the Liouvillians for the interaction with the left and right contact separately

$$\gamma_{ab,ab} = \gamma_{ab,ab}^L + \gamma_{ab,ab}^R, \quad (2.47)$$

since we are constrained to second order perturbation theory in the tunneling amplitudes. Since we have  $\tilde{d}_A = A_2^\dagger = A_1 = \tilde{d}_A$  and  $\tilde{d}_B = A_4^\dagger = A_3 = \tilde{d}_B$ , we obtain for the left-associated dampening coefficients

$$\begin{aligned}\gamma_{ab,ab}^L &= \gamma_{12}(E_b - E_a) |\langle a | A_2 | b \rangle|^2 + \gamma_{21}(E_b - E_a) |\langle a | A_1 | b \rangle|^2, \\ \gamma_{ab,ab}^R &= \gamma_{34}(E_b - E_a) |\langle a | A_4 | b \rangle|^2 + \gamma_{43}(E_b - E_a) |\langle a | A_3 | b \rangle|^2.\end{aligned}\quad (2.48)$$

Figure 2.4: Configuration space of a serial double quantum dot coupled to two leads, yielding a rate equation for the populations in the system energy eigenbasis (red). The only allowed coherences of equally charged states (yellow) decouple and decay in the long-term limit. Due to the hybridization of the two levels, electrons may jump directly from the left contact to right-localized modes and vice versa, such that in principle all transitions are driven by both contacts, albeit with different strength. In the Coulomb-blockade limit, transitions to the doubly occupied state are strongly suppressed (small arrowheads), such that the system dimension can be reduced.



In the wideband (flatband) limit  $\Gamma_{L/R}(\omega) = \Gamma_{L/R}$ , we obtain for the nonvanishing transition rates in the energy eigenbasis

$$\begin{aligned}
\gamma_{0-,0-}^L &= \Gamma_L \gamma_+ [1 - f_L(\epsilon - \sqrt{\Delta^2 + T^2})], & \gamma_{0-,0-}^R &= \Gamma_R \gamma_- [1 - f_R(\epsilon - \sqrt{\Delta^2 + T^2})], \\
\gamma_{0+,0+}^L &= \Gamma_L \gamma_- [1 - f_L(\epsilon + \sqrt{\Delta^2 + T^2})], & \gamma_{0+,0+}^R &= \Gamma_R \gamma_+ [1 - f_R(\epsilon + \sqrt{\Delta^2 + T^2})], \\
\gamma_{-2,-2}^L &= \Gamma_L \gamma_- [1 - f_L(\epsilon + U + \sqrt{\Delta^2 + T^2})], & \gamma_{-2,-2}^R &= \Gamma_R \gamma_+ [1 - f_R(\epsilon + U + \sqrt{\Delta^2 + T^2})], \\
\gamma_{+2,+2}^L &= \Gamma_L \gamma_+ [1 - f_L(\epsilon + U - \sqrt{\Delta^2 + T^2})], & \gamma_{+2,+2}^R &= \Gamma_R \gamma_- [1 - f_R(\epsilon + U - \sqrt{\Delta^2 + T^2})], \\
\gamma_{-0,-0}^L &= \Gamma_L \gamma_+ f_L(\epsilon - \sqrt{\Delta^2 + T^2}), & \gamma_{-0,-0}^R &= \Gamma_R \gamma_- f_R(\epsilon - \sqrt{\Delta^2 + T^2}), \\
\gamma_{+0,+0}^L &= \Gamma_L \gamma_- f_L(\epsilon + \sqrt{\Delta^2 + T^2}), & \gamma_{+0,+0}^R &= \Gamma_R \gamma_+ f_R(\epsilon + \sqrt{\Delta^2 + T^2}), \\
\gamma_{-2,-2-}^L &= \Gamma_L \gamma_- f_L(\epsilon + U + \sqrt{\Delta^2 + T^2}), & \gamma_{-2,-2-}^R &= \Gamma_R \gamma_+ f_R(\epsilon + U + \sqrt{\Delta^2 + T^2}), \\
\gamma_{+2,+2+}^L &= \Gamma_L \gamma_+ f_L(\epsilon + U - \sqrt{\Delta^2 + T^2}), & \gamma_{+2,+2+}^R &= \Gamma_R \gamma_- f_R(\epsilon + U - \sqrt{\Delta^2 + T^2}),
\end{aligned} \tag{2.49}$$

with the dimensionless coefficients

$$\gamma_{\pm} = \frac{1}{2} \left[ 1 \pm \frac{\Delta}{\sqrt{\Delta^2 + T^2}} \right] \tag{2.50}$$

arising from the matrix elements of the system coupling operators. This rate equation can also be visualized with a network, see Fig. 2.4. We note that although both reservoirs drive all transitions, their relative strength is different, and we do not have a simple situation as discussed previously in Eq. (2.9). Consequently, the stationary state of the rate equation cannot be written as some grand-canonical equilibrium state, which is most conveniently shown by disproving the relations  $\bar{\rho}_{--}/\bar{\rho}_{00} = e^{-\beta(E_- - E_0 - \mu)}$ ,  $\bar{\rho}_{++}/\bar{\rho}_{00} = e^{-\beta(E_+ - E_0 - \mu)}$  and  $\bar{\rho}_{++}/\bar{\rho}_{--} = e^{-\beta(E_+ - E_-)}$ .

As the simplest example of the resulting rate equation, we study the high-bias and Coulomb-blockade limit  $f_{L/R}(\epsilon + U \pm \sqrt{\Delta^2 + T^2}) \rightarrow 0$  and  $f_L(\epsilon \pm \sqrt{\Delta^2 + T^2}) \rightarrow 1$  and  $f_R(\epsilon \pm \sqrt{\Delta^2 + T^2}) \rightarrow 0$  when the onsite-energies are degenerate such that  $\Delta \rightarrow 0$  (such that  $\gamma_{\pm} \rightarrow 1/2$ ). This removes any dependence on the internal tunneling amplitude  $T$ . Consequently, derived quantities such as e.g. the current will not depend on  $T$  either and we would obtain a current even when  $T \rightarrow 0$  (where we have a disconnected structure). However, precisely in this limit (i.e.,  $\Delta \rightarrow 0$  and  $T \rightarrow 0$ ), the

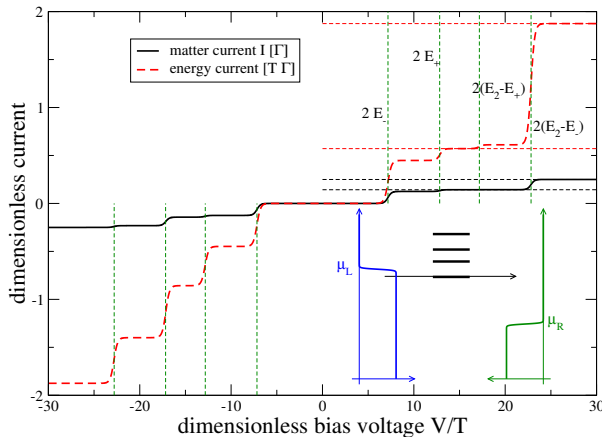


Figure 2.5: Plot of matter (solid black) and energy (dashed red) currents. At sufficiently low temperatures, the steps in the currents occur for positive bias voltage at  $\mu_L = V/2 \in \{E_- - E_0, E_+ - E_0, E_2 - E_+, E_2 - E_-\}$ . The inset displays the configuration of these transition energies relative to left (blue) and right (green) Fermi functions taken at  $V = 10T$ . Then, only the lowest transition energy (arrow) is inside the transport window, such that transport is dominated by transitions between  $|-\rangle$  and  $|0\rangle$ . Other parameters have been chosen as  $\mu_L = -\mu_R = V/2$ ,  $\Gamma_L = \Gamma_R = \Gamma$ ,  $\epsilon_A = 4T$ ,  $\epsilon_B = 6T$ ,  $U = 5T$ , and  $\beta T = 10$ .

two levels  $E_-$  and  $E_+$  become energetically degenerate, and a simple rate equation description is not applicable. The take-home message of this failure is that one should not use plug and play formulas without learning about their limits. Therefore, keeping in mind that  $T \neq 0$ , the resulting Liouvillian reads

$$\mathcal{L} = \frac{1}{2} \begin{pmatrix} -2\Gamma_L & \Gamma_R & \Gamma_R & 0 \\ \Gamma_L & -\Gamma_R & 0 & \Gamma_L + \Gamma_R \\ \Gamma_L & 0 & -\Gamma_R & \Gamma_L + \Gamma_R \\ 0 & 0 & 0 & -2(\Gamma_L + \Gamma_R) \end{pmatrix}, \quad (2.51)$$

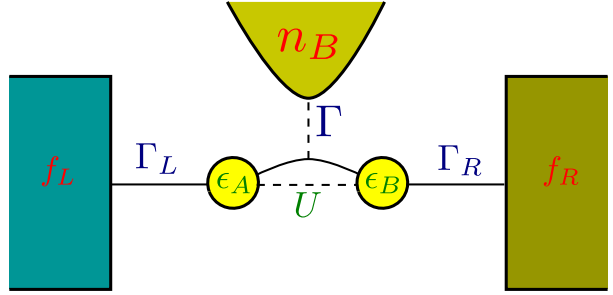
where it becomes visible that the doubly occupied state will simply decay and may therefore – since we are interested in the long-term dynamics – be eliminated completely

$$\mathcal{L}_{\text{CBHB}} = \frac{1}{2} \begin{pmatrix} -2\Gamma_L & \Gamma_R & \Gamma_R \\ \Gamma_L & -\Gamma_R & 0 \\ \Gamma_L & 0 & -\Gamma_R \end{pmatrix}. \quad (2.52)$$

**Exercise 23** (Stationary DQD currents). *Calculate the stationary currents entering the right reservoir.*

At finite bias voltages, it becomes of course harder to calculate steady states and stationary currents. However, for low temperatures, the Fermi functions will behave similar to step functions, and the transport window becomes sharp. Then, by enlarging the bias voltage, the transport window is opened, and the currents will exhibit steps when a new transport channel is inside the transport window, see Fig. 2.5. A further obvious observation is that at zero bias voltage, we have vanishing currents. This must happen at equal temperatures. The entropy production in this case is fully determined by the matter current  $\dot{S}_i = \beta(\mu_L - \mu_R)\bar{I}_M$ , where  $\bar{I}_M$  denotes the current from left to right. Identifying  $P_{\text{diss}} = +(\mu_L - \mu_R)\bar{I}_M$  with the power dissipated by the device, the entropy production just becomes  $\dot{S}_i = \beta P_{\text{diss}} \geq 0$ .

Figure 2.6: Sketch of two quantum dots that are separately tunnel-coupled to their adjacent reservoir in the conventional way by rates  $\Gamma_L$  and  $\Gamma_R$ . The mere Coulomb interaction  $U$  only allows for the exchange of energy between the dots, but with phonons present (rounded terminals), tunneling between  $A$  and  $B$  becomes possible (dotted and dashed). The device may act as a thermoelectric generator converting thermal gradients into power.



## BMS decoherence

Our discussion has so far neglected the evolution of coherences, which is valid when these decay in the long-term limit. We still want to confirm that. First, only the coherences between states of equal charge are allowed  $\rho_{-+} = \rho_{+-}^*$ , such that it suffices to look only at this coherence. Examining the BMS master equation yields under the assumption of a non-degenerate system ( $E_0 < E_- < E_+ < E_2$ ) and using that many other rates vanish for the evolution of the coherence

$$\dot{\rho}_{-+} = \kappa \rho_{-+}, \quad \kappa = i(E_+ - E_- + \sigma_{++} - \sigma_{--}) - \frac{1}{2}(\gamma_{0-,0-} + \gamma_{2-,2-} + \gamma_{0+,0+} + \gamma_{2+,2+}), \quad (2.53)$$

which tells us with regard to Eq. (2.49) that the coherences will just decay, since the rates in the second argument are positive and the matrix elements  $\sigma_{--}$  and  $\sigma_{++}$  of the Lamb-shift Hamiltonian are real. Therefore, any superpositions in the system energy eigenbasis decay. Vectorizing the relevant density matrix elements populations as  $(\rho_{00}, \rho_{--}, \rho_{++}, \rho_{22}, \rho_{-+}, \rho_{+-})^T$ , the Lindbladian thus assumes the form

$$\mathcal{L} = \begin{pmatrix} \mathcal{L}_{\text{pop}} & \mathbf{0} & \mathbf{0} \\ \mathbf{0} & \kappa & 0 \\ \mathbf{0} & 0 & \kappa^* \end{pmatrix}, \quad (2.54)$$

where  $\mathcal{L}_{\text{pop}}$  is the  $4 \times 4$  rate matrix previously discussed. The block structure separating the evolution of coherences and populations is characteristic for the BMS approximation when the system Hamiltonian is non-degenerate.

## 2.7 Example: Phonon-Assisted Tunneling

### Model definition

We consider here a three-terminal system, comprised as before of two quantum dots. The left dot is tunnel-coupled to the left lead, the right dot to the right, but in addition, tunneling between the dots is now triggered by a third (bosonic) reservoir that does not change the particle content. That is, without the bosonic reservoir (e.g. phonons or photons) the model would not support a steady state matter current – which is in contrast to the previous model

The system is described by the Hamiltonian

$$H_S = \epsilon_A d_A^\dagger d_A + \epsilon_B d_B^\dagger d_B + U d_A^\dagger d_A d_B^\dagger d_B \quad (2.55)$$

with on-site energies  $\epsilon_A < \epsilon_B$  and Coulomb interaction  $U$ . Since there is no internal tunneling, its energy eigenstates coincide with the localized basis  $|n_A, n_B\rangle$  with the dot occupations  $n_A, n_B \in \{0, 1\}$ . This structure makes it particularly simple to derive a master equation in rate equation representation. The jumps between states are triggered by the electronic tunneling Hamiltonians and the electron-phonon interaction

$$H_I = \sum_k \left( t_{kL} d_A c_{kL}^\dagger + t_{kL}^* c_{kL} d_A^\dagger \right) + \sum_k \left( t_{kR} d_B c_{kR}^\dagger + t_{kR}^* c_{kR} d_B^\dagger \right) + \left( d_A d_B^\dagger + d_B d_A^\dagger \right) \otimes \sum_q \left( h_q a_q + h_q^* a_q^\dagger \right), \quad (2.56)$$

where  $c_{k\alpha}$  are fermionic and  $a_q$  bosonic annihilation operators. The three reservoirs

$$H_B = \sum_k \epsilon_{kL} c_{kL}^\dagger c_{kL} + \sum_k \epsilon_{kR} c_{kR}^\dagger c_{kR} + \sum_q \omega_q a_q^\dagger a_q \quad (2.57)$$

are assumed to remain in separate thermal equilibrium states, such that the reservoir density matrix is assumed to be a product of the single density matrices. This automatically implies that the expectation value of linear combinations of the coupling operators vanishes.

## BMS rate equations

In the weak-coupling limit, the rate matrix will be additively decomposed into contributions resulting from the electronic ( $L, R$ ) and bosonic ( $B$ ) reservoirs  $\mathcal{L} = \mathcal{L}_L + \mathcal{L}_R + \mathcal{L}_B$ . From our results with the single-electron transistor, we may readily reproduce the rates for the electronic jumps. Ordering the basis as  $\rho_{00,00}$ ,  $\rho_{10,10}$ ,  $\rho_{01,01}$ , and  $\rho_{11,11}$  and using for simplicity the wide-band limit  $\Gamma_\alpha(\omega) \approx \Gamma_\alpha$  these read

$$\mathcal{L}_L = \Gamma_L \begin{pmatrix} -f_L(\epsilon_A) & 1 - f_L(\epsilon_A) & 0 & 0 \\ +f_L(\epsilon_A) & -[1 - f_L(\epsilon_A)] & 0 & 0 \\ 0 & 0 & -f_L(\epsilon_A + U) & 1 - f_L(\epsilon_A + U) \\ 0 & 0 & +f_L(\epsilon_A + U) & -[1 - f_L(\epsilon_A + U)] \end{pmatrix}$$

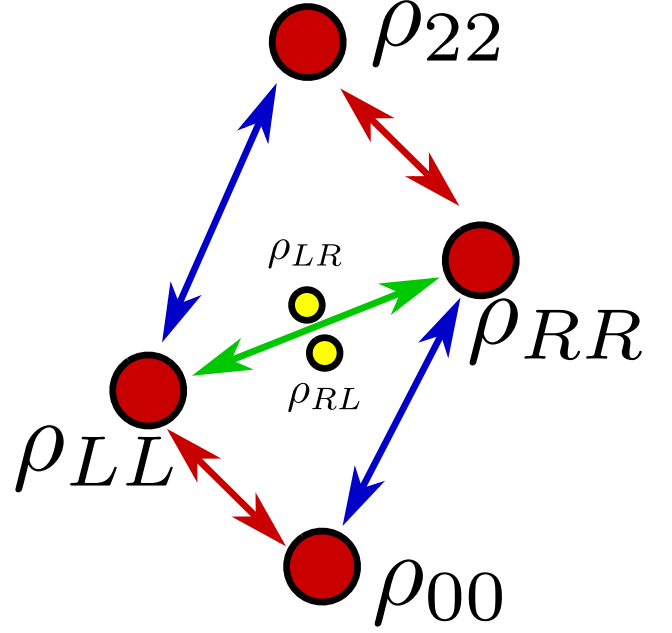
$$\mathcal{L}_R = \Gamma_R \begin{pmatrix} -f_R(\epsilon_B) & 0 & 1 - f_R(\epsilon_B) & 0 \\ 0 & -f_R(\epsilon_B + U) & 0 & 1 - f_R(\epsilon_B + U) \\ +f_R(\epsilon_B) & 0 & -[1 - f_R(\epsilon_B)] & 0 \\ 0 & +f_R(\epsilon_B + U) & 0 & -[1 - f_R(\epsilon_B + U)] \end{pmatrix}, \quad (2.58)$$

where the electronic tunneling rates are as usual obtained via (in the wide-band limit)  $\Gamma_\alpha \approx \Gamma_\alpha(\omega) = 2\pi \sum_k |t_{k\alpha}|^2 \delta(\omega - \epsilon_{k\alpha})$  from the microscopic tunneling amplitudes  $t_{k\alpha}$ . We note that the Fermi functions are evaluated at the energy difference of the jump to which they refer. Although energy may be transferred between the left and right junctions without the presence of phonons, it is not possible to transfer charges.

For the spin-boson example, we have also already calculated the correlation function for the phonons for a spin-boson model in Sec. 1.3.6. Since the reservoir coupling operator is identical, we may use our result from Eq. (1.150).

$$\gamma(\omega) = \Gamma(+\omega)\Theta(+\omega)[1 + n_B(+\omega)] + \Gamma(-\omega)\Theta(-\omega)n_B(-\omega) = \tilde{\Gamma}(\omega)[1 + n_B(\omega)], \quad (2.59)$$

Figure 2.7: Configuration space of the four populations with allowed transitions. Only two coherences of equally charged states can be created, but they decouple from the evolution of populations and decay. Each of the reservoirs (blue for left, red for right, green for phonon) can for this model only trigger specific transitions.



where  $\Gamma(\omega) = 2\pi \sum_k |h_k|^2 \delta(\omega - \omega_k)$  was the spectral coupling density and  $n_B(\omega)$  denoted the Bose-Einstein distribution function and  $\tilde{\Gamma}(\omega)$  the analytic continuation of  $\Gamma(\omega)$  to the complete real axis as an odd function. For consistency, we just note that the KMS condition is obeyed. With this, we may readily evaluate the rates due to the phonon reservoirs, i.e., we have with  $\Gamma = \Gamma(\epsilon_B - \epsilon_A)$

$$\mathcal{L}_B = \Gamma \begin{pmatrix} 0 & 0 & 0 & 0 \\ 0 & -n_B(\epsilon_B - \epsilon_A) & 1 + n_B(\epsilon_B - \epsilon_A) & 0 \\ 0 & +n_B(\epsilon_B - \epsilon_A) & -[1 + n_B(\epsilon_B - \epsilon_A)] & 0 \\ 0 & 0 & 0 & 0 \end{pmatrix}. \quad (2.60)$$

These rate equations just describe the evolution of the population in the energy eigenbasis, the coherences decouple from that, see Fig. 2.7.

## BMS currents

The rate matrices in Eqs. (2.58) and (2.60) can be used to determine all currents. We have a three terminal system, where the phonon terminal only allows for the exchange of energy, i.e., in total we can calculate five non-vanishing currents. With the conservation laws on matter and energy currents, we can at steady state eliminate two of these, and the entropy production rate becomes

$$\begin{aligned} \dot{\mathcal{S}}_i &= -\beta_{\text{ph}} \bar{I}_E^B - \beta_L (\bar{I}_E^L - \mu_L \bar{I}_M^L) - \beta_R (\bar{I}_E^R - \mu_R \bar{I}_M^R) \\ &= -\beta_{\text{ph}} \bar{I}_E^B - \beta_L (\bar{I}_E^L - \mu_L \bar{I}_M^L) + \beta_R (\bar{I}_E^L + \bar{I}_E^B - \mu_R \bar{I}_M^L) \\ &= (\beta_R - \beta_{\text{ph}}) \bar{I}_E^B + (\beta_R - \beta_L) \bar{I}_E^L + (\beta_L \mu_L - \beta_R \mu_R) \bar{I}_M^L, \end{aligned} \quad (2.61)$$

which has the characteristic affinity-flux form. In usual electronic setups, the electronic temperatures will be the same  $\beta_{\text{el}} = \beta_L = \beta_R$ , such that the entropy production further reduces to

$$\dot{\mathcal{S}}_i = (\beta_{\text{el}} - \beta_{\text{ph}}) \bar{I}_E^B + \beta_{\text{el}} (\mu_L - \mu_R) \bar{I}_M^L \geq 0, \quad (2.62)$$

where we can identify the term  $(\mu_L - \mu_R) \bar{I}_M^L$  as a power consumed or produced by the device. Furthermore, we note that the device obeys the tight-coupling property: Every electron traversing

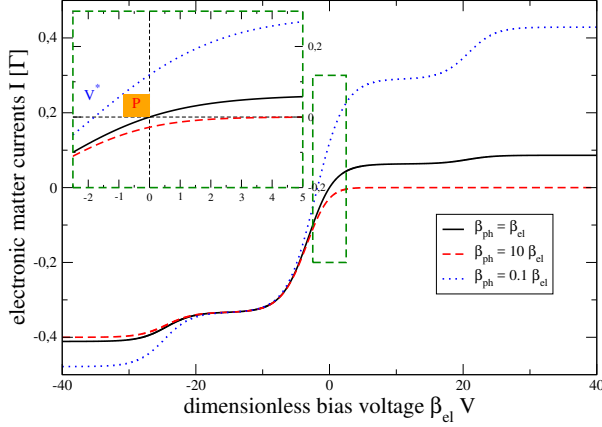


Figure 2.8: Electronic matter current in units of  $\Gamma_L = \Gamma_R = \Gamma$  versus dimensionless bias voltage  $\beta_{\text{el}}V$ . For low phonon temperatures  $\beta_{\text{ph}}(\epsilon_B - \epsilon_A) \gg 1$ , the current cannot flow from left to right, such that the system acts as a rectifier (dashed red). For large phonon temperatures  $\beta_{\text{ph}}(\epsilon_B - \epsilon_A) \ll 1$ , the energy driving the current against the bias (see zoomed inset) is supplied by the phonon bath. Other parameters:  $\beta_{\text{el}}\epsilon_B = 2$ ,  $\beta_{\text{el}}\epsilon_A = 0$ ,  $\beta_{\text{el}}U = 10$ ,  $J_B = \Gamma$ ,  $\beta_L = \beta_R = \beta_{\text{el}}$ , and  $\mu_L = +V/2 = -\mu_R$ .

the system from left to right must absorb energy  $\epsilon_B - \epsilon_A$  from the phonon reservoir  $\bar{I}_E^B = (\epsilon_B - \epsilon_A)\bar{I}_M^L$ . Therefore, the entropy production can also be written as

$$\dot{\bar{S}}_i = [(\beta_{\text{el}} - \beta_{\text{ph}})(\epsilon_B - \epsilon_A) + \beta_{\text{el}}(\mu_L - \mu_R)]\bar{I}_M^L \geq 0. \quad (2.63)$$

We note that the prefactor of the matter current vanishes at

$$V^* = \mu_L^* - \mu_R^* = \left( \frac{T_{\text{el}}}{T_{\text{ph}}} - 1 \right) (\epsilon_B - \epsilon_A). \quad (2.64)$$

Since the prefactor switches sign at this voltage, the matter current must vanish at this voltage, too – otherwise the entropy production would not be positive. Without calculation, we have therefore found that at bias voltage  $V^*$  the current must vanish.

Noting that the total entropy production is positive does not imply that all contributions are separately positive. Fig. 2.8 displays the current as a function of the bias voltage for different electronic and phonon temperature configurations. It is visible that at zero bias, the matter current does not vanish when electron and phonon temperatures are not chosen equal.

We concentrate on the simple case discussed before and use  $\beta_L = \beta_R = \beta_{\text{el}}$  and  $\beta_{\text{ph}} = \beta_B$ . In regions where the current runs against the bias, the power

$$P = -(\mu_L - \mu_R)\bar{I}_M^L \quad (2.65)$$

becomes positive, and we can define an efficiency via

$$\eta = \frac{-(\mu_L - \mu_R)\bar{I}_M^L}{\dot{Q}_{\text{in}}}\Theta(P), \quad (2.66)$$

where  $\dot{Q}_{\text{in}}$  is the heat entering the system from the hot reservoir. The sole purpose of the Heaviside function is just to avoid misinterpretations of the efficiency. Consequently, when the phonon temperature is larger than the electron temperature  $T_{\text{ph}} > T_{\text{el}}$ , the input heat is given by the positive energy flow from the hot phonon bath into the system, such that – due to the tight-coupling property – the efficiency becomes trivially dependent on the bias voltage

$$\eta_{T_{\text{ph}} > T_{\text{el}}} = \frac{P}{\bar{I}_E^B}\Theta(P) = -\frac{V}{\epsilon_B - \epsilon_A}\Theta(P). \quad (2.67)$$

At first sight, one might think that this efficiency could become larger than one. It should be kept in mind however that it is only valid in regimes where the power (2.65) is positive, which limits the applicability of these efficiencies to voltages within  $V = 0$  and  $V = V^*$  from Eq. (2.64). The maximum efficiency is reached at  $V = V^*$  and reads

$$\eta_{T_{\text{ph}} > T_{\text{el}}} < \eta_{\text{max}} = 1 - \frac{T_{\text{el}}}{T_{\text{ph}}} = \eta_{\text{Ca}}, \quad (2.68)$$

and thus, the efficiency is upper-bounded by Carnot efficiency

$$\eta_{\text{Ca}} = 1 - \frac{T_{\text{cold}}}{T_{\text{hot}}}. \quad (2.69)$$

In the opposite case, where  $T_{\text{ph}} < T_{\text{el}}$ , the input heat is given by the sum of the energy currents entering from the hot electronic leads  $\dot{Q}_{\text{in}} = \dot{Q}^L + \dot{Q}^R = \bar{I}_E^L + \bar{I}_E^R + P = -\bar{I}_E^B + P$ , such that the efficiency becomes

$$\eta_{T_{\text{ph}} < T_{\text{el}}} = \frac{P}{-\bar{I}_E^B + P} = \frac{(\mu_L - \mu_R)}{(\epsilon_B - \epsilon_A) + (\mu_L - \mu_R)} = \frac{1}{1 + \frac{\epsilon_B - \epsilon_A}{\mu_L - \mu_R}}, \quad (2.70)$$

which also trivially depends on the bias voltage. Inserting the maximum bias voltage with positive power in Eq. (2.64) we obtain the maximum efficiency

$$\eta_{T_{\text{ph}} < T_{\text{el}}} < \frac{1}{1 + \frac{1}{\frac{T_{\text{el}}}{T_{\text{ph}}}-1}} = 1 - \frac{T_{\text{ph}}}{T_{\text{el}}}, \quad (2.71)$$

which is also just the Carnot efficiency.

Unfortunately, Carnot efficiencies are reached at vanishing current, i.e., at zero power. At these parameters, a thermoelectric device is useless. It is therefore more practical to consider the efficiency at maximum power. However, since the currents depend in a highly nonlinear fashion on all parameters (coupling constants, temperatures, chemical potentials, and system parameters), this becomes a numerical optimization problem – unless one restricts the analysis to the linear response regime.

Also the evolution of the coherences decomposes additively. The contribution of the electronic leads to the decay of coherences is similar as in Eq. (2.53), just the limit  $T \rightarrow 0$  has to be taken in the rates. However, we do now have an additional contribution from the phonons that lead to a non-vanishing rate  $\gamma_{-+,-+}$  and further increases the decay of coherences.

## 2.8 Example: Attainability of cooling

If a system couples to two reservoirs allowing only for energy exchange, the second law will tell us that heat can only flow from the hot one to the cold one. However, with three terminals, such a construction is in principle possible. Then, one could use heat from a work reservoir ( $w$ ) to pump heat from a cold reservoir ( $c$ ) into a hot reservoir ( $h$ ).

So we consider the case

$$\beta_c > \beta_h, \beta_w, \quad (2.72)$$

or  $T_c < T_h, T_w$ . The second law reads at steady state

$$-\beta_c \bar{I}_E^{(c)} - \beta_h \bar{I}_E^{(h)} - \beta_w \bar{I}_E^{(w)} = (\beta_w - \beta_c) \bar{I}_E^{(c)} + (\beta_w - \beta_h) \bar{I}_E^{(h)} \geq 0, \quad (2.73)$$

where we have used that  $\bar{I}_E^{(c)} + \bar{I}_E^{(h)} + \bar{I}_E^{(w)} = 0$ . To pump heat from the cold reservoir into the hot one, we require  $\bar{I}_E^{(c)} > 0$  and  $\bar{I}_E^{(h)} < 0$ . Since  $\beta_w - \beta_c < 0$  we see that the first term is negative. Therefore, to meet a positive entropy production rate, the temperatures have to obey a hierarchy

$$\beta_c > \beta_h > \beta_w, \quad (2.74)$$

such that the work reservoir needs to be the hottest one of all.

## Two-level system

One can easily show that cooling does not work if the system is just a two-level one with  $E_0 < E_1$ : Assuming a vectorization of  $\text{vec}(\rho) = (\rho_{00}, \rho_{11})^T$ , the BMS rate matrix in the system energy eigenbasis then becomes under the usual additivity assumptions

$$\mathcal{L}_2 = \Gamma_c \begin{pmatrix} -n_c & +(1+n_c) \\ +n_c & -(1+n_c) \end{pmatrix} + \Gamma_h \begin{pmatrix} -n_h & +(1+n_h) \\ +n_h & -(1+n_h) \end{pmatrix} + \Gamma_w \begin{pmatrix} -n_w & +(1+n_w) \\ +n_w & -(1+n_w) \end{pmatrix}, \quad (2.75)$$

where the Bose distribution reads

$$n_\nu = \frac{1}{e^{\beta_\nu \Delta E} - 1}, \quad \Delta E = E_1 - E_0 > 0. \quad (2.76)$$

The stationary solution of the two-level system becomes

$$\begin{aligned} \bar{P}_0 &= \frac{\Gamma_c(1+n_c) + \Gamma_h(1+n_h) + \Gamma_w(1+n_w)}{\Gamma_c(1+2n_c) + \Gamma_h(1+2n_h) + \Gamma_w(1+2n_w)} = \frac{1 + \bar{n}}{1 + 2\bar{n}}, \\ \bar{P}_1 &= \frac{\Gamma_c n_c + \Gamma_h n_h + \Gamma_w n_w}{\Gamma_c(1+2n_c) + \Gamma_h(1+2n_h) + \Gamma_w(1+2n_w)} = \frac{\bar{n}}{1 + 2\bar{n}}, \end{aligned} \quad (2.77)$$

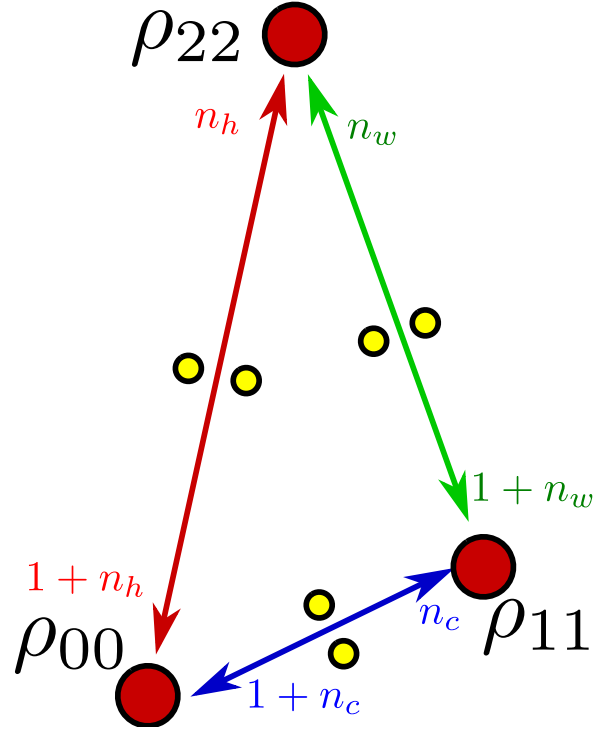
and we see that it just depends on some average thermal parameter  $\bar{n} = \frac{\Gamma_c n_c + \Gamma_h n_h + \Gamma_w n_w}{\Gamma_c + \Gamma_h + \Gamma_w}$ . We can use it to calculate the stationary energy current from the cold reservoir into the system

$$\bar{I}_E^{(c)} = (E_1 - E_0) \frac{\Gamma_c [\Gamma_h(n_c - n_h) + \Gamma_w(n_c - n_w)]}{\Gamma_c(1+2n_c) + \Gamma_h(1+2n_h) + \Gamma_w(1+2n_w)} < 0. \quad (2.78)$$

A two level system cannot be used to cool the cold reservoir (at least not under the weak coupling assumptions that we used to derive the master equation). This follows from  $\beta_c > \beta_w$  and  $\beta_c > \beta_h$ , which implies  $n_c < n_w$  and auch  $n_c < n_h$ , since in the Bose distributions we always have the same energy difference entering. Furthermore we see that for  $\Gamma_w \rightarrow 0$  we recover the energy current through a two-level two-terminal system, which will always flow from hot to cold

$$\lim_{\Gamma_w \rightarrow 0} \bar{I}_E^{(c)} = (E_1 - E_0) \frac{\Gamma_c \Gamma_h (n_c - n_h)}{\Gamma_c(1+2n_c) + \Gamma_h(1+2n_h)}. \quad (2.79)$$

Figure 2.9: Configuration space of a generic three level system. Individual transitions between energy levels are (dominantly) driven selectively by the cold (blue), the hot (red), and the work (green) reservoirs, whereas coherences are assumed to decouple. By tuning the energy levels, it is possible to drive the system through a cycle dominantly in a counterclockwise direction, thus effectively absorbing heat from the cold and work reservoirs cooling them, and dumping it into the hot reservoir (heating it). One realization of this model could be via phonon-assisted tunneling in the Coulomb-blockade limit, compare Fig. 2.7.



### Three-level system

The situation is different for a three-level system

$$E_0 < E_1 < E_2. \quad (2.80)$$

Here, it is possible to cool the cold reservoir, when the transition  $E_0 \leftrightarrow E_2$  is (dominantly) driven by the hot reservoir, the transition  $E_1 \leftrightarrow E_2$  by the work reservoir, and the transition  $E_0 \leftrightarrow E_1$  by the cold reservoir. Such a selective coupling could be realized by the spectral densities of the reservoirs being peaked around the fitting transition energies. Alternatively, one could enforce this on the level of the coupling Hamiltonian. For example, the interaction  $H_I^{(c)} = [|E_0\rangle\langle E_1| + |E_1\rangle\langle E_0|] \otimes \sum_k (h_{kc}b_{kc} + h_{kc}^*b_{kc}^\dagger)$  would selectively drive transitions between the lowest and first excited state. Assuming that such a selective coupling can be implemented with bosonic reservoirs, the BMS rate matrix becomes for the vectorization  $vec(\rho) = (\rho_{00}, \rho_{11}, \rho_{22})^T$

$$\mathcal{L}_3 = \begin{pmatrix} -\Gamma_c n_c - \Gamma_h n_h & \Gamma_c(1 + n_c) & \Gamma_h(1 + n_h) \\ \Gamma_c n_c & -\Gamma_c(1 + n_c) - \Gamma_w n_w & \Gamma_w(1 + n_w) \\ \Gamma_h n_h & \Gamma_w n_w & -\Gamma_h(1 + n_h) - \Gamma_w(1 + n_w) \end{pmatrix}, \quad (2.81)$$

compare also Fig. 2.9. Here, different transition energies enter the Bose distributions

$$n_c = \frac{1}{e^{\beta_c(E_1 - E_0)} - 1}, \quad n_h = \frac{1}{e^{\beta_h(E_2 - E_0)} - 1}, \quad n_w = \frac{1}{e^{\beta_w(E_2 - E_1)} - 1}, \quad (2.82)$$

and  $\Gamma_c = \Gamma_c(E_1 - E_0)$ ,  $\Gamma_h = \Gamma_h(E_2 - E_0)$  as well as  $\Gamma_w = \Gamma_w(E_2 - E_1)$ . Again, we can calculate the stationary state analytically and from that the current entering the system from the hot reservoir, which is a bit lengthy (not shown). When the temperature of the work reservoir goes to infinity however  $n_w \rightarrow \infty$ , one obtains the simpler expression

$$\lim_{n_w \rightarrow \infty} \bar{I}_E^{(c)} = (E_1 - E_0) \frac{\Gamma_c \Gamma_h (n_c - n_h)}{\Gamma_c(1 + 3n_c) + \Gamma_h(1 + 3n_h)}. \quad (2.83)$$

Now, since the Bose distributions have different energies in their arguments, one can actually achieve  $n_c > n_h$  whenever

$$\beta_h(E_2 - E_0) > \beta_c(E_1 - E_0), \quad (2.84)$$

which despite  $\beta_c > \beta_h$  can be reached by a corresponding configuration of the energy levels. Altogether, one needs at least three energy levels for cooling. To calculate the coefficient of performance, we need the energy current entering the system from the work reservoir

$$\lim_{n_w \rightarrow \infty} \bar{I}_E^{(w)} = (E_2 - E_1) \frac{\Gamma_c \Gamma_h (n_c - n_h)}{\Gamma_c (1 + 3n_c) + \Gamma_h (1 + 3n_h)}. \quad (2.85)$$

With this, the coefficient of performance becomes

$$\text{COP}_{\text{cooling}} = \frac{E_1 - E_0}{E_2 - E_1} \Theta(n_c - n_h) \leq \frac{T_c}{T_h - T_c}, \quad (2.86)$$

which can be shown with Eq. (2.84).



# Chapter 3

## Full Counting Statistics

Previous definitions of currents were based on the phenomenologic identification of the change of a system observable (energy, particle number) with additive contributions from the reservoirs. Sometimes however one is also interested in more information beyond the mean values, i.e., the statistics of single jumps into the reservoir. In Full Counting Statistics (FCS) for example one is interested in the probability distribution  $P_n(t)$  denoting the net number of particles  $n \in \mathbb{Z}$  transferred to a specific reservoir after time  $t$ . This can be generalized to full energy counting statistics, which we will also consider in this chapter.

### 3.1 Phenomenologic Introduction of counting fields

#### 3.1.1 Single jump type

Suppose that by some method we can identify jump terms between different states in the master equation, i.e., we can separate the total dissipator as

$$\mathcal{L} = \mathcal{L}_0 + \mathcal{L}_1, \quad (3.1)$$

where  $\mathcal{L}_1$  denotes the jump term and  $\mathcal{L}_0$  the jump-free evolution (containing the isolated dynamics of the system or un-monitored jumps). For the rate matrix (2.40) of the SET for example, we could ask for the total number of jumps over the left barrier. Then, a suitable decomposition would be

$$\mathcal{L}_0 = \begin{pmatrix} -\Gamma_L f_L - \Gamma_R f_R & \Gamma_R(1 - f_R) \\ \Gamma_R f_R & -\Gamma_R(1 - f_R) - \Gamma_L(1 - f_L) \end{pmatrix}, \quad \mathcal{L}_1 = \begin{pmatrix} 0 & \Gamma_L(1 - f_L) \\ \Gamma_L f_L & 0 \end{pmatrix}. \quad (3.2)$$

We would like to have an expansion of the total propagator

$$\mathcal{P}(t) = e^{\mathcal{L}t} \quad : \quad \rho(t) = \mathcal{P}(t)\rho_0, \quad (3.3)$$

that makes the number of such jumps explicit. One way to obtain such an expansion proceeds similar to the time evolution operator in the interaction picture for closed systems. Considering  $\mathcal{L}_0$  as the free evolution and  $\mathcal{L}_1$  as the perturbation, we transform to another picture by using the **free propagator**  $\mathcal{P}_0$

$$\rho(t) = \mathcal{P}_0(t)\tilde{\rho}(t), \quad \mathcal{P}_0(t) = e^{\mathcal{L}_0 t}. \quad (3.4)$$

Inserting this in the evolution equation for  $\rho$ , we obtain an equation for  $\tilde{\rho}$

$$\dot{\tilde{\rho}} = e^{-\mathcal{L}_0 t} \mathcal{L}_1 e^{\mathcal{L}_0 t} \tilde{\rho}. \quad (3.5)$$

Formally integrating yields

$$\tilde{\rho}(t) = \rho_0 + \int_0^t e^{-\mathcal{L}_0 t_1} \mathcal{L}_1 e^{\mathcal{L}_0 t_1} \tilde{\rho}(t_1) dt_1. \quad (3.6)$$

In this equation, we can now recursively insert the l.h.s., yielding the expansion

$$\begin{aligned} \tilde{\rho}(t) &= \rho_0 + \int_0^t dt_1 e^{-\mathcal{L}_0 t_1} \mathcal{L}_1 e^{\mathcal{L}_0 t_1} \rho_0 + \int_0^t dt_1 \int_0^{t_1} dt_2 e^{-\mathcal{L}_0 t_1} \mathcal{L}_1 e^{\mathcal{L}_0 t_1} e^{-\mathcal{L}_0 t_2} \mathcal{L}_1 e^{\mathcal{L}_0 t_2} \rho_0 + \dots \\ &= \left[ \mathbf{1} + \int_0^t dt_1 e^{-\mathcal{L}_0 t_1} \mathcal{L}_1 e^{\mathcal{L}_0 t_1} + \int_0^t dt_1 \int_0^{t_1} dt_2 e^{-\mathcal{L}_0 t_1} \mathcal{L}_1 e^{\mathcal{L}_0(t_1-t_2)} \mathcal{L}_1 e^{\mathcal{L}_0 t_2} + \dots \right] \rho_0. \end{aligned} \quad (3.7)$$

Relabeling the ordering of times and transforming back into the original frame then yields

$$\begin{aligned} \rho(t) &= \left[ e^{\mathcal{L}_0 t} + \int_0^t dt_1 e^{\mathcal{L}_0(t-t_1)} \mathcal{L}_1 e^{\mathcal{L}_0(t_1-0)} + \int_0^t dt_2 \int_0^{t_2} dt_1 e^{\mathcal{L}_0(t-t_2)} \mathcal{L}_1 e^{\mathcal{L}_0(t_2-t_1)} \mathcal{L}_1 e^{\mathcal{L}_0(t_1-0)} \right. \\ &\quad \left. \dots + \int_0^t dt_n \int_0^{t_n} dt_{n-1} \dots \int_0^{t_2} dt_1 e^{\mathcal{L}_0(t-t_n)} \mathcal{L}_1 e^{\mathcal{L}_0(t_n-t_{n-1})} \mathcal{L}_1 \dots \mathcal{L}_1 e^{\mathcal{L}_0(t_1-0)} + \dots \right] \rho_0. \end{aligned} \quad (3.8)$$

Thereby, we have decomposed the full propagator into a series of jumps

$$\begin{aligned} \mathcal{P}(t) &= e^{\mathcal{L}_0(t-0)} + \int_0^t e^{\mathcal{L}_0(t-t_1)} \mathcal{L}_1 e^{\mathcal{L}_0(t_1-0)} dt_1 \\ &\quad + \int_0^t dt_2 \int_0^{t_2} dt_1 e^{\mathcal{L}_0(t-t_2)} \mathcal{L}_1 e^{\mathcal{L}_0(t_2-t_1)} \mathcal{L}_1 e^{\mathcal{L}_0(t_1-0)} + \dots, \\ &= \mathcal{P}_0(t-0) + \int_0^t dt_1 \mathcal{P}_0(t-t_1) \mathcal{L}_1 \mathcal{P}_0(t_1-0) \\ &\quad + \int_0^t dt_2 \int_0^{t_2} dt_1 \mathcal{P}_0(t-t_2) \mathcal{L}_1 \mathcal{P}_0(t_2-t_1) \mathcal{L}_1 \mathcal{P}_0(t_1-0) + \dots, \end{aligned} \quad (3.9)$$

which has the appealing interpretation that we have periods of free evolutions interrupted by single jump events, see Fig. 3.1.

This decomposition can alternatively be obtained with the Laplace transform of the propagator

$$\mathcal{P}(z) = \int_0^\infty \mathcal{P}(t) e^{-zt} dt = \sum_{n=0}^\infty \frac{\mathcal{L}^n}{n!} \int_0^\infty t^n e^{-zt} dt = \sum_{n=0}^\infty \frac{\mathcal{L}^n}{n!} \frac{n!}{z^{n+1}} = \frac{1}{z} \left[ \mathbf{1} - \frac{\mathcal{L}}{z} \right]^{-1} = [z\mathbf{1} - \mathcal{L}]^{-1}. \quad (3.10)$$

It is simpler to expand the Laplace-transform of the propagator

$$\begin{aligned} \mathcal{P}(z) &= [z\mathbf{1} - \mathcal{L}_0 - \mathcal{L}_1]^{-1} = [(z\mathbf{1} - \mathcal{L}_0)(\mathbf{1} - (z\mathbf{1} - \mathcal{L}_0)^{-1} \mathcal{L}_1)]^{-1} \\ &= (\mathbf{1} - (z\mathbf{1} - \mathcal{L}_0)^{-1} \mathcal{L}_1)^{-1} (z\mathbf{1} - \mathcal{L}_0)^{-1}. \end{aligned} \quad (3.11)$$

At this time, it is useful to introduce the Laplace transform of the free propagator

$$\mathcal{P}_0(z) = [z\mathbf{1} - \mathcal{L}_0]^{-1} = \int_0^\infty e^{\mathcal{L}_0 t} e^{-zt} dt. \quad (3.12)$$

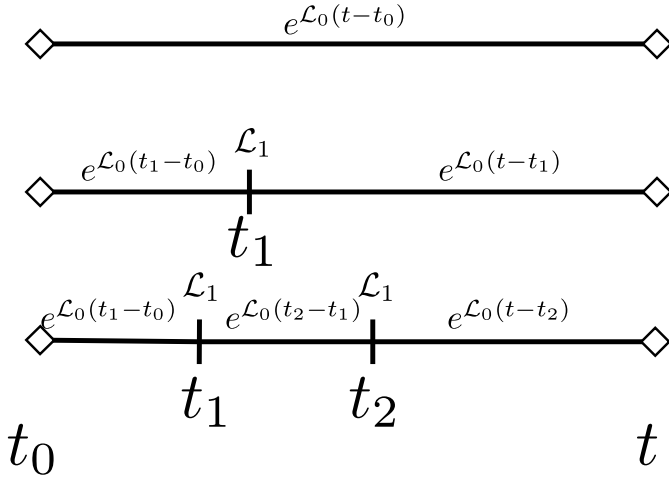


Figure 3.1: Illustration of the first three terms in the series expansion in Eq. (3.9). Periods of free evolution (lines) are interrupted by instantaneous jumps (marks). In the end, one has to integrate over all times at which jumps may occur.

Using it, we can expand the full propagator as

$$\mathcal{P}(z) = \sum_{n=0}^{\infty} [\mathcal{P}_0(z)\mathcal{L}_1]^n \mathcal{P}_0(z) = \mathcal{P}_0(z) + \mathcal{P}_0(z)\mathcal{L}_1\mathcal{P}_0(z) + \mathcal{P}_0(z)\mathcal{L}_1\mathcal{P}_0(z)\mathcal{L}_1\mathcal{P}_0(z) + \dots \quad (3.13)$$

We remark that the convolution property holds also for matrix-valued functions (provided we do not change their order)

$$\begin{aligned} \int_0^{\infty} dt e^{-zt} \int_0^t d\tau \mathcal{A}(t-\tau)\mathcal{B}(\tau) &= \int_0^{\infty} d\tau \int_{\tau}^{\infty} dt \mathcal{A}(t-\tau)e^{-zt}\mathcal{B}(\tau) \\ &= \int_0^{\infty} \left[ \int_0^{\infty} dt' \mathcal{A}(t')e^{-zt'} \right] e^{-z\tau}\mathcal{B}(\tau) d\tau = \mathcal{A}(z)\mathcal{B}(z). \end{aligned} \quad (3.14)$$

Here, we have exchanged in the first equality sign the integrals, using that the total integration region is the same. Applying this recursively, we can indeed show that (3.13) is equivalent to the convolution series (3.9).

The benefit of the series expansion (3.9) is that it yields a decomposition where we can readily write down the probabilities for  $n$  jump events during time  $t$

$$P_n(t) = \text{Tr} \left\{ \int_0^t dt_n \dots \int_0^{t_2} dt_1 e^{\mathcal{L}_0(t-t_n)} \mathcal{L}_1 \dots \mathcal{L}_1 e^{\mathcal{L}_0(t_2-t_1)} \mathcal{L}_1 e^{\mathcal{L}_0(t_1-0)} \rho_0 \right\}, \quad (3.15)$$

which looks way more convenient in Laplace space

$$P_n(z) = \text{Tr} \{ [\mathcal{P}_0(z)\mathcal{L}_1]^n \mathcal{P}_0(z)\rho_0 \}. \quad (3.16)$$

But suppose we are only given the full Lindbladian  $\mathcal{L} = \mathcal{L}_0 + \mathcal{L}_1$ . Is there a convenient way to sort out only those contributions that have exactly  $n$  jump events, without the need to perform a jump (or Dyson) series expansion?

Taking the identity

$$\frac{1}{2\pi} \int_{-\pi}^{+\pi} e^{+in\chi} e^{-im\chi} d\chi = \delta_{nm} \quad (3.17)$$

into account, it becomes quite obvious that one can infer the statistics of such jumps with following replacement

$$\mathcal{L}_1 \rightarrow \mathcal{L}_1 e^{+i\chi}, \quad \mathcal{L} \rightarrow \mathcal{L}(\chi) = \mathcal{L}_0 + \mathcal{L}_1 e^{+i\chi} \quad (3.18)$$

in the full propagator  $\mathcal{P}(\chi, t) = e^{\mathcal{L}(\chi)t}$ . Then, terms with powers  $\mathcal{L}_1^n$  go as  $e^{+in\chi}$ , and we can project on them by performing an appropriate integration according to Eq. (3.17).

The new variable  $\chi$  is conventionally called **counting field**. Then, we can use the orthonormality relation (3.17) to conclude

$$P_n(t) = \frac{1}{2\pi} \int_{-\pi}^{+\pi} \text{Tr} \{ \mathcal{P}(\chi, t) \rho_0 \} e^{-in\chi} d\chi, \quad P_n(z) = \frac{1}{2\pi} \int_{-\pi}^{+\pi} \text{Tr} \{ \mathcal{P}(\chi, z) \rho_0 \} e^{-in\chi} d\chi. \quad (3.19)$$

The corresponding Moment-generating function is given by the Fourier transform of the probability distribution, and we can infer the definition below.

**Def. 12** (Moment- and Cumulant-Generating function). *For a generalized generator  $\mathcal{L}(\chi)$ , the moment-generating function for an initial state  $\rho_0$  is*

$$M(\chi, t) = \text{Tr} \{ e^{\mathcal{L}(\chi)t} \rho_0 \}. \quad (3.20)$$

*Once this function is known, all moments can be computed by differentiation with respect to the counting field*

$$\langle n^k \rangle_t = \sum_n n^k P_n(t) = (-i\partial_\chi)^k M(\chi, t) \Big|_{\chi=0}. \quad (3.21)$$

*The cumulant-generating function is given by*

$$C(\chi, t) = \ln M(\chi, t), \quad (3.22)$$

*and by differentiation with respect to the counting field all cumulants are recovered  $\langle\langle n^k \rangle\rangle_t = (-i\partial_\chi)^k C(\chi, t) \Big|_{\chi=0}$ .*

An easy way to see that moments can be obtained by differentiation with respect to the counting field  $\chi$  is to invert the FT in Eq. (3.19)

$$M(\chi, t) = \sum_n e^{+in\chi} P_n(t). \quad (3.23)$$

This makes it quite obvious that  $\langle n^k \rangle = (-i\partial_\chi)^k M(\chi, t) \Big|_{\chi \rightarrow 0}$ . Cumulants and moments are of course related, we just summarize relations for the lowest few cumulants

$$\begin{aligned} \langle\langle n \rangle\rangle &= \langle n \rangle, \\ \langle\langle n^2 \rangle\rangle &= \langle n^2 \rangle - \langle n \rangle^2, \\ \langle\langle n^3 \rangle\rangle &= \langle n^3 \rangle - 3 \langle n \rangle \langle n^2 \rangle + 2 \langle n \rangle^3, \\ \langle\langle n^4 \rangle\rangle &= \langle n^4 \rangle - 4 \langle n \rangle \langle n^3 \rangle - 3 \langle n^2 \rangle^2 + 12 \langle n \rangle^2 \langle n^2 \rangle - 6 \langle n \rangle^4. \end{aligned} \quad (3.24)$$

Obviously, the first two cumulants are just related to the **mean of a distribution** and the **width of a distribution**. For unimodal distributions, the third cumulant (skewness) and the fourth cumulant (kurtosis) describe the shape of the distribution near its maximum. In contrast to moments, higher cumulants are inert when a trivial transformation such as a simple shift is performed on a probability distribution.

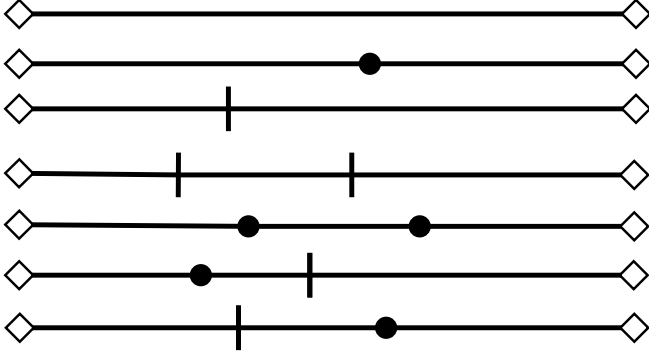


Figure 3.2: Illustration of the first 7 terms in the series expansion in Eq. (3.26). Periods of free evolution (lines) are interrupted by instantaneous jumps of the first (marks) or second (balls) type. In practice, many diagrams may vanish as e.g. for a system hosting at most one electron one will not observe two electrons jumping out subsequently.

### 3.1.2 Different jump types

So how is it then possible to count different jumps? Regarding the example of the SET, this could mean that one could distinguish jumps into the system over the left barrier and jumps out of the system over the left barrier. We can base this on the already existing expansion. By further splitting the free Liouvillian  $\mathcal{L}_0 = \mathcal{L}_{00} + \mathcal{L}_2$  we would obtain the decomposition

$$\mathcal{P}_0(z) = \sum_{m=0}^{\infty} [\mathcal{P}_{00}(z)\mathcal{L}_2]^m \mathcal{P}_{00}(z), \quad (3.25)$$

which we can insert in Eq. (3.13). The first terms of the resulting expansion would read

$$\begin{aligned} \mathcal{P}(z) &= \mathcal{P}_{00}(z) + \mathcal{P}_{00}(z)\mathcal{L}_1\mathcal{P}_{00}(z) + \mathcal{P}_{00}(z)\mathcal{L}_2\mathcal{P}_{00}(z) \\ &\quad + \mathcal{P}_{00}(z)\mathcal{L}_1\mathcal{P}_{00}(z)\mathcal{L}_1\mathcal{P}_{00}(z) + \mathcal{P}_{00}(z)\mathcal{L}_2\mathcal{P}_{00}(z)\mathcal{L}_2\mathcal{P}_{00}(z) \\ &\quad + \mathcal{P}_{00}(z)\mathcal{L}_1\mathcal{P}_{00}(z)\mathcal{L}_2\mathcal{P}_{00}(z) + \mathcal{P}_{00}(z)\mathcal{L}_2\mathcal{P}_{00}(z)\mathcal{L}_1\mathcal{P}_{00}(z) + \dots \end{aligned} \quad (3.26)$$

This becomes pretty involved very soon, and a diagrammatic representation is more useful, see Fig. 3.2. However, we see that with the replacement  $\mathcal{L}_1 \rightarrow \mathcal{L}_1 e^{+i\chi}$  and  $\mathcal{L}_2 \rightarrow \mathcal{L}_2 e^{+i\xi}$  the probability of getting  $n$  jumps of type  $\mathcal{L}_1$  and  $m$  jumps of type  $\mathcal{L}_2$  can be obtained via

$$P_{nm}(z) = \frac{1}{2\pi} \int_{-\pi}^{+\pi} d\chi \frac{1}{2\pi} \int_{-\pi}^{+\pi} d\xi \text{Tr} \{ \mathcal{P}(\chi, \xi, z) \rho_0 \} e^{-in\chi} e^{-im\xi}, \quad (3.27)$$

and similar for the temporal version.

### 3.1.3 Net particle transfers

An important special case arises when we are interested in all trajectories that only lead to a net difference. For example, we may be interested in the net number of particles leaving the system to a certain reservoir. Then, we could count the outgoing jumps ( $\mathcal{L}_+$ ) and the ingoing jumps ( $\mathcal{L}_-$ ) at first separately. From the resulting distribution  $P_{n_{\text{out}}, n_{\text{in}}}(t)$  describing the joint distribution of  $n_{\text{out}} \in \mathbb{Z}^+$  outgoing and  $n_{\text{in}} \in \mathbb{Z}^+$  ingoing jumps during time  $t$ , the required information can be reconstructed

$$P_n(t) = \sum_{n_{\text{out}}, n_{\text{in}}=0}^{\infty} P_{n_{\text{out}}, n_{\text{in}}}(t) \delta_{n_{\text{out}} - n_{\text{in}}, n}. \quad (3.28)$$

Here,  $P_n(t)$  describes the probability of having net  $n \in \mathbb{Z}$  particle transfers into the monitored reservoir. To project out the trajectories that only have the net  $n = n_{\text{out}} - n_{\text{in}}$  particle exchange, we can simply use the replacement  $\mathcal{L}_+ \rightarrow \mathcal{L}_+ e^{+ix}$  and  $\mathcal{L}_- \rightarrow \mathcal{L}_- e^{-ix}$

$$P_n(t) = \frac{1}{2\pi} \int_{-\pi}^{+\pi} d\chi \text{Tr} \{ \mathcal{P}(+\chi, -\chi, t) \rho_0 \} e^{-inx}. \quad (3.29)$$

This means that we can simply use  $\xi = -\chi$  to define the decomposition

$$\mathcal{L}(\chi) = \mathcal{L}_0 + e^{+ix} \mathcal{L}_+ + e^{-ix} \mathcal{L}_- \quad (3.30)$$

and use the standard definition of the moment-generating function  $M(\chi, t) = \text{Tr} \{ e^{\mathcal{L}(\chi)t} \rho_0 \}$  and the derived cumulant-generating function.

### 3.1.4 Long-term dynamics of cumulants

The clear advantage of the description by cumulants however lies in the fact that the long-term evolution of the cumulant-generating function is usually given by the dominant eigenvalue of the Liouvillian

$$C(\chi, t) \approx \lambda(\chi)t, \quad (3.31)$$

where  $\lambda(\chi)$  is the (uniqueness assumed) eigenvalue of the Liouvillian that vanishes at zero counting field  $\lambda(0) = 0$ . For this reason, the dominant eigenvalue is also interpreted as the cumulant-generating function of the stationary current. We recall that the Liouville superoperator is in general non-hermitian and may not have a spectral representation. Nevertheless, we can represent it in Jordan Block form

$$\mathcal{L}(\chi) = Q(\chi) \mathcal{L}_J(\chi) Q^{-1}(\chi), \quad (3.32)$$

where  $Q(\chi)$  is a (non-unitary) similarity matrix and  $\mathcal{L}_J(\chi)$  contains the eigenvalues of the Liouvillian on its diagonal – distributed in blocks with a size corresponding to the eigenvalue multiplicity. We assume that there exists one stationary state  $\bar{\rho}$ , i.e., one eigenvalue  $\lambda(\chi)$  with  $\lambda(0) = 0$  and that all other eigenvalues have a larger negative real part near  $\chi = 0$ . Then, we use this decomposition in the matrix exponential to estimate its long-term evolution

$$\begin{aligned} M(\chi, t) &= \text{Tr} \{ e^{\mathcal{L}(\chi)t} \rho_0 \} = \text{Tr} \left\{ e^{Q(\chi) \mathcal{L}_J(\chi) Q^{-1}(\chi)t} \rho_0 \right\} = \text{Tr} \left\{ Q(\chi) e^{\mathcal{L}_J(\chi)t} Q^{-1}(\chi) \rho_0 \right\} \\ &\rightarrow \text{Tr} \left\{ Q(\chi) \begin{pmatrix} e^{\lambda(\chi)t} & & & \\ & 0 & & \\ & & \ddots & \\ & & & 0 \end{pmatrix} Q^{-1}(\chi) \rho_0 \right\} \\ &= e^{\lambda(\chi)t} \text{Tr} \left\{ Q(\chi) \begin{pmatrix} 1 & & & \\ & 0 & & \\ & & \ddots & \\ & & & 0 \end{pmatrix} Q^{-1}(\chi) \rho_0 \right\} = e^{\lambda(\chi)t} c(\chi) \end{aligned} \quad (3.33)$$

with some polynomial  $c(\chi)$  depending on the matrix  $Q(\chi)$ . This implies that the **cumulant-generating function**

$$C(\chi, t) \equiv \ln M(\chi, t) \xrightarrow{t \rightarrow \infty} \lambda(\chi)t + \ln c(\chi) \approx \lambda(\chi)t \quad (3.34)$$

becomes linear in  $\lambda(\chi)$  and  $t$  for large times. The cumulants can be conveniently determined once the dominant eigenvalue of the Liouvillian is known.

### 3.1.5 Dynamics of current and noise

One is not always in the fortunate position to have the dominant eigenvalue of the Liouvillian as an analytic function of  $\chi$  (as  $\mathcal{L}(\chi)$  becomes usually a large matrix). However, for the important quantities current and the noise, one can derive simplified expressions that only involve the time-dependent density matrix.

With the **generalized density matrix**

$$\rho(\chi, t) = e^{\mathcal{L}(\chi)t} \rho_0, \quad (3.35)$$

we can adopt the convention that  $\rho'(\chi, t) = \partial_\chi \rho(\chi, t)$  and  $\dot{\rho}(\chi, t) = \partial_t \rho(\chi, t)$ . Then, the time-dependent current becomes

$$\begin{aligned} I(t) &\equiv \frac{d}{dt} \langle n(t) \rangle = -i \partial_\chi \text{Tr} \left\{ \frac{d}{dt} \rho(\chi, t) \right\} \Big|_{\chi=0} = -i \partial_\chi \text{Tr} \{ \mathcal{L}(\chi) \rho(\chi, t) \} \Big|_{\chi=0} \\ &= -i \text{Tr} \{ \mathcal{L}'(0) \rho(0, t) \} - i \text{Tr} \{ \mathcal{L}(0) \rho'(0, t) \} \\ &= -i \text{Tr} \{ \mathcal{L}'(0) \rho(t) \}, \end{aligned} \quad (3.36)$$

where we have used that  $\text{Tr} \{ \mathcal{L}(0) \hat{O} \} = 0$  for any operator  $\hat{O}$  due to the trace-conservation obeyed by  $\mathcal{L}(0)$ . Even simpler, in the long-term limit we may use the stationary state  $\mathcal{L}(0) \bar{\rho} = 0$

$$\bar{I} = -i \text{Tr} \{ \mathcal{L}'(0) \bar{\rho} \}. \quad (3.37)$$

The noise becomes

$$\begin{aligned} S(t) &\equiv \frac{d}{dt} (\langle n^2(t) \rangle - \langle n(t) \rangle^2) = (-i \partial_\chi)^2 \text{Tr} \{ \mathcal{L}(\chi) \rho(\chi, t) \} \Big|_{\chi=0} - 2I(t) \cdot \langle n(t) \rangle \\ &= -\text{Tr} \{ \mathcal{L}''(0) \rho(t) \} - 2\text{Tr} \{ \mathcal{L}'(0) \rho'(0, t) \} + 2 [\text{Tr} \{ \mathcal{L}'(0) \rho(t) \}] \cdot [\text{Tr} \{ \rho'(0, t) \}] \\ &= -\text{Tr} \{ \mathcal{L}''(0) \rho(t) \} - 2\text{Tr} \{ \mathcal{L}'(0) \sigma(t) \}, \end{aligned} \quad (3.38)$$

where we have defined the auxiliary matrix

$$\sigma(t) = \partial_\chi \frac{\rho(\chi, t)}{\text{Tr} \{ \rho(\chi, t) \}} \Big|_{\chi=0} = \rho'(0, t) - \rho(t) \text{Tr} \{ \rho'(0, t) \}. \quad (3.39)$$

It obeys the differential equation

$$\begin{aligned} \frac{d}{dt} \sigma(t) &= \partial_\chi \frac{\mathcal{L}(\chi) \rho(\chi, t)}{\text{Tr} \{ \rho(\chi, t) \}} \Big|_{\chi=0} - \partial_\chi \frac{\rho(\chi, t)}{\text{Tr} \{ \rho(\chi, t) \}^2} \text{Tr} \{ \mathcal{L}(\chi) \rho(\chi, t) \} \Big|_{\chi=0} \\ &= \mathcal{L}'(0) \rho(t) + \mathcal{L}(0) \sigma(t) - \rho(t) \text{Tr} \{ \mathcal{L}'(0) \rho(t) \}, \end{aligned} \quad (3.40)$$

and is subject to the initial condition  $\sigma(0) = \mathbf{0}$ .

Summarizing, to obtain both time-dependent current  $I(t)$  and noise  $S(t)$

$$\begin{aligned} I(t) &= -i \text{Tr} \{ \mathcal{L}'(0) \rho(t) \}, \\ S(t) &= -\text{Tr} \{ \mathcal{L}''(0) \rho(t) \} - 2\text{Tr} \{ \mathcal{L}'(0) \sigma(t) \}, \end{aligned} \quad (3.41)$$

one has to solve the coupled (nonlinear) differential equations

$$\begin{aligned} \dot{\rho} &= \mathcal{L} \rho(t), \\ \dot{\sigma} &= [\mathcal{L}'(0) - \text{Tr} \{ \mathcal{L}'(0) \rho(t) \}] \rho(t) + \mathcal{L}(0) \sigma(t), \end{aligned} \quad (3.42)$$

subject to the initial conditions  $\rho(0) = \rho_0$  and  $\sigma(0) = \mathbf{0}$ . Under this evolution, the trace of  $\sigma$  remains conserved, such that  $\sigma(t)$  is always a traceless operator. However, when only interested in the long-term limit, we can linearize this by inserting the stationary current. Encoding the trace of  $\bar{\rho}$  and  $\bar{\sigma}$  into rows of a large matrix, this eventually amounts to solving the equation

$$\begin{pmatrix} & \mathcal{L}(0) & \\ & & \\ 1 & \dots & 1 \end{pmatrix} \begin{pmatrix} | \\ \bar{\rho} \\ | \end{pmatrix} = \begin{pmatrix} 0 \\ \vdots \\ 0 \\ 1 \end{pmatrix} \quad (3.43)$$

first for the steady state  $\bar{\rho}$  (the last row in the matrix implements the normalization). Then, one solves with the stationary current  $\bar{I} = -i\text{Tr}\{\mathcal{L}'(0)\bar{\rho}\}$  the equation

$$\begin{pmatrix} & \mathcal{L}(0) & \\ & & \\ 1 & \dots & 1 \end{pmatrix} \begin{pmatrix} | \\ \bar{\sigma} \\ | \end{pmatrix} = \begin{pmatrix} i\bar{I}\bar{\rho} - \mathcal{L}'(0)\bar{\rho} \\ | \\ 0 \end{pmatrix} \quad (3.44)$$

for  $\bar{\sigma}$ . Inserting the results into (3.41) then also yields the stationary noise.

### 3.1.6 Example: The single-electron transistor

We will illustrate these findings with the simple rate equation of the SET with two junctions. For such rate equations, we can naturally interpret the off-diagonal matrix elements as jump terms. Counting, for example the particles entering the system from the left as positive and leaving to the left as negative, we would get the generalized Liouvillian

$$\mathcal{L}(\chi) = \begin{pmatrix} -\Gamma_L f_L & +\Gamma_L(1-f_L)e^{-i\chi} \\ +\Gamma_L f_L e^{+i\chi} & -\Gamma_L(1-f_L) \end{pmatrix} + \begin{pmatrix} -\Gamma_R f_R & +\Gamma_R(1-f_R) \\ +\Gamma_R f_R & -\Gamma_R(1-f_R) \end{pmatrix}. \quad (3.45)$$

Application of the trace formula for the current yields the known result

$$\bar{I}_M^{(L)} = -i\text{Tr}\{\mathcal{L}'(0)\bar{\rho}\} = (1, 1) \begin{pmatrix} 0 & -\Gamma_L(1-f_L) \\ +\Gamma_L f_L & 0 \end{pmatrix} \begin{pmatrix} 1 - \bar{f} \\ \bar{f} \end{pmatrix} = \dots = \frac{\Gamma_L \Gamma_R}{\Gamma_L + \Gamma_R} (f_L - f_R), \quad (3.46)$$

where  $\bar{f} = (\Gamma_L f_L + \Gamma_R f_R)/(\Gamma_L + \Gamma_R)$ .

The full moment-generating function can be obtained by exponentiating the Liouvillian, but it is simpler to consider its dominant eigenvalue. For simplicity, we will first discuss the **infinite bias regime**  $f_L \rightarrow 1$  and  $f_R \rightarrow 0$

$$\mathcal{L}^\infty(\chi) = \begin{pmatrix} -\Gamma_L & \Gamma_R \\ +\Gamma_L e^{+i\chi} & -\Gamma_R \end{pmatrix} \quad (3.47)$$

Then, we get two eigenvalues

$$\lambda_\pm^\infty(\chi) = \frac{1}{2} \left( -\Gamma_L - \Gamma_R \pm \sqrt{(\Gamma_L - \Gamma_R)^2 + 4e^{+i\chi}\Gamma_L\Gamma_R} \right), \quad (3.48)$$

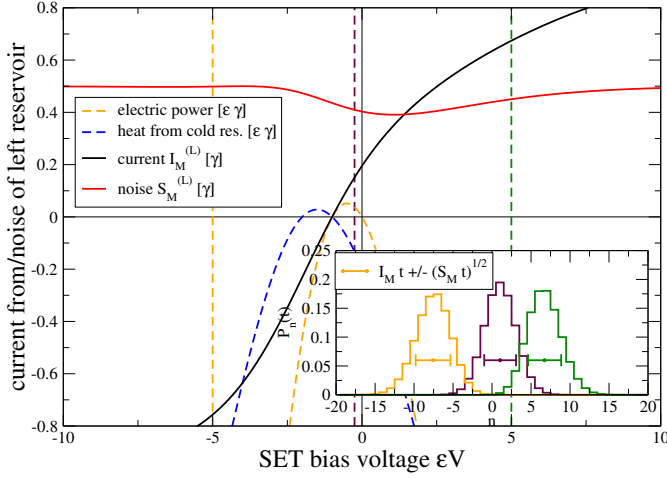


Figure 3.3: Stationary matter current through the SET versus bias voltage, as in Fig. 2.2. The dashed curves indicate the generated electric power and the heat current entering from the cold (right) reservoir, and there are two regions where the device acts as a heat engine or refrigerator. The inset shows the distribution of the net number of particles leaving the left reservoir after time  $t$  at the vertically indicated positions. Parameters:  $\Gamma_L = \Gamma_R = 2\gamma$ ,  $\beta_L\epsilon = 0.5$ ,  $\beta_R\epsilon = 1.5$ ,  $\gamma t = 10$ .

and it is visible that  $\lambda_+^\infty(0) = 0$ , such that  $\lambda_{\text{dom}}^\infty(\chi) = \lambda_+^\infty(\chi)$  is the sought-after generating function for the cumulants. In the long-time limit, the first cumulants become

$$\begin{aligned}
 \langle\langle n \rangle\rangle &= \frac{\Gamma_L \Gamma_R}{\Gamma_L + \Gamma_R} t, \\
 \langle\langle n^2 \rangle\rangle &= \frac{\Gamma_L \Gamma_R}{\Gamma_L + \Gamma_R} \frac{\Gamma_L^2 + \Gamma_R^2}{(\Gamma_L + \Gamma_R)^2} t, \\
 \langle\langle n^3 \rangle\rangle &= \frac{\Gamma_L \Gamma_R}{\Gamma_L + \Gamma_R} \frac{\Gamma_L^4 - 2\Gamma_L^3 \Gamma_R + 6\Gamma_L^2 \Gamma_R^2 - 2\Gamma_L \Gamma_R^3 + \Gamma_R^4}{(\Gamma_L + \Gamma_R)^4} t
 \end{aligned} \tag{3.49}$$

**Exercise 24** (Cumulants). *Show that the above formulas hold.*

At finite bias, the statistics can be computed as well. In particular, we can now evaluate the reliability of the thermoelectric generator that converted heat into electric power. For  $\mu_L - \mu_R < 0$ , we need to transport electrons from left to right to generate positive electric power from heat. We have already calculated the mean current in Fig. 2.2. Repeating this now, we can numerically compute the associated probabilities in the long-term limit

$$P_n(t) = \frac{1}{2\pi} \int_{-\pi}^{+\pi} \text{Tr} \{ e^{\mathcal{L}(\chi)t - in\chi} \bar{\rho} \} d\chi \tag{3.50}$$

and compare these with the mean  $\langle n \rangle \approx I_M t = -i\lambda'(0)t$  and noise  $\langle\langle n^2 \rangle\rangle \approx S_M t = -\lambda''(0)t$  obtained from the long-term cumulants. This is depicted in Fig. 3.3. While for the short times considered, the machine works stochastically (magenta distribution in the inset), this improves for large times. The mean of the distribution grows linearly in time, and so does the second cumulant. The width however will only grow as  $\sqrt{t}$ , such that for long times, the heat engine can be considered as reliable.

Alternatively, we can count different things, e.g. the jumps over the right junction, the total number of outgoing or ingoing jumps, the total number of jumps etc.

**Exercise 25** (Total number of jumps at infinite bias). Calculate the long-term cumulant-generating function in the infinite bias limit  $f_L \rightarrow 1$  and  $f_R \rightarrow 0$  for the probability  $P_n(t)$  of measuring  $n$  jumps in total. How is the first cumulant related to the current?

For example, one may be interested in the total number of jumps when the dot is only coupled to a single equilibrium reservoir

$$\mathcal{L}(\chi) = \Gamma \begin{pmatrix} -f & +(1-f)e^{+i\chi} \\ +fe^{+i\chi} & -1+f \end{pmatrix}. \quad (3.51)$$

The dominant eigenvalue is given by

$$\lambda(\chi) = \frac{\Gamma}{2} \left( -1 + \sqrt{1 - 4(1 - e^{+2i\chi})f(1-f)} \right). \quad (3.52)$$

From it, we can determine the average value of total jumps for long times

$$\langle n \rangle = 2\Gamma t f(1-f) \leq \frac{\Gamma t}{2}. \quad (3.53)$$

One concludes that the average number of jumps vanishes at zero temperature (where either  $f = 0$  or  $f = 1$ ) and becomes maximal at infinite temperature (where  $f \rightarrow 1/2$ ).

### 3.1.7 Example: Absorbtion refrigerator

Revisiting our example of the three-level cooler (or absorbtion refrigerator) from Sec. 2.8, we can generalize the rate matrix in (2.81) to

$$\mathcal{L}_3(\chi) = \begin{pmatrix} -\Gamma_c n_c - \Gamma_h n_h & \Gamma_c(1+n_c)e^{-i\chi} & \Gamma_h(1+n_h) \\ \Gamma_c n_c e^{+i\chi} & -\Gamma_c(1+n_c) - \Gamma_w n_w & \Gamma_w(1+n_w) \\ \Gamma_h n_h & \Gamma_w n_w & -\Gamma_h(1+n_h) - \Gamma_w(1+n_w) \end{pmatrix}. \quad (3.54)$$

This allows to compute the average number of cooling cycle operations, which is positive if on average we are cooling the cold reservoirs and becomes negative when on average we are heating it. The FCS now allows for more detailed statements on the reliability of this engine. Using the trace formula for the current, we reproduce Eq. (2.83) up to a factor of  $E_1 - E_0$ , which is due to the fact that we are not counting energies but absorbtion and emission events. The FCS analysis shows that the device does not work deterministically, see Fig. 3.4.

In general, the dominant eigenvalue of a  $3 \times 3$  matrix is hard to obtain. However, in the interesting limit where  $n_w \rightarrow \infty$ , we see that the transition between the levels 1 and 2 is much faster than the others, such that we may coarse-grain the equation to reduce its dimension. Introducing

$$\rho_{12} = \rho_{11} + \rho_{22}, \quad (3.55)$$

we can write the equation for all populations

$$\frac{d}{dt} \begin{pmatrix} \rho_{00} \\ \rho_{11} \\ \rho_{22} \end{pmatrix} = \begin{pmatrix} -\Gamma_c n_c - \Gamma_h n_h & \Gamma_c(1+n_c)e^{-i\chi} & \Gamma_h(1+n_h) \\ \Gamma_c n_c e^{+i\chi} & -\Gamma_c(1+n_c) - \Gamma_w n_w & \Gamma_w(1+n_w) \\ \Gamma_h n_h & \Gamma_w n_w & -\Gamma_h(1+n_h) - \Gamma_w(1+n_w) \end{pmatrix} \begin{pmatrix} \rho_{00} \\ \rho_{11} \\ \rho_{22} \end{pmatrix} \quad (3.56)$$

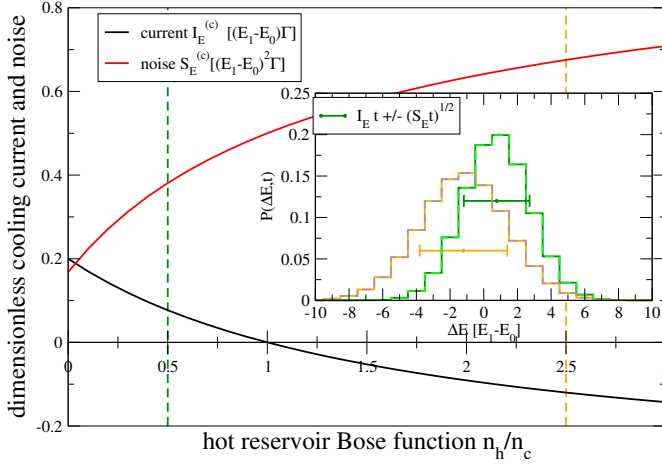


Figure 3.4: Plot of the energy current and noise from the cold reservoir vs. Bose distribution of the hot reservoir (in units of the cold reservoir distribution). The inset (taken at vertical dashed lines of same color) demonstrates that the mean of the distribution is slightly positive in the cooling regime, but a large noise spoils the reliability of the cooler. Solid curves correspond to Eq. (3.55), whereas dashed curves correspond to Eq. (3.60). Parameters:  $\Gamma_c = \Gamma_h = \Gamma_w = \Gamma$ ,  $n_w = 1000$ ,  $n_c = 1$ ,  $\Gamma\Delta t = 10$ .

as a reduced (but non-Markovian equation for the probabilities  $\rho_{00}$  and  $\rho_{12}$

$$\begin{aligned}\dot{\rho}_{00} &= -[\Gamma_c n_c + \Gamma_h n_h] \rho_{00} + \left[ \Gamma_c (1 + n_c) e^{-i\chi} \frac{\rho_{11}}{\rho_{12}} + \Gamma_h (1 + n_h) \frac{\rho_{22}}{\rho_{12}} \right] \rho_{12} \\ \dot{\rho}_{12} &= +[\Gamma_c n_c e^{+i\chi} + \Gamma_h n_h] \rho_{00} - \left[ \Gamma_c (1 + n_c) \frac{\rho_{11}}{\rho_{12}} + \Gamma_h (1 + n_h) \frac{\rho_{22}}{\rho_{12}} \right] \rho_{12}.\end{aligned}\quad (3.57)$$

This is non-Markovian, since in we still need to know  $\rho_{11}$  and  $\rho_{22}$  to compute the rates in the large brackets. However, observing that  $\frac{\rho_{11}}{\rho_{12}}$  and  $\frac{\rho_{22}}{\rho_{12}}$  are just the conditional probabilities of being in state 1 or 2, provided the system is in the coarse-grained state 12, we can replace these values in the limit  $n_w \rightarrow \infty$  by their stationary values

$$\lim_{n_w \rightarrow \infty} \frac{\rho_{11}}{\rho_{12}} = \lim_{n_w \rightarrow \infty} \frac{\rho_{22}}{\rho_{12}} = \frac{1}{2},\quad (3.58)$$

which then leaves us with a reduced Markovian equation for just two variables

$$\frac{d}{dt} \begin{pmatrix} \rho_{00} \\ \rho_{12} \end{pmatrix} = \begin{pmatrix} -\Gamma_c n_c - \Gamma_h n_h & \frac{\Gamma_c}{2} (1 + n_c) e^{-i\chi} + \frac{\Gamma_h}{2} (1 + n_h) \\ +\Gamma_c n_c e^{+i\chi} + \Gamma_h n_h & -\frac{\Gamma_c}{2} (1 + n_c) - \frac{\Gamma_h}{2} (1 + n_h) \end{pmatrix} \begin{pmatrix} \rho_{00} \\ \rho_{12} \end{pmatrix}.\quad (3.59)$$

For this, the dominant eigenvalue can be computed analytically, and the agreement of the resulting FCS with that of the full model is excellent for large  $n_w$  (compare inset of Fig. 3.4).

## 3.2 Energy-resolved Counting Statistics

If we do not ask about the number of particles exchanged with the reservoir, but about the total energy exchanged with it, we can count the energy by counting different transitions as different jumps. For example, for a rate equation describing jumps between energy eigenstates  $E_n$  with

$$\dot{p}_n = \sum_{\nu} \sum_m W_{nm}^{(\nu)} p_m - \sum_{\nu} \sum_m W_{mn}^{(\nu)} p_n,\quad (3.60)$$

we can count jumps with different energy transfers differently, e.g. with different counting fields for different allowed transitions. The qubit absorption refrigerator (3.55) from the previous section

would for example allow to count the full energetic exchanges by counting quanta exchanged with all reservoirs separately

$$\mathcal{L}_3(\chi, \xi, \sigma) = \begin{pmatrix} -\Gamma_c n_c - \Gamma_h n_h & \Gamma_c(1 + n_c)e^{-i\chi} & \Gamma_h(1 + n_h)e^{-i\xi} \\ \Gamma_c n_c e^{+i\chi} & -\Gamma_c(1 + n_c) - \Gamma_w n_w & \Gamma_w(1 + n_w)e^{-i\sigma} \\ \Gamma_h n_h e^{+i\xi} & \Gamma_w n_w e^{+i\sigma} & -\Gamma_h(1 + n_h) - \Gamma_w(1 + n_w) \end{pmatrix}. \quad (3.61)$$

For each of the counting fields, we have the net number of quanta  $N_c$ ,  $N_h$ ,  $N_w$  transferred to the system. The total energy transferred into the system is then

$$\Delta E = N_c(E_1 - E_0) + N_h(E_2 - E_0) + N_w(E_2 - E_1). \quad (3.62)$$

However, when we are only interested in the net energy transfer, this overcounting is not necessary. We can also directly count the energy with a single **energy counting field**  $\xi$

$$\mathcal{L}_3(\xi) = \begin{pmatrix} -\Gamma_c n_c - \Gamma_h n_h & \Gamma_c(1 + n_c)e^{-i\xi(E_1 - E_0)} & \Gamma_h(1 + n_h)e^{-i\xi(E_2 - E_0)} \\ \Gamma_c n_c e^{+i\xi(E_1 - E_0)} & -\Gamma_c(1 + n_c) - \Gamma_w n_w & \Gamma_w(1 + n_w)e^{-i\xi(E_2 - E_1)} \\ \Gamma_h n_h e^{+i\xi(E_2 - E_0)} & \Gamma_w n_w e^{+i\xi(E_2 - E_1)} & -\Gamma_h(1 + n_h) - \Gamma_w(1 + n_w) \end{pmatrix}. \quad (3.63)$$

Then, the whole formalism goes through as before.

Although intuitively clear, we want to show that these distributions are equivalent. Let  $P_{n_1, n_2}(t)$  be the particle counting distribution with  $n_i \in \mathbb{Z}$ , and

$$P(E, t) \equiv \sum_{n_1, n_2} P_{n_1, n_2}(t) \delta(n_1 \Delta E_1 + n_2 \Delta E_2, E) \quad (3.64)$$

be the sought-after energy-resolved distribution. Furthermore, we denote the moment-generating function of the particle-resolved distribution by  $M(\chi_1, \chi_2, t)$ . Then, the moment-generating function of the energy-resolved distribution becomes

$$\begin{aligned} M(\xi, t) &\equiv \sum_E P(E, t) e^{+iE\xi} = \sum_E \sum_{n_1, n_2} P_{n_1, n_2}(t) \delta(n_1 \Delta E_1 + n_2 \Delta E_2, E) e^{+i(n_1 \Delta E_1 + n_2 \Delta E_2)\xi} \\ &= \frac{1}{(2\pi)^2} \int_{-\pi/2}^{+\pi/2} d\chi_1 \int_{-\pi/2}^{+\pi/2} d\chi_2 M(\chi_1, \chi_2, t) \sum_{n_1, n_2} e^{-in_1(\chi_1 - \Delta E_1 \xi)} e^{-in_2(\chi_2 - \Delta E_2 \xi)} \\ &= M(\Delta E_1 \xi, \Delta E_2 \xi). \end{aligned} \quad (3.65)$$

Here  $\xi$  is the counting field for energy. Since this argument also holds for multiple counting fields, we can generally count energies in the same way. The difference however is that now the counting fields have dimension of inverse energy, such that e.g. cumulants of different order have different dimension.

### 3.3 Waiting times and Full Counting Statistics

We will also briefly discuss the relation between full counting statistics and waiting times, see also Ref. [14]. Suppose we have a decomposition of the Liouville superoperator into  $n$  jump terms

$$\mathcal{L} = \mathcal{L}_0 + \mathcal{L}_1 + \dots + \mathcal{L}_n, \quad (3.66)$$

where  $\mathcal{L}_{i>0}$  describes a jump of type  $i$  and  $\mathcal{L}_0$  the no-jump evolution. With the FCS, we can ask for the probabilities of having  $n_i$  jumps of type  $i$  during a time interval  $\Delta t$ . In contrast, a **waiting time distribution**  $P_{ij}(\tau)$  denotes the distribution of times between two jump events  $\mathcal{L}_i$  and  $\mathcal{L}_j$ .

A trivial example of a waiting time distribution can be easily constructed from the FCS by asking for the average waiting time for the first jump to occur [4]. From the FCS, the probability of observing no jump from in  $[t_0, t] = [0, t]$  is given by  $P_0(t) = \text{Tr} \{e^{\mathcal{L}_0 t} \rho_0\}$ . Then, the probability  $W(t)dt$  that the jump occurs in the next time interval  $[t, t + dt]$  is  $W(t)dt = P_0(t) - P_0(t + dt)$ . From this, we conclude that the derivative

$$W(t) = -\dot{P}_0 = -\text{Tr} \{ \mathcal{L}_0 e^{\mathcal{L}_0 t} \rho_0 \} \quad (3.67)$$

is the sought-after waiting time distribution for the system to remain in the initial state  $\rho_0$ , until it leaves it with a jump. Since we always have  $W(\tau) \geq 0$  (the probability of no-jump occurring  $P_0(t)$  can only decrease in time) and  $\int_0^\infty W(\tau) d\tau = -P_0(\infty) + P_0(0) = 1$  (using  $P_0(0) = 1$ ), this is a valid probability density.

However, the waiting time problem can be formulated much more generally. For example, we can ask for the waiting time distribution between two successive jump events, i.e., for the time between a jump of type  $i$  followed by a jump of type  $j$ . This will of course depend on the initial state, such that to avoid ambiguities one usually chooses it to be the steady state  $\rho_0 = \bar{\rho}$ , obeying  $\mathcal{L}\bar{\rho} = 0$ . We also note that we assume that there exists only one steady state. First, to meaningfully define the waiting time distribution, we have to ask ourselves about the density matrix after the first jump has occurred. From the series expansion of the propagator (3.9), we see for a single jump type that

$$\int_0^{\Delta t} e^{\mathcal{L}_0(\Delta t - t_1)} \mathcal{L}_1 e^{\mathcal{L}_0 t_1} dt_1 \approx \Delta t \mathcal{L}_1 + \mathcal{O}\{\Delta t^2\}. \quad (3.68)$$

This is the part that is applied to the density matrix for all trajectories with a single jump. Accordingly, the density matrix after the particular jump is proportional to  $\mathcal{L}_1 \rho$ . For different jump types we just replace  $\mathcal{L}_1 \rightarrow \mathcal{L}_i$  and renormalize, such that the **conditional density matrix** right after a jump of type  $\mathcal{L}_i$  is given by

$$\rho_0^{(i)} = \frac{\Delta t \mathcal{L}_i \bar{\rho}}{\text{Tr} \{ \Delta t \mathcal{L}_i \bar{\rho} \}} = \frac{\mathcal{L}_i \bar{\rho}}{\text{Tr} \{ \mathcal{L}_i \bar{\rho} \}}. \quad (3.69)$$

Here, one conventionally uses the stationary density matrix  $\bar{\rho}$  with  $\mathcal{L}\bar{\rho} = 0$  as the initial state right before the jump (the resulting waiting time distribution will then be valid at steady state). We can now take this as the initial state and ask for the probability that no second jump of any type occurs up to time  $t$ :  $P_0^i(t) = \text{Tr} \{ e^{\mathcal{L}_0 t} \rho_0^{(i)} \}$ . The corresponding waiting time distribution to remain in this initial state would – in complete analogy to our previous arguments – be given by

$$W^i(\tau) = -\text{Tr} \{ \mathcal{L}_0 e^{\mathcal{L}_0 \tau} \rho_0^{(i)} \} = \text{Tr} \{ (\mathcal{L} - \mathcal{L}_0) e^{\mathcal{L}_0 \tau} \rho_0^{(i)} \} = \sum_{j=1}^N \text{Tr} \{ \mathcal{L}_j e^{\mathcal{L}_0 \tau} \rho_0^{(i)} \} \equiv \sum_{j=1}^N W^{ji}(\tau). \quad (3.70)$$

Here, we have used trace conservation of  $\mathcal{L} = \mathcal{L}_0 + \sum_{j=1}^N \mathcal{L}_j$ , and the intuition that the quantity

$$\rho^{(j,i)}(\tau) = \mathcal{L}_j e^{\mathcal{L}_0 \tau} \rho_0^{(i)}, \quad (3.71)$$

is a conditional density matrix for initial state  $\rho_0^{(i)}$  followed by a jump-free evolution for time  $\tau$ , finally ended by a jump of type  $j$ . This leads to the definition below.

**Def. 13** (Waiting time distribution). *For a Liouvillian decomposition  $\mathcal{L} = \mathcal{L}_0 + \sum_{i=1}^N \mathcal{L}_i$  with jump terms  $\mathcal{L}_i$  and steady state  $\mathcal{L}\bar{\rho} = 0$ , the waiting time distributions between an initial jump of type  $i$  and a successive jump of type  $j$  are defined as*

$$W^{ji}(\tau) = \frac{\text{Tr} \{ \mathcal{L}_j e^{\mathcal{L}_0 \tau} \mathcal{L}_i \bar{\rho} \}}{\text{Tr} \{ \mathcal{L}_i \bar{\rho} \}}. \quad (3.72)$$

The waiting times defined this way are positive when our probability interpretation of the Dyson series holds. However, they are not always normalized to one, since a jump  $i$  may not necessarily be followed by a jump  $j$ . For only a single jump type, and defining the initial state as that right after a jump  $\rho_0 = \mathcal{L}_1 \bar{\rho} / \text{Tr} \{ \mathcal{L}_1 \bar{\rho} \}$ , this reduces to the previously discussed phenomenologic example

$$W^{11}(\tau) = \frac{\text{Tr} \{ \mathcal{L}_1 e^{\mathcal{L}_0 \tau} \mathcal{L}_1 \bar{\rho} \}}{\text{Tr} \{ \mathcal{L}_1 \bar{\rho} \}} = \text{Tr} \{ (\mathcal{L} - \mathcal{L}_0) e^{\mathcal{L}_0 \tau} \rho_0 \} = -\text{Tr} \{ \mathcal{L}_0 e^{\mathcal{L}_0 \tau} \rho_0 \}. \quad (3.73)$$

As an example, we can consider the single resonant level with the splitting  $\mathcal{L} = \mathcal{L}_0 + \mathcal{L}_1 + \mathcal{L}_2$ , where

$$\mathcal{L}_0 = \Gamma \begin{pmatrix} -f & 0 \\ 0 & -(1-f) \end{pmatrix}, \quad \mathcal{L}_1 = \Gamma \begin{pmatrix} 0 & 0 \\ f & 0 \end{pmatrix}, \quad \mathcal{L}_2 = \Gamma \begin{pmatrix} 0 & 1-f \\ 0 & 0 \end{pmatrix}. \quad (3.74)$$

The steady state of the full Liouvillian is given by  $\bar{\rho} = (1-f, f)^T$ . Then, we can compute the waiting time distributions

$$W(\tau) = \begin{pmatrix} 0 & \Gamma f e^{-\Gamma f \tau} \\ \Gamma(1-f) e^{-\Gamma(1-f)\tau} & 0 \end{pmatrix}. \quad (3.75)$$

This shows that it is not possible to observe two successive jumps of the same type in this system, it can only hold a single electron. Consequently, there is only the distribution of remaining empty  $W^{12}(\tau)$  and the waiting time distribution of remaining filled  $W^{21}(\tau)$ , which are both normalized.

For completeness, we also revisit the SET in the infinite bias regime with the splitting

$$\mathcal{L}_0 = \begin{pmatrix} -\Gamma_L & 0 \\ 0 & -\Gamma_R \end{pmatrix}, \quad \mathcal{L}_1 = \begin{pmatrix} 0 & 0 \\ +\Gamma_L & 0 \end{pmatrix}, \quad \mathcal{L}_2 = \begin{pmatrix} 0 & +\Gamma_R \\ 0 & 0 \end{pmatrix}. \quad (3.76)$$

The steady state is given by  $\rho = (\Gamma_R, \Gamma_L)^T / (\Gamma_L + \Gamma_R)$ , and the waiting time distributions become

$$W(\tau) = \begin{pmatrix} 0 & \Gamma_L e^{-\Gamma_L \tau} \\ \Gamma_R e^{-\Gamma_R \tau} & 0 \end{pmatrix}. \quad (3.77)$$

Here,  $\Gamma_L e^{-\Gamma_L \tau}$  is the distributions for the empty dot, and  $\Gamma_R e^{-\Gamma_R \tau}$  corresponds to the filled dot. Whenever the dot has been emptied to the right lead, its waiting time distribution  $W^{12}(\tau)$  (of remaining empty) is governed by the rates of the left lead. Similarly, as the filled dot can only be depleted via the right lead, we find that  $W^{21}(\tau)$  (of remaining filled) is governed by the rates of the right reservoir.

### 3.4 Microscopic derivation of counting fields

Sometimes, we are interested not only in the number of particles but also e.g. in the energy transferred into the reservoir. Alternatively, one could be interested in other observables of the reservoir, where at the level of the Hamiltonian it is not immediately apparent how these reservoir observables are changed by individual terms. Therefore, we also consider another microscopic way of deriving generalized master equations here. At this point, we only assume that the observable of interest  $\hat{O}$  commutes with the reservoir Hamiltonian  $[\hat{O}, H_B] = 0$ . The observable in the reservoir can already initially take infinite values – after all, a reservoir can contain an infinite amount of particles. To say by how much the observable has changed during some time interval  $t$ , one introduces a two-point measurement scheme [15]. The first measurement at time 0 defines the initial value of the observable, and the second measurement at time  $t$  its final value. The difference then tells us by how much the observable has changed in between.

We will employ the spectral decomposition of the observable (mostly, one is concerned with observables such as the Hamiltonian  $\hat{H}_B$  or the particle number operator  $\hat{N}_B$  of the reservoir)

$$\hat{O} = \sum_{\ell} O_{\ell} |\ell\rangle \langle \ell|. \quad (3.78)$$

Upon the specific outcome  $\ell$ , the initial measurement projects the bath density matrix to

$$\bar{\rho}_B \xrightarrow{\ell} \frac{|\ell\rangle \langle \ell| \bar{\rho}_B |\ell\rangle \langle \ell|}{P_{\ell}} = \frac{\bar{\rho}_B^{(\ell)}}{P_{\ell}}, \quad (3.79)$$

where  $P_{\ell} = \text{Tr} \{ |\ell\rangle \langle \ell| \bar{\rho}_B \}$  denotes the probability for the outcome  $\ell$ . Since we only measure a reservoir observable and initially, system and reservoir are assumed to be in a product state  $\rho_{\text{tot}}(0) = \rho_S(0) \otimes \bar{\rho}_B$ , this does not affect the system density matrix. The initial value  $O_{\ell}$  is now our reference point with respect to which we define the change. Since we do not only want a generating function specific to a certain initial value, we perform a weighted average over all outcomes to define the moment-generating function

$$M(\chi, t) = \sum_{\ell} \text{Tr} \left\{ e^{i\chi(\hat{O}-O_{\ell})} \mathbf{U}(t) \rho_S^0 \otimes \bar{\rho}_B^{(\ell)} \mathbf{U}^{\dagger}(t) \right\}, \quad (3.80)$$

where we see that the probability  $P_{\ell}$  has cancelled due to the weighted average. We note that this equation has been written down in the interaction picture, where due to our assumption  $[H_B, \hat{O}] = 0$ , the reservoir observable did not pick up a time dependence. Clearly, computing derivatives with respect to  $\chi$  pulls down powers of  $(\hat{O} - O_{\ell})$  in the usual way, such that the above function generates moments of the distribution of observable changes with respect to the initial measurement.

We now evaluate the moment-generating function as

$$\begin{aligned} M(\chi, t) &= \sum_{\ell} \text{Tr} \left\{ e^{+i(\hat{O}-O_{\ell})\chi} \mathbf{U}(t) \rho_S^0 \otimes \bar{\rho}_B^{(\ell)} \mathbf{U}^{\dagger}(t) \right\} \\ &= \sum_{\ell} \text{Tr} \left\{ e^{+i\hat{O}\frac{\chi}{2}} \mathbf{U}(t) e^{-iO_{\ell}\frac{\chi}{2}} \rho_S^0 \otimes \bar{\rho}_B^{(\ell)} e^{-iO_{\ell}\frac{\chi}{2}} \mathbf{U}^{\dagger}(t) e^{+i\hat{O}\frac{\chi}{2}} \right\} \\ &= \sum_{\ell} \text{Tr} \left\{ e^{+i\hat{O}\frac{\chi}{2}} \mathbf{U}(t) e^{-i\hat{O}\frac{\chi}{2}} \rho_S^0 \otimes \bar{\rho}_B^{(\ell)} e^{-i\hat{O}\frac{\chi}{2}} \mathbf{U}^{\dagger}(t) e^{+i\hat{O}\frac{\chi}{2}} \right\} \\ &= \text{Tr} \left\{ \mathbf{U}_{+\frac{\chi}{2}}(t) \rho_0 \otimes \left( \sum_{\ell} \bar{\rho}_B^{(\ell)} \right) \mathbf{U}_{-\frac{\chi}{2}}^{\dagger}(t) \right\} = \text{Tr} \left\{ \mathbf{U}_{+\frac{\chi}{2}}(t) \rho_0 \otimes \bar{\rho}_B \mathbf{U}_{-\frac{\chi}{2}}^{\dagger}(t) \right\} \end{aligned} \quad (3.81)$$

Here, we have used that  $O_\ell$  is just a number (first line) and also that  $e^{-iO_\ell\chi/2}\bar{\rho}_B^{(\ell)}e^{-iO_\ell\chi/2} = e^{-i\hat{O}\chi/2}\bar{\rho}_B^{(\ell)}e^{-i\hat{O}\chi/2}$  by construction, cf. Eq. (3.80). Instead of the usual bath density matrix, we have now used its averaged initial value after the projection

$$\bar{\bar{\rho}}_B = \sum_{\ell} |\ell\rangle \langle \ell| \bar{\rho}_B |\ell\rangle \langle \ell|. \quad (3.82)$$

Depending on measurement and initial state, this may or may not have any effect on the statistics. In the cases where  $\bar{\rho}_B$  is already diagonal in the system energy eigenbasis and we measure an observable like energy, we simply get that  $\bar{\bar{\rho}}_B = \bar{\rho}_B$ .

Eventually, this defines a generalized **time evolution operator with counting field**

$$\mathbf{U}_{+\frac{\chi}{2}}(t) = e^{+i\hat{O}\frac{\chi}{2}}\mathbf{U}(t)e^{-i\hat{O}\frac{\chi}{2}}. \quad (3.83)$$

This object obeys the same initial condition as the normal time evolution operator. In a similar way, we define a generalized **interaction Hamiltonian with counting field**

$$\mathbf{H}_I\left(\frac{\chi}{2}, t\right) = e^{+i\hat{O}\frac{\chi}{2}}\mathbf{H}_I(t)e^{-i\hat{O}\frac{\chi}{2}} = \sum_{\alpha} \mathbf{A}_{\alpha}(t) \otimes e^{+i\hat{O}\frac{\chi}{2}}\mathbf{B}_{\alpha}(t)e^{-i\hat{O}\frac{\chi}{2}}. \quad (3.84)$$

Since in the expansion of the conventional time evolution operator in Eqns. (1.118) and (1.119) we can simply insert identities  $\mathbf{1} = e^{+i\hat{O}\frac{\chi}{2}}e^{-i\hat{O}\frac{\chi}{2}}$ , this then implies

$$\begin{aligned} \mathbf{U}_{+\frac{\chi}{2}}(t) &= \mathbf{1} - i \int_0^t \mathbf{H}_I\left(+\frac{\chi}{2}, t_1\right) dt_1 - \int_0^t dt_1 dt_2 \mathbf{H}_I\left(+\frac{\chi}{2}, t_1\right) \mathbf{H}_I\left(+\frac{\chi}{2}, t_2\right) \Theta(t_1 - t_2) + \dots, \\ \mathbf{U}_{-\frac{\chi}{2}}^\dagger(t) &= \mathbf{1} + i \int_0^t \mathbf{H}_I\left(-\frac{\chi}{2}, t_1\right) dt_1 - \int_0^t dt_1 dt_2 \mathbf{H}_I\left(-\frac{\chi}{2}, t_1\right) \mathbf{H}_I\left(-\frac{\chi}{2}, t_2\right) \Theta(t_2 - t_1) + \dots \end{aligned} \quad (3.85)$$

Based on this evolution, we can now follow e.g. the coarse-graining derivation of a master equation in Sec. 1.3.5 with using only minor modifications

$$[\mathbf{1} + t\mathcal{L}_t(\chi) + \dots] \rho_S^0 \stackrel{!}{=} \text{Tr}_B \left\{ \mathbf{U}_{+\chi/2}(t) \rho_S^0 \otimes \bar{\bar{\rho}}_B \mathbf{U}_{-\chi/2}^\dagger(t) \right\}. \quad (3.86)$$

Using the same assumptions as there (vanishing of first order, initially factorizing state) we get

$$\begin{aligned} t\mathcal{L}_t(\chi)\rho_S^0 &= + \int_0^t dt_1 dt_2 \text{Tr}_B \left\{ \mathbf{H}_I\left(+\frac{\chi}{2}, t_2\right) \rho_S^0 \otimes \bar{\bar{\rho}}_B \mathbf{H}_I\left(-\frac{\chi}{2}, t_1\right) \right\} \\ &\quad - \int_0^t dt_1 dt_2 \Theta(t_1 - t_2) \text{Tr}_B \left\{ \mathbf{H}_I\left(+\frac{\chi}{2}, t_1\right) \mathbf{H}_I\left(+\frac{\chi}{2}, t_2\right) \rho_S^0 \otimes \bar{\bar{\rho}}_B \right\} \\ &\quad - \int_0^t dt_1 dt_2 \Theta(t_2 - t_1) \text{Tr}_B \left\{ \rho_S^0 \otimes \bar{\bar{\rho}}_B \mathbf{H}_I\left(-\frac{\chi}{2}, t_1\right) \mathbf{H}_I\left(-\frac{\chi}{2}, t_2\right) \right\} \\ &= \sum_{\alpha\beta} \int_0^t dt_1 dt_2 \left[ C_{\alpha\beta}^\chi(t_1, t_2) \mathbf{A}_\beta(t_2) \rho_S^0 \mathbf{A}_\alpha(t_1) \right. \\ &\quad \left. - C_{\alpha\beta}^0(t_1, t_2) \Theta(t_1 - t_2) \mathbf{A}_\alpha(t_1) \mathbf{A}_\beta(t_2) \rho_S^0 - C_{\alpha\beta}^0(t_1, t_2) \Theta(t_2 - t_1) \rho_S^0 \mathbf{A}_\alpha(t_1) \mathbf{A}_\beta(t_2) \right], \end{aligned} \quad (3.87)$$

$$C_{\alpha\beta}^\chi(t_1, t_2) \equiv \text{Tr} \left\{ e^{-i\hat{O}\frac{\chi}{2}} \mathbf{B}_\alpha(t_1) e^{+i\hat{O}\frac{\chi}{2}} e^{+i\hat{O}\frac{\chi}{2}} \mathbf{B}_\beta(t_2) e^{-i\hat{O}\frac{\chi}{2}} \bar{\bar{\rho}}_B \right\}. \quad (3.88)$$

Thereby, we have introduced a generalized **correlation function with counting fields**. Furthermore, we have used that the counting field has no effect in all terms where the reservoir density matrix appears left or right to the reservoir coupling operators, since due to  $[O, \bar{\rho}_B] = 0$  we have

$$\begin{aligned} \text{Tr}_B \left\{ e^{+i\hat{O}\chi/2} \mathbf{B}_\alpha(t_1) e^{-i\hat{O}\chi/2} e^{+i\hat{O}\chi/2} \mathbf{B}_\beta(t_2) e^{-i\hat{O}\chi/2} \bar{\rho}_B \right\} &= C_{\alpha\beta}^0(t_1, t_2) = C_{\alpha\beta}(t_1, t_2), \\ \text{Tr}_B \left\{ \bar{\rho}_B e^{-i\hat{O}\chi/2} \mathbf{B}_\alpha(t_1) e^{+i\hat{O}\chi/2} e^{-i\hat{O}\chi/2} \mathbf{B}_\beta(t_2) e^{+i\hat{O}\chi/2} \right\} &= C_{\alpha\beta}^0(t_1, t_2), \end{aligned} \quad (3.89)$$

such that these terms just involve the conventional correlation function. In contrast, in the terms where the reservoir density matrix is sandwiched by two coupling operators, these are transformed with a different sign of the counting fields, such that here a contribution remains.

**Def. 14** (Generalized Correlation Function). *The generalized reservoir correlation function is defined as*

$$C_{\alpha\beta}^\chi(t_1, t_2) = \text{Tr} \left\{ e^{-i\hat{O}\frac{\chi}{2}} \mathbf{B}_\alpha(t_1) e^{+i\hat{O}\frac{\chi}{2}} e^{+i\hat{O}\frac{\chi}{2}} \mathbf{B}_\beta(t_2) e^{-i\hat{O}\frac{\chi}{2}} \bar{\rho}_B \right\}. \quad (3.90)$$

If in addition  $[H_B, \bar{\rho}_B] = 0$ , this simplifies with  $\tau = t_1 - t_2$

$$C_{\alpha\beta}^\chi(\tau) = \text{Tr} \left\{ e^{-i\hat{O}\chi} \mathbf{B}_\alpha(\tau) e^{+i\hat{O}\chi} B_\beta \bar{\rho}_B \right\} \quad (3.91)$$

So in effect, all derivations go through as before, the difference is that the generalized correlation functions have to be used in terms where the system density matrix is sandwiched. Furthermore, if  $\hat{O} = H_B$  is the reservoir energy, we find simply that  $C_{\alpha\beta}^\chi(\tau) = C_{\alpha\beta}(\tau - \chi)$ .

This definition can be used to complete the coarse-graining master equation to the counting-field dependent case, in complete analogy to Sec. 1.3.5.

**Def. 15** (Generalized CG Master Equation). *An interaction Hamiltonian of the form  $H_I = \sum_\alpha A_\alpha \otimes B_\alpha$  with reservoir observable  $\hat{O}$  leads in the interaction picture to the generalized master equation*

$$\begin{aligned} \dot{\rho}_S &= -i \left[ \frac{1}{2i\tau} \int_0^\tau dt_1 \int_0^\tau dt_2 \sum_{\alpha\beta} C_{\alpha\beta}^0(t_1, t_2) \text{sgn}(t_1 - t_2) \mathbf{A}_\alpha(t_1) \mathbf{A}_\beta(t_2), \rho_S \right] \\ &+ \frac{1}{\tau} \int_0^\tau dt_1 \int_0^\tau dt_2 \sum_{\alpha\beta} \left[ C_{\alpha\beta}^\chi(t_1, t_2) \mathbf{A}_\beta(t_2) \rho_S \mathbf{A}_\alpha(t_1) - \frac{C_{\alpha\beta}^0(t_1, t_2)}{2} \{ \mathbf{A}_\alpha(t_1) \mathbf{A}_\beta(t_2), \rho_S \} \right]. \end{aligned} \quad (3.92)$$

We see that the counting-field dependence only affects the terms with the density matrix in the middle, which we would phenomenologically have identified as jump terms. The solution to this master equation defines a generalized density matrix for the system  $\rho_S(\chi, t)$ , and the moment-generating function is then obtained via  $M(\chi, t) = \text{Tr} \{ \rho_S(\chi, t) \}$  as usual. Furthermore, the BMS limit is obtained as before with  $\tau \rightarrow \infty$ . If we choose  $\hat{O} = H_B$  or  $\hat{O} = N_B$  to count energy or particle number of the reservoir, the convention is such that contributions transferred into the reservoir count positive.

### 3.4.1 Example: transient SRL energy current

Let us consider the energy current entering the single resonant level (SRL), i.e., a single quantum dot coupled to a reservoir. The Hamiltonian reads (we implicitly use the mapping to tensor products)

$$H = \epsilon d^\dagger d + d \otimes \sum_k t_k c_k^\dagger + d^\dagger \otimes \sum_k t_k^* c_k + \sum_k \epsilon_k c_k^\dagger c_k. \quad (3.93)$$

We define  $B_1 = \sum_k t_k c_k^\dagger$ ,  $B_2 = B_1^\dagger$ ,  $A_1 = d$ , and  $A_2 = d^\dagger$ . If we are interested in the energy entering the reservoir  $\hat{O} = H_B$ , the observable obviously commutes with the reservoir density matrix, when this is held at a thermal state. Then, since the bath density matrix is already diagonal in the measurement basis, we also have  $\bar{\rho}_B = \bar{\rho}_B$ . The generalized correlation functions then become

$$\begin{aligned} C_{12}^\chi(\tau) &= \frac{1}{2\pi} \int \Gamma(\omega) f(\omega) e^{-i\omega\chi} e^{+i\omega\tau} d\omega = \frac{1}{2\pi} \int \Gamma(-\omega) f(-\omega) e^{+i\omega\chi} e^{-i\omega\tau}, \\ C_{21}^\chi(\tau) &= \frac{1}{2\pi} \int \Gamma(\omega) [1 - f(\omega)] e^{+i\omega\chi} e^{-i\omega\tau}. \end{aligned} \quad (3.94)$$

From this, we can read off the Fourier transforms of the correlation functions

$$\gamma_{12}^\chi(\omega) = \Gamma(-\omega) f(-\omega) e^{+i\omega\chi}, \quad \gamma_{21}^\chi(\omega) = \Gamma(+\omega) [1 - f(+\omega)] e^{+i\omega\chi}. \quad (3.95)$$

When we want to evaluate the BMS rate equation (simply use coarse-graining with  $\tau \rightarrow \infty$ ), we get for the transition rates

$$\gamma_{ab,ab} = \sum_{\alpha\beta} \gamma_{\alpha\beta}(E_b - E_a) \langle a | A_\beta | b \rangle \langle a | A_\alpha^\dagger | b \rangle^*, \quad (3.96)$$

which in our case become dependent on the counting field

$$\gamma_{01,01}^\chi = \gamma_{21}^\chi(+\epsilon) = \Gamma(\epsilon) [1 - f(\epsilon)] e^{+\epsilon\chi}, \quad \gamma_{10,10}^\chi = \gamma_{12}^\chi(-\epsilon) = \Gamma(\epsilon) f(\epsilon) e^{-\epsilon\chi}, \quad (3.97)$$

and our generalized rate matrix becomes

$$\mathcal{L}(\chi) = \Gamma(\epsilon) \begin{pmatrix} -f(\epsilon) & +[1 - f(\epsilon)] e^{+\epsilon\chi} \\ +f(\epsilon) e^{-\epsilon\chi} & -[1 - f(\epsilon)] \end{pmatrix}. \quad (3.98)$$

These are precisely the differences we would have guessed from a rate equation representation. The sign convention here has been chosen such that currents count positively when they enter the reservoir. If we would count the number of particles instead, we just need to replace  $\epsilon \rightarrow 1$  in the above equation. However, for many examples, a full microscopic derivation is actually required to obtain a consistent treatment, see below.

### 3.4.2 Example: SET monitored by a quantum point contact

The microscopic Hamiltonian for the SET was

$$H_{SET} = \epsilon d^\dagger d + \sum_{k\nu} \left[ t_{k\nu} d c_{k\nu}^\dagger + t_{k\nu}^* c_{k\nu} d^\dagger \right] + \sum_{k\nu} \epsilon_{k\nu} c_{k\nu}^\dagger c_{k\nu}. \quad (3.99)$$

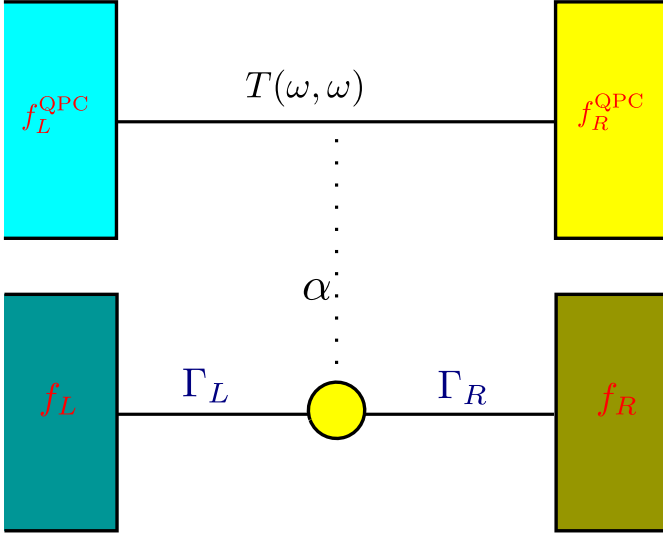


Figure 3.5: Sketch of an SET (bottom) with two leads that is additionally coupled to a QPC (top) consisting of two directly coupled leads. The tunneling through the QPC is modified by the presence of an electron on the SET dot (dotted line). The microscopic derivation of counting fields allows to track the particles transferred through the QPC with a generalized master equation for the SET dot alone.

It would be straightforward to derive the exchange of energy and particles with the two leads  $\nu \in \{L, R\}$  of the SET as demonstrated above for the SRL. However, we consider the SET additionally coupled to a quantum point contact (QPC)

$$H_{QPC} = \sum_{\nu} \sum_k \varepsilon_{k\nu} \gamma_{k\nu}^{\dagger} \gamma_{k\nu} \quad (3.100)$$

as depicted in Fig. 3.5. The tunneling through the QPC circuit is modified by the presence of electrons on the SET

$$H_I = \underbrace{(1 - \alpha d^{\dagger} d)}_A \otimes \underbrace{\sum_{kk'} [t_{kk'} \gamma_{kL} \gamma_{k'R}^{\dagger} + t_{kk'}^* \gamma_{k'R} \gamma_{kL}^{\dagger}]}_B. \quad (3.101)$$

Here, the case  $\alpha = 0$  just represents the bare tunneling through the QPC with  $t_{kk'}$  denoting tunneling amplitudes and  $\gamma_{k\nu}$  annihilating electrons of mode  $k$  in the QPC lead  $\nu$ . The parameter  $0 < \alpha < 1$  models a modification of the QPC tunneling in presence of an electron on the SET dot. We note that this QPC reservoir denotes a nonequilibrium reservoir and thereby does not fit the setting of chapter 2.

For brevity we also only consider the coupling operators to the QPC (we have already discussed the SET in Sec. 2.1) and as reservoir observable, we are interested in the number of electrons transferred to the right QPC reservoir

$$\hat{O} = \sum_k \gamma_{kR}^{\dagger} \gamma_{kR}, \quad (3.102)$$

provided the QPC reservoirs are at local thermal equilibrium states

$$\bar{\rho}_B = \frac{e^{-\beta_L \sum_k (\varepsilon_{kL} - \mu_L) \gamma_{kL}^{\dagger} \gamma_{kL}}}{Z_L} \frac{e^{-\beta_R \sum_k (\varepsilon_{kR} - \mu_R) \gamma_{kR}^{\dagger} \gamma_{kR}}}{Z_R} = \bar{\bar{\rho}}_B. \quad (3.103)$$

Since  $[H_{QPC}, \bar{\rho}_B] = 0$ , the generalized correlation function becomes

$$\begin{aligned}
C^\xi(\tau) &= \text{Tr} \left\{ e^{-i\hat{O}\xi} e^{+iH_{QPC}\tau} B e^{-iH_{QPC}\tau} e^{+i\hat{O}\xi} B \bar{\rho}_B \right\} \\
&= \sum_{kk'qq'} \text{Tr} \left\{ \left[ t_{kk'} \gamma_{kL} \gamma_{k'R}^\dagger e^{+i(\varepsilon_{k'R} - \varepsilon_{kL})\tau} e^{-i\xi} + t_{kk'}^* \gamma_{k'R} \gamma_{kL}^\dagger e^{-i(\varepsilon_{k'R} - \varepsilon_{kL})\tau} e^{+i\xi} \right] \times \right. \\
&\quad \left. \times \left[ t_{qq'} \gamma_{qL} \gamma_{q'R}^\dagger + t_{qq'}^* \gamma_{q'R} \gamma_{qL}^\dagger \right] \bar{\rho}_B \right\} \\
&= \sum_{kk'qq'} t_{kk'} t_{qq'}^* e^{+i(\varepsilon_{k'R} - \varepsilon_{kL})\tau} e^{-i\xi} \text{Tr} \left\{ \gamma_{kL} \gamma_{k'R}^\dagger \gamma_{q'R} \gamma_{qL}^\dagger \bar{\rho}_B \right\} \\
&\quad + \sum_{kk'qq'} t_{kk'}^* t_{qq'} e^{-i(\varepsilon_{k'R} - \varepsilon_{kL})\tau} e^{+i\xi} \text{Tr} \left\{ \gamma_{k'R} \gamma_{kL}^\dagger \gamma_{qL} \gamma_{q'R}^\dagger \bar{\rho}_B \right\} \\
&= e^{-i\xi} \sum_{kk'} |t_{kk'}|^2 e^{+i(\varepsilon_{k'R} - \varepsilon_{kL})\tau} [1 - f_L(\varepsilon_{kL})] f_R(\varepsilon_{k'R}) \\
&\quad + e^{+i\xi} \sum_{kk'} |t_{kk'}|^2 e^{-i(\varepsilon_{k'R} - \varepsilon_{kL})\tau} f_L(\varepsilon_{kL}) [1 - f_R(\varepsilon_{k'R})] \\
&= e^{-i\xi} \frac{1}{(2\pi)^2} \int d\omega \int d\omega' T(\omega, \omega') e^{+i(\omega' - \omega)\tau} [1 - f_L(\omega)] f_R(\omega') \\
&\quad + e^{+i\xi} \frac{1}{(2\pi)^2} \int d\omega \int d\omega' T(\omega, \omega') e^{-i(\omega' - \omega)\tau} f_L(\omega) [1 - f_R(\omega')], \tag{3.104}
\end{aligned}$$

where we have introduced the dimensionless **transmission**

$$T(\omega, \omega') = (2\pi)^2 \sum_{kk'} |t_{kk'}|^2 \delta(\omega - \varepsilon_{kL}) \delta(\omega' - \varepsilon_{k'R}). \tag{3.105}$$

The FT of the correlation function accordingly can be expressed by a convolution integral

$$\begin{aligned}
\gamma^\xi(\Omega) &= \int C^\xi(\tau) e^{+i\Omega\tau} d\tau \\
&= \frac{e^{-i\xi}}{2\pi} \int d\omega T(\omega, \omega - \Omega) [1 - f_L(\omega)] f_R(\omega - \Omega) + \frac{e^{+i\xi}}{2\pi} \int d\omega T(\omega, \omega + \Omega) f_L(\omega) [1 - f_R(\omega + \Omega)]. \tag{3.106}
\end{aligned}$$

These terms have the appealing interpretation of an electron transfer from right to left (first) or from left to right (second term) while the energy  $\Omega$  is absorbed from the system, and we see that the sign of the counting field matches this interpretation.

Now, to compute the transition rates (for the SET quantum dot we do not have coherences), we have to evaluate

$$\gamma_{ab,ab}^\xi = \gamma^\xi(E_b - E_a) |\langle a | (1 - \alpha d^\dagger) | b \rangle|^2. \tag{3.107}$$

Since the coupling operator is just diagonal, the only allowed transition rates are

$$\gamma_{00,00}^\xi = \gamma^\xi(0), \quad \gamma_{11,11}^\xi = \gamma^\xi(0) |1 - \alpha|^2, \tag{3.108}$$

Eventually, this leads to the QPC-induced rate matrix

$$\begin{aligned}
\mathcal{L}_{\text{QPC}}(\xi) &= \begin{pmatrix} 1 & 0 \\ 0 & |1 - \alpha|^2 \end{pmatrix} C_{\text{QPC}}(\xi), \\
C_{\text{QPC}}(\xi) &= \left[ \frac{e^{-i\xi}}{2\pi} \int T(\omega, \omega) [1 - f_L(\omega)] f_R(\omega) + \frac{e^{+i\xi}}{2\pi} \int T(\omega, \omega) f_L(\omega) [1 - f_R(\omega)] \right], \tag{3.109}
\end{aligned}$$

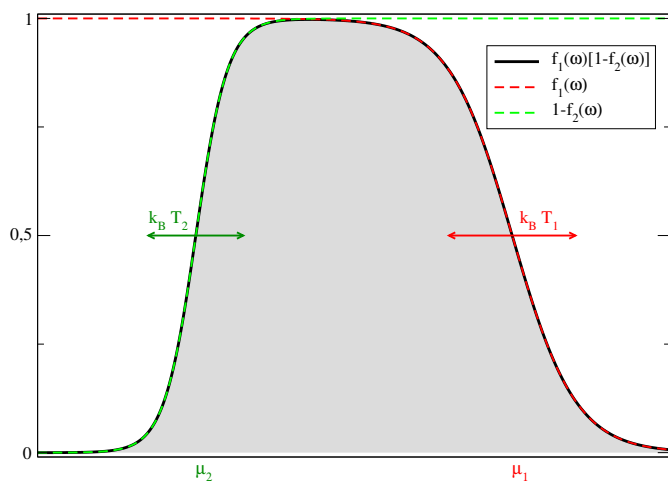


Figure 3.6: Integrand in Eq. (3.112). At zero temperature at both contacts, we obtain a product of two step functions and the area under the curve is given by the difference  $\mu_1 - \mu_2$  as soon as  $\mu_1 > \mu_2$  (and zero otherwise).

which has to be added to the dissipators of the SET leads (2.40). The function  $C_{\text{QPC}}(\xi)$  denotes the cumulant-generating function of the unperturbed (low-transparency) QPC, and that  $T(\omega, \omega + \Omega)$  is only evaluated at  $\Omega = 0$  reflects the fact that the SET and the QPC do not exchange energy, i.e., the transport through the QPC remains ballistic. The fact that this time, the counting fields occur on the diagonal is related to the fact that the QPC charge transfers are not associated to jumps of the SET dot itself. If we assume that the SET dot is empty all the time, the associated QPC current is just determined by the free generating function of the QPC

$$I_0 = (-i\partial_\xi)C_{\text{QPC}}(\xi)|_{\xi=0} = \frac{1}{2\pi} \int T(\omega, \omega)[f_L(\omega) - f_R(\omega)]d\omega, \quad (3.110)$$

which is also known as **Landauer formula**. The isolated QPC can also be treated non-perturbatively, such that its full generating function (i.e., nonperturbative  $t_{kk'}$ ) can be derived (see e.g. [16]), such that we have only derived a small  $T(\omega, \omega)$  approximation to the full generating function. For a filled SET dot all the time, one simply gets  $I_1 = |1 - \alpha|^2 I_0$ .

**Exercise 26** (QPC current). *Show that the stationary state of the SET is unaffected by the additional QPC dissipator and calculate the stationary current through the QPC for Liouillian  $\mathcal{L}(\xi) = \mathcal{L}_{\text{SET}} + \mathcal{L}_{\text{QPC}}(\xi)$ .*

If we assume that  $T(\omega, \omega') = T$  is a flat function (at least in the region where the product of the Fermi functions is finite), these integrals can actually be solved analytically: The structure of the Fermi functions demonstrates that the shift  $\Omega$  can be included in the chemical potentials. Therefore, we consider integrals of the type

$$I = \int f_1(\omega) [1 - f_2(\omega)] d\omega. \quad (3.111)$$

At zero temperature, these should behave as  $I \approx (\mu_1 - \mu_2)\Theta(\mu_1 - \mu_2)$ , where  $\Theta(x)$  denotes the Heaviside- $\Theta$  function, which follows from the structure of the integrand, see Fig. 3.6. For finite temperatures, the value of the integral can also be calculated, for simplicity we constrain ourselves

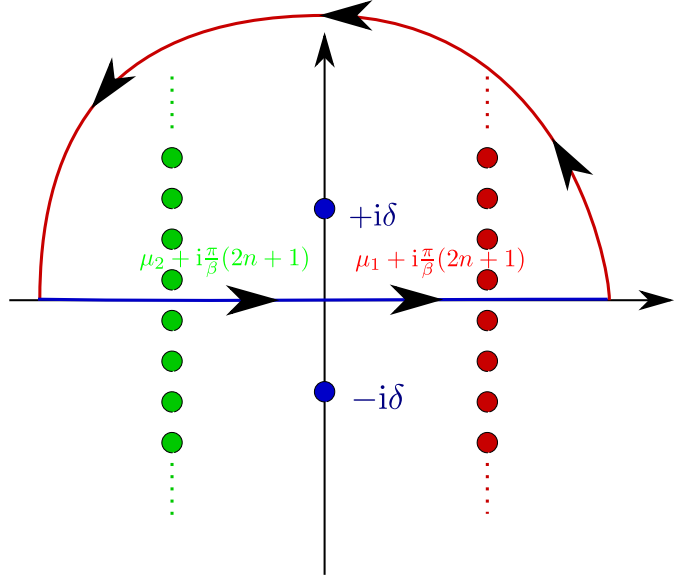


Figure 3.7: Poles and integration contour for Eq. (3.112) in the complex plane. The integral along the real axis (blue line) closed by an arc (red curve) in the upper complex plane, along which (due to the regulator) the integrand vanishes sufficiently fast.

to the (experimentally relevant) case of equal temperatures ( $\beta_1 = \beta_2 = \beta$ ), for which we obtain

$$\begin{aligned} I &= \int \frac{1}{(e^{\beta(\mu_2 - \omega)} + 1)(e^{-\beta(\mu_1 - \omega)} + 1)} d\omega \\ &= \lim_{\delta \rightarrow \infty} \int \frac{1}{(e^{\beta(\mu_2 - \omega)} + 1)(e^{-\beta(\mu_1 - \omega)} + 1)} \frac{\delta^2}{\delta^2 + \omega^2} d\omega, \end{aligned} \quad (3.112)$$

where we have introduced the Lorentzian-shaped regulator to enforce convergence. By identifying the poles of the integrand

$$\begin{aligned} \omega_{\pm}^* &= \pm i\delta, \\ \omega_{1,n}^* &= \mu_1 + i\frac{\pi}{\beta}(2n+1), \\ \omega_{2,n}^* &= \mu_2 + i\frac{\pi}{\beta}(2n+1), \end{aligned} \quad (3.113)$$

where  $n \in \{0, \pm 1, \pm 2, \pm 3, \dots\}$  we can solve the integral by using the residue theorem, see also Fig. 3.7 for the integration contour. Finally, we obtain for the integral

$$\begin{aligned} I &= 2\pi i \lim_{\delta \rightarrow \infty} \left\{ \text{Res } f_1(\omega) [1 - f_2(\omega)] \frac{\delta^2}{\delta^2 + \omega^2} \Big|_{\omega = +i\delta} + \sum_{n=0}^{\infty} \text{Res } f_1(\omega) [1 - f_2(\omega)] \frac{\delta^2}{\delta^2 + \omega^2} \Big|_{\omega = \mu_1 + i\frac{\pi}{\beta}(2n+1)} \right. \\ &\quad \left. + \sum_{n=0}^{\infty} \text{Res } f_1(\omega) [1 - f_2(\omega)] \frac{\delta^2}{\delta^2 + \omega^2} \Big|_{\omega = \mu_2 + i\frac{\pi}{\beta}(2n+1)} \right\} \\ &= \frac{\mu_1 - \mu_2}{1 - e^{-\beta(\mu_1 - \mu_2)}}, \end{aligned} \quad (3.114)$$

which automatically obeys the simple zero-temperature ( $\beta \rightarrow \infty$ ) limit.

With the replacements  $\mu_1 \rightarrow \mu_R + \Omega$  and  $\mu_2 \rightarrow \mu_L$  or  $\mu_1 \rightarrow \mu_L$  and  $\mu_2 \rightarrow \mu_R - \Omega$ , respectively, we can evaluate both terms in the reservoir correlation function, which becomes

$$\gamma^\xi(\Omega) = e^{-i\xi} \frac{T}{2\pi} \frac{\Omega - V}{1 - e^{-\beta(\Omega - V)}} + e^{+i\xi} \frac{T}{2\pi} \frac{\Omega + V}{1 - e^{-\beta(\Omega + V)}}, \quad (3.115)$$

where  $V = \mu_L - \mu_R$  is the QPC bias voltage. We see that for  $\mu_L \gg \mu_R$ , only the term with  $e^{+i\xi}$  remains, and  $\gamma^\xi(\Omega) \approx e^{+i\xi}T(\Omega + V)$ . In contrast, for  $\mu_L \ll \mu_R$ , we have  $\gamma^\xi(\Omega) \approx e^{-i\xi}T(\Omega - V)$ . This just expresses the fact that for large QPC bias voltage, the current across the QPC becomes unidirectional.

When we now consider the case  $\{\Gamma_L, \Gamma_R\} \ll \{TV, |1 - \alpha|^2TV\}$ , we approach a bistable system, where for a nearly stationary SET the QPC transmits many charges. Then, the QPC current measured at finite times will be large when the SET dot is empty and reduced otherwise. In this case, the counting statistics approaches the case of telegraph noise. When the dot is empty or filled throughout respectively, the current can easily be determined as

$$I_0 = \frac{T}{2\pi}V \left[ \frac{1}{1 - e^{-\beta V}} - \frac{1}{e^{+\beta V} - 1} \right] = \frac{T}{2\pi}V, \quad I_1 = |1 - \alpha|^2 I_0. \quad (3.116)$$

For finite time intervals  $\Delta t$ , the number of electrons tunneling through the QPC  $\Delta n$  is determined by the probability distribution

$$P_{\Delta n}(\Delta t) = \frac{1}{2\pi} \int_{-\pi}^{+\pi} \text{Tr} \{ e^{\mathcal{L}(\xi)\Delta t - i\Delta n\xi} \rho(t) \} d\xi, \quad (3.117)$$

where  $\rho(t)$  represents the initial density matrix. This quantity can e.g. be evaluated numerically. When  $\Delta t$  is not too large (such that the stationary state is not really reached) and not too small (such that there are sufficiently many particles tunneling through the QPC to meaningfully define a current), a continuous measurement of the QPC current maps to a fixed-point iteration as follows: Now we care about the change of the density matrix when we actually measure a particular change of the particle number. Formally, it would be given by the corresponding propagator

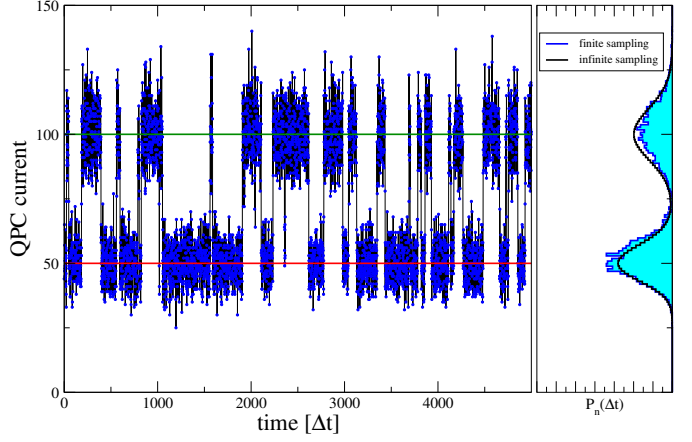
$$\mathcal{P}^{(n)}(\Delta t) = \frac{1}{2\pi} \int_{-\pi}^{+\pi} e^{\mathcal{L}(\xi)\Delta t - i\Delta n\xi} d\xi, \quad (3.118)$$

which has to be applied to the initial density matrix upon measuring a transfer of  $n$  particles into the reservoir. Afterwards, we need to renormalize, such that, upon measurement of  $n$  particle transfers

$$\rho \rightarrow \frac{\mathcal{P}^{(n)}(\Delta t)\rho}{\text{Tr} \{ \mathcal{P}^{(n)}(\Delta t)\rho \}}. \quad (3.119)$$

For the generation of a realistic trajectory under continuous monitoring, it is now essential to use the density matrix after the measurement as the initial state for the next iteration. This ensures that e.g. after measuring a large current it is in the next step more likely to measure a large current again than a low current and vice versa. Consequently, the ratio of measured particles divided by measurement time gives a current estimate  $I(t) \approx \frac{\Delta n}{\Delta t}$  for the time interval. Such current trajectories are used to track the full counting statistics through quantum point contacts, see Fig. 3.8. In this way, the QPC acts as a detector for the counting statistics of the SET circuit. Finally, we note that for an SET, a QPC only acts as a reliable detector for the occupation of the SET dot. However, when the SET transport is unidirectional (large SET bias), we can infer from this also the number of charges transferred through the SET.

Figure 3.8: Numerical simulation of the time-resolved QPC current for infinite SET and high QPC bias. The QPC current allows to reconstruct the FCS of the SET, since each current blip from low (red line) to high (green line) current corresponds to an electron leaving the SET to its right junction. Parameters:  $\Gamma_L\Delta t = \Gamma_R\Delta t = 0.01$ ,  $\beta V \rightarrow +\infty$ ,  $TV/(2\pi) = 100.0$ ,  $|1 - \alpha|^2 TV/(2\pi) = 50.0$ ,  $f_L = 1.0$ ,  $f_R = 0.0$ . The right panel shows the corresponding probability distribution  $P_n(\Delta t)$  versus  $n = I\Delta t$ , where the blue curve is sampled from the finite range of the left panel and the black curve is the theoretical limit for infinitely long times.



### 3.4.3 Example: pure dephasing model

We revisit the pure dephasing model

$$H = \Omega\sigma^z + \sigma^z \otimes \sum_k \left( h_k b_k + h_k^* b_k^\dagger \right) + \sum_k \omega_k b_k^\dagger b_k \quad (3.120)$$

and consider the total energy radiated into the reservoir, such that  $\hat{O} = \sum_k \omega_k b_k^\dagger b_k$ . In Sec. 1.3.6, we already learned by solving the model exactly that populations (in the eigenbasis of  $\sigma^z$ ) would remain constant and coherences would simply decay, such that an initial quantum superposition is transformed into a statistical mixture. With counting fields, we can however also track the energy radiated into the reservoir, which we can compare to the exact solution.

First, we derive the generalized master equation with counting fields. Again we have  $\bar{\rho}_B = \bar{\rho}_B$ , and we can get away with a single correlation function

$$\begin{aligned} C^X(t) &= \text{Tr}_B \left\{ e^{-iH_B\chi} \sum_k \left( h_k b_k e^{-i\omega_k t} + h_k^* b_k^\dagger e^{+i\omega_k t} \right) e^{+iH_B\chi} \sum_q \left( h_q b_q + h_q^* b_q^\dagger \right) \bar{\rho}_B \right\} \\ &= \sum_k |h_k|^2 \left[ e^{+i\omega_k \chi} e^{-i\omega_k t} [1 + n_B(\omega_k)] + e^{-i\omega_k \chi} e^{+i\omega_k t} n_B(\omega_k) \right] \\ &= \frac{1}{2\pi} \int_0^\infty \Gamma(\omega) \left[ e^{+i\omega \chi} e^{-i\omega t} [1 + n_B(\omega)] + e^{-i\omega \chi} e^{+i\omega t} n_B(\omega) \right] d\omega \\ &= \frac{1}{2\pi} \int d\omega e^{-i\omega t} \left[ \Theta(\omega) \Gamma(\omega) [1 + n_B(\omega)] e^{+i\omega \chi} + \Theta(-\omega) \Gamma(-\omega) n_B(-\omega) e^{+i\omega \chi} \right]. \end{aligned} \quad (3.121)$$

Here, we have not rewritten the correlation function as a single term due to the occurrence of the counting field.

With  $\sigma_z^2 = \mathbf{1}$  we can again ignore the Lamb-shift contribution, and the coarse-graining master equation (3.93) becomes

$$\begin{aligned} \dot{\rho} &= \frac{1}{2\pi\tau} \int_0^\tau dt_1 \int_0^\tau dt_2 \int d\omega \Theta(\omega) \Gamma(\omega) [1 + n_B(\omega)] e^{-i\omega(t_1-t_2)} \left[ e^{+i\omega \chi} \sigma^z \rho \sigma^z - \rho \right] \\ &\quad + \frac{1}{2\pi\tau} \int_0^\tau dt_1 \int_0^\tau dt_2 \int d\omega \Theta(-\omega) \Gamma(-\omega) n_B(-\omega) e^{-i\omega(t_1-t_2)} \left[ e^{+i\omega \chi} \sigma^z \rho \sigma^z - \rho \right]. \end{aligned} \quad (3.122)$$

We can also write this as

$$\begin{aligned}\dot{\boldsymbol{\rho}} &= [\gamma_-(\chi, \tau)\sigma^z \boldsymbol{\rho}\sigma^z - \gamma_-(0, \tau)\boldsymbol{\rho}] + [\gamma_+(\chi, \tau)\sigma^z \boldsymbol{\rho}\sigma^z - \gamma_+(0, \tau)\boldsymbol{\rho}] , \\ \gamma_+(\chi, \tau) &= \int \Theta(\omega)\Gamma(\omega)[1 + n_B(\omega)]e^{+i\omega\chi} \frac{\tau}{2\pi} \text{sinc}^2 \left[ \frac{\omega\tau}{2} \right] d\omega , \\ \gamma_-(\chi, \tau) &= \int \Theta(-\omega)\Gamma(-\omega)n_B(-\omega)e^{+i\omega\chi} \frac{\tau}{2\pi} \text{sinc}^2 \left[ \frac{\omega\tau}{2} \right] d\omega .\end{aligned}\quad (3.123)$$

This Liouvillian is just diagonal

$$\begin{aligned}\dot{\boldsymbol{\rho}}_{00} &= [\gamma_-(\chi, \tau) - \gamma_-(0, \tau) + \gamma_+(\chi, \tau) - \gamma_+(0, \tau)] \boldsymbol{\rho}_{00} , \\ \dot{\boldsymbol{\rho}}_{11} &= [\gamma_-(\chi, \tau) - \gamma_-(0, \tau) + \gamma_+(\chi, \tau) - \gamma_+(0, \tau)] \boldsymbol{\rho}_{11} , \\ \dot{\boldsymbol{\rho}}_{01} &= -[\gamma_-(\chi, \tau) + \gamma_-(0, \tau) + \gamma_+(\chi, \tau) + \gamma_+(0, \tau)] \boldsymbol{\rho}_{01} ,\end{aligned}\quad (3.124)$$

and likewise for  $\boldsymbol{\rho}_{10}$ . When setting the counting field to zero, we also recover Eq. (1.156). This demonstrates that the counting field also enters the evolution of coherences.

By exploiting the trace conservation, the cumulant-generating function becomes

$$C(\chi, t) = \ln \text{Tr} \{ e^{\mathcal{L}(\chi)t} \rho_0 \} = [\gamma_-(\chi, \tau) - \gamma_-(0, \tau) + \gamma_+(\chi, \tau) - \gamma_+(0, \tau)] t . \quad (3.125)$$

The average energy radiated into the reservoir until time  $t = \tau$  then becomes

$$\begin{aligned}\Delta E(\tau) &= \int \Theta(\omega)\omega\Gamma(\omega)[1 + n_B(\omega)] \frac{\tau^2}{2\pi} \text{sinc}^2 \left( \frac{\omega\tau}{2} \right) d\omega + \int \Theta(-\omega)\omega\Gamma(-\omega)n_B(-\omega) \frac{\tau^2}{2\pi} \text{sinc}^2 \left( \frac{\omega\tau}{2} \right) d\omega \\ &= \int_0^\infty \omega\Gamma(\omega) \frac{\tau^2}{2\pi} \text{sinc}^2 \left( \frac{\omega\tau}{2} \right) d\omega = \frac{2}{\pi} \int_0^\infty \frac{\Gamma(\omega)}{\omega} \sin^2 \left( \frac{\omega\tau}{2} \right) d\omega .\end{aligned}\quad (3.126)$$

We see that the temperature of the reservoir eventually has no effect on this energy.

To obtain the exact solution for the radiated energy, we can use the exact Heisenberg picture (bold symbols) dynamics.

$$\begin{aligned}\frac{d}{dt} \boldsymbol{\sigma}^z &= ie^{+iHt} [H, \boldsymbol{\sigma}^z] e^{-iHt} = 0 , \\ \frac{d}{dt} \mathbf{b}_k &= -i\omega_k \mathbf{b}_k - ih_k^* \boldsymbol{\sigma}^z , \\ \frac{d}{dt} \mathbf{b}_k^\dagger &= +i\omega_k \mathbf{b}_k^\dagger + ih_k \boldsymbol{\sigma}^z .\end{aligned}\quad (3.127)$$

These equations are solved by  $\boldsymbol{\sigma}^z(t) = \boldsymbol{\sigma}^z$  and

$$\begin{aligned}\mathbf{b}_k(t) &= b_k e^{-i\omega_k t} + \frac{h_k^*}{\omega_k} \boldsymbol{\sigma}^z (e^{-i\omega_k t} - 1) , \\ \mathbf{b}_k^\dagger(t) &= b_k^\dagger e^{+i\omega_k t} + \frac{h_k}{\omega_k} \boldsymbol{\sigma}^z (e^{+i\omega_k t} - 1) ,\end{aligned}\quad (3.128)$$

which also respect the initial condition  $\mathbf{b}_k(0) = b_k$ . Therefore, the total expectation value of the reservoir energy becomes

$$\begin{aligned}\langle E \rangle_t &= \sum_k \omega_k \text{Tr} \left\{ \left( e^{+i\omega_k t} \mathbf{b}_k^\dagger + \frac{h_k}{\omega_k} (e^{+i\omega_k t} - 1) \boldsymbol{\sigma}^z \right) \left( e^{-i\omega_k t} b_k + \frac{h_k^*}{\omega_k} (e^{-i\omega_k t} - 1) \boldsymbol{\sigma}^z \right) \rho_S^0 \otimes \rho_B \right\} \\ &= \langle E \rangle_0 + \sum_k \frac{|h_k|^2}{\omega_k} [2 - 2 \cos(\omega_k t)] = \langle E \rangle_0 + \frac{2}{\pi} \int_0^\infty \frac{\Gamma(\omega)}{\omega} \sin^2 \left( \frac{\omega t}{2} \right) d\omega ,\end{aligned}\quad (3.129)$$

and we see that the difference agrees exactly with our previously computed mean value for coarse-graining (3.127), derived using energy counting fields, when the coarse-graining time is chosen as physical time  $\tau = t$ .

**Exercise 27** (Energetic noise). *Show that also for the second cumulant of the radiated energy the results from the generalized coarse-graining master equation and the exact solution agree*

$$\langle\langle E^2 \rangle\rangle = \frac{2}{\pi} \int_0^\infty \Gamma(\omega) [1 + 2n_B(\omega)] \sin^2\left(\frac{\omega t}{2}\right) d\omega.$$

### 3.4.4 Example: spin current

So far, our considerations only involved simple observables such as particle number or energy of the reservoir. However, it is quite straightforward to consider more general ones as well. When dealing with electronic transport, we did not take the spin of electrons into account, since all involved processes were not sensitive to it, such that its inclusion would amount to a factor of two.

This changes of course when a magnetic field is involved. For example, a magnetic field localized to the SET dot would lead to a Zeeman-splitting term

$$H_S = (\epsilon + b)d_\uparrow^\dagger d_\uparrow + (\epsilon - b)d_\downarrow^\dagger d_\downarrow + U d_\uparrow^\dagger d_\uparrow d_\downarrow^\dagger d_\downarrow, \quad (3.130)$$

where  $\epsilon$  is the on-site energy in absence of a magnetic field, the energetic splitting is proportional to the magnetic field  $b$  (including Bohr magneton and  $g$ -factor), and  $U$  is the Coulomb interaction energy. The tunnel interaction does not depend on the spin

$$H_I = \sum_k \sum_{\nu \in \{L,R\}} \sum_{\sigma \in \{\uparrow,\downarrow\}} [t_{k\nu} d_\nu^\dagger c_{k\nu\sigma} + \text{h.c.}], \quad (3.131)$$

and the reservoirs will not be sensitive to the spin either (assuming that the magnetic field is only present inside the system)

$$H_B = \sum_k \sum_{\nu \in \{L,R\}} \epsilon_{k\nu} \sum_{\sigma \in \{\uparrow,\downarrow\}} c_{k\nu\sigma}^\dagger c_{k\nu\sigma}, \quad (3.132)$$

see Fig. 3.9. A suitable observable for the FCS would now be the total spin of the right reservoir

$$\hat{O} = S_R = \sum_k \left[ c_{kR\uparrow}^\dagger c_{kR\uparrow} - c_{kR\downarrow}^\dagger c_{kR\downarrow} \right]. \quad (3.133)$$

For this choice, the calculations required for the computation of the reservoir correlation function can be explicitly performed. The right reservoir coupling operators are equipped with an additional counting field

$$\begin{aligned} e^{-iS_{RX}} e^{+iH_B t} c_{kR\uparrow} e^{-iH_B t} e^{+iS_{RX}} &= e^{-i\epsilon_{kR} t} e^{+i\chi} c_{kR\uparrow}, \\ e^{-iS_{RX}} e^{+iH_B t} c_{kR\downarrow} e^{-iH_B t} e^{+iS_{RX}} &= e^{-i\epsilon_{kR} t} e^{-i\chi} c_{kR\downarrow}, \end{aligned} \quad (3.134)$$

where we have stoically used  $e^{+i\alpha c_k^\dagger c_k} c_k e^{-i\alpha c_k^\dagger c_k} = e^{-i\alpha} c_k$ . Analogous expressions are obtained for the right creation operators, whereas the left reservoir coupling operators just acquire the usual

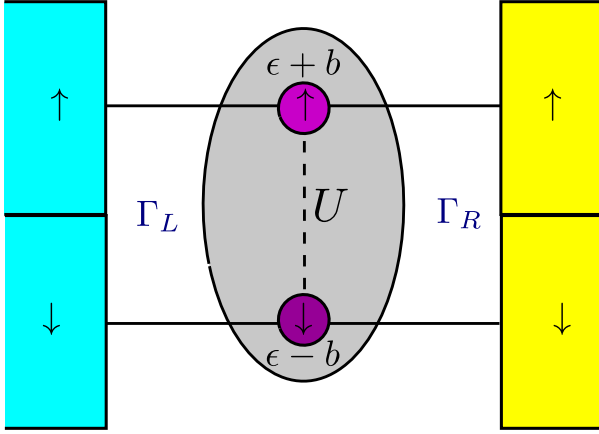


Figure 3.9: Sketch of an SET with spin resolution and a local Zeeman-splitting term  $b$  proportional to the applied magnetic field. This can be understood as two separate spinless quantum dots, one for each spin species. Since the two electrons actually reside on the same physical dot, Coulomb interaction  $U$  cannot be neglected.

interaction picture dynamics without counting field. Under the assumption that the magnetic field does not vanish  $|b| \gg t_{k\nu}$ , the secular master equation can be derived the usual way: From the counting fields, we get the only modified correlation functions

$$\begin{aligned} \gamma_{34\uparrow}^{\chi}(\omega) &= \Gamma_R(\omega)[1 - f_R(\omega)]e^{+i\chi}, & \gamma_{43\uparrow}^{\chi}(\omega) &= \Gamma_R(-\omega)f_R(-\omega)e^{-i\chi}, \\ \gamma_{34\downarrow}^{\chi}(\omega) &= \Gamma_R(\omega)[1 - f_R(\omega)]e^{-i\chi}, & \gamma_{43\downarrow}^{\chi}(\omega) &= \Gamma_R(-\omega)f_R(-\omega)e^{+i\chi}. \end{aligned} \quad (3.135)$$

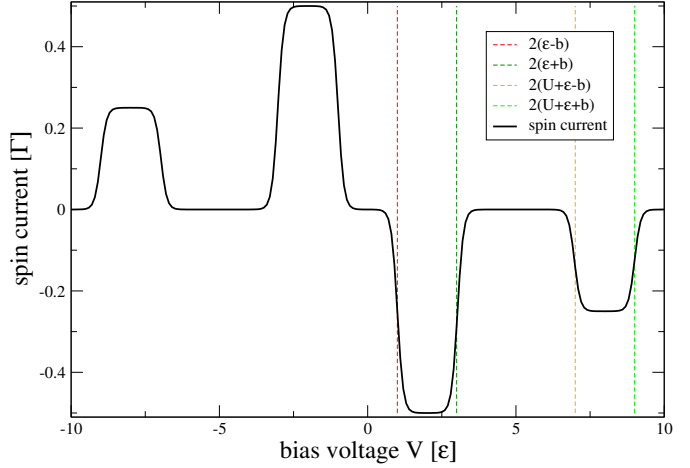
The system energy eigenbasis becomes

$$\begin{aligned} |E_0\rangle &= |0\rangle = |0, 0\rangle, & E_0 &= 0, \\ |E_{\downarrow}\rangle &= |\downarrow\rangle = |0, 1\rangle, & E_{\downarrow} &= \epsilon - b, \\ |E_{\uparrow}\rangle &= |\uparrow\rangle = |1, 0\rangle, & E_{\uparrow} &= \epsilon + b, \\ |E_2\rangle &= |\uparrow\downarrow\rangle = |1, 1\rangle, & E_2 &= 2\epsilon + U. \end{aligned} \quad (3.136)$$

With furthermore assuming the wideband limit  $\Gamma_{\nu}(\omega) = \Gamma_{\nu}$ , we can directly write the generalized rate equation for the populations ordered as  $(\rho_{00}, \rho_{\downarrow\downarrow}, \rho_{\uparrow\uparrow}, \rho_{22})^T$  as

$$\begin{aligned} \mathcal{L}(\chi) = & \Gamma_L \begin{pmatrix} -f_L(\epsilon - b) & +[1 - f_L(\epsilon - b)] & 0 & 0 \\ +f_L(\epsilon - b) & -[1 - f_L(\epsilon - b)] & 0 & 0 \\ 0 & 0 & -f_L(U + \epsilon - b) & +[1 - f_L(U + \epsilon - b)] \\ 0 & 0 & +f_L(U + \epsilon - b) & -[1 - f_L(U + \epsilon - b)] \end{pmatrix} \\ & + \Gamma_L \begin{pmatrix} -f_L(\epsilon + b) & 0 & +[1 - f_L(\epsilon + b)] & 0 \\ 0 & -f_L(U + \epsilon + b) & 0 & +[1 - f_L(U + \epsilon + b)] \\ +f_L(\epsilon + b) & 0 & -[1 - f_L(\epsilon + b)] & 0 \\ 0 & +f_L(U + \epsilon + b) & 0 & -[1 - f_L(U + \epsilon + b)] \end{pmatrix} \\ & + \Gamma_R \begin{pmatrix} -f_R(\epsilon - b) & +[1 - f_R(\epsilon - b)]e^{-i\chi} & 0 & 0 \\ +f_R(\epsilon - b)e^{+i\chi} & -[1 - f_R(\epsilon - b)] & 0 & 0 \\ 0 & 0 & -f_R(U + \epsilon - b) & +[1 - f_R(U + \epsilon - b)]e^{-i\chi} \\ 0 & 0 & +f_R(U + \epsilon - b)e^{+i\chi} & -[1 - f_R(U + \epsilon - b)] \end{pmatrix} \\ & + \Gamma_R \begin{pmatrix} -f_R(\epsilon + b) & 0 & +[1 - f_R(\epsilon + b)]e^{+i\chi} & 0 \\ 0 & -f_R(U + \epsilon + b) & 0 & +[1 - f_R(U + \epsilon + b)]e^{+i\chi} \\ +f_R(\epsilon + b)e^{-i\chi} & 0 & -[1 - f_R(\epsilon + b)] & 0 \\ 0 & +f_R(U + \epsilon + b)e^{-i\chi} & 0 & -[1 - f_R(U + \epsilon + b)] \end{pmatrix}. \end{aligned} \quad (3.137)$$

Figure 3.10: Spin current through a quantum dot with a Zeeman spin valve. At the first vertical line, the transition  $\epsilon - b$  enters the transport window, such that dominantly  $\downarrow$ -spins are transported from left to right. When the second transition  $\epsilon + b$  enters, also  $\uparrow$  spins participate in transport with exactly the same transmission probability, such that the spin current vanishes. This symmetry is again broken and restored when the transitions  $U + \epsilon - b$  and  $U + \epsilon + b$  enter the transport window. Parameters  $\Gamma_L = \Gamma_R = \Gamma$ ,  $\beta\epsilon = 20$ ,  $U = 3\epsilon$ ,  $b = \epsilon/2$ ,  $\mu_L = +V/2 = -\mu_R$ .



Here, the counting of different spin species enters with opposite sign, and the formalism puts the counting field at exactly those positions where we would expect it. Not surprisingly, the system can act as a **spin valve**, which e.g. for positive magnetic fields and finite positive bias voltages moves the energies of  $\uparrow$  spins outside the transport window and just lets  $\downarrow$  spins pass, thus yielding a negative spin current contribution, see Fig. 3.10.

## 3.5 Symmetries in Full Counting Statistics

### 3.5.1 Mathematical Motivation

The probability distribution  $P_n(t)$  is given by the inverse Fourier transform of the moment-generating function

$$P_n(t) = \frac{1}{2\pi} \int_{-\pi}^{+\pi} M(\chi, t) e^{-in\chi} d\chi = \frac{1}{2\pi} \int_{-\pi}^{+\pi} e^{C(\chi, t) - in\chi} d\chi. \quad (3.138)$$

Accordingly, a symmetry in the cumulant-generating function (or moment-generating function) of the form

$$C(-\chi, t) = C(+\chi + i\alpha, t) \quad (3.139)$$

leads to a symmetry of the probabilities

$$\begin{aligned} \frac{P_{+n}(t)}{P_{-n}(t)} &= \frac{\frac{1}{2\pi} \int_{-\pi}^{+\pi} e^{C(\chi, t) - in\chi} d\chi}{\frac{1}{2\pi} \int_{-\pi}^{+\pi} e^{C(\chi, t) + in\chi} d\chi} = \frac{\int_{-\pi}^{+\pi} e^{C(\chi, t) - in\chi} d\chi}{\int_{-\pi}^{+\pi} e^{C(-\chi, t) - in\chi} d\chi} \\ &= \frac{\int_{-\pi}^{+\pi} e^{C(\chi, t) - in\chi} d\chi}{\int_{-\pi}^{+\pi} e^{C(\chi + i\alpha, t) - in\chi} d\chi} = \frac{\int_{-\pi}^{+\pi} e^{C(\chi, t) - in\chi} d\chi}{\int_{-\pi + i\alpha}^{+\pi + i\alpha} e^{C(\chi, t) - in[\chi - i\alpha]} d\chi} \\ &= \frac{\int_{-\pi}^{+\pi} e^{C(\chi, t) - in\chi} d\chi}{e^{-n\alpha} \int_{-\pi}^{+\pi} e^{C(\chi, t) - in\chi} d\chi} \\ &= e^{+n\alpha}, \end{aligned} \quad (3.140)$$

where we have used in the last step that the counting field always enters as a function of  $e^{\pm ix}$ . This automatically implies that  $C(-\pi + i\sigma, t) = C(+\pi + i\sigma, t)$  for all real numbers  $\sigma$ , such that we can add two further integration paths from  $-\pi$  to  $-\pi + i\alpha$  and from  $+\pi + i\alpha$  to  $+\pi$  to the integral in the denominator. The value of the cumulant-generating function along these paths is the same, such that due to the different integral orientation there is no net change. Finally, using analyticity of the integrand, we deform the integration contour in the denominator, leaving two identical integrals in numerator and denominator. Note that the system may be very far from thermodynamic equilibrium but still obey a symmetry of the form (3.140), which leads to a fluctuation theorem of the form (3.141) being valid far from equilibrium.

As example, we consider the SET. The characteristic polynomial  $\mathcal{D}(\chi) = |\mathcal{L}(\chi) - \lambda \mathbf{1}|$  of the Liouvillian (3.46) and therefore also all eigenvalues obeys the symmetry

$$\mathcal{D}(-\chi) = \mathcal{D}\left(+\chi + i \ln \left[ \frac{f_L(1-f_R)}{(1-f_L)f_R} \right]\right) = \mathcal{D}(\chi + i[(\beta_R - \beta_L)\epsilon + \beta_L\mu_L - \beta_R\mu_R]). \quad (3.141)$$

**Exercise 28** (Eigenvalue Symmetry). (1 points)

Compute the characteristic polynomial of the Liouvillian (3.46) and confirm the symmetry (3.142).

which leads to the fluctuation theorem

$$\lim_{t \rightarrow \infty} \frac{P_{+n}(t)}{P_{-n}(t)} = e^{n[(\beta_R - \beta_L)\epsilon + \beta_L\mu_L - \beta_R\mu_R]}. \quad (3.142)$$

We note that the exponent does not depend on the microscopic details of the model ( $\Gamma_\alpha$ ) but only on thermodynamic quantities. Indeed, we had computed the entropy production rate for this model before

$$\dot{S}_i = [(\beta_R - \beta_L)\epsilon + \beta_L\mu_L - \beta_R\mu_R] I_M, \quad (3.143)$$

with  $I_M$  denoting the matter current from left to right and  $I_E = \epsilon I_M$ . Therefore, in the exponent, we simply have the integrated (long-term) entropy production.

We would obtain the same result for a DQD coupled to two terminals. For equal temperatures  $\beta_L = \beta_R = \beta$ , this becomes with  $V = \mu_L - \mu_R$

$$\lim_{t \rightarrow \infty} \frac{P_{+n}(t)}{P_{-n}(t)} = e^{n\beta V}, \quad (3.144)$$

which directly demonstrates that for large times the average transferred particle number

$$\langle n(t) \rangle = \sum_{n=-\infty}^{+\infty} n P_n(t) = \sum_{n=1}^{\infty} n [P_{+n}(t) - P_{-n}(t)] = \sum_{n=1}^{\infty} n P_n(t) [1 - e^{-n\beta V}] \quad (3.145)$$

always follows the voltage, i.e., for  $V > 0$  we also have  $\langle n(t) \rangle > 0$  and vice versa. We can interpret the exponent in Eq. (3.143) in terms of the entropy that has been produced: The quantity  $n\epsilon$  describes the energy that has traversed the SET for large times, and consequently, the term in the exponent approximates the entropy production, which is for large times simply proportional to the number of particles that have travelled from left to right

$$\Delta S_i \approx (\beta_R - \beta_L) n\epsilon + (\beta_L\mu_L - \beta_R\mu_R) n. \quad (3.146)$$

Therefore, we can interpret the fluctuation theorem also as a stochastic manifestation of the second law

$$\frac{P(+\Delta S_i)}{P(-\Delta S_i)} = e^{+\Delta S_i}. \quad (3.147)$$

Here, trajectories with a negative entropy production  $\Delta S_i$  are not forbidden. They are just less likely to occur than their positive-production counterparts, such that – on average – the second law is always obeyed.

The SET has the property of **tight coupling** between energy and matter currents: Every electron carries the same energy. For more general systems, where this property is not present, one still obtains a fluctuation theorem for the entropy production. Then, the combined counting statistics of energy and matter currents is necessary to obtain it. Furthermore, one will for an  $n$ -terminal system need  $2n$  counting fields to quantify the entropy production. In the long-term limit, one can use conservation laws, such that the maximum number of counting fields is given by  $2n - 2$ , which can be further reduced when one has further symmetries (like tight-coupling).

### 3.5.2 Microscopic discussion for multiple counting fields

In general, we can decide to count matter and energy exchanges with all  $N$  junctions of our model. Then, our Liouvillian depends on counting fields for both matter and energy at all these junctions  $\mathcal{L} \rightarrow \mathcal{L}(\boldsymbol{\chi}, \boldsymbol{\xi})$ , where  $\boldsymbol{\chi} = (\chi_1, \dots, \chi_N)$  denotes the matter and  $\boldsymbol{\xi} = (\xi_1, \dots, \xi_N)$  the energy counting fields. Let us further assume that our model leads to an additive rate equation

$$\dot{P}_a = \sum_{\nu} \sum_{b \neq a} \gamma_{ab}^{(\nu)} e^{+i(N_a - N_b)\chi_{\nu}} e^{+i(E_a - E_b)\xi_{\nu}} P_b - \sum_{\nu} \sum_{b \neq a} \gamma_{ba}^{(\nu)} P_a. \quad (3.148)$$

Here,  $\gamma_{ab}$  denotes the rate from  $b$  to  $a$  and  $E_a$  and  $N_a$  denote the corresponding energies and particle numbers. We have inserted the particle counting field  $\chi_{\nu}$  and energy counting field  $\xi_{\nu}$  for exchanges with reservoir  $\nu$  adopting the convention that contributions entering the system are counted positively. The rates obey the detailed balance property (1.101)

$$\frac{\gamma_{ab}^{(\nu)}}{\gamma_{ba}^{(\nu)}} = e^{\beta_{\nu}[(E_b - E_a) - \mu_{\nu}(N_b - N_a)]}. \quad (3.149)$$

Writing this in matrix notation

$$\dot{\mathbf{P}} = \mathcal{W}(\boldsymbol{\chi}, \boldsymbol{\xi}) \mathbf{P}, \quad (3.150)$$

we note that the counting fields would only enter the off-diagonal entries due to our assumptions. Then, we can show the following symmetry relation

$$\mathcal{W}^T(-\boldsymbol{\chi} - i\mathbf{A}, -\boldsymbol{\xi} - i\mathbf{B}) = \mathcal{W}(\boldsymbol{\chi}, \boldsymbol{\xi}), \quad \mathbf{B} = (\beta_1, \dots, \beta_N)^T, \quad \mathbf{A} = -(\mu_1\beta_1, \dots, \mu_N\beta_N)^T, \quad (3.151)$$

where  $T$  denotes the transpose. In components, this means (we do assume  $a \neq b$ )

$$\begin{aligned} \gamma_{ba}^{(\nu)} e^{+i(-\chi_{\nu} - iA_{\nu})(N_b - N_a)} e^{+i(-\xi_{\nu} - iB_{\nu})(E_b - E_a)} &= \gamma_{ab}^{(\nu)} e^{+\beta_{\nu}(E_a - E_b)} e^{-\beta_{\nu}\mu_{\nu}(N_a - N_b)} \times \\ &\quad \times e^{-i(-\chi_{\nu} - iA_{\nu})(N_a - N_b)} e^{-i(-\xi_{\nu} - iB_{\nu})(E_a - E_b)} \\ &\stackrel{!}{=} \gamma_{ab,ab}^{(\nu)} e^{+i\chi_{\nu}(N_a - N_b)} e^{+i\xi_{\nu}(E_a - E_b)}. \end{aligned} \quad (3.152)$$

In the first equality sign, we have inserted the local detailed balance relation specific to reservoir  $\nu$ . Now, solving for the coefficients we see that this is fulfilled when  $A_\nu = -\mu_\nu\beta_\nu$  and  $B_\nu = \beta_\nu$ , proving our relation (3.152).

This symmetry transfers to the long-term cumulant-generating function. The eigenvalues  $\lambda_\alpha(\boldsymbol{\chi}, \boldsymbol{\xi})$  of the rate matrix solve the characteristic polynomial at all  $\boldsymbol{\chi}$  and  $\boldsymbol{\xi}$

$$|\mathcal{W}(\boldsymbol{\chi}, \boldsymbol{\xi}) - \lambda_\alpha(\boldsymbol{\chi}, \boldsymbol{\xi})| = 0. \quad (3.153)$$

Evaluating this at shifted values we see that

$$\begin{aligned} & |\mathcal{W}(-\boldsymbol{\chi} - \mathbf{iA}, -\boldsymbol{\xi} - \mathbf{iB}) - \lambda_\alpha(-\boldsymbol{\chi} - \mathbf{iA}, -\boldsymbol{\xi} - \mathbf{iB}) \cdot \mathbf{1}| \\ &= |\mathcal{W}^T(-\boldsymbol{\chi} - \mathbf{iA}, -\boldsymbol{\xi} - \mathbf{iB}) - \lambda_\alpha(-\boldsymbol{\chi} - \mathbf{iA}, -\boldsymbol{\xi} - \mathbf{iB}) \cdot \mathbf{1}| \\ &= |\mathcal{W}(\boldsymbol{\chi}, \boldsymbol{\xi}) - \lambda_\alpha(-\boldsymbol{\chi} - \mathbf{iA}, -\boldsymbol{\xi} - \mathbf{iB}) \cdot \mathbf{1}|, \end{aligned} \quad (3.154)$$

where we have used that the eigenvalues do not change under transposition for an arbitrary quadratic matrix. Therefore, the eigenvalues and in particular the long-term cumulant-generating function inherit this symmetry

$$\lim_{t \rightarrow \infty} C(-\boldsymbol{\chi} - \mathbf{iA}, -\boldsymbol{\xi} - \mathbf{iB}, t) = \lim_{t \rightarrow \infty} C(\boldsymbol{\chi}, \boldsymbol{\xi}, t). \quad (3.155)$$

Before, we have learned for the example that a symmetry relation of the form  $C(-\chi - i\alpha, t) = C(+\chi, t)$  implies a fluctuation theorem of the form  $P_{+n}(t)/P_{-n}(t) = e^{-n\alpha}$ . Now, applying this to  $2N$  dimensions, we conclude

$$\lim_{t \rightarrow \infty} \frac{P_{+\Delta\mathbf{N}, +\Delta\mathbf{E}}(t)}{P_{-\Delta\mathbf{N}, -\Delta\mathbf{E}}(t)} = e^{-(\Delta\mathbf{E} \cdot \mathbf{B} + \Delta\mathbf{N} \cdot \mathbf{A})} = e^{-\sum_\nu \beta_\nu [\Delta E_\nu - \mu_\nu \Delta N_\nu]}. \quad (3.156)$$

In the exponent, we recognize the integrated entropy change of the reservoirs, which in the long-term limit for a transport setup becomes the total entropy production, since the system contribution is negligible. Therefore, the interpretation of the above formula is as follows: Each trajectory with an exchange of  $\Delta\mathbf{N}$  particles and an energy of  $\Delta\mathbf{E}$  is associated with an entropy production of  $\Delta_i S = -\sum_\nu \beta_\nu [\Delta E_\nu - \mu_\nu \Delta N_\nu]$ . Then, the fluctuation theorem corresponds to a stochastic formulation of the second law

**Def. 16** (Crooks fluctuation theorem). *A stochastic formulation of the second law is given by Crooks fluctuation theorem*

$$\frac{P_{+\Delta_i S}}{P_{-\Delta_i S}} = e^{+\Delta_i S}, \quad (3.157)$$

where  $\Delta_i S$  is the total entropy production.

The Crooks relation [17] is more quantitative than the average statement of the second law discussed before. We just check here that the second law follows from it

$$\begin{aligned} \langle \Delta_i S \rangle &= \sum_{\Delta_i S} \Delta_i S P_{\Delta_i S} = \sum_{\Delta_i S > 0} \Delta_i S [P_{+\Delta_i S} - P_{-\Delta_i S}] \\ &= \sum_{\Delta_i S > 0} \Delta_i S P_{-\Delta_i S} \underbrace{\left[ \frac{P_{+\Delta_i S}}{P_{-\Delta_i S}} - 1 \right]}_{\geq 0} \geq 0. \end{aligned} \quad (3.158)$$

We note that Eq. (3.157) only holds at large times, since for finite times, the entropy change of the system has to be taken into account.

# Chapter 4

## Transport in the strong coupling limit

The present treatment of open quantum systems allowed far-reaching statements on the quantum thermodynamic behaviour, albeit in quite narrow parameter regimes. During the derivation of such master equations we performed weak-coupling approximations between system and reservoir, and consequently we cannot expect these simple master equations to hold beyond the weak-coupling limit. The approaches we discuss here are not perturbative in the system reservoir coupling strength but can either correspond to exact solutions or are perturbative in other parameters. Then, with some modifications one can also treat the strong-coupling limit with master equations. Even for two-terminal transport however as in Fig. 4.1, the fuzzy boundary between system and reservoir may require redefinitions of the boundary.

### 4.1 Exactly solvable models: The Fano-Anderson model

An important class for benchmarking perturbative approaches are exactly solvable models, where the total Hamiltonian is a quadratic form of bosonic or fermionic annihilation and creation operators. For example, the Fano Anderson model (SET) can be solved along a similar route as the SRL. The system, bath, and interaction Hamiltonians are given by

$$\begin{aligned} H_S &= \epsilon d^\dagger d, & H_B &= \sum_k \epsilon_{kL} c_{kL}^\dagger c_{kL} + \sum_k \epsilon_{kR} c_{kR}^\dagger c_{kR}, \\ H_I &= \sum_k \left( t_{kL} d c_{kL}^\dagger + t_{kL}^* c_{kL} d^\dagger \right) + \sum_k \left( t_{kR} d c_{kR}^\dagger + t_{kR}^* c_{kR} d^\dagger \right), \end{aligned} \quad (4.1)$$

where  $d$  is a fermionic annihilation operator on the dot and  $c_{k\nu}$  are fermionic annihilation operators of an electron in the  $k$ -th mode of lead  $\nu$ . Obviously, this corresponds to a quadratic fermionic Hamiltonian, which can in principle be solved exactly by various methods such as e.g. non-equilibrium Greens functions [18] or even the equation-of-motion approach [19]. Such quadratic models are useful to study exact transport properties [20] or exact master equations [21].

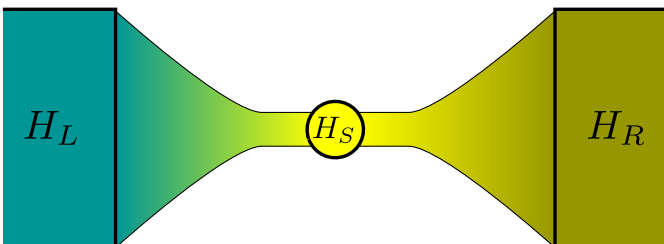


Figure 4.1: Sketch of a two-terminal transport scenario in the strong coupling limit. The boundaries between system and reservoir are defined by the observer and will not comply with weak-coupling assumptions.

### 4.1.1 Heisenberg Picture Dynamics

To be as self-contained as possible, we here simply compute the Heisenberg equations of motion for the system and bath annihilation operators (we denote operators in the Heisenberg picture by boldface symbols)

$$\begin{aligned} \dot{\mathbf{d}} &= -i\epsilon\mathbf{d} + i \sum_k [t_{kL}^* \mathbf{c}_{kL} + t_{kR}^* \mathbf{c}_{kR}] , \\ \dot{\mathbf{c}}_{kL} &= -i\epsilon_{kL} \mathbf{c}_{kL} + it_{kL} \mathbf{d} , \quad \dot{\mathbf{c}}_{kR} = -i\epsilon_{kR} \mathbf{c}_{kR} + it_{kR} \mathbf{d} . \end{aligned} \quad (4.2)$$

Surprisingly, this system is already closed and we obtain its solution by performing a Laplace transform [22]

$$\begin{aligned} z\tilde{d}(z) - d &= -i\epsilon\tilde{d}(z) + i \sum_k [t_{kL}^* \tilde{c}_{kL}(z) + t_{kR}^* \tilde{c}_{kR}(z)] , \\ z\tilde{c}_{kL}(z) - c_{kL} &= -i\epsilon_{kL} \tilde{c}_{kL}(z) + it_{kL} \tilde{d}(z) , \quad z\tilde{c}_{kR}(z) - c_{kR} = -i\epsilon_{kR} \tilde{c}_{kR}(z) + it_{kR} \tilde{d}(z) . \end{aligned} \quad (4.3)$$

In the above equations, we can eliminate the operators  $\tilde{c}_{kL}(z)$  and  $\tilde{c}_{kR}(z)$  in analogy to Sec. 1.3.8 (where we considered one reservoir and the sign of the  $t_k$  was opposite). This yields for the dot annihilation operator

$$\tilde{d}(z) = \frac{d + i \sum_k \left( \frac{t_{kL}^* c_{kL}}{z + i\epsilon_{kL}} + \frac{t_{kR}^* c_{kR}}{z + i\epsilon_{kR}} \right)}{z + i\epsilon + \sum_k \left( \frac{|t_{kL}|^2}{z + i\epsilon_{kL}} + \frac{|t_{kR}|^2}{z + i\epsilon_{kR}} \right)} \equiv \tilde{f}(z)d + \sum_k (\tilde{g}_{kL}(z)c_{kL} + \tilde{g}_{kR}(z)c_{kR}) , \quad (4.4)$$

where we have introduced the functions  $\tilde{g}_{k\nu}(z)$  and  $\tilde{f}(z)$ . This expression also yields the solution for the operators of the right lead modes

$$\tilde{c}_{k\nu}(z) = \frac{1}{z + i\epsilon_{k\nu}} c_{k\nu} + \frac{it_{k\nu}}{z + i\epsilon_{k\nu}} \tilde{d}(z) . \quad (4.5)$$

Inverting the Laplace transform may now be achieved by identifying the poles and applying the residue theorem. In the wide-band limit discussed below, this becomes particularly simple.

### 4.1.2 Asymptotic evolution

To find the full time evolution of the operators in the Heisenberg picture, we have to compute the inverse Laplace transform of

$$\begin{aligned} \tilde{f}(z) &= \frac{1}{z + i\epsilon + \sum_k \left( \frac{|t_{kL}|^2}{z + i\epsilon_{kL}} + \frac{|t_{kR}|^2}{z + i\epsilon_{kR}} \right)} , \\ \tilde{g}_{k\nu}(z) &= \frac{it_{k\nu}^*}{[z + i\epsilon_{k\nu}] \left[ z + i\epsilon + \sum_k \left( \frac{|t_{kL}|^2}{z + i\epsilon_{kL}} + \frac{|t_{kR}|^2}{z + i\epsilon_{kR}} \right) \right]} , \end{aligned} \quad (4.6)$$

which heavily depends on the number of modes and their distribution in the reservoir. Any system with a finite number of reservoir modes, for example, will exhibit recurrences to the initial state.

Only systems with a continuous spectrum of reservoir modes can be expected to yield a stationary system state. To obtain that limit, we approximate the summation over discrete modes by an integral formally by introducing the energy-dependent **tunnel rate** or **spectral density**

$$\Gamma_\nu(\omega) = 2\pi \sum_k |t_{k\nu}|^2 \delta(\omega - \epsilon_{k\nu}). \quad (4.7)$$

To obtain simple results, we will specifically assume a Lorentzian-shaped tunneling rate [23]

$$\Gamma_\nu(\omega) = \frac{\Gamma_\nu \delta_\nu^2}{\omega^2 + \delta_\nu^2}. \quad (4.8)$$

The simple pole structure of such tunneling rates renders analytic calculations simple. Superpositions of many Lorentzian shapes with shifted centers may approximate quite general tunneling rates [24]. With this, we get

$$\begin{aligned} \tilde{f}(z) &\approx \frac{1}{z + i\epsilon + \int \frac{1}{2\pi} \left( \frac{\Gamma_L \delta_L^2}{\omega^2 + \delta_L^2} + \frac{\Gamma_R \delta_R^2}{\omega^2 + \delta_R^2} \right) \frac{1}{z+i\omega} d\omega} = \frac{1}{z + i\epsilon + \frac{1}{2} \left( \frac{\Gamma_L \delta_L}{z + \delta_L} + \frac{\Gamma_R \delta_R}{z + \delta_R} \right)}, \\ \tilde{g}_{k\nu}(z) &\approx \frac{it_{k\nu}^*}{(z + i\epsilon_{k\nu}) \left[ z + i\epsilon + \int \frac{1}{2\pi} \left( \frac{\Gamma_L \delta_L^2}{\omega^2 + \delta_L^2} + \frac{\Gamma_R \delta_R^2}{\omega^2 + \delta_R^2} \right) \frac{1}{z+i\omega} d\omega \right]} \\ &= \frac{1}{[z + i\epsilon_{k\nu}] \left[ z + i\epsilon + \frac{1}{2} \left( \frac{\Gamma_L \delta_L}{z + \delta_L} + \frac{\Gamma_R \delta_R}{z + \delta_R} \right) \right]}. \end{aligned} \quad (4.9)$$

To obtain sufficiently simple results, we assume the **wide-band limit**  $\delta_\nu \rightarrow \infty$  (within which the tunneling rates are flat), where one obtains the simple expression

$$\begin{aligned} \tilde{f}(z) &\rightarrow \frac{1}{z + i\epsilon + (\Gamma_L + \Gamma_R)/2}, \\ \tilde{g}_{k\nu}(z) &\rightarrow \frac{it_{k\nu}^*}{(z + i\epsilon_{k\nu}) [z + i\epsilon + (\Gamma_L + \Gamma_R)/2]}. \end{aligned} \quad (4.10)$$

Inserting the inverse Laplace transforms of these expressions

$$\begin{aligned} f(t) &\rightarrow e^{-i\epsilon t} e^{-\Gamma t/2}, \\ g_{k\nu}(t) &\rightarrow \frac{t_{k\nu}^* (e^{-i\epsilon t} e^{-\Gamma t/2} - e^{-i\epsilon_{k\nu} t})}{\epsilon_{k\nu} - \epsilon + i\Gamma/2} \end{aligned} \quad (4.11)$$

(with  $\Gamma \equiv \Gamma_L + \Gamma_R$ ) into the equations for the dot then yields in the long-term limit

$$\mathbf{d}(t) = \sum_k g_{kL}(t) c_{kL} + \sum_k g_{kR}(t) c_{kR} \quad (4.12)$$

allows to express the dot Heisenberg operator in terms of the initial or Schrödinger picture operators.

Specifically, we get in the long-term limit

$$\mathbf{d}(t) \rightarrow - \sum_k \frac{t_{kL}^* e^{-i\epsilon_{kL} t}}{\epsilon_{kL} - \epsilon + i\Gamma/2} c_{kL} - \sum_k \frac{t_{kR}^* e^{-i\epsilon_{kR} t}}{\epsilon_{kR} - \epsilon + i\Gamma/2} c_{kR}, \quad (4.13)$$

where we see that asymptotically, the initial occupation of the dot is not relevant.

Using Eq. (4.5), also the right lead modes can be expressed in terms of the Schrödinger picture operators

$$\begin{aligned}\tilde{c}_{kR}(z) &= \frac{it_{kR}}{(z + i\epsilon_{kR})(z + i\epsilon + \Gamma/2)}d + \frac{1}{z + i\epsilon_{kR}}c_{kR} \\ &\quad - \sum_q \frac{t_{kR}t_{qL}^*}{(z + i\epsilon_{kR})(z + i\epsilon_{qL})(z + i\epsilon + \Gamma/2)}c_{qL} \\ &\quad - \sum_q \frac{t_{kR}t_{qR}^*}{(z + i\epsilon_{kR})(z + i\epsilon_{qR})(z + i\epsilon + \Gamma/2)}c_{qR}.\end{aligned}\quad (4.14)$$

Now, performing the inverse Laplace transform and neglecting all transient dynamics, we obtain the asymptotic evolution of the annihilation operators in the Heisenberg picture

$$\begin{aligned}c_{kR}(t) &\rightarrow \left(-\frac{t_{kR}e^{-i\epsilon_{kR}t}}{\epsilon_{kR} - \epsilon + i\Gamma/2}\right)d + e^{-i\epsilon_{kR}t}c_{kR} \\ &\quad + \sum_q \frac{t_{kR}t_{qL}^*}{\epsilon_{kR} - \epsilon_{qL}} \left(\frac{e^{-i\epsilon_{qL}t}}{\epsilon_{qL} - \epsilon + i\Gamma/2} - \frac{e^{-i\epsilon_{kR}t}}{\epsilon_{kR} - \epsilon + i\Gamma/2}\right)c_{qL} \\ &\quad + \sum_q \frac{t_{kR}t_{qR}^*}{\epsilon_{kR} - \epsilon_{qR}} \left(\frac{e^{-i\epsilon_{qR}t}}{\epsilon_{qR} - \epsilon + i\Gamma/2} - \frac{e^{-i\epsilon_{kR}t}}{\epsilon_{kR} - \epsilon + i\Gamma/2}\right)c_{qR}.\end{aligned}\quad (4.15)$$

### 4.1.3 Time-dependent and stationary occupation

The full time-dependent occupation  $n(t) = \langle d^\dagger(t)d(t) \rangle$  is found by inverting the Laplace transform. For the moment we do it formally and already perform the expectation value

$$\begin{aligned}n(t) &= \left\langle \left[ f^*(t)d^\dagger + \sum_k \left( g_{kL}^*(t)c_{kL}^\dagger + g_{kR}^*(t)c_{kR}^\dagger \right) \right] \left[ f(t)d + \sum_k \left( g_{kL}(t)c_{kL} + g_{kR}(t)c_{kR} \right) \right] \right\rangle \\ &= |f(t)|^2 n_0 + \sum_k \left( |g_{kL}(t)|^2 f_L(\epsilon_{kL}) + |g_{kR}(t)|^2 f_R(\epsilon_{kR}) \right),\end{aligned}\quad (4.16)$$

where we have used a product state as an initial one

$$\rho_0 = \rho_S^0 \frac{e^{-\beta_L(H_L - \mu_L N_L)}}{Z_L} \frac{e^{-\beta_R(H_R - \mu_R N_R)}}{Z_R}\quad (4.17)$$

with the lead Hamiltonians  $H_\nu = \sum_k \epsilon_{k\nu} c_{k\nu}^\dagger c_{k\nu}$  and the lead particle numbers  $N_\nu = \sum_k c_{k\nu}^\dagger c_{k\nu}$ . These eventually yield the only non-vanishing expectation values  $n_0 = \langle d^\dagger d \rangle$  and  $f_\nu(\epsilon_{k\nu}) = \langle c_{k\nu}^\dagger c_{k\nu} \rangle$ . Inverse lead temperatures  $\beta_\nu$  and chemical potentials  $\mu_\nu$  thereby only enter implicitly in the Fermi functions.

we obtain by switching to a continuum representation

$$\begin{aligned}n(t) &= e^{-\Gamma t} n_0 + \sum_k \sum_\nu |t_{k\nu}|^2 f_\nu(\epsilon_{k\nu}) 4 \frac{1 - 2e^{-\Gamma t/2} \cos[(\epsilon_{k\nu} - \epsilon)t] + e^{-\Gamma t}}{\Gamma^2 + 4(\epsilon_{k\nu} - \epsilon)^2} \\ &= e^{-\Gamma t} n_0 + \sum_\nu \int d\omega \Gamma_\nu f_\nu(\omega) \frac{4}{2\pi} \frac{1 - 2e^{-\Gamma t/2} \cos[(\omega - \epsilon)t] + e^{-\Gamma t}}{\Gamma^2 + 4(\omega - \epsilon)^2}.\end{aligned}\quad (4.18)$$

This is just the generalization of Eq. (1.182) to more reservoirs. The long-term limit can – due to  $\Gamma > 0$  – be determined easily, and the stationary occupation becomes

$$\bar{n} = \sum_{\nu} \int d\omega \Gamma_{\nu} f_{\nu}(\omega) \frac{2}{\pi} \frac{1}{\Gamma^2 + 4(\omega - \epsilon)^2}. \quad (4.19)$$

With the above formula for the stationary occupation valid for the wide-band limit, one can easily demonstrate the following:

- At infinite bias  $f_L(\omega) = 1$  and  $f_R(\omega) = 0$ , the stationary occupation approaches  $\bar{n} \rightarrow \Gamma_L/(\Gamma_L + \Gamma_R)$ , regardless of the coupling strength. A similar result is of course obtained for reverse infinite bias where  $\bar{n} \rightarrow \Gamma_R/(\Gamma_L + \Gamma_R)$ .
- When the quantum dot is coupled weakly to a single bath only (e.g.  $\Gamma_R(\omega) = 0$ ), the stationary occupation approaches the Fermi distribution of the coupled lead, evaluated at the dot energy (e.g.  $\bar{n} = f_L(\epsilon) + \mathcal{O}\{\Gamma_L\}$ ). This implies that for weak coupling to an equilibrium reservoir, the system will equilibrate with the temperature and chemical potential of the reservoir, consistent with what one expects from a master equation approach.
- When the dot is coupled weakly to both reservoirs, the stationary state approaches

$$\bar{n} \rightarrow \frac{\Gamma_L f_L(\epsilon) + \Gamma_R f_R(\epsilon)}{\Gamma_L + \Gamma_R}, \quad (4.20)$$

which is also obtained within a master equation approach, compare Sec. 2.5.

**Exercise 29** (Weak Coupling Limit). *Show that Eq. (4.19) reduces in the weak coupling limit to Eq. (4.20) by using a representation of the Dirac-Delta distribution*

$$\delta(x) = \lim_{\epsilon \rightarrow 0} \frac{1}{\pi} \frac{\epsilon}{x^2 + \epsilon^2}.$$

- In contrast, for the strong-coupling limit, the stationary occupation will be suppressed  $\bar{n} \rightarrow 0$ , as the exact solution for the stationary state is no longer localized on the dot.

#### 4.1.4 Stationary Current

For simplicity, we will only consider the stationary current from left to right here. It can be defined as the long-term limit of the change of particle numbers at the right lead

$$I_M = \lim_{t \rightarrow \infty} \frac{d}{dt} \left\langle \sum_k c_{kR}^{\dagger} c_{kR} \right\rangle = - \lim_{t \rightarrow \infty} \frac{d}{dt} \left\langle \sum_k c_{kL}^{\dagger} c_{kL} \right\rangle, \quad (4.21)$$

which we can evaluate in the Heisenberg picture as we did for the stationary occupation

$$I = i \sum_k t_{kR} \left\langle \mathbf{c}_{kR}^{\dagger}(t) \mathbf{d}(t) \right\rangle + \text{h.c.} \quad (4.22)$$

The r.h.s. of the above equation is also known as **current operator**.

From Eq. (4.15) we can obtain the long-term asymptotic evolution of the right lead occupation

$$\begin{aligned}
N_R \rightarrow & \sum_k \frac{|t_{kR}|^2}{(\epsilon_{kR} - \epsilon)^2 + \Gamma^2/4} n_0 + N_R^0 \\
& - \sum_{kq} \left[ \frac{t_{kR} t_{qR}^*}{\epsilon_{kR} - \epsilon_{qR}} e^{+i\epsilon_{kR}t} \left( \frac{e^{-i\epsilon_{qR}t}}{\epsilon_{qR} - \epsilon + i\Gamma/2} - \frac{e^{-i\epsilon_{kR}t}}{\epsilon_{kR} - \epsilon + i\Gamma/2} \right) \delta_{kq} f_R(\epsilon_{kR}) + \text{h.c.} \right] \\
& + \sum_{kq} \frac{|t_{kR}|^2 |t_{qL}|^2}{(\epsilon_{kR} - \epsilon_{qL})^2} \left( \frac{e^{+i\epsilon_{qL}t}}{\epsilon_{qL} - \epsilon - i\Gamma/2} - \frac{e^{+i\epsilon_{kR}t}}{\epsilon_{kR} - \epsilon - i\Gamma/2} \right) \\
& \quad \times \left( \frac{e^{-i\epsilon_{qL}t}}{\epsilon_{qL} - \epsilon + i\Gamma/2} - \frac{e^{-i\epsilon_{kR}t}}{\epsilon_{kR} - \epsilon + i\Gamma/2} \right) f_L(\epsilon_{qL}) \\
& + \sum_{kq} \frac{|t_{kR}|^2 |t_{qR}|^2}{(\epsilon_{kR} - \epsilon_{qR})^2} \left( \frac{e^{+i\epsilon_{qR}t}}{\epsilon_{qR} - \epsilon - i\Gamma/2} - \frac{e^{+i\epsilon_{kR}t}}{\epsilon_{kR} - \epsilon - i\Gamma/2} \right) \\
& \quad \times \left( \frac{e^{-i\epsilon_{qR}t}}{\epsilon_{qR} - \epsilon + i\Gamma/2} - \frac{e^{-i\epsilon_{kR}t}}{\epsilon_{kR} - \epsilon + i\Gamma/2} \right) f_R(\epsilon_{qR}). \tag{4.23}
\end{aligned}$$

Introducing the tunneling rates in the wide-band limit  $\Gamma_\nu \approx \Gamma_\nu(\omega) = \sum_k |t_{k\nu}|^2 \delta(\omega - \epsilon_{k\nu})$ , we can represent the right lead occupation by integrals

$$\begin{aligned}
N_R \rightarrow & \frac{1}{2\pi} \int d\omega \frac{\Gamma_R}{(\omega - \epsilon)^2 + \Gamma^2/4} n_0 + N_R^0 - \frac{1}{2\pi} \int d\omega \Gamma_R f_R(\omega) \left[ \frac{4 + 4i\omega t - 2t(\Gamma + 2i\epsilon)}{(2\omega + i\Gamma - 2\epsilon)^2} + \text{h.c.} \right] \\
& + \frac{1}{4\pi^2} \int d\omega d\omega' (\Gamma_L \Gamma_R f_L(\omega') + \Gamma_R^2 f_R(\omega')) \frac{1}{(\omega - \omega')^2} \left| \frac{e^{-i\omega't}}{\omega' - \epsilon + i\Gamma/2} - \frac{e^{-i\omega t}}{\omega - \epsilon + i\Gamma/2} \right|^2. \tag{4.24}
\end{aligned}$$

Whereas the first two terms are constant and do not contribute to the current, all other terms yield a non-vanishing contribution. The long-term limit of the time-derivative of the very last term is a bit involved to determine. It can be found, for example, by using properties of the Laplace transform. To evaluate the current, we therefore consider the limit

$$\begin{aligned}
F(\omega') & \equiv \lim_{t \rightarrow \infty} \frac{d}{dt} \int d\omega \frac{1}{(\omega - \omega')^2} \left| \frac{e^{-i\omega't}}{\omega' - \epsilon + i\Gamma/2} - \frac{e^{-i\omega t}}{\omega - \epsilon + i\Gamma/2} \right|^2 \\
& = \lim_{z \rightarrow 0} z \int_0^\infty dt e^{-zt} \frac{d}{dt} \int d\omega \frac{1}{(\omega - \omega')^2} \left| \frac{e^{-i\omega't}}{\omega' - \epsilon + i\Gamma/2} - \frac{e^{-i\omega t}}{\omega - \epsilon + i\Gamma/2} \right|^2 \\
& = \frac{8\pi}{\Gamma^2 + 4(\omega' - \epsilon)^2}, \tag{4.25}
\end{aligned}$$

which with its Lorentzian shape converges for small  $\Gamma$  towards a Dirac-Delta distribution. Eventually, the current becomes

$$\begin{aligned}
I_M & = -\frac{1}{\pi} \int d\omega \Gamma_R f_R(\omega) \frac{\Gamma/2}{(\omega - \epsilon)^2 + (\Gamma/2)^2} + \frac{1}{\pi\Gamma} \int d\omega (\Gamma_L \Gamma_R f_L(\omega) + \Gamma_R^2 f_R(\omega)) \frac{\Gamma/2}{(\omega - \epsilon)^2 + (\Gamma/2)^2} \\
& = \frac{\Gamma_L \Gamma_R}{\Gamma_L + \Gamma_R} \int d\omega [f_L(\omega) - f_R(\omega)] \frac{1}{\pi} \frac{\Gamma/2}{(\omega - \epsilon)^2 + (\Gamma/2)^2}. \tag{4.26}
\end{aligned}$$

Comparing this with the **Landauer formula**, according to which the current can be expressed as  $I_M = \frac{1}{2\pi} \int d\omega T(\omega) [f_L(\omega) - f_R(\omega)]$ , we can read off the **transmission** of the SET in the wideband

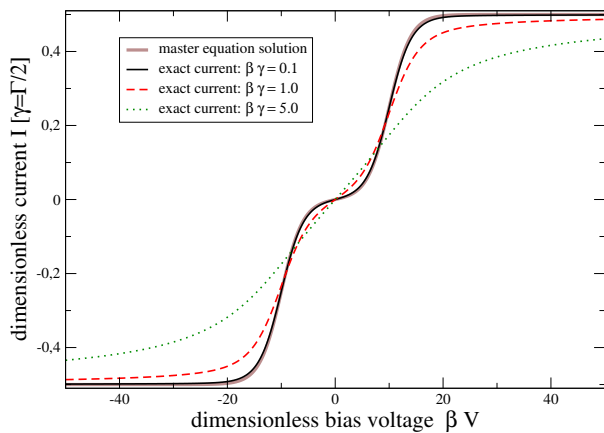


Figure 4.2: Plot of the electronic matter current (in units of  $\gamma = \Gamma_L = \Gamma_R = \Gamma/2$ ) versus the bias voltage for symmetric tunneling rates and equal electronic temperatures  $\beta_L = \beta_R = \beta$  and dot level  $\beta\epsilon = 5$ . For small coupling strength, exact (black solid) and master equation solution (brown bold) coincide for all bias voltages. For stronger couplings (red dashed and green dotted, respectively), the determination of the dot level  $\epsilon$  from the current is no longer possible.

limit

$$T_{\text{SET}}(\omega) = \frac{\Gamma_L \Gamma_R}{(\omega - \epsilon)^2 + (\Gamma_L + \Gamma_R)^2/4}. \quad (4.27)$$

The integrals in the above expression can be solved analytically by analysis in the complex plane, but here we will be content with the above integral representation, which can also be found using non-equilibrium Greens functions [18]. For consistency, we note that the current is antisymmetric under exchange of left and right leads as expected.

In the weak-coupling limit  $\Gamma \rightarrow 0$ , the current reduces to the known result (2.41)

$$I_M = \frac{\Gamma_L \Gamma_R}{\Gamma_L + \Gamma_R} [f_L(\epsilon) - f_R(\epsilon)], \quad (4.28)$$

which at equal temperatures left and right implies that the current always flows from the lead with larger chemical potential to the one with lower chemical potential.

**Exercise 30** (Weak-Coupling Limit). *Show that Eq. (4.28) follows from Eq. (4.26) when  $\Gamma \rightarrow 0$ .*

Finally, we note further that, in the infinite bias limit ( $f_L(\omega) \rightarrow 1$  and  $f_R(\omega) \rightarrow 0$ ), the current becomes  $I = \Gamma_L \Gamma_R / (\Gamma_L + \Gamma_R)$ , which is independent of the coupling strength and also consistent with Eq. (4.28). We have already seen that the master equation approach applied to the same problem reproduces Eq. (4.28) and therefore coincides with the exact result in the infinite bias limit.

Fig. 4.2 demonstrates the effect of increasing but symmetric coupling strengths  $\Gamma_L = \Gamma_R = \gamma$  on the current. Whereas the weak-coupling result is well approximated when  $\beta\gamma \ll 1$ , one may observe significant deviations for strong couplings. In the shown example, spectroscopy of the dot level  $\epsilon$  via detecting steps in the  $I - V$  characteristics is therefore only possible in the weak-coupling limit.

An analogous result can be obtained for the stationary energy current  $I_E = \frac{1}{2\pi} \int \omega T(\omega) [f_L(\omega) - f_R(\omega)] d\omega$ , and one can show that for such Landauer-type transport, the second law is obeyed  $(\beta_R - \beta_L)I_E + (\beta_L \mu_L - \beta_R \mu_R)I_M \geq 0$  [25].

## 4.2 Polaron master equation

### 4.2.1 Single bosonic reservoir

We consider an arbitrary system described by  $H_S$  (which may contain interactions) via a single coupling operator  $S = S^\dagger$  to a bosonic reservoir

$$H = H_S + \sum_k \omega_k \left[ b_k^\dagger + \frac{h_k}{\omega_k} S \right] \left[ b_k + \frac{h_k^*}{\omega_k} S \right], \quad (4.29)$$

with reservoir energies  $\omega_k$ , bosonic annihilation operators  $b_k$ , and spontaneous emission amplitudes  $h_k$ . Importantly, we note that – if  $H_S$  has a lower spectral bound – the above Hamiltonian has a lower spectral bound for all values of the coupling strength  $h_k$ . Upon expansion, this leads to a term

$$\Delta H_S = \sum_k \frac{|h_k|^2}{\omega_k} S^2 = \frac{1}{2\pi} \int_0^\infty \frac{J(\omega)}{\omega} d\omega S^2 \quad (4.30)$$

that renormalizes the system Hamiltonian and is typically neglected in weak-coupling treatments. When for example following the minimal coupling procedure, such a term will however arise generically. In our discussion here, we will keep it.

Now, the unitary **polaron transform**

$$U_P = \exp \left\{ S \sum_k \left( \frac{h_k^*}{\omega_k} b_k^\dagger - \frac{h_k}{\omega_k} b_k \right) \right\} \quad (4.31)$$

can be defined for arbitrary coupling operators  $S$  and has the following properties

$$\begin{aligned} U_P S U_P^\dagger &= S, \\ U_P b_k U_P^\dagger &= b_k - \frac{h_k^*}{\omega_k} S, \quad U_P b_k^\dagger U_P^\dagger = b_k^\dagger - \frac{h_k}{\omega_k} S, \end{aligned} \quad (4.32)$$

where the first line follows trivially and the last two lines can be shown with the **Hadamard lemma**

$$e^{+A} B e^{-A} = \sum_{m=0}^{\infty} \frac{1}{m!} [A, B]_m \quad : \quad [A, B]_0 = B, \quad [A, B]_{m+1} = [A, [A, B]_m]. \quad (4.33)$$

In the polaron picture, the total Hamiltonian therefore becomes

$$H' = U_P H U_P^\dagger = U_P H_S U_P^\dagger + \sum_k \omega_k b_k^\dagger b_k. \quad (4.34)$$

Now, if  $[H_S, S] = 0$  as e.g. in the pure dephasing model (compare Sec. 1.3.6), we would have  $U_P H_S U_P^\dagger = H_S$  and the model was completely decoupled in the polaron frame. However, realistic models will usually not do us this favor, and  $U_P H_S U_P^\dagger$  will involve terms mediating the interaction between system and reservoirs. The usual approach to derive a polaron master equation now defines a modified system Hamiltonian by the requirement that the first order expectation value

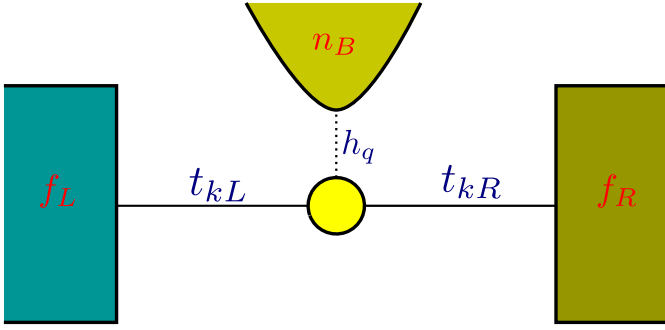


Figure 4.3: Sketch of a single-electron transistor that is capacitively coupled to a phonon reservoir. The interaction in the original Hamiltonian is of the pure dephasing type, i.e., to lowest order the SET energy will not be changed by the phonons. A conventional master equation treatment would yield no phonon effect on the SET dynamics.

of the interaction between system and reservoir should vanish in a thermal equilibrium state of the reservoir

$$\begin{aligned}
 H' &= U_P H_S U_P^\dagger + \sum_k \omega_k b_k^\dagger b_k \\
 &= \underbrace{\text{Tr}_B \left\{ U_P H_S U_P^\dagger \frac{e^{-\beta \omega_k b_k^\dagger b_k}}{Z} \right\}}_{H'_S} + \underbrace{\left[ U_P H_S U_P^\dagger - \text{Tr}_B \left\{ U_P H_S U_P^\dagger \frac{e^{-\beta \omega_k b_k^\dagger b_k}}{Z} \right\} \right]}_{H'_I} + \underbrace{\sum_k \omega_k b_k^\dagger b_k}_{H'_B}. \quad (4.35)
 \end{aligned}$$

The first term defines a renormalized system Hamiltonian, the second term denotes the system-reservoir interaction which by construction obeys  $\text{Tr}_B \{ H'_I e^{-\beta H'_B} / Z \} = 0$ , and the last term the reservoir contribution. In particular, we note that in this frame, in the strong coupling limit  $h_k \rightarrow \infty$ , none of these terms diverges. When deriving a master equation in this frame, instead of being perturbative in the  $h_k$ , we are rather perturbative in the term in square brackets, such that there exist regimes where the polaron master equation can be used to treat the strong-coupling limit.

### 4.2.2 Multiple reservoir example: Phonon-coupled single electron transistor

As before, we consider a quantum dot model that is additionally coupled to phonons. To keep the analysis simple however, we follow Ref. [26] by considering an SET that is coupled to one, many, or even a continuum of phonon modes as depicted in Fig. 4.3.

#### Model

We write the full Hamiltonian as  $H = H_{\text{SET}} + H_I + H_B^{\text{ph}}$ , where the SET Hamiltonian is given by

$$H_{\text{SET}} = \epsilon d^\dagger d + \sum_{\nu \in \{L, R\}} \sum_k \left[ \epsilon_{k\nu} c_{k\nu}^\dagger c_{k\nu} + t_{k\nu} d c_{k\nu}^\dagger + t_{k\nu}^* c_{k\nu} d^\dagger \right]. \quad (4.36)$$

In addition, the central dot of the SET now interacts with a phonon reservoir

$$H_I = d^\dagger d \otimes \sum_{q=1}^Q [h_q a_q + h_q^* a_q^\dagger], \quad H_B^{\text{ph}} = \sum_{q=1}^Q \omega_q a_q^\dagger a_q \quad (4.37)$$

containing  $Q$  phonon modes. Obviously, the interaction commutes with the central dot part of the SET Hamiltonian. Therefore, if one would conventionally derive a master equation for the

population dynamics of the central quantum dot, the additional phonon bath would not affect the populations of the central dot at all – the interaction is of pure-dephasing type.

In general however, this cannot be true: The interaction does not commute with the total SET Hamiltonian, and therefore one must expect the phonons to have some effect. Indeed, extensive calculations with only a single phonon mode whose dynamics is completely taken into account have revealed a strong suppression of the electronic current when strongly-coupled phonons are present. This phenomenon has been termed Franck-Condon blockade [27].

To treat such cases within a master equation approach, we apply a transformation to the full Hamiltonian  $H' = UHU^\dagger$  with the unitary operator

$$U = \exp \left\{ d^\dagger d \sum_q \left( \frac{h_q^*}{\omega_q} a_q^\dagger - \frac{h_q}{\omega_q} a_q \right) \right\} \equiv e^{d^\dagger d A}. \quad (4.38)$$

The above transformation is known as polaron or Lang-Firzov transformation [28, 29]. Obviously, the electronic leads are unaffected by the transformation, since  $Uc_{k\nu}U^\dagger = c_{k\nu}$ , and also the central dot part is inert  $Ud^\dagger dU^\dagger = d^\dagger d$ . There are multiple ways of proving the following relations

$$\begin{aligned} UdU^\dagger &= de^{-A}, & Ud^\dagger U^\dagger &= d^\dagger e^{+A}, \\ Ua_q U^\dagger &= a_q - \frac{h_q^*}{\omega_q} d^\dagger d, & Ua_q^\dagger U^\dagger &= a_q^\dagger - \frac{h_q}{\omega_q} d^\dagger d. \end{aligned} \quad (4.39)$$

**Exercise 31** (Polaron transformation). *Show the validity of Eqs. (4.39).*

These immediately also imply the relation

$$Ua_q^\dagger a_q U^\dagger = a_q^\dagger a_q - \frac{d^\dagger d}{\omega_q} (h_q a_q + h_q^* a_q^\dagger) + \frac{|h_q|^2}{\omega_q^2} d^\dagger d. \quad (4.40)$$

After the polaron transformation, the Hamiltonian therefore reads

$$\begin{aligned} H' &= \left( \epsilon - \sum_q \frac{|h_q|^2}{\omega_q} \right) d^\dagger d + \sum_{k\nu} \epsilon_{k\nu} c_{k\nu}^\dagger c_{k\nu} + \sum_q \omega_q a_q^\dagger a_q \\ &\quad + \sum_{k\nu} \left( t_{k\nu} d c_{k\nu}^\dagger e^{-A} + t_{k\nu}^* c_{k\nu} d^\dagger e^{+A} \right), \end{aligned} \quad (4.41)$$

and thereby admits a new decomposition into system and bath Hamiltonians, see also Fig. 4.4. Most obvious, we observe a shift of the electronic level  $\epsilon \rightarrow \epsilon' = \epsilon - \sum_q \frac{|h_q|^2}{\omega_q}$ . Second, the electronic tunneling terms between central dot and the adjacent leads now become dressed by exponential operators

$$H'_I = \sum_{k\nu} \left[ t_{k\nu} d c_{k\nu}^\dagger e^{-\sum_q \left( \frac{h_q^*}{\omega_q} a_q^\dagger - \frac{h_q}{\omega_q} a_q \right)} + t_{k\nu}^* c_{k\nu} d^\dagger e^{+\sum_q \left( \frac{h_q^*}{\omega_q} a_q^\dagger - \frac{h_q}{\omega_q} a_q \right)} \right], \quad (4.42)$$

which demonstrates that every single electronic jump from the central dot to the leads may now trigger multiple phonon emissions or absorptions. This implies that a perturbative treatment in  $t_{k\nu}$  still enables for a non-perturbative treatment of the phonon absorption and emission amplitudes  $h_q$ . Furthermore, this leads to the somewhat non-standard situation that already in the interaction Hamiltonian one has now operators from different reservoirs occurring in a product, which implies interesting properties for the correlation functions.

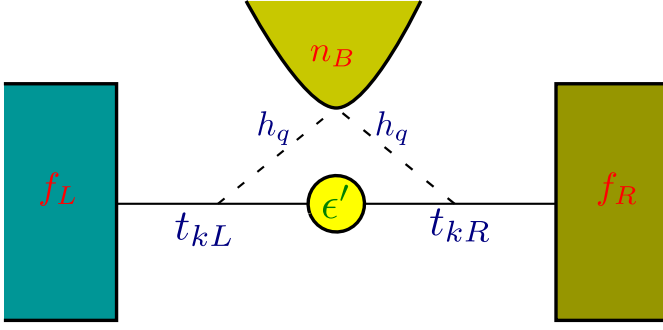


Figure 4.4: After the polaron transformation, direct coupling between the central quantum dot and the phonons in Fig. 4.3 is transformed to the electronic tunnel couplings. The electron-phonon coupling may be treated non-perturbatively (dash-dotted lines) when the electronic tunnel couplings are treated perturbatively (dashed lines).

### Reservoir equilibrium in the polaron picture

Before we proceed further by deriving a master equation in the displaced polaron frame, we remark that the solution from the displaced frame has to be transformed back to the original picture. A rate equation in the displaced frame implies that the full density matrix in the polaron frame is given by a product state of system and reservoir, where the phonon reservoir density matrix is given by the thermal equilibrium state  $\rho'(t) = \rho'_S(t) \bar{\rho}_B^{(L)} \bar{\rho}_B^{(R)} \frac{e^{-\beta_{\text{ph}} H'_B}}{Z'_{\text{ph}}}$ . The transformation back to the initial frame is given by the inverse polaron transformation

$$\begin{aligned} \rho(t) &= U^\dagger \rho'(t) U = U^\dagger \rho'_S(t) \bar{\rho}_B^{(L)} \bar{\rho}_B^{(R)} U U^\dagger \frac{e^{-\beta_{\text{ph}} H'_B}}{Z'_{\text{ph}}} U \\ &= U^\dagger \rho'_S(t) U \bar{\rho}_B^{(L)} \bar{\rho}_B^{(R)} \frac{e^{-\beta_{\text{ph}} U^\dagger H'_B U}}{Z'_{\text{ph}}}, \end{aligned} \quad (4.43)$$

where we have used that the polaron transformation (4.38) leaves the electronic reservoirs untouched. When the system density matrix does not exhibit coherences  $\rho'_S(t) = P_E(t) d d^\dagger + P_F(t) d^\dagger d$ , the unitary transformation will leave it untouched, such that only the reservoir part will be modified. With  $H'_B = \sum_q \omega_q a_q^\dagger a_q$  we can with the inverse transformations of Eq. (4.39)

$$\begin{aligned} U^\dagger H'_B U &= \sum_q \omega_q a_q^\dagger a_q + d^\dagger d \otimes \sum_q (h_q a_q + h_q^* a_q^\dagger) + \sum_q \frac{|h_q|^2}{\omega_q} d^\dagger d \\ &= d^\dagger d \otimes \sum_q \left( \omega_q a_q^\dagger a_q + h_q a_q + h_q^* a_q^\dagger + \frac{|h_q|^2}{\omega_q} \mathbf{1} \right) + d d^\dagger \otimes \sum_q \omega_q a_q^\dagger a_q \end{aligned} \quad (4.44)$$

represent the operator in the exponential as a sum of commuting operators. Since for all operators  $AB = BA = \mathbf{0}$  we have  $e^{A+B} = e^A e^B$  we conclude

$$\begin{aligned} e^{-\beta_{\text{ph}} U^\dagger H'_B U} &= e^{-\beta_{\text{ph}} d^\dagger d \otimes \sum_q \omega_q (a_q^\dagger + h_q/\omega_q)(a_q + h_q^*/\omega_q)} e^{-\beta_{\text{ph}} d d^\dagger \otimes \sum_q \omega_q a_q^\dagger a_q} \\ &= \left[ \mathbf{1} + d^\dagger d \left( e^{-\beta_{\text{ph}} \sum_q \omega_q (a_q^\dagger + h_q/\omega_q)(a_q + h_q^*/\omega_q)} - \mathbf{1} \right) \right] \left[ \mathbf{1} + d d^\dagger \left( e^{-\beta_{\text{ph}} \sum_q \omega_q a_q^\dagger a_q} - \mathbf{1} \right) \right] \\ &= d^\dagger d e^{-\beta_{\text{ph}} \sum_q \omega_q (a_q^\dagger + h_q/\omega_q)(a_q + h_q^*/\omega_q)} + d d^\dagger e^{-\beta_{\text{ph}} \sum_q \omega_q a_q^\dagger a_q}. \end{aligned} \quad (4.45)$$

Comparing with the initial Hamiltonian, the phonon part of the first term in the last line is nothing but the thermal phonon state under the side constraint that the SET dot is filled. Formally, this can be seen by replacing  $d^\dagger d \rightarrow 1$  in Eq. (4.37). Similarly, the other term is the thermalized phonon state when the SET dot is empty. Therefore, preparing the reservoir in a thermal state in

the polaron-transformed frame implies that in the original frame, the reservoir state is conditioned on the state of the system. Inserting the assumption that there are no coherences in the system  $\rho'_S(t) = P_E(t)dd^\dagger + P_F(t)d^\dagger d$ , the full density matrix in the original frame becomes

$$\rho(t) = P_E(t)dd^\dagger \bar{\rho}_B^{(L)} \bar{\rho}_B^{(R)} \otimes \frac{e^{-\beta_{\text{ph}} \sum_q \omega_q a_q^\dagger a_q}}{Z'_{\text{ph}}} + P_F(t)d^\dagger d \bar{\rho}_B^{(L)} \bar{\rho}_B^{(R)} \otimes \frac{e^{-\beta_{\text{ph}} \sum_q \omega_q (a_q^\dagger + h_q/\omega_q)(a_q + h_q^*/\omega_q)}}{Z'_{\text{ph}}}. \quad (4.46)$$

Therefore, when the SET dot is occupied, the phonon state is given by a displaced thermal state, whereas when the SET dot is empty, it is just given by the thermal state corresponding to the original phonon Hamiltonian. The phonon dynamics thereby follows the system state immediately, which goes beyond the conventional Born approximation.

### Polaron Rate Equation for discrete phonon modes

In the transformed frame, we do now proceed to derive a rate equation for the SET dot populations. We choose to count the phonons emitted into the phonon bath, to test the applicability of the counting field formalism. Here, we will use  $N_{\text{ph}} = \sum_q a_q^\dagger a_q$  as the reservoir observable of interest. Identifying the bath coupling operators in the interaction Hamiltonian (4.42) as

$$B_{1\nu} = \sum_k t_{k\nu} c_{k\nu}^\dagger e^{-A}, \quad B_{2\nu} = \sum_k t_{k\nu}^* c_{k\nu} e^{+A} \quad (4.47)$$

it becomes quite obvious that the reservoir correlation functions will now simultaneously contain contributions from electronic and phonon reservoirs. Recalling the definition 14 of the generalized correlation function, we obtain a simple product form between electronic and phononic contributions

$$\begin{aligned} C_{12}^{\nu, \chi}(\tau) &= \langle \mathbf{B}_{1\nu}(\tau) B_{2\nu} \rangle = C_{12, \text{el}}^\nu(\tau) C_{12, \text{ph}}^\chi(\tau), \\ C_{21}^{\nu, \chi}(\tau) &= \langle \mathbf{B}_{2\nu}(\tau) B_{1\nu} \rangle = C_{21, \text{el}}^\nu(\tau) C_{21, \text{ph}}^\chi(\tau). \end{aligned} \quad (4.48)$$

Here, the electronic contributions are just the conventional ones known from the SET

$$\begin{aligned} C_{12, \text{el}}^\nu(\tau) &= \sum_k |t_{k\nu}|^2 f_\nu(\epsilon_{k\nu}) e^{+i\epsilon_{k\nu}\tau} = \frac{1}{2\pi} \int \Gamma_\nu(-\omega) f_\nu(-\omega) e^{-i\omega\tau} d\omega, \\ C_{21, \text{el}}^\nu(\tau) &= \sum_k |t_{k\nu}|^2 [1 - f_\nu(\epsilon_{k\nu})] e^{-i\epsilon_{k\nu}\tau} = \frac{1}{2\pi} \int \Gamma_\nu(\omega) [1 - f_\nu(\omega)] e^{-i\omega\tau} d\omega. \end{aligned} \quad (4.49)$$

In contrast, the phonon contributions are given by

$$C_{12, \text{ph}}^\chi(\tau) = \left\langle e^{-iN_{\text{ph}}\chi} e^{-\mathbf{A}(\tau)} e^{+iN_{\text{ph}}\chi} e^{+\mathbf{A}} \right\rangle, \quad C_{21, \text{ph}}^\chi(\tau) = \left\langle e^{-iN_{\text{ph}}\chi} e^{+\mathbf{A}(\tau)} e^{+iN_{\text{ph}}\chi} e^{-\mathbf{A}} \right\rangle, \quad (4.50)$$

with the phonon operator in the interaction picture

$$\mathbf{A}(\tau) = \sum_q \left( \frac{h_q^*}{\omega_q} a_q^\dagger e^{+i\omega_q\tau} - \frac{h_q}{\omega_q} a_q e^{-i\omega_q\tau} \right). \quad (4.51)$$

We note that by  $h_q \rightarrow -h_q$ , we transform  $C_{12,\text{ph}}^\chi(\tau) \rightarrow C_{21,\text{ph}}^\chi(\tau)$ , such that we actually only need to calculate one correlation function. To calculate phonon contribution to the correlation function, we can exploit that (with  $\mathbf{A}^X(\tau) = e^{-iN_{\text{ph}}\chi} \mathbf{A}(\tau) e^{+iN_{\text{ph}}\chi}$ )

$$[\mathbf{A}^X(\tau), A] = 2i \sum_q \frac{|h_q|^2}{\omega_q^2} \sin(\omega_q \tau - \chi) \quad (4.52)$$

is just a number, which implies – using the Baker-Campbell-Hausdorff relation

$$\begin{aligned} e^{-\mathbf{A}^X(\tau)} e^{+A} &= e^{A - \mathbf{A}^X(\tau) - 1/2[\mathbf{A}^X(\tau), A]} \\ &= e^{\sum_q \left( \frac{h_q^*}{\omega_q} a_q^\dagger (1 - e^{+i(\omega_q \tau - \chi)}) - \frac{h_q}{\omega_q} a_q (1 - e^{-i(\omega_q \tau - \chi)}) \right)} e^{-i \sum_q \frac{|h_q|^2}{\omega_q^2} \sin(\omega_q \tau - \chi)}. \end{aligned} \quad (4.53)$$

For a thermal reservoir, the phonon correlation function can be written as a product of single-mode correlation functions  $C_{12,\text{ph}}^\chi(\tau) = \prod_{q=1}^Q C_{12,\text{ph}}^{\chi,q}(\tau)$ , where the single mode contributions read

$$\begin{aligned} C_{\text{ph}}^{\chi,q}(\tau) &= \left\langle e^{\frac{h_q^*}{\omega_q} a_q^\dagger (1 - e^{+i(\omega_q \tau - \chi)}) - \frac{h_q}{\omega_q} a_q (1 - e^{-i(\omega_q \tau - \chi)})} e^{-i \frac{|h_q|^2}{\omega_q^2} \sin(\omega_q \tau - \chi)} \right\rangle \\ &= \left\langle e^{\frac{h_q^*}{\omega_q} a_q^\dagger (1 - e^{+i(\omega_q \tau - \chi)})} e^{-\frac{h_q}{\omega_q} a_q (1 - e^{-i(\omega_q \tau - \chi)})} \right\rangle e^{-\frac{|h_q|^2}{\omega_q^2} (1 - e^{-i(\omega_q \tau - \chi)})}. \end{aligned} \quad (4.54)$$

By expanding the exponentials, we can evaluate the expectation value for thermal states, where the probability of having  $n$  quanta in the mode  $q$  is given by  $P_n = (1 - e^{-\beta_{\text{ph}} \omega_q}) e^{-n \beta_{\text{ph}} \omega_q}$  as

$$\begin{aligned} \left\langle e^{\alpha_q^* a_q^\dagger} e^{-\alpha_q a_q} \right\rangle &= \sum_{n,m=0}^{\infty} \frac{(\alpha_q^*)^n}{n!} \frac{(-\alpha_q)^m}{m!} \sum_{\ell=0}^{\infty} P_\ell \langle \ell | (a_q^\dagger)^n (a_q)^m | \ell \rangle \\ &= \sum_{n=0}^{\infty} \frac{(-1)^n |\alpha_q|^{2n}}{(n!)^2} \sum_{\ell=0}^{\infty} P_\ell \langle \ell | (a_q^\dagger)^n (a_q)^n | \ell \rangle = \sum_{\ell=0}^{\infty} P_\ell \sum_{n=0}^{\ell} \frac{(-1)^n |\alpha_q|^{2n}}{(n!)^2} \frac{\ell!}{(\ell - n)!} \\ &= \sum_{\ell=0}^{\infty} P_\ell \mathcal{L}_\ell(|\alpha_q|^2) = e^{-|\alpha_q|^2 n_B^q} \end{aligned} \quad (4.55)$$

with the Bose distribution  $n_B^q = [e^{\beta_{\text{ph}} \omega_q} - 1]^{-1}$  and Legendre polynomials, defined by the Rodriguez formula [30]

$$\mathcal{L}_n(x) = \frac{1}{2^n n!} \frac{d^n}{dx^n} [x^2 - 1]^n. \quad (4.56)$$

The single-mode contributions thus become with  $\alpha_q = \frac{h_q}{\omega_q} (1 - e^{-i(\omega_q \tau - \chi)})$

$$C_{\text{ph}}^{\chi,q}(\tau) = \exp \left\{ \frac{|h_q|^2}{\omega_q^2} \left[ e^{-i(\omega_q \tau - \chi)} (1 + n_B^q) + e^{+i(\omega_q \tau - \chi)} n_B^q - (1 + 2n_B^q) \right] \right\}, \quad (4.57)$$

such that finally, we obtain for the phonon correlation function

$$C_{12,\text{ph}}^\chi(\tau) = \exp \left\{ \sum_q \frac{|h_q|^2}{\omega_q^2} \left[ e^{-i(\omega_q \tau - \chi)} (1 + n_B^q) + e^{+i(\omega_q \tau - \chi)} n_B^q - (1 + 2n_B^q) \right] \right\}. \quad (4.58)$$

The fact that the transformation  $h_q \rightarrow -h_q$  leaves this result invariant implies that the phonon contribution is always the same in Eq. (4.48), such that we can drop the indices 12 and 21. Furthermore, we see that the phonon counting field occurs at the positions where one might have intuitively expected them. We note that the phonon correlation function obeys the KMS condition.

**Exercise 32** (KMS condition). *Show that the phonon correlation function (4.58) obeys the KMS condition  $C(\tau) = C(-\tau - i\beta_{\text{ph}})$*

The observation that in the phonon correlation function (4.57) the terms proportional to  $(1 + n_B^q)$  correspond to the emission of a phonon into the phonon reservoir and terms proportional to  $n_B^q$  alone are responsible for the absorption of a phonon from the reservoir enables one to derive the full phonon counting statistics from the model. Formally expanding the single mode correlation function into multiple emission ( $m'$ ) and absorption ( $m$ ) events we would obtain a decomposition in the net number of phonon absorbtions by the phonon bath  $n = m' - m$ , where  $C_{\text{ph}}^{\chi,q}(\tau) = \sum_{n=-\infty}^{+\infty} C_{\text{ph}}^{q,n}(\tau) e^{in\chi}$ , and  $C_{\text{ph}}^{q,n}(\tau) = \frac{1}{2\pi} \int_{-\pi}^{+\pi} C_{\text{ph}}^{\chi,q}(\tau) e^{-in\chi} d\chi$  can be determined by the inverse Fourier transform. In particular, using that

$$C_{\text{ph}}^q(\tau) = e^{-\frac{|h_q|^2}{\omega_q^2}(1+2n_B^q)} \sum_{m,m'=0}^{\infty} \left( \frac{|h_q|^2}{\omega_q^2} \right)^{m+m'} \frac{(n_B^q)^m (1+n_B^q)^{m'}}{m!m'} e^{i(m-m')\omega_q\tau} \quad (4.59)$$

one can show that by introducing the net number of phonon absorbtions by the phonon bath  $n = m' - m$ , the correlation function can be represented as (below, we drop the counting field  $\chi \rightarrow 0$ , since we have an interpretation for each term)

$$C_{\text{ph}}^q(\tau) = \sum_{n=-\infty}^{+\infty} e^{-in\omega_q\tau} e^{-\frac{|h_q|^2}{\omega_q^2}(1+2n_B^q)} \left( \frac{1+n_B^q}{n_B^q} \right)^{\frac{n}{2}} \mathcal{J}_n \left( 2 \frac{|h_q|^2}{\omega_q^2} \sqrt{n_B^q(1+n_B^q)} \right), \quad (4.60)$$

where  $\mathcal{J}_n(x)$  denotes the modified Bessel function of the first kind [30] – defined by the solution of the differential equation  $z^2 \mathcal{J}_n''(z) + z \mathcal{J}_n'(z) - (z^2 + n^2) \mathcal{J}_n(z) = 0$ . Introducing for multiple modes the notation  $\mathbf{n} = (n_1, \dots, n_Q)$ ,  $\boldsymbol{\omega} = (\omega_1, \dots, \omega_Q)$ , we therefore have for the full multi-mode phonon correlation function the representation

$$\begin{aligned} C_{\text{ph}}(\tau) &= \sum_{\mathbf{n}} e^{-i\mathbf{n}\cdot\boldsymbol{\omega}\tau} \prod_{q=1}^Q \left[ e^{-\frac{|h_q|^2}{\omega_q^2}(1+2n_B^q)} \left( \frac{1+n_B^q}{n_B^q} \right)^{\frac{n_q}{2}} \mathcal{J}_{n_q} \left( 2 \frac{|h_q|^2}{\omega_q^2} \sqrt{n_B^q(1+n_B^q)} \right) \right] \\ &= \sum_{\mathbf{n}} e^{-i\mathbf{n}\cdot\boldsymbol{\omega}\tau} C_{\text{ph}}^{\mathbf{n}}, \end{aligned} \quad (4.61)$$

where the simple exponential prefactor enables to calculate the Fourier transform of the full correlation function. In particular if only a single phonon mode is present, this enables a simple calculation of the Fourier transform of the complete electron-phonon correlation function

$$\begin{aligned} \gamma_{12}^{\nu}(\omega) &= \sum_{\mathbf{n}_{\nu}} \gamma_{12,\text{el}}^{\nu}(\omega - \mathbf{n}_{\nu} \cdot \boldsymbol{\omega}) C_{\text{ph}}^{\mathbf{n}_{\nu}} = \sum_{\mathbf{n}_{\nu}} \gamma_{12,\mathbf{n}_{\nu}}^{\nu}(\omega), \\ \gamma_{21}^{\nu}(\omega) &= \sum_{\mathbf{n}_{\nu}} \gamma_{21,\text{el}}^{\nu}(\omega - \mathbf{n}_{\nu} \cdot \boldsymbol{\omega}) C_{\text{ph}}^{\mathbf{n}_{\nu}} = \sum_{\mathbf{n}_{\nu}} \gamma_{21,\mathbf{n}_{\nu}}^{\nu}(\omega). \end{aligned} \quad (4.62)$$

Here, the terms  $\gamma_{12, \mathbf{n}_\nu}^\nu$  are interpreted as the emission of  $\mathbf{n}_\nu$  phonons into the phonon reservoir whilst an electron jumps from lead  $\nu$  onto the SET dot, whereas  $\gamma_{21, \mathbf{n}_\nu}^\nu$  accounts for the emission of  $\mathbf{n}_\nu$  when an electron is emitted to lead  $\nu$ . Now, the bosonic KMS relation

$$C_{\text{ph}}^{-\mathbf{n}_\nu} = e^{-\beta_{\text{ph}} \mathbf{n}_\nu \cdot \boldsymbol{\omega}} C_{\text{ph}}^{+\mathbf{n}_\nu} \quad (4.63)$$

together with properties of the Fermi functions implies a KMS-type relation for the full correlation function

$$\gamma_{12, +\mathbf{n}_\nu}^\nu(-\omega) = e^{-\beta_\nu(\omega - \mu_\nu + \mathbf{n}_\nu \cdot \boldsymbol{\omega})} e^{+\beta_{\text{ph}} \mathbf{n}_\nu \cdot \boldsymbol{\omega}} \gamma_{21, -\mathbf{n}_\nu}^\nu(+\omega), \quad (4.64)$$

which now involves both the electronic and phononic temperatures.

**Exercise 33** (KMS condition). *Show the validity of relation (4.64).*

However, we note that when these temperatures are equal, the usual local detailed balance relations are reproduced. Deriving a secular-type rate equation for the dot occupation is now straightforward, the probabilities for finding the dot empty or filled are governed by the rate matrix

$$\mathcal{L} = \sum_{\nu \in \{L, R\}} \sum_{\mathbf{n}_\nu} \begin{pmatrix} -\gamma_{12, \mathbf{n}_\nu}^\nu(-\epsilon') & +\gamma_{21, -\mathbf{n}_\nu}^\nu(+\epsilon') \\ +\gamma_{12, \mathbf{n}_\nu}^\nu(-\epsilon') & -\gamma_{21, -\mathbf{n}_\nu}^\nu(+\epsilon') \end{pmatrix}, \quad (4.65)$$

where  $\gamma_{12, \mathbf{n}_\nu}^\nu(-\epsilon')$  denotes the rate for an electron jumping onto the SET dot from lead  $\nu$  whilst simultaneously emitting  $\mathbf{n}_\nu$  phonons of the various modes into the phonon reservoir. Correspondingly,  $\gamma_{21, -\mathbf{n}_\nu}^\nu(+\epsilon')$  denotes the rate for the inverse process. Having identified the rates for the various involved processes, we can proceed by introducing counting fields. For a three-terminal system with the phononic junction only allowing for energy exchange and with conservation laws on the total energy and particle number we can expect three counting fields to be sufficient for tracking the full entropy production. These can – for example – be the matter transfer from left to right and the energy emitted to the phonon bath counted separately for electronic jumps, such that we have the counting-field dependent version

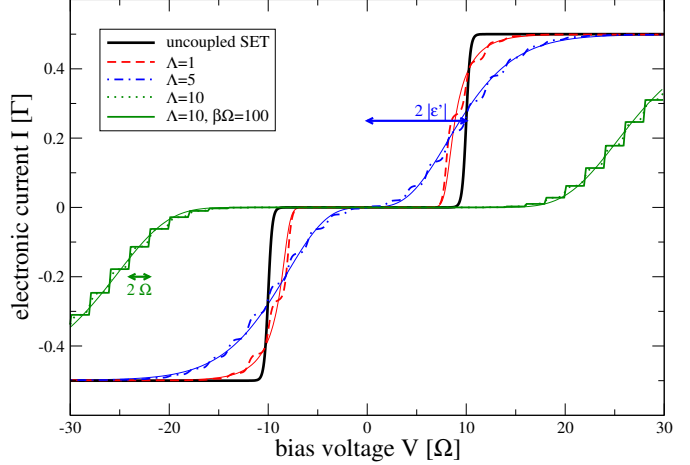
$$\begin{aligned} \mathcal{L}(\chi, \xi_L, \xi_R) = & \begin{pmatrix} -\gamma_{12, \mathbf{n}_L}^L(-\epsilon') & +\gamma_{21, -\mathbf{n}_L}^L(+\epsilon') e^{-i\mathbf{n}_L \cdot \Omega \xi_L} \\ +\gamma_{12, \mathbf{n}_L}^L(-\epsilon') e^{+i\mathbf{n}_L \cdot \Omega \xi_L} & -\gamma_{21, -\mathbf{n}_L}^L(+\epsilon') \end{pmatrix} \\ & + \begin{pmatrix} -\gamma_{12, \mathbf{n}_R}^R(-\epsilon') & +\gamma_{21, -\mathbf{n}_R}^R(+\epsilon') e^{+i\chi} e^{-i\mathbf{n}_R \cdot \Omega \xi_R} \\ +\gamma_{12, \mathbf{n}_R}^R(-\epsilon') e^{-i\chi} e^{+i\mathbf{n}_R \cdot \Omega \xi_R} & -\gamma_{21, -\mathbf{n}_R}^R(+\epsilon') \end{pmatrix}, \end{aligned} \quad (4.66)$$

which enables one to reconstruct all energy and matter currents and thus the full entropy flow.

Here, we will first investigate the impact of the phonon presence on the electronic matter current. If one is only interested in the electronic current, we may set  $\xi_L = \xi_R = 0$ . The transition rates in the above Liouvillian become particularly simple in the case of a single phonon mode

$$\begin{aligned} \gamma_{12, +n}^\nu(-\epsilon') &= \Gamma_\nu(\epsilon' + n\Omega) f_\nu(\epsilon' + n\Omega) e^{-\Lambda(1+2n_B)} \left( \frac{1+n_B}{n_B} \right)^{\frac{n}{2}} \mathcal{J}_n \left( 2\Lambda \sqrt{n_B(1+n_B)} \right), \\ \gamma_{21, -n}^\nu(+\epsilon') &= \Gamma_\nu(\epsilon' + n\Omega) [1 - f_\nu(\epsilon' + n\Omega)] e^{-\Lambda(1+2n_B)} \left( \frac{n_B}{1+n_B} \right)^{\frac{n}{2}} \mathcal{J}_n \left( 2\Lambda \sqrt{n_B(1+n_B)} \right), \end{aligned} \quad (4.67)$$

Figure 4.5: Electronic matter current versus bias voltage applied to the SET for vanishing (bold black) and increasing (dashed red, dash-dotted blue, and dotted green, respectively) coupling strengths  $\Lambda = |h|^2/\Omega^2 = J_0$  to a single phonon mode of frequency  $\Omega$  (bold curves) or to a continuum of phonon modes distributed according to an ohmic model (thin solid curves in background). The Franck-Condon blockade can within this model be understood in terms of a renormalization of the effective dot level  $\epsilon' = \epsilon - \Lambda\Omega$ , which – when  $\Lambda\Omega \gg \epsilon$  will lead to current suppression. Furthermore, the steps in the electronic current observed for sufficiently low temperatures (solid green) admit for the transport spectroscopy of the phonon frequency  $\Omega$ . In the multi-mode case (thin solid curves, for  $\omega_c = \Omega$  and  $J_0 = \Lambda$ ), current suppression due to the level renormalization is also observed but the steps in the current are no longer visible. Other parameters:  $\Gamma_L = \Gamma_R = \Gamma$ ,  $\beta_L = \beta_R = \beta_{\text{ph}} = \beta$ ,  $\beta\Omega = 10$  (except the thin green curve),  $\epsilon = 5\Omega$ ,  $J_0 = \Lambda$ ,  $\omega_c = \Omega$ .



where  $\Lambda = \frac{|h|^2}{\Omega^2}$  denotes the dimensionless coupling strength to the single phonon mode which is occupied according to  $n_B = [e^{\beta_{\text{ph}}\Omega} - 1]^{-1}$ . The resulting electronic matter current is depicted in Fig. 4.5.

Surprisingly, the simple  $2 \times 2$  rate matrix predicts many signatures in the electronic current. For example, in the electronic matter current one can read off the renormalized dot level at sufficiently low electronic temperatures. In addition however, low temperatures also allow to determine the phonon frequency from the width of the multiple plateaus.

### Thermodynamic interpretation

The present rate equation does not directly fit the scheme in Sec. 2.3, since the contribution of the three reservoirs to the rates is not additive. Nevertheless, an interpretation in terms of stochastic thermodynamics is possible.

The strong modification of the electronic current is due to the fact that the phonons allow for processes that would normally be forbidden, see Fig. 4.6 In the trajectory in the figure, first an electron jumps in from the left lead to the initially empty SET whilst absorbing two phonons. The change of the system energy by  $\Delta E = +\epsilon' = \Delta E_L + \Delta E_{\text{ph}}$  is supplied by both the left lead  $\Delta E_L = \epsilon' - 2\Omega$  and the phonon bath  $\Delta E_{\text{ph}} = +2\Omega$ . In the second step, the electron leaves the dot towards the right lead whilst again absorbing three phonons. Again, the change of the system energy by  $-\epsilon'$  is supplied by the right lead  $\Delta E_R = -(\epsilon' + 3\Omega)$  and the phonon both  $\Delta E_{\text{ph}} = +3\Omega$ . These energy and matter transfers can be used to construct the total heat exchanged between the reservoirs and thereby also the total entropy production in the steady state.

To relate the thermodynamic interpretation more to the modified local detailed balance relation,

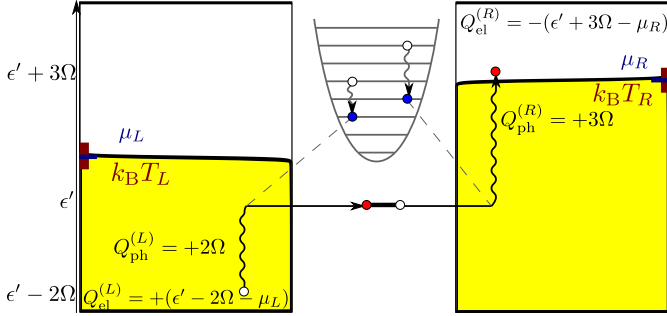


Figure 4.6: Sketch of the energetics of the problem for a single phonon mode, slightly adapted from Ref. [26]. For sufficiently low electronic temperatures, the dot level has to be between  $\mu_L$  and  $\mu_R$  to allow for transport, such that an electronic transfer from left to right would be extremely unlikely for the depicted situation. With phonons at sufficiently large temperature however, it is possible to realize trajectories where the missing energy is supplied by the phonon bath. The indicated heat transfers from reservoirs into the system allow for a complete reconstruction of the entropy flows even for single trajectories.

let us now for simplicity restrict ourselves to the case of a single phonon mode (the generalization to multiple modes is also possible). Formally, the rates corresponding to emission or absorption of different phonon numbers enter additively in Eq. (4.65). This enables one to see the phonon reservoir as a whole collection of infinitely many virtual phonon reservoirs that admit only for the emission or absorption of a certain number of phonons with the same frequency each time an electron is transferred across the SET junctions. This view enables one to adopt the previous definition of the entropy flow, where the index  $\nu$  labeling the reservoir may now assume infinitely many values  $\nu \rightarrow (\nu, n)$ , where  $\nu \in \{L, R\}$  denotes the junction across which an electron is transferred and  $n$  denotes the virtual phonon reservoir from or to which only  $n$  phonons may be absorbed or emitted at once. Recalling that  $\mathcal{L}_{EF}^{(\nu, n)}$  denotes the rate for an electron to leave the dot towards lead  $\nu$  whilst absorbing  $n$  phonons from the reservoir and  $\mathcal{L}_{FE}^{(\nu, n)}$  the rate of the inverse process, i.e., for an electron to enter the dot from lead  $\nu$  whilst emitting  $n$  phonons into the reservoir, the local detailed balance relation becomes – with the rates in Eq. (4.67)

$$\begin{aligned} \ln \left( \frac{\mathcal{L}_{FE}^{(\nu, n)}}{\mathcal{L}_{EF}^{(\nu, n)}} \right) &= \ln \left( \frac{\gamma_{12, +n}(-\epsilon')}{\gamma_{21, -n}(+\epsilon')} \right) = \ln \left[ \frac{f_\nu(\epsilon' + n\Omega)}{1 - f_\nu(\epsilon' + n\Omega)} \left( \frac{1 + n_B}{n_B} \right)^n \right] \\ &= \ln \left[ e^{-\beta_\nu(\epsilon' + n\Omega - \mu_\nu)} e^{+n\beta_{\text{ph}}\Omega} \right] = -\beta_\nu(\epsilon' + n\Omega - \mu_\nu) + \beta_{\text{ph}}n\Omega, \end{aligned} \quad (4.68)$$

such that the entropy flow from the virtual reservoir (recall that  $\nu \rightarrow (\nu, n)$ ) becomes

$$\begin{aligned} \dot{S}_e^{(\nu, n)} &= \mathcal{L}_{EF}^{(\nu, n)} \bar{P}_F \ln \left( \frac{\mathcal{L}_{FE}^{(\nu, n)}}{\mathcal{L}_{EF}^{(\nu, n)}} \right) + \mathcal{L}_{FE}^{(\nu, n)} \bar{P}_E \ln \left( \frac{\mathcal{L}_{EF}^{(\nu, n)}}{\mathcal{L}_{FE}^{(\nu, n)}} \right) \\ &= \left[ \mathcal{L}_{EF}^{(\nu, n)} \bar{P}_F - \mathcal{L}_{FE}^{(\nu, n)} \bar{P}_E \right] \ln \left( \frac{\mathcal{L}_{FE}^{(\nu, n)}}{\mathcal{L}_{EF}^{(\nu, n)}} \right) \\ &= \beta_\nu (I_E^{(\nu, n)} - \mu_\nu I_M^{(\nu, n)}) + \beta_{\text{ph}} I_E^{(n, \nu, \text{ph})} = \dot{S}_{e, \text{el}}^{(\nu, n)} + \dot{S}_{e, \text{ph}}^{(\nu, n)}, \end{aligned} \quad (4.69)$$

which is additive in electronic and phononic contributions. Here, we have introduced the energy flows corresponding to the emission or absorption of  $n$  phonons. The total energy flows are given

by

$$I_E^\nu = \sum_n I_E^{(\nu,n)} = \sum_n [\gamma_{12,+n}(-\epsilon')\bar{P}_E - \gamma_{21,-n}(+\epsilon')\bar{P}_F] (\epsilon' + n\Omega),$$

$$I_E^{\text{ph}} = \sum_n [I_E^{(n,L,\text{ph})} + I_E^{(n,R,\text{ph})}] = \sum_n \sum_\nu [\gamma_{21,-n}(+\epsilon')\bar{P}_F - \gamma_{12,+n}(-\epsilon')\bar{P}_R] n\Omega, \quad (4.70)$$

whereas the total electronic matter current from lead  $\nu$  is given by

$$I_M^\nu = \sum_n I_E^{(\nu,n)} = \sum_n [\gamma_{12,+n}(-\epsilon')\bar{P}_E - \gamma_{21,-n}(+\epsilon')\bar{P}_F]. \quad (4.71)$$

Similarly, the total entropy flow from the electronic leads is obtained by summing over all different  $n$ , and the total entropy flow from the phonon reservoirs is obtained by summing over the contributions from different  $n$  and different  $\nu$

$$\dot{S}_e^{(\nu)} = \sum_n \dot{S}_{e,\text{el}}^{(\nu,n)}$$

$$\dot{S}_e^{\text{ph}} = \sum_n \left( \dot{S}_{e,\text{ph}}^{(L,n)} + \dot{S}_{e,\text{ph}}^{(R,n)} \right). \quad (4.72)$$

Altogether, the system obeys the laws of thermodynamics, which results in an overall positive entropy production. Consequently, we just note here that it is possible to verify a fluctuation theorem for entropy production, i.e., for  $P_{n,e_{\text{ph}}^L,e_{\text{ph}}^R}(t)$  denoting the probability for trajectories with  $n$  electrons having traversed the SET from left to right and having emitted energy  $e_{\text{ph}}^L = \mathbf{n}_L \cdot \boldsymbol{\omega}$  to the phonon reservoir during electronic jumps over the left and energy  $e_{\text{ph}}^R = \mathbf{n}_R \cdot \boldsymbol{\omega}$  during jumps over the right barrier. In detail, it reads [26]

$$\lim_{t \rightarrow \infty} \frac{P_{+n,+e_{\text{ph}}^L,+e_{\text{ph}}^R}(t)}{P_{-n,-e_{\text{ph}}^L,-e_{\text{ph}}^R}(t)} = e^{[(\beta_R - \beta_L)\epsilon' + (\beta_L \mu_L - \beta_R \mu_R)]n + (\beta_{\text{ph}} - \beta_L)e_{\text{ph}}^L + (\beta_{\text{ph}} - \beta_R)e_{\text{ph}}^R}, \quad (4.73)$$

and it is straightforward to see that it reduces to the conventional fluctuation theorem when all temperatures are equal.

Disregarding the phonon counting statistics, we note that the system also obeys a fluctuation theorem involving the electronic transfer statistics only

$$\lim_{t \rightarrow \infty} \frac{P_{+n}(t)}{P_{-n}(t)} = e^{n\mathcal{A}_{\text{eff}}}, \quad (4.74)$$

where the effective affinity  $\mathcal{A}_{\text{eff}}$  is however not related to the entropy production, it does, for example, depend on the details of the coupling.

### Polaron Rate Equation for continuum phonon modes

Also for a continuum of phonon modes it is possible to obtain a master equation representation. Here, we directly represent the phonon correlation function (4.58), taking a counting field for the energy of the phonon reservoir into account. This then yields

$$C_{\text{ph}}^\xi(\tau) = \exp \left\{ \int_0^\infty d\omega \frac{J(\omega)}{\omega^2} [e^{-i\omega(\tau-\xi)}(1 + n_B(\omega)) + e^{+i\omega(\tau-\xi)}n_B(\omega) - (1 + 2n_B(\omega))] \right\}, \quad (4.75)$$

where we have introduced the spectral density  $J(\omega) = \sum_q |h_q|^2 \delta(\omega - \omega_q)$ , and  $\xi$  is a counting field responsible for the energy of the phonon reservoir. When we choose the common ohmic parametrization  $J(\omega) = J_0 \omega e^{-\omega/\omega_c}$  with dimensionless coupling strength  $J_0$  and cutoff frequency  $\omega_c$ , the integral can be solved exactly. Writing the Bose-Einstein distributions as a geometric series and resumming all separate integral contribution, we finally obtain for the phonon correlation function

$$C_{\text{ph}}^\xi(\tau) = \left[ \frac{\Gamma\left(\frac{1+\beta_{\text{ph}}\omega_c+i(\tau-\xi)\omega_c}{\beta_{\text{ph}}\omega_c}\right) \Gamma\left(\frac{1+\beta_{\text{ph}}\omega_c-i(\tau-\xi)\omega_c}{\beta_{\text{ph}}\omega_c}\right)}{\Gamma^2\left(\frac{1+\beta_{\text{ph}}\omega_c}{\beta_{\text{ph}}\omega_c}\right) (1+i(\tau-\xi)\omega_c)} \right]^{J_0}, \quad (4.76)$$

where  $\Gamma(x) = \int_0^\infty t^{x-1} e^{-t} dt$  denotes the  $\Gamma$ -function. The observation that  $C_{\text{ph}}^\xi(\tau) = C_{\text{ph}}(\tau - \xi)$  (generally true for energy counting and an initial state that is diagonal in the energy eigenbasis) leads to the relation

$$\gamma_{\text{ph}}^\xi(\omega) = e^{+i\omega\xi} \gamma_{\text{ph}}(\omega). \quad (4.77)$$

We note from Eq. (4.75) that for particular parametrizations of the spectral coupling density one can expect that for large times the phonon correlation functions may remain finite  $\lim_{t \rightarrow \infty} C_{\text{ph}}(\tau) \neq 0$ . However, the total correlation function is given by a product of electronic (which decay) and phonon correlation functions. Its Fourier transform (that enters the rates) can be calculated numerically from a convolution integral

$$\begin{aligned} \gamma_{12}^{\nu, \xi_\nu}(-\epsilon') &= \frac{1}{2\pi} \int d\omega \Gamma_\nu(-\omega) f_\nu(-\omega) \gamma_{\text{ph}}(-\epsilon' - \omega) e^{-i(\epsilon' + \omega)\xi_\nu}, \\ \gamma_{21}^{\nu, \xi_\nu}(+\epsilon') &= \frac{1}{2\pi} \int d\omega \Gamma_\nu(+\omega) [1 - f_\nu(+\omega)] \gamma_{\text{ph}}(+\epsilon' - \omega) e^{+i(\epsilon' - \omega)\xi_\nu}, \end{aligned} \quad (4.78)$$

and enters in this case a rate matrix of the form

$$\mathcal{L}(\chi, \xi_L, \xi_R) = \begin{pmatrix} -\gamma_{12}^L(-\epsilon') & +\gamma_{21}^{L, \xi_L}(+\epsilon') \\ +\gamma_{12}^{L, \xi_L}(-\epsilon') & -\gamma_{21}^L(+\epsilon') \end{pmatrix} + \begin{pmatrix} -\gamma_{12}^R(-\epsilon') & +\gamma_{21}^{R, \xi_R}(+\epsilon') e^{+i\chi} \\ +\gamma_{12}^{R, \xi_R}(-\epsilon') e^{-i\chi} & -\gamma_{21}^R(+\epsilon') \end{pmatrix}, \quad (4.79)$$

from which the electronic matter current can be directly deduced. With the choices  $J_0 = \frac{|h|^2}{\Omega^2}$  and  $\omega_c = \Omega$  the electronic current is for high temperatures quite similar as if one would have only a single phonon mode. Also the symmetries are similar to that of Eq. (4.66), and a similar fluctuation theorem arises from that. The crucial difference however is that at low temperatures, the phonon plateaus are no longer visible – compare the thin solid versus the bold curves in Fig. 4.5. Since for the continuum model many different phonon frequencies contribute, this is expected. Interestingly however, the current suppression due to the presence of the phonons (Franck-Condon blockade) is also visible for a continuum of phonon modes.

### 4.3 Bosonic reaction-coordinate mappings

Polaron transforms are only one way to approach the strong-coupling limit. They may not always be applicable, which is why also other transforms have been used.

### 4.3.1 Bosonic Bogoliubov transforms

In a nutshell, Bogoliubov transforms (compare lecture on Advanced Mathematical Methods) map bosonic (or fermionic) creation and annihilation operators to new bosonic (or fermionic) creation and annihilation operators while leaving their (anti-)commutation relations invariant.

**Def. 17** (Bosonic Bogoliubov transform). *A bosonic Bogoliubov transform is a linear mapping between bosonic annihilation and creation operators, which preserves the corresponding bosonic commutation relations*

$$a_k = \sum_q [u_{kq}b_q + v_{kq}b_q^\dagger], \quad \begin{aligned} [a_k, a_{k'}^\dagger] &= \delta_{kk'}, & [a_k, a_{k'}] &= 0, \\ [b_k, b_{k'}^\dagger] &= \delta_{kk'}, & [b_k, b_{k'}] &= 0, \end{aligned} \quad (4.80)$$

where  $u_{kq}, v_{kq} \in \mathbb{C}$ .

The demand that the commutation relations must be preserved puts additional constraints on the a priori unknown coefficients  $u_{kq}$  and  $v_{kq}$ . For example, from the commutation relations we obtain the conditions

$$\begin{aligned} [a_k, a_{k'}^\dagger] &= \sum_q (u_{kq}u_{k'q}^* - v_{kq}v_{k'q}^*) = \delta_{kk'}, \\ [a_k, a_{k'}] &= \sum_q (u_{kq}v_{k'q} - v_{kq}u_{k'q}) = 0, \end{aligned} \quad (4.81)$$

where we note that the equation  $[a_k^\dagger, a_{k'}^\dagger] = 0$  just adds the conjugate of the second constraint.

- A simple but special solution to these equations is to choose  $v_{kk'} = 0$ . Then, creation and annihilation operators are not mixed, the second of Eq. (4.81) is trivially fulfilled, and the first reduces to a unitarity condition  $\sum_q u_{kq}u_{k'q}^* = \delta_{kk'}$  on the matrix formed by the  $u_{kq}$ . In this case, the Bogoliubov transform therefore reduces to a unitary transform between annihilation operators. An even more trivial example of unitary Bogoliubov transforms is the multiplication of the creation and annihilation operators by a phase factor (absence of any mixing): When discussing operator transforms, we noted that time-dependent phase factors would e.g. arise in the interaction picture.
- Another special case is obtained when parametrizing the  $u_{kq}$  and  $v_{kq}$  by an orthogonal matrix

$$u_{kq} = \frac{1}{2} \left( \frac{\alpha_k}{\beta_q} + \frac{\beta_q}{\alpha_k} \right) \Lambda_{kq}, \quad v_{kq} = \frac{1}{2} \left( \frac{\alpha_k}{\beta_q} - \frac{\beta_q}{\alpha_k} \right) \Lambda_{kq}, \quad \sum_q \Lambda_{kq}\Lambda_{k'q} = \delta_{kk'} \quad (4.82)$$

with  $\alpha_k \in \mathbb{R}$  and  $\beta_q \in \mathbb{R}$ . Direct insertion shows that the bosonic commutation relations are automatically preserved under such a Bogoliubov transform.

In the general case, interpreting the coefficients as matrix elements  $u_{kq} = (U)_{kq}$  and  $v_{kq} = (V)_{kq}$  as elements of matrices, we can also write these relations as

$$UU^\dagger - VV^\dagger = \mathbf{1}, \quad UV^T - VU^T = \mathbf{0}. \quad (4.83)$$

Now, arranging the  $U$  and  $V$  matrices in an enlarged matrix

$$W = \begin{pmatrix} U^T & V^\dagger \\ V^T & U^\dagger \end{pmatrix}, \quad W^T = \begin{pmatrix} U & V \\ V^* & U^* \end{pmatrix}, \quad (4.84)$$

where  $A^T$  denotes the transpose of the matrix  $A$ , we see that we can encode the conditions (4.83) – or conjugate (transposes) thereof – into a single relation on the matrix  $W$

$$W^T \begin{pmatrix} \mathbf{0} & +\mathbf{1} \\ -\mathbf{1} & \mathbf{0} \end{pmatrix} W = \begin{pmatrix} \mathbf{0} & +\mathbf{1} \\ -\mathbf{1} & \mathbf{0} \end{pmatrix}. \quad (4.85)$$

Such matrices  $W$  are called **symplectic**, they have unit determinant and form a group under matrix multiplication. Consequently, in general Bogoliubov transforms are symplectic transforms of the creation and annihilation operators. Fortunately, even in the non-trivial cases, the symplectic transform is not completely fixed, which gives us the freedom to recast the Hamiltonian into a specific form.

Formally vectorizing the creation and annihilation operators, the Bogoliubov transform can then be written as

$$\begin{pmatrix} \vdots \\ a_k \\ \vdots \\ \hline \vdots \\ a_k^\dagger \\ \vdots \end{pmatrix} = \left( \begin{array}{c|c} U & V \\ \hline V^* & U^* \end{array} \right) \begin{pmatrix} \vdots \\ b_k \\ \vdots \\ \hline \vdots \\ b_k^\dagger \\ \vdots \end{pmatrix} = W^T \begin{pmatrix} \vdots \\ b_k \\ \vdots \\ \hline \vdots \\ b_k^\dagger \\ \vdots \end{pmatrix}. \quad (4.86)$$

### 4.3.2 Two-mode example

We consider a bosonic reservoir with just two modes that is coupled via the dimensionless operator  $S = S^\dagger$  to some arbitrary system  $H_S$

$$\begin{aligned} H &= H_S + \omega_1 \left[ a_1^\dagger + \frac{\lambda_1}{\omega_1} S \right] \left[ a_1 + \frac{\lambda_1}{\omega_1} S \right] + \omega_2 \left[ a_2^\dagger + \frac{\lambda_2}{\omega_2} S \right] \left[ a_2 + \frac{\lambda_2}{\omega_2} S \right] \\ &= H_S + \left( \frac{\lambda_1^2}{\omega_1} + \frac{\lambda_2^2}{\omega_2} \right) S^2 + S[\lambda_1(a_1 + a_1^\dagger) + \lambda_2(a_2 + a_2^\dagger)] + \omega_1 a_1^\dagger a_1 + \omega_2 a_2^\dagger a_2. \end{aligned} \quad (4.87)$$

This Hamiltonian has a lower bound for all values of the couplings  $\lambda_i$ , provided that  $\omega_i > 0$  and  $H_S$  has a lower bound. If  $H_S = \omega a^\dagger a$  and  $S = \alpha a + \alpha^* a^\dagger$  were bosonic and the full Hamiltonian  $H$  was at most quadratic, one could use a general three-mode Bogoliubov transform to write it as a sum of non-interacting modes  $H = \Omega_0 c_0^\dagger c_0 + \Omega_1 c_1^\dagger c_1 + \Omega_2 c_2^\dagger c_2$ . However, we want to generalize later-on to infinite-size systems, where this approach cannot be applied and, additionally,  $H_S$  need not be a bosonic operator in general.

We therefore use the two-mode **Bogoliubov transform**

$$\begin{aligned}
a_1 &= \frac{1}{2} \left( \frac{\alpha_1}{\beta_1} + \frac{\beta_1}{\alpha_1} \right) \Lambda_{11} b_1 + \frac{1}{2} \left( \frac{\alpha_1}{\beta_2} + \frac{\beta_2}{\alpha_1} \right) \Lambda_{12} b_2 \\
&\quad + \frac{1}{2} \left( \frac{\alpha_1}{\beta_1} - \frac{\beta_1}{\alpha_1} \right) \Lambda_{11} b_1^\dagger + \frac{1}{2} \left( \frac{\alpha_1}{\beta_2} - \frac{\beta_2}{\alpha_1} \right) \Lambda_{12} b_2^\dagger, \\
a_2 &= \frac{1}{2} \left( \frac{\alpha_2}{\beta_1} + \frac{\beta_1}{\alpha_2} \right) \Lambda_{21} b_1 + \frac{1}{2} \left( \frac{\alpha_2}{\beta_2} + \frac{\beta_2}{\alpha_2} \right) \Lambda_{22} b_2 \\
&\quad + \frac{1}{2} \left( \frac{\alpha_2}{\beta_1} - \frac{\beta_1}{\alpha_2} \right) \Lambda_{21} b_1^\dagger + \frac{1}{2} \left( \frac{\alpha_2}{\beta_2} - \frac{\beta_2}{\alpha_2} \right) \Lambda_{22} b_2^\dagger,
\end{aligned} \tag{4.88}$$

and likewise for the creation operators. By construction, this transform preserves the bosonic commutation relations. The unknown parameters hidden in the orthogonal matrix  $\Lambda_{kq}$  can be fixed by demanding that the Hamiltonian after the transformation does not include couplings between  $H_S$  and the second transformed mode. In particular, with

$$\Lambda = \begin{pmatrix} \lambda_1 \alpha_1 & -\lambda_2 \alpha_2 \\ +\lambda_2 \alpha_2 & \lambda_1 \alpha_1 \end{pmatrix} \frac{1}{\sqrt{\lambda_1^2 \alpha_1^2 + \lambda_2^2 \alpha_2^2}} \tag{4.89}$$

we see that

$$\lambda_1 (a_1 + a_1^\dagger) + \lambda_2 (a_2 + a_2^\dagger) = \frac{\sqrt{\lambda_1^2 \alpha_1^2 + \lambda_2^2 \alpha_2^2}}{\beta_1} (b_1 + b_1^\dagger), \tag{4.90}$$

such that the coupling is now only between  $H_S$  and the first transformed mode. However, this does not decouple the second transformed mode, since by inserting the same transformation into the term  $\omega_1 a_1^\dagger a_1 + \omega_2 a_2^\dagger a_2$ , we will automatically generate an interaction between the modes: Since the transformation is linear, the resulting operator will again be at most quadratic between the annihilation and creation operators. In principle, this may also generate terms like  $b_1^2$  and  $b_2^2$ , but we still have the freedom to choose the  $\alpha_i$  and  $\beta_i$  to prevent the generation of such terms.

- For example, by choosing  $\alpha_i = \beta_i = 1$ , the Bogoliubov transform becomes a unitary transform that does not mix between creation and annihilation operators, which allows to write

$$\omega_1 a_1^\dagger a_1 + \omega_2 a_2^\dagger a_2 = E_0 + \Omega_1 b_1^\dagger b_1 + \Omega_2 b_2^\dagger b_2 + \Lambda_2 \left( b_1^\dagger b_2 + b_2^\dagger b_1 \right), \tag{4.91}$$

where the new frequencies  $\Omega_i$  and the residual coupling  $\Lambda_2$  are functions of the  $\lambda_i$  and  $\omega_i$ , see Fig. 4.7. Interestingly, after the mapping the residual interaction between modes  $b_1$  and  $b_2$  preserves the quasiparticle number. Since we can identify

$$\Lambda_1 = \sqrt{\lambda_1^2 \alpha_1^2 + \lambda_2^2 \alpha_2^2} / \beta_1, \tag{4.92}$$

we see that in the strong-coupling limit  $\lambda_i \rightarrow \infty$ , the system-reaction coordinate coupling will also diverge  $\Lambda_1 \rightarrow \infty$ . However, the matrix elements of the orthogonal matrix  $\Lambda$  will remain finite also in this limit, since its entries are normalized. Therefore, the residual coupling  $\Lambda_2$  will remain finite.

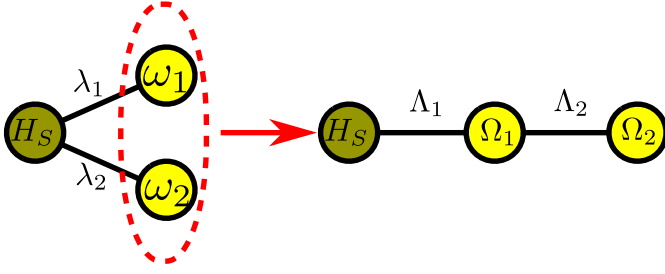


Figure 4.7: Effect of the two-mode Bogoliubov transform. The system (orange) coupled initially to two  $a$  modes via couplings  $\lambda_1$  and  $\lambda_2$  is after the transformation coupled only to the  $b_1$  mode via  $\Lambda_1$ , which is then coupled to the  $b_2$  mode via  $\Lambda_2$ . Strong-coupling effects can be treated by treating  $H_S$  and the  $b_1$  mode explicitly.

- Other choices of  $\alpha_i$  and  $\beta_i$  lead to decompositions of the form

$$\omega_1 a_1^\dagger a_1 + \omega_2 a_2^\dagger a_2 = E_0 + \Omega_1 b_1^\dagger b_1 + \Omega_2 b_2^\dagger b_2 + \Lambda_2 (b_1 + b_1^\dagger)(b_2 + b_2^\dagger), \quad (4.93)$$

which leads to the same situation as in Fig. 4.7, but various combinations may be used. In any case, the coupling  $\Lambda_2$  need not diverge as  $\lambda_i \rightarrow \infty$ , as the transformation needs to respect the bosonic commutation relations.

If more modes are involved, the transformations become larger, such that to find the suitable mapping transform, larger algebraic problems have to be solved. In particular, for an infinite size reservoir, one will have to resort to other means of finding the suitable transformation.

### 4.3.3 Derivation of the mapping

We postulate the equivalence of the following Hamiltonians. First, we have

$$\begin{aligned} H &= H_S + \sum_k \omega_k \left( a_k^\dagger + \frac{t_k}{\omega_k} S \right) \left( a_k + \frac{t_k}{\omega_k} S \right) \\ &= \left( H_S + \sum_k \frac{t_k^2}{\omega_k} S^2 \right) + S \sum_k t_k (a_k + a_k^\dagger) + \sum_k \omega_k a_k^\dagger a_k, \end{aligned} \quad (4.94)$$

where  $H_S = H_S^\dagger$  is an arbitrary system Hamiltonian with a lower spectral bound and  $S = S^\dagger$  is an arbitrary dimensionless system operator that couples the system to a bath of harmonic oscillators with spontaneous emission/absorption amplitudes  $t_k$  and energies  $\omega_k$ . Note that we have absorbed any phase in the bosonic operators and thereby assume  $t_k \in \mathbb{R}$ . These amplitudes enter the original **spectral density** as before

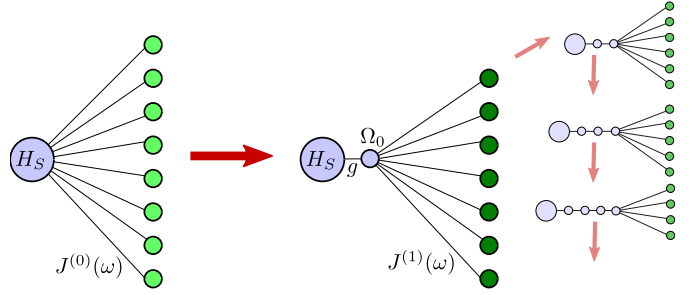
$$J^{(0)}(\omega) = 2\pi \sum_k |t_k|^2 \delta(\omega - \omega_k). \quad (4.95)$$

Obviously, the Hamiltonian also has a lower spectral bound.

Second, we say that (up to a possible shift)

$$\begin{aligned} H &= H_S + \Omega_0 \left( b^\dagger + \frac{g}{\Omega_0} S \right) \left( b + \frac{g}{\Omega_0} S \right) + \sum_k \Omega_k \left( b_k^\dagger + \frac{h_k}{\Omega_k} (b + b^\dagger) \right) \left( b_k + \frac{h_k}{\Omega_k} (b + b^\dagger) \right) \\ &= H_S + \Omega_0 b^\dagger b + gS(b + b^\dagger) + \frac{g^2}{\Omega_0} S^2 + \sum_k \frac{h_k^2}{\Omega_k} (b + b^\dagger)^2 + (b + b^\dagger) \sum_k h_k (b_k + b_k^\dagger) + \sum_k \Omega_k b_k^\dagger b_k, \end{aligned} \quad (4.96)$$

Figure 4.8: Sketch of the reaction-coordinate mapping. The original star-shaped interaction is transformed into a setup where the system couples to the reaction-coordinate, which then couples to all the modes of the residual reservoir. The magnitude of  $J^{(0)}(\omega)$  only maps to the magnitude of  $g$ , such that arbitrarily strong couplings can be treated, provided  $J^{(1)}(\omega)$  admits a perturbative treatment. Recursive application of the mapping leads to a chain representation of the reservoir.



where  $b$  denotes a **reaction coordinate** (RC) and the  $b_k$  **residual reservoir** modes. The reaction coordinate has energy  $\Omega_0$  and is coupled to the original system via the coupling constant  $g$ . The coupling between the reaction coordinate and the residual reservoir is described by the  $h_k$  amplitudes, and treating these perturbatively it is useful to define the residual **spectral density** via

$$J^{(1)}(\omega) = 2\pi \sum_k |h_k|^2 \delta(\omega - \Omega_k). \quad (4.97)$$

The intended mapping is visualized in Fig. 4.8.

The mapping shall be achieved by means of a Bogoliubov transform

$$\bar{a}_k = u_{k0}b + \sum_{q \geq 1} u_{kq}b_q + v_{k0}b^\dagger + \sum_{q \geq 1} v_{kq}b_q^\dagger \quad (4.98)$$

and similar for the creation operator. To maintain the bosonic character of the new modes, the coefficients  $u_{kq}$  and  $v_{kq}$  have to obey the relations

$$\begin{aligned} 0 &= \sum_q (u_{kq}v_{k'q} - v_{kq}u_{k'q}), \\ \delta_{kk'} &= \sum_q (u_{kq}u_{k'q}^* - v_{kq}v_{k'q}^*). \end{aligned} \quad (4.99)$$

This is automatically obeyed when we choose them via

$$u_{kq} = \frac{1}{2} \left( \sqrt{\frac{\omega_k}{\Omega_q}} + \sqrt{\frac{\Omega_q}{\omega_k}} \right) \Lambda_{kq}, \quad v_{kq} = \frac{1}{2} \left( \sqrt{\frac{\omega_k}{\Omega_q}} - \sqrt{\frac{\Omega_q}{\omega_k}} \right) \Lambda_{kq}, \quad (4.100)$$

with the unknown orthogonality transformation  $\Lambda$  obeying

$$\sum_q \Lambda_{kq} \Lambda_{k'q} = \delta_{kk'}. \quad (4.101)$$

Here,  $q = 0$  maps to the annihilation and creation operators of the RC.

### Energy and coupling strength of the RC

Inserting the transformation and comparing the terms linear in  $S$  yields that the first column of the orthogonal transformation has to be chosen as  $\Lambda_{k0} = \frac{t_k}{g} \sqrt{\frac{\omega_k}{\Omega_0}}$  and the other ones just orthogonal.

Since every row of the orthogonal transformation needs to be normalized  $\sum_k \Lambda_{k0}^2 = 1$ , we readily obtain the coupling strength to the RC

$$1 = \frac{1}{2\pi g^2 \Omega_0} \int_0^\infty \omega J^{(0)}(\omega) d\omega. \quad (4.102)$$

Comparing the terms quadratic in  $S$  yields the relation

$$\frac{g^2}{\Omega_0} = \frac{1}{2\pi} \int_0^\infty \frac{J^{(0)}(\omega)}{\omega} d\omega. \quad (4.103)$$

Furthermore, the terms with  $b^\dagger b$  yield

$$\Omega_0 = \frac{1}{2\pi g^2} \int_0^\infty \omega J^{(0)}(\omega) d\omega. \quad (4.104)$$

The first and the last of these equations are just the same, and combining the first and the second we can deduce **energy and coupling strength of the RC**

$$\Omega_0^2 = \frac{\int_0^\infty \omega J^{(0)}(\omega) d\omega}{\int_0^\infty \frac{J^{(0)}(\omega)}{\omega} d\omega}, \quad g^2 = \frac{1}{2\pi \Omega_0} \int_0^\infty \omega J^{(0)}(\omega) d\omega. \quad (4.105)$$

This is slightly different from the mapping that arises without a manifest lower spectral bound [31]. We remark that  $J^{(0)}(\omega)$ ,  $\Lambda$ , and  $g$  all have dimensions of energy. Furthermore, by comparing the terms with  $(b + b^\dagger)^2$  we already get a relation between original and transformed spectral densities

$$\frac{4g^2}{2\pi} \int \frac{J^{(1)}(\omega)}{\omega} d\omega = \frac{1}{2\pi \Omega_0^2} \int_0^\infty \omega^3 J^{(0)}(\omega) d\omega - \frac{1}{2\pi} \int_0^\infty \omega J^{(0)}(\omega) d\omega, \quad (4.106)$$

which however is unfortunately not explicit.

### Mapping of spectral density

We first consider the Heisenberg equations of motion for an arbitrary system observable  $\mathbf{A} = e^{+iHt} \mathbf{A} e^{-iHt}$ , which become  $\dot{\mathbf{A}} = e^{+iHt} [H, \mathbf{A}_S] e^{-iHt}$ , in the original picture, i.e., based on Eq. (4.94). Specifically, we get (bold symbols denote the Heisenberg picture)

$$\begin{aligned} \dot{\mathbf{A}} &= i\mathbf{S}_1 + i\mathbf{S}_2 \sum_k t_k (\mathbf{a}_k + \mathbf{a}_k^\dagger), \\ \dot{\mathbf{a}}_k &= -i\omega_k \mathbf{a}_k - it_k \mathbf{S}, \\ \dot{\mathbf{a}}_k^\dagger &= +i\omega_k \mathbf{a}_k^\dagger + it_k \mathbf{S}, \end{aligned} \quad (4.107)$$

with

$$\begin{aligned} \mathbf{S}_1 &= e^{+iHt} \left[ H_S + \sum_k \frac{t_k^2}{\omega_k} S^2, A \right] e^{-iHt}, \\ \mathbf{S}_2 &= e^{+iHt} [S, A] e^{-iHt}. \end{aligned} \quad (4.108)$$

Next, we perform an FT with the convention that  $\Im z \geq 0$

$$A(z) = \int \mathbf{A} e^{+izt} dt. \quad (4.109)$$

This will convert the equations into algebraic ones – we use an overbar to denote the transformed creation operator and use the convolution theorem

$$\begin{aligned}
izA(z) &= iS_1(z) + \frac{i}{2\pi} \int dz' S_2(z') \sum_k t_k [a_k(z-z') + \bar{c}_k(z-z')], \\
iza_k(z) &= -i\omega_k a_k(z) - it_k S(z), \\
iz\bar{c}_k(z) &= +i\omega_k \bar{c}_k(z) + it_k S(z),
\end{aligned} \tag{4.110}$$

of which we can eliminate the last two and insert it in the first, yielding

$$zA(z) = S_1(z) + \frac{1}{2\pi} \int dz' S_2(z') \sum_k t_k^2 \left[ \frac{1}{z-z'-\omega_k} - \frac{1}{z-z'+\omega_k} \right] S(z-z') \tag{4.111}$$

Now, we do the same as before, but in the transformed picture based on (4.96), where the Heisenberg equations become

$$\begin{aligned}
\dot{\mathbf{A}} &= i\mathbf{S}_1 + i\mathbf{S}_2 g(\mathbf{b} + \mathbf{b}^\dagger), \\
\dot{\mathbf{b}} &= -i\Omega_0 \mathbf{b} - ig\mathbf{S} - 2i \sum_k \frac{h_k^2}{\Omega_k} (\mathbf{b} + \mathbf{b}^\dagger) - i \sum_k h_k (\mathbf{b}_k + \mathbf{b}_k^\dagger), \\
\dot{\mathbf{b}}^\dagger &= +i\Omega_0 \mathbf{b}^\dagger + ig\mathbf{S} + 2i \sum_k \frac{h_k^2}{\Omega_k} (\mathbf{b} + \mathbf{b}^\dagger) + i \sum_k h_k (\mathbf{b}_k + \mathbf{b}_k^\dagger), \\
\dot{\mathbf{b}}_k &= -ih_k (\mathbf{b} + \mathbf{b}^\dagger) - i\Omega_k \mathbf{b}_k, \\
\dot{\mathbf{b}}_k^\dagger &= +ih_k (\mathbf{b} + \mathbf{b}^\dagger) + i\Omega_k \mathbf{b}_k^\dagger.
\end{aligned} \tag{4.112}$$

We proceed as before: We Fourier-transform all equations

$$\begin{aligned}
zA(z) &= S_1(z) + \frac{1}{2\pi} \int S_2(z') g[b(z-z') + \bar{b}(z-z')] dz', \\
zb(z) &= -\Omega_0 b(z) - gS(z) - 2 \sum_k \frac{h_k^2}{\Omega_k} [b(z) + \bar{b}(z)] - \sum_k h_k [b_k(z) + \bar{b}_k(z)], \\
z\bar{b}(z) &= +\Omega_0 \bar{b}(z) + gS(z) + 2 \sum_k \frac{h_k^2}{\Omega_k} [b(z) + \bar{b}(z)] + \sum_k h_k [b_k(z) + \bar{b}_k(z)], \\
zb_k(z) &= -h_k [b(z) + \bar{b}(z)] - \Omega_k b_k(z), \\
z\bar{b}_k(z) &= +h_k [b(z) + \bar{b}(z)] + \Omega_k \bar{b}_k(z),
\end{aligned} \tag{4.113}$$

then eliminate

$$b_k(z) = \frac{-h_k}{z + \Omega_k} [b(z) + \bar{b}(z)], \quad \bar{b}_k(z) = \frac{+h_k}{z - \Omega_k} [b(z) + \bar{b}(z)], \tag{4.114}$$

and then successively  $\bar{b}(z) - b(z)$ , yielding an equation for  $\bar{b}(z) + b(z)$

$$\left[ \frac{z^2}{\Omega_0} - \Omega_0 - 4 \sum_k \frac{h_k^2}{\Omega_k} - 4 \sum_k \frac{h_k^2 \Omega_k}{z^2 - \Omega_k^2} \right] [b(z) + \bar{b}(z)] = 2gS(z). \tag{4.115}$$

Inserting this in the first equation yields

$$\begin{aligned} zA(z) &= S_1(z) + \frac{g}{2\pi} \int S_2(z') [b(z-z') + \bar{b}(z-z')] dz' \\ &= S_1(z) + \frac{2g^2}{2\pi} \int S_2(z') \left[ \frac{1}{\frac{(z-z')^2}{\Omega_0} - \Omega_0 - 4 \sum_k \frac{h_k^2}{\Omega_k} - 4 \sum_k \frac{h_k^2 \Omega_k}{(z-z')^2 - \Omega_k^2}} \right] S(z-z') dz'. \end{aligned} \quad (4.116)$$

Finally, we can compare Eq. (4.111) and Eq. (4.116), which yields a relation between the spectral densities

$$\sum_k t_k^2 \left[ \frac{1}{z-z'-\omega_k} - \frac{1}{z-z'+\omega_k} \right] = \frac{2g^2}{\frac{(z-z')^2}{\Omega_0} - \Omega_0 - 4 \sum_k \frac{h_k^2}{\Omega_k} - 4 \sum_k \frac{h_k^2 \Omega_k}{(z-z')^2 - \Omega_k^2}}. \quad (4.117)$$

Going to the continuum limit then implies

$$\frac{1}{\pi} \int_0^\infty \frac{J^{(0)}(\omega)\omega}{(z-z')^2 - \omega^2} d\omega = \frac{2g^2}{\frac{(z-z')^2}{\Omega_0} - \Omega_0 - \frac{4}{2\pi} \int_0^\infty \frac{J^{(1)}(\omega)}{\omega} d\omega - \frac{4}{2\pi} \int_0^\infty \frac{J^{(1)}(\omega)\omega}{(z-z')^2 - \omega^2} d\omega}. \quad (4.118)$$

Introducing the **Cauchy transform of an odd function**  $J(\omega)$  via

$$W(z) = \frac{2}{\pi} \int_0^\infty \frac{\omega J(\omega)}{\omega^2 - z^2} d\omega = \frac{1}{\pi} \int_{-\infty}^{+\infty} \frac{J(\omega')}{\omega' - z} d\omega', \quad (4.119)$$

we see that it has the appealing property

$$\begin{aligned} W(\omega + i0^+) &= \lim_{\epsilon \rightarrow 0^+} \frac{1}{\pi} \int_{-\infty}^{+\infty} \frac{J(\omega') d\omega'}{\omega' - \omega - i\epsilon} = \lim_{\epsilon \rightarrow 0^+} \frac{1}{\pi} \int_{-\infty}^{+\infty} \frac{J(\omega') [\omega' - \omega + i\epsilon]}{(\omega' - \omega)^2 + \epsilon^2} d\omega' \\ &= \frac{1}{\pi} \mathcal{P} \int \frac{J(\omega')}{\omega' - \omega} d\omega' + iJ(\omega), \end{aligned} \quad (4.120)$$

where we have used a representation of the Dirac-Delta function and  $\mathcal{P}$  denotes the Cauchy principal value. Computing the Cauchy transform of both spectral densities we can write Eq. (4.118) as

$$-\frac{1}{2} W^{(0)}(z-z') = \frac{2g^2}{\frac{(z-z')^2}{\Omega_0} - \Omega_0 - \frac{2}{\pi} \int_0^\infty \frac{J^{(1)}(\omega)}{\omega} d\omega + W^{(1)}(z-z')} \quad (4.121)$$

Rearranging this for  $W^{(1)}(z-z')$  and evaluating at  $z-z' = \omega + i0^+$  eventually yields the sought-after relation between the spectral densities

$$J^{(1)}(\omega) = \frac{4g^2 J^{(0)}(\omega)}{\left[ \frac{1}{\pi} \mathcal{P} \int \frac{J^{(0)}(\omega')}{\omega - \omega'} d\omega' \right]^2 + [J^{(0)}(\omega)]^2}. \quad (4.122)$$

To summarize, the mapping between Hamiltonians (4.94) and (4.96) is realized by the **phonon mapping**.

**Def. 18** (phonon mapping). *The phonon-form of the reaction coordinate mapping for Hamiltonians with lower spectral bound is realized by the transformations for reaction coordinate energy  $\Omega_0$ , coupling strength  $g$ , and residual spectral density  $J^{(1)}(\omega)$ , that are fully defined by the original spectral density*

$$\begin{aligned} \Omega_0^2 &= \frac{\int_0^\infty \omega J^{(0)}(\omega) d\omega}{\int_0^\infty \frac{J^{(0)}(\omega)}{\omega} d\omega}, & g^2 &= \frac{1}{2\pi\Omega_0} \int_0^\infty \omega J^{(0)}(\omega) d\omega, \\ J^{(1)}(\omega) &= \frac{4g^2 J^{(0)}(\omega)}{\left[ \frac{1}{\pi} \mathcal{P} \int \frac{J^{(0)}(\omega')}{\omega - \omega'} d\omega' \right]^2 + [J^{(0)}(\omega)]^2}, \end{aligned} \quad (4.123)$$

where the analytic continuation  $J^{(0)}(-\omega) = -J^{(0)}(\omega)$  is understood.

- The first observation is that if we rescale the original spectral density by a factor  $\alpha$ ,  $g^2$  will scale proportional to  $\alpha$  as well, such that this factor  $\alpha$  will cancel in the numerator and denominator. Thereby, the ultrastrong coupling limit in the original frame  $\alpha \rightarrow \infty$  will have absolutely no effect on the coupling strength to the residual reservoir. Rather, the coupling strength to the residual reservoir will depend on the shape of the original spectral density.
- By redefining  $S = (b + b^\dagger)$  in Eq. (4.96) and absorbing the reaction coordinate terms into  $H_S$ , we see that the form of (4.94) is fully reproduced, such that the mapping transformation can be iterated recursively, until one of the involved integrals diverges. For the recursive application, the above definition can be used with simply replacing  $J^{(0)}(\omega) \rightarrow J^{(n)}(\omega)$  and  $J^{(1)}(\omega) \rightarrow J^{(n+1)}(\omega)$ .
- Finally, for spectral densities that have a finite support, i.e., which are non-vanishing only inside a region  $\omega \in [0, \omega_m]$ , one can show that the mapping transformations lead to the limiting spectral density [32]

$$\bar{J}(\omega) = \omega \sqrt{1 - \frac{\omega^2}{\omega_m^2}} \Theta(\omega_m^2 - \omega^2), \quad (4.124)$$

known as **Rubin spectral density**. Direct insertion into the mapping relation shows that it reproduces itself under the mapping.

#### 4.3.4 Application: Spin-boson model

We consider a single-reservoir scenario with

$$H = \frac{\omega}{2} \sigma^z + \sum_k \frac{t_k^2}{\omega_k} S^2 + S \sum_k t_k (a_k + a_k^\dagger) + \sum_k \omega_k a_k^\dagger a_k, \quad (4.125)$$

where  $S = \sigma^z$  can implement either the exactly solvable pure-dephasing limit and  $S = \sigma^x$  would be a dissipative spin-boson model. Since in these cases  $S^2 = \mathbf{1}$ , the renormalization term corresponds to a trivial shift. To compare with an available exact solution, we will consider the pure-dephasing

limit  $S = \sigma^z$  here, but the method is applicable more generally. The original spectral density shall be

$$J^{(0)}(\omega) = 2\pi \sum_k |t_k|^2 \delta(\omega - \omega_k) = \Gamma \frac{\omega \delta^7}{[(\omega - \epsilon)^2 + \delta^2]^2 [(\omega + \epsilon)^2 + \delta^2]^2}, \quad (4.126)$$

where  $\Gamma$  denotes an overall coupling strength, and for  $\epsilon > \delta > 0$  the parameter  $\epsilon$  describes roughly the position of the maximum and  $\delta$  roughly the width around the maximum. All these parameters have dimension of energy. This special spectral density is chosen to perform the mapping analytically.

Accordingly, the transformed model reads

$$H = \frac{\omega}{2} \sigma^z + \Omega_0 \left( b^\dagger + \frac{g}{\Omega_0} S \right) \left( b + \frac{g}{\Omega_0} S \right) + \sum_k \Omega_k \left( b_k^\dagger + \frac{h_k}{\Omega_k} (b + b^\dagger) \right) \left( b_k + \frac{h_k}{\Omega_k} (b + b^\dagger) \right), \quad (4.127)$$

where the energy of the RC and the coupling strength become

$$\Omega_0^2 = \frac{(\delta^2 + \epsilon^2)^2}{5\delta^2 + \epsilon^2}, \quad g^2 = \frac{\Gamma \delta^4 \sqrt{5\delta^2 + \epsilon^2}}{64(\delta^2 + \epsilon^2)^2}. \quad (4.128)$$

The mapping transformation can be computed explicitly, where the transformed spectral density becomes ohmic

$$J^{(1)}(\omega) = \frac{16\omega \delta^3 \sqrt{5\delta^2 + \epsilon^2}}{\omega^4 + \omega^2(6\delta^2 - 2\epsilon^2) + (5\delta^2 + \epsilon^2)^2}, \quad (4.129)$$

which does not depend on the coupling strength  $\Gamma$  (demonstrating that it can be chosen arbitrarily large). With introducing the supersystem renormalization (for the chosen spectral density, everything converges)

$$\Omega_0 \cdot \Delta \equiv \sum_k \frac{h_k^2}{\Omega_k} = \frac{1}{2\pi} \int_0^\infty \frac{J^{(1)}(\omega)}{\omega} d\omega, \quad (4.130)$$

we can identify a new decomposition into supersystem  $H'_S$  and residual reservoir  $H'_B$  via  $H = H'_S + H'_B + H'_I$  with

$$\begin{aligned} H'_S &= \frac{\omega}{2} \sigma^z + \Omega_0 \left( b^\dagger + \frac{g}{\Omega_0} S \right) \left( b + \frac{g}{\Omega_0} S \right) + \Omega_0 \Delta (b + b^\dagger)^2, \\ H'_I &= (b + b^\dagger) \sum_k h_k (b_k + b_k^\dagger), \quad H'_B = \sum_k \Omega_k b_k^\dagger b_k, \end{aligned} \quad (4.131)$$

for which we can derive and solve a master equation in the usual way. For the sake of simplicity we will not bother to derive a Lindblad master equation but will simply use the Redfield master equation (1.63), but now for the supersystem

$$\begin{aligned} \dot{\rho} &= -i[H'_S, \rho] - \int_0^\infty C(+\tau) \left[ (b + b^\dagger), e^{-iH'_S \tau} (b + b^\dagger) e^{+iH'_S \tau} \rho(t) \right] d\tau \\ &\quad - \int_0^\infty C(-\tau) \left[ \rho(t) e^{-iH'_S \tau} (b + b^\dagger) e^{+iH'_S \tau}, (b + b^\dagger) \right] d\tau. \end{aligned} \quad (4.132)$$

Here,  $C(\tau)$  is the correlation function for the residual bath

$$C(\tau) = \frac{1}{2\pi} \int \gamma(\omega) e^{-i\omega\tau} d\omega = \frac{1}{2\pi} \int J^{(1)}(\omega) [1 + n_B(\omega)] e^{-i\omega\tau} d\omega, \quad (4.133)$$

which under the assumption of weak residual coupling (for which we have derived the master equation) is still approximately in a thermal state with the same temperature. The half-sided Fourier transform can be performed by finding the eigenbasis of the supersystem Hamiltonian  $H'_S |a'\rangle = E'_a |a'\rangle$ , such that

$$\int_0^\infty C(\tau) e^{-iH'_S\tau} (b + b^\dagger) e^{+iH'_S\tau} d\tau = \sum_{ab} \langle a' | (b + b^\dagger) | b' \rangle \int_0^\infty C(\tau) e^{-i(E'_a - E'_b)\tau} d\tau |a'\rangle \langle b'|. \quad (4.134)$$

Now, the remaining half-sided integral can be evaluated via

$$\begin{aligned} \int_0^\infty C(\tau) e^{+i(E'_b - E'_a)\tau} d\tau &= \int \Theta(\tau) C(\tau) e^{+i(E'_b - E'_a)\tau} d\tau = \int d\omega \gamma(\omega) \left[ \frac{1}{2\pi} \int d\tau e^{+i(E'_b - E'_a - \omega)\tau} \frac{1}{2} [1 + \text{sgn}(\tau)] \right] \\ &= \frac{\gamma(E'_b - E'_a)}{2} + \frac{i}{2\pi} \mathcal{P} \int \frac{\gamma(\omega)}{E'_b - E'_a - \omega} d\omega \approx \frac{\gamma(E'_b - E'_a)}{2} \end{aligned} \quad (4.135)$$

where in the last equality sign we have neglected the Lamb shift. The dissipator can then be established numerically, after obtaining the eigenbasis of  $H'_S$ .

The solution for the supersystem  $\rho(t)$  then allows to compute observables such as the absolute value of coherences

$$|\rho_{01}| = \left| \frac{1}{2} \text{Tr} \{ (\sigma^x + i\sigma^y) \rho(t) \} \right|, \quad (4.136)$$

which can be directly compared with the exact solution in Eq. (1.148). Likewise, we had established that due to global energy conservation, the energy radiated into the reservoir must stem from the interaction

$$\frac{d}{dt} \left\langle \sum_k \omega_k a_k^\dagger a_k \right\rangle = -\frac{d}{dt} \left\langle \sigma^z \sum_k t_k (a_k + a_k^\dagger) \right\rangle = -\frac{d}{dt} g \langle \sigma^z (b + b^\dagger) \rangle, \quad (4.137)$$

where the last expression is now accessible within the master equation formulation of the supersystem and can be compared with the exact solution for the current obtain from the time derivative of Eq. (3.130), provided the supersystem is initialized as

$$\rho_0 = \rho_S^0 \otimes \frac{e^{-\beta\Omega[b^\dagger b + \Delta(b+b^\dagger)^2]}}{Z_{RC}}, \quad (4.138)$$

where the first factor is the initial state of the spin (including e.g. coherences) and the second part comes from the reduced thermal state of the reaction coordinate. The result is depicted in Fig. 4.9. One can see that the transient evolution of coherences is extremely well captured with the RC approach. By further increasing the bosonic cutoff  $N_c$ , the solution well approaches the exact one. The total radiated current however does not yet approximate the exact solution well (even for  $N_c \rightarrow \infty$ ), which roots in the Markovian approximation applied to the supersystem ( $\delta\beta \approx 1$  does not fully justify a Markovian treatment). The bottom-line is that a time-local (and in this sense Markovian) treatment of the supersystem includes non-Markovian effects in the original system.

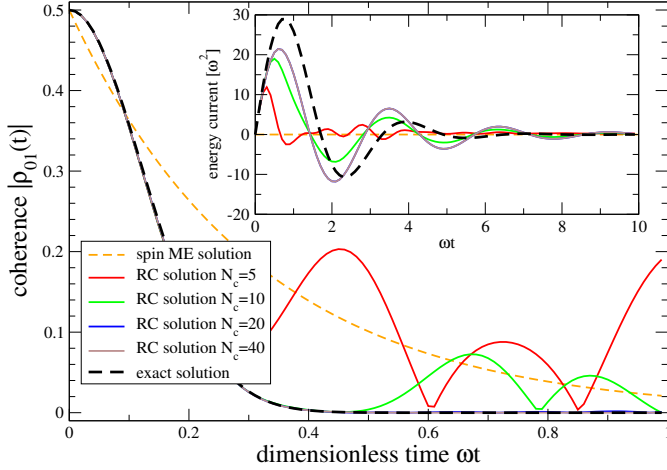


Figure 4.9: Evolution of coherences in the pure-dephasing spin boson model and energy radiated into the reservoir versus dimensionless time. Whereas the naive master equation for the single spin predicts simple exponential decay and a vanishing energy current (orange dashed), treatment of the supersystem (solid curves) approximates the exact solution (bold dashed black) much better, depending on the bosonic cutoff chosen. To compute the currents (inset) more accurately, further mappings would be necessary. Parameters:  $\Gamma\beta = 10000$ ,  $\delta\beta = 1$ ,  $\epsilon\beta = 2$ ,  $\omega\beta = 1$ .

## 4.4 Fermionic reaction-coordinate mappings

As for bosonic systems, similar Bogoliubov transforms exist for fermionic systems. The only difference is that they preserve the fermionic anticommutation relations.

### 4.4.1 Fermionic Bogoliubov transforms

**Def. 19** (Fermionic Bogoliubov transform). *A fermionic Bogoliubov transform is a linear mapping between fermionic annihilation and creation operators, which preserves the corresponding fermionic anticommutation relations*

$$c_k = \sum_q [u_{kq}d_q + v_{kq}d_q^\dagger], \quad \begin{cases} \{c_k, c_{k'}^\dagger\} = \delta_{kk'}, & \{c_k, c_{k'}\} = 0, \\ \{d_k, d_{k'}^\dagger\} = \delta_{kk'}, & \{d_k, d_{k'}\} = 0, \end{cases} \quad (4.139)$$

where  $u_{kq}, v_{kq} \in \mathbb{C}$ .

In analogy to the bosonic case, the constraints that the coefficients  $u_{kq}$  and  $v_{kq}$  have to obey can be written as

$$\sum_q (u_{kq}u_{k'q}^* + v_{kq}v_{k'q}^*) = \delta_{kk'}, \quad \sum_q (u_{kq}v_{k'q} + v_{kq}u_{k'q}) = 0, \quad (4.140)$$

or in matrix notation

$$UU^\dagger + VV^\dagger = \mathbf{1}, \quad UV^\top + VU^\top = \mathbf{0}. \quad (4.141)$$

In the following, we will only treat the case of particle-conserving interactions (relevant e.g. for electronic tunneling), such that when we consider just  $V = 0$ , again  $U$  just needs to be a unitary transformation to obey the preservation of the anticommutation relations. Another simplification is that we will not bother to write the Hamiltonian in a manifestly positive form, since for fermions the spectrum is always bounded from below.

### 4.4.2 Two-mode example

Consider the fermionic Hamiltonian

$$H = H_S + \left( t_1 d^\dagger c_1 + t_1^* c_1^\dagger d \right) + \left( t_2 d^\dagger c_2 + t_2^* c_2^\dagger d \right) + \varepsilon_1 c_1^\dagger c_1 + \varepsilon_2 c_2^\dagger c_2, \quad (4.142)$$

where  $H_S$  may contain arbitrary interactions and  $d$  is an operator in the system. A unitary Bogoliubov transform of the reservoir modes only

$$c_1 = u_{11}d_1 + u_{12}d_2, \quad c_2 = u_{21}d_1 + u_{22}d_2, \quad (4.143)$$

and analogous for the creation operators can now be chosen to achieve an effective decoupling of the system and the second mode  $d_2$ . Inserting this transformation

$$\begin{aligned} H = H_S + [ & d^\dagger(t_1 u_{11} + t_2 u_{21})d_1 + d^\dagger(t_1 u_{12} + t_2 u_{22})d_2 + \text{h.c.}] \\ & + \varepsilon_1 \left( u_{11}^* d_1^\dagger + u_{12}^* d_2^\dagger \right) (u_{11}d_1 + u_{12}d_2) + \varepsilon_2 \left( u_{21}^* d_1^\dagger + u_{22}^* d_2^\dagger \right) (u_{21}d_1 + u_{22}d_2), \end{aligned} \quad (4.144)$$

and we see that by fulfilling  $(t_1 u_{12} + t_2 u_{22}) = 0$  we can achieve a decoupling of the system and the second mode. This is for example implemented by the choice

$$U = \frac{1}{\sqrt{|t_1|^2 + |t_2|^2}} \begin{pmatrix} +t_1^* & -t_2 \\ +t_2^* & +t_1 \end{pmatrix}, \quad (4.145)$$

which eventually yields

$$\begin{aligned} H = H_S + \left[ \underbrace{\sqrt{|t_1|^2 + |t_2|^2}}_{T_1} d^\dagger d_1 + \text{h.c.} \right] & + \underbrace{\frac{\varepsilon_1 |t_1|^2 + \varepsilon_2 |t_2|^2}{|t_1|^2 + |t_2|^2}}_{\varepsilon_1} d_1^\dagger d_1 + \underbrace{\frac{\varepsilon_1 |t_2|^2 + \varepsilon_2 |t_1|^2}{|t_1|^2 + |t_2|^2}}_{\varepsilon_2} d_2^\dagger d_2 \\ & + \left[ \underbrace{\frac{t_1 t_2}{|t_1|^2 + |t_2|^2}}_{T_2} (\varepsilon_2 - \varepsilon_1) d_1^\dagger d_2 + \text{h.c.} \right], \end{aligned} \quad (4.146)$$

which has the same interpretation as Fig. 4.7 with the appropriately renamed parameters. As before, we see that as  $t_i \rightarrow \infty$ , only  $T_1$  diverges, whereas  $\varepsilon_i$  and also  $T_2$  remain finite. Therefore, an explicit treatment of only the first mode allows for a perturbative treatment also in the strong-coupling limit.

### 4.4.3 Derivation of the mapping

We postulate the equivalence of the Hamiltonians

$$\begin{aligned} H &= H_S + c \sum_k t_k^* c_k^\dagger - c^\dagger \sum_k t_k c_k + \sum_k \varepsilon_k c_k^\dagger c_k \\ &= H_S + \lambda c d^\dagger - \lambda c^\dagger d + \varepsilon d^\dagger d + d \sum_k T_k^* d_k^\dagger - d^\dagger \sum_k T_k d_k + \sum_k \varepsilon_k d_k^\dagger d_k. \end{aligned} \quad (4.147)$$

In the first one,  $t_k$  gives rise to the original spectral density

$$\Gamma^{(0)}(\omega) = 2\pi \sum_k |t_k|^2 \delta(\omega - \epsilon_k), \quad (4.148)$$

and in the second Hamiltonian,  $\lambda$  and  $\varepsilon$  denote coupling and energy of the reaction coordinate, respectively. Also, the amplitudes  $T_k$  and energies  $\varepsilon_k$  define the residual spectral density

$$\Gamma^{(1)}(\omega) = 2\pi \sum_k |T_k|^2 \delta(\omega - \varepsilon_k). \quad (4.149)$$

Thus, the difference to the bosonic case is that no extra term is required to grant the existence of a lower bound and also that the spectral densities can be defined also for negative frequencies, such that no analytic continuation is necessary. The transformation shall be implemented by a unitary variant of the Bogoliubov transform

$$c_k = \sum_q u_{kq} d_q, \quad (4.150)$$

and specifically we identify  $d_0 = d$  as the reaction coordinate.

### Energy and coupling strength

Thereby, it has to hold that

$$\lambda d = \sum_k t_k c_k, \quad \lambda d^\dagger = \sum_k t_k^* c_k^\dagger, \quad (4.151)$$

and similar for the conjugate transpose, such that by computing e.g. the anticommutator of the two terms above we get the relation

$$\lambda^2 = \sum_k |t_k|^2, \quad (4.152)$$

which defines the coupling strength of the reaction coordinate. Solving for  $d$ , we get

$$d = \sum_k \frac{t_k}{\lambda} c_k = \sum_k (U^\dagger)_{0k} c_k = \sum_k u_{k0}^* c_k \quad \Longrightarrow \quad u_{k0} = \frac{t_k^*}{\lambda}. \quad (4.153)$$

Finally, the term that generates the energy of the reaction coordinate must generate from the reservoir Hamiltonian, such that

$$\varepsilon d^\dagger d = \sum_k \epsilon_k |u_{k0}|^2 d^\dagger d = \sum_k \epsilon_k \frac{|t_k|^2}{\lambda^2} d^\dagger d. \quad (4.154)$$

This yields the energy of the reaction coordinate

$$\varepsilon = \sum_k \epsilon_k \frac{|t_k|^2}{\lambda^2}. \quad (4.155)$$

In the continuum limit, we can get the coupling and energy from integrals over the complete energies

$$\lambda^2 = \frac{1}{2\pi} \int \Gamma^{(0)}(\omega) d\omega, \quad \varepsilon = \frac{1}{2\pi\lambda^2} \int \omega \Gamma^{(0)}(\omega) d\omega. \quad (4.156)$$

### Mapping of the spectral density

To find the mapping relation for the spectral density, we set up the Heisenberg equations of motion for both realizations of the total Hamiltonian. For simplicity, we only consider the Heisenberg equations for the creation and annihilation operators (in principle, any observable can be constructed from these). In the original representation, they become

$$\dot{c} = i[H_S, c] + i \sum_k t_k c_k = iS(t) + i \sum_k t_k c_k, \quad \dot{c}_k = it_k^* c - i\epsilon_k c_k, \quad (4.157)$$

and similarly for the creation operators. Since at this level they do not mix, we consider only the annihilation operators. Fourier-transformation yields

$$zc(z) = S(z) + \sum_k t_k c_k(z), \quad zc_k(z) = t_k^* c(z) - \epsilon_k c_k(z). \quad (4.158)$$

Eliminating the second equation then gives

$$zc(z) = S_1(z) + \sum_k \frac{|t_k|^2}{z + \epsilon_k} c(z). \quad (4.159)$$

In contrast, the mapped representation yields

$$\dot{c} = iS(t) + i\lambda d, \quad \dot{d} = -i\lambda c - i\epsilon d + i \sum_k T_k d_k, \quad \dot{d}_k = iT_k^* d - i\epsilon_k d_k. \quad (4.160)$$

Fourier-transforming and eliminating the non-system variables then gives

$$zc(z) = S(z) - \frac{\lambda^2}{z + \epsilon - \sum_k \frac{|T_k|^2}{z + \epsilon_k}} c(z), \quad (4.161)$$

and from comparison we get the relation

$$\sum_k \frac{|t_k|^2}{z + \epsilon_k} = -\frac{\lambda^2}{z + \epsilon - \sum_k \frac{|T_k|^2}{z + \epsilon_k}}. \quad (4.162)$$

Converting the sums to integrals and evaluating at  $z = -\omega + i\delta$  when  $\delta \rightarrow 0^+$  we obtain a mapping relation between the fermionic spectral densities just as before.

Summarizing, we obtain the fermionic particle mapping.

**Def. 20** (Fermionic particle mapping). *The particle form of the reaction-coordinate mapping for fermionic tunneling Hamiltonians provides the reaction coordinate coupling  $\lambda$ , the energy  $\epsilon$ , and the residual spectral density  $\Gamma^{(1)}(\omega)$*

$$\begin{aligned} \lambda^2 &= \frac{1}{2\pi} \int \Gamma^{(0)}(\omega) d\omega, & \epsilon &= \frac{1}{2\pi\lambda^2} \int \omega \Gamma^{(0)}(\omega) d\omega, \\ \Gamma^{(1)}(\omega) &= \frac{4\lambda^2 \Gamma^{(0)}(\omega)}{\left[ \frac{1}{\pi} \mathcal{P} \int \frac{\Gamma^{(0)}(\omega')}{\omega - \omega'} d\omega' \right]^2 + [\Gamma^{(0)}(\omega)]^2}. \end{aligned} \quad (4.163)$$

- As before, the transformed spectral density remains invariant under trivial rescalings of the original one.
- As before, the mapping can be performed recursively.
- For spectral densities with a finite support, i.e., nonvanishing ones in the interval  $\omega \in [\epsilon - \delta, \epsilon + \delta]$ , the mapping converges to a semicircle-shaped spectral density

$$\bar{\Gamma}(\omega) = \delta \sqrt{1 - \left(\frac{\omega - \epsilon}{\delta}\right)^2} \Theta(\delta^2 - (\omega - \epsilon)^2). \quad (4.164)$$

#### 4.4.4 Application: Single-electron transistor

We consider the SET

$$H = \epsilon d^\dagger d + \sum_{\nu} \sum_k \left[ \epsilon_{k\nu} c_{k\nu}^\dagger c_{k\nu} + (t_{k\nu} d^\dagger c_{k\nu} + \text{h.c.}) \right] \quad (4.165)$$

with two leads  $\nu \in \{L, R\}$  described by Lorentzian spectral densities

$$\Gamma_{\alpha}^{(0)}(\omega) = 2\pi \sum_k |t_{k\nu}|^2 \delta(\omega - \epsilon_{k\nu}) = \Gamma_{\alpha} \frac{\delta_{\alpha}^2}{(\omega - \epsilon_{\alpha})^2 + \delta_{\alpha}^2}, \quad (4.166)$$

where  $\alpha \in \{L, R\}$  denotes the lead,  $\Gamma_{\alpha}$  the coupling strength,  $\delta_{\alpha}$  the width, and  $\epsilon_{\alpha}$  the frequency with the strongest coupling. The wideband limit is implemented with  $\delta_{\alpha} \rightarrow \infty$ .

Introducing a separate reaction coordinate for each reservoir, the model is transformed into a triple quantum dot (TQD) structure

$$H = H_{TQD} + \sum_{\nu} \sum_k \left[ \epsilon_{k\nu} d_{k\nu}^\dagger d_{k\nu} + (T_{k\nu} d_{k\nu}^\dagger d_{k\nu} + \text{h.c.}) \right],$$

$$H_{TQD} = \epsilon_L d_L^\dagger d_L + \epsilon d^\dagger d + \epsilon_R d_R^\dagger d_R + (\lambda_L d^\dagger d_L + \lambda_R d^\dagger d_R + \text{h.c.}), \quad (4.167)$$

where the coupling strengths and energies of the RC, respectively, become

$$\lambda_{\nu} = \sqrt{\frac{\Gamma_{\nu} \delta_{\nu}}{2}}, \quad \epsilon_{\nu} = \epsilon_{\nu}. \quad (4.168)$$

Here, for the computation of the RC energy one can actually use symmetry arguments or use the principal value as otherwise the integral is not convergent. The computation of the principal value integral yields

$$\begin{aligned} \mathcal{P} \int \frac{\Gamma_{\nu}^{(0)}(\omega')}{\omega - \omega'} d\omega' &= 2\pi i \left[ \text{Res}_{\omega' = \epsilon_{\nu} + i\delta} \frac{\Gamma_{\nu}^{(0)}(\omega')}{\omega - \omega'} + \frac{1}{2} \text{Res}_{\omega' = \omega} \frac{\Gamma_{\nu}^{(0)}(\omega')}{\omega - \omega'} \right] \\ &= \frac{\pi \Gamma_{\nu} \delta_{\nu} (\omega - \epsilon_{\nu})}{(\omega - \epsilon_{\nu})^2 + \delta_{\nu}^2}, \end{aligned} \quad (4.169)$$

which eventually allows to compute the residual spectral density

$$\Gamma_{\nu}^{(1)}(\omega) = 2\pi \sum_k |T_{k\nu}|^2 \delta(\omega - \epsilon_{k\nu}) = 2\delta_{\nu}, \quad (4.170)$$

which is just flat. An additional transformation could not be performed here, since the spectral densities would just diverge. We can now solve the model with various approaches.

- First, since the model is exactly solvable, we can use e.g. nonequilibrium Greens functions or the Laplace transform method used in Sec. 4.1 (without invoking the wideband limit on the single dot or applying it to the TQD) to obtain an exact solution for the stationary currents in terms of a Landauer representation

$$I_M = \frac{1}{2\pi} \int d\omega T(\omega) [f_L(\omega) - f_R(\omega)] d\omega, \quad (4.171)$$

where the transmission becomes

$$T(\omega) = \frac{\Gamma_L^{(0)}(\omega)\Gamma_R^{(0)}(\omega)}{\left[\omega - \epsilon - \frac{1}{2\pi} \mathcal{P} \int \frac{\Gamma_L^{(0)}(\omega') + \Gamma_R^{(0)}(\omega')}{\omega - \omega'} d\omega'\right]^2 + \left[\frac{\Gamma_L^{(0)}(\omega') + \Gamma_R^{(0)}(\omega')}{2}\right]^2}. \quad (4.172)$$

- Second, we can use the naive master equation for the SET as discussed explicitly in Sec. 2.1. From this, we know that the current  $I_M$  will scale linearly with the coupling strength if symmetrically coupled  $\Gamma_L = \Gamma_R$ .
- Third, we can derive the BMS rate equations (1.82) for the resulting triple-dot system, which are sometimes referred to as global Lindblad equations, since their Lindblad operators are expressible by the energy eigenbasis of the TQD. Without coherences in the energy eigenbasis, this will correspond to a classical stochastic process switching between the energy eigenstates of the TQD (which can for our example actually be analytically calculated). This master equation is globally of Lindblad form, and therefore the dynamics will be contractive (or Markovian), such that the TQD density matrix will always approach its steady state as enforced by Spohn's inequality. However, the dynamics of the central dot alone does not follow a master equation and may be non-Markovian. The reduced density matrix of the central dot is always diagonal

$$\rho_c(t) = \begin{pmatrix} 1 - P_1(t) & 0 \\ 0 & P_1(t) \end{pmatrix}, \quad (4.173)$$

and is thereby fully determined by the probability of the central dot being occupied  $P_1(t) = \text{Tr} \{d^\dagger d \rho(t)\}$ . Likewise its stationary limit is given by  $\bar{P}_1 = \text{Tr} \{d^\dagger d \bar{\rho}\}$ , such that the trace distance between the single-electron density matrix and its stationary limit  $T(\rho_c(t), \bar{\rho}_c) = |P_1(t) - \bar{P}_1|$  or likewise the quantum relative entropy between these states may actually temporarily increase. This hallmarks a non-Markovian effect, demonstrating that the TQD Lindblad equation provides a Markovian embedding for a non-Markovian evolution of the central dot.

- Fourth, we can use the nonsecular master equation (1.63) for the triple quantum dot, which is not of Lindblad form but will approximately preserve the density matrix properties when applied within its range of validity (weak residual coupling  $\beta_\nu \delta_\nu \ll 1$ ). In this case, a temporarily increasing trace distance to the stationary state may already be observed in the supersystem.
- Fifth, since the mapping to the triple quantum dot picture does not require the strong-coupling limit, we can also compare with the case where the internal amplitudes  $\lambda_\nu$  and the residual amplitudes  $T_{k\nu}$  are of the same order by defining the transformation to the

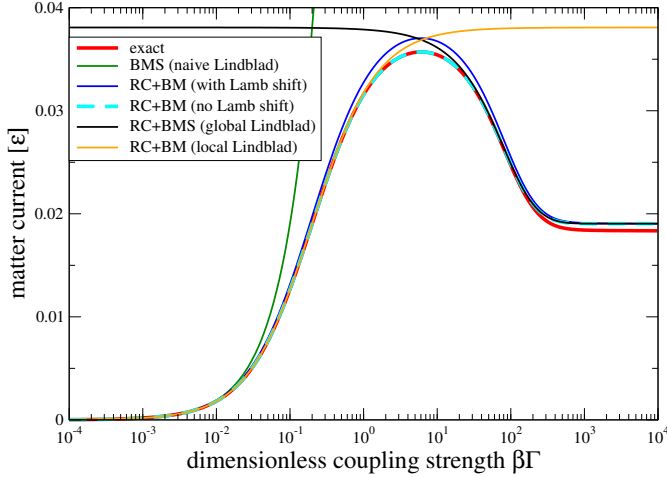


Figure 4.10: Plot of the matter current versus dimensionless coupling strength at a fixed non-equilibrium scenario. Lindblad approaches (green, black, orange) capture the exact solution (red) only in suitable regimes, whereas the Redfield master equation (light dashed blue and solid blue) recover the exact solution over various orders. In particular the naive SET Lindblad (green) captures only the weak-coupling regime. In contrast, the failure of the BMS for the TQD (black) fails at weak coupling since the secular approximation is not applicable. Parameters:  $\Gamma_L = \Gamma_R = \Gamma$ ,  $\beta_L \epsilon = \beta_R \epsilon = 1$ ,  $\mu_L = +\epsilon$ ,  $\mu_R = -\epsilon$ ,  $\delta_L = \delta_R = 0.1\epsilon$ ,  $\epsilon_L = \epsilon_R = \epsilon$ .

interaction picture differently. This results in a **local Lindblad** master equation [33] for the triple quantum dot

$$\begin{aligned} \dot{\rho} = & -i[H_{TQD}, \rho] \\ & + \Gamma_L^{(1)}(\epsilon_L)[1 - f_L(\epsilon_L)] \left[ d_L \rho d_L^\dagger - \frac{1}{2} \{ d_L^\dagger d_L, \rho \} \right] + \Gamma_L^{(1)}(\epsilon_L) f_L(\epsilon_L) \left[ d_L^\dagger \rho d_L - \frac{1}{2} \{ d_L d_L^\dagger, \rho \} \right] \\ & + \Gamma_R^{(1)}(\epsilon_R)[1 - f_R(\epsilon_R)] \left[ d_R \rho d_R^\dagger - \frac{1}{2} \{ d_R^\dagger d_R, \rho \} \right] + \Gamma_R^{(1)}(\epsilon_R) f_R(\epsilon_R) \left[ d_R^\dagger \rho d_R - \frac{1}{2} \{ d_R d_R^\dagger, \rho \} \right], \end{aligned} \quad (4.174)$$

where the coupling between the left and right dots is only mediated by the triple dot Hamiltonian  $H_{TQD}$ .

The results of these considerations are shown in Fig. 4.10. One can see that a single Lindblad approach – at least of the forms mentioned – is not able to capture the behaviour of the exact solution for all coupling strengths, whereas the Redfield master equation, despite not obeying the Lindblad form, captures its features much better over a wide range of parameters. Nevertheless, for particular regimes suitable Lindblad descriptions exist.

## 4.5 Reduced stationary state

In the strong-coupling limit, we no longer expect the local Gibbs state  $e^{-\beta H_S}/Z_S$  to be the stationary state of the system. Rather, one might expect it to be given by the reduced density matrix of the total Gibbs state

$$\bar{\rho}_S \approx \text{Tr}_B \left\{ \frac{e^{-\beta(H_S + H_B + H_I)}}{Z} \right\}, \quad (4.175)$$

which would only coincide with the system-local Gibbs state when  $H_I \rightarrow 0$  (vanishingly weak coupling), which goes along our results for the conventional master equation. Since the reaction coordinate mappings allow for arbitrarily strong coupling between the original system and reservoir, we can test when the resulting stationary state in the supersystem is consistent with these expectations.

In particular, we assume that the coupling between the supersystem and residual reservoir is small, such that we can apply the master equation formalism to the supersystem

$$H'_S = H_S + H_{RC} + H_I, \quad (4.176)$$

composed of system and reaction coordinate. For the standard quantum-optical master equation (based in general on Born-Markov and secular approximations) it is known that for a single reservoir the stationary state will approach the system-local Gibbs state, now associated with the supersystem

$$\bar{\rho}'_S = \frac{e^{-\beta H'_S}}{\text{Tr}_{S,RC} \{e^{-\beta H'_S}\}}. \quad (4.177)$$

We define a **Hamiltonian of mean force**  $H^*$  via the relation

$$e^{-\beta H^*} \equiv \frac{\text{Tr}_B \{e^{-\beta(H_S+H_I+H_B)}\}}{\text{Tr}_B \{e^{-\beta H_B}\}}. \quad (4.178)$$

It can be seen as an effective Hamiltonian for the system in the strong coupling limit. In the weak-coupling limit ( $H_I \rightarrow 0$ ) we get  $H^* \rightarrow H_S$ . By construction, the Hamiltonian of mean force obeys

$$e^{-\beta H^*} = \frac{\text{Tr}_{RC,B'} \{e^{-\beta(H'_S+\lambda H'_I+H'_B)}\}}{\text{Tr}_{RC,B'} \{e^{-\beta(H_{RC}+\lambda H'_I+H'_B)}\}} = \frac{\text{Tr}_{RC} \{e^{-\beta H'_S}\}}{\text{Tr}_{RC} \{e^{-\beta H_{RC}}\}} + \mathcal{O}\{\lambda\}. \quad (4.179)$$

Here,  $\lambda$  serves as a dimensionless bookkeeping parameter for the coupling between the reaction coordinate and the residual reservoir. With Eq. (4.177), this implies that the reduced steady state of the original system becomes

$$\bar{\rho}_S = \text{Tr}_{RC} \{\bar{\rho}'_S\} = \frac{\text{Tr}_{RC} \{e^{-\beta H'_S}\}}{\text{Tr}_{S,RC} \{e^{-\beta H'_S}\}} = \frac{e^{-\beta H^*} \text{Tr}_{RC} \{e^{-\beta H_{RC}}\}}{\text{Tr}_{S,RC} \{e^{-\beta H'_S}\}} + \mathcal{O}\{\lambda\}, \quad (4.180)$$

where we have used the defining equation of the Hamiltonian for mean force in the last step. By performing the trace over the system  $\text{Tr}_S \{e^{-\beta H^*}\}$  in Eq. (4.179), we get the relation

$$\text{Tr}_S \{e^{-\beta H^*}\} = \frac{\text{Tr}_{S,RC} \{e^{-\beta H'_S}\}}{\text{Tr}_{RC} \{e^{-\beta H_{RC}}\}}, \quad (4.181)$$

and thereby we eventually can express the stationary state as the Gibbs state of the Hamiltonian of mean force

$$\bar{\rho}_S = \frac{e^{-\beta H^*}}{\text{Tr}_S \{e^{-\beta H^*}\}} + \mathcal{O}\{\lambda\}. \quad (4.182)$$

That means, when the coupling between the supersystem and the residual reservoir (i.e. the transformed spectral density) is small, the approach recovers the reduced steady state (4.175) of the global Gibbs state. In the regime where we can describe the evolution of the supersystem with a conventional master equation, the RC approach correctly predicts relaxation to the reduced steady state of the global Gibbs state.

# Chapter 5

## Periodically driven systems

Transport can be manipulated by driving a system, a conventional example of this is just a pump, where the usual direction of transport can be reversed by investing work. Such pumps can also be implemented for quantum systems, and an experimentally particularly relevant example is the case of periodic driving, characterized by a time-dependent system Hamiltonian

$$H_S(t) = H_S(t + T) \quad \Omega = \frac{2\pi}{T}, \quad (5.1)$$

with period  $T$  and frequency  $\Omega$ . The restriction of driving only the system Hamiltonian can be extended to driving also the interaction, since then a suitable redefinition, based e.g. on reaction-coordinate mappings as discussed in the previous chapter, can be used to recover system-only-driven case [34]. For more details on periodically driven systems see e.g. [35].

### 5.1 Closed systems

#### 5.1.1 Floquet theory

We want to solve the periodically driven Schrödinger equation

$$|\dot{\Psi}\rangle = -iH(t)|\Psi(t)\rangle \quad : \quad H(t+T) = H(t) \quad (5.2)$$

with a periodically driven Hamiltonian with period  $T = 2\pi/\Omega$ .

The **Floquet theorem** states that a solution to this equation is given by

$$|\Phi_r(t)\rangle = e^{-i\epsilon_r t} |r(t)\rangle, \quad (5.3)$$

where the **quasienergies**  $\epsilon_r$  are real and the periodic **Floquet states**  $|r(t)\rangle = |r(t+T)\rangle$  form a complete and orthonormal basis at every instant in time. From this, we already note a certain ambiguity. With replacing

$$\epsilon_r \rightarrow \epsilon_r + m\Omega = \epsilon_{rm}, \quad |r(t)\rangle \rightarrow e^{+im\Omega t} |r(t)\rangle = |r_m(t)\rangle \quad (5.4)$$

we obtain another set of solutions with exactly the same properties. To remove this ambiguity, it is standard to choose  $m$  such that all quasienergies lie in the first Brillouin zone

$$-\frac{\Omega}{2} < \epsilon_{rm} \leq +\frac{\Omega}{2}. \quad (5.5)$$

In the following, we will adopt this convention and drop the index  $m$ . Knowing the quasienergies and Floquet states allows to construct the full quantum dynamics for a given initial condition  $|\Psi(t)\rangle = \sum_r c_r^0 e^{-i\epsilon_r t} |r(t)\rangle$ , that determines the coefficients  $c_r^0$ . To find the quasienergies and Floquet states we insert this into the Schrödinger equation, which yields

$$[H(t) - i\partial_t] |r(t)\rangle = \epsilon_r |r(t)\rangle . \quad (5.6)$$

This is the relevant equation that needs to be solved for the time-dependent Floquet states  $|r(t)\rangle$  and quasienergies  $\epsilon_r$ , such that the latter lie in the first Brillouin zone.

An alternative formulation of the Floquet theorem for the driven Schrödinger equation would be that the time evolution operator from 0 to  $t$  can be expressed as a product of a unitary kick operator with the period of the driving and and the evolution under an effective Floquet Hamiltonian

$$U(t) = U_{\text{kick}}(t) e^{-i\bar{H}t} \quad : \quad U_{\text{kick}}(t+T) = U_{\text{kick}}(t), \quad U_{\text{kick}}(nT) = \mathbf{1} . \quad (5.7)$$

Expressing the time evolution operator instead in terms of Floquet states and quasienergies we have

$$U(t) = \sum_r e^{-i\epsilon_r t} |r(t)\rangle \langle r(0)| , \quad (5.8)$$

and in particular we have due to the periodicity of  $|r(t+T)\rangle = |r(t)\rangle$  that

$$U(T) = \sum_r e^{-i\epsilon_r T} |r(0)\rangle \langle r(0)| \stackrel{!}{=} e^{-i\bar{H}T} \quad \Longrightarrow \quad \bar{H} = \sum_r \epsilon_r |r(0)\rangle \langle r(0)| , \quad (5.9)$$

which provides a realization of the Floquet Hamiltonian in terms of quasienergies  $\epsilon_r$  and Floquet states  $|r(0)\rangle$ . From this, also the kick operator can be found

$$\begin{aligned} U_{\text{kick}}(t) &= U(t) e^{+i\bar{H}t} = \left[ \sum_r e^{-i\epsilon_r t} |r(t)\rangle \langle r(0)| \right] \left[ \sum_q e^{+i\epsilon_q t} |q(0)\rangle \langle q(0)| \right] \\ &= \sum_r |r(t)\rangle \langle r(0)| , \end{aligned} \quad (5.10)$$

from which we can see its unitarity and periodic properties.

In effect, we can express any operator in the Heisenberg picture as

$$\begin{aligned} \mathbf{A}(t) &= U^\dagger(t, 0) \mathbf{A} U(t, 0) = \sum_{rr'} e^{+i(\epsilon_r - \epsilon_{r'})t} \langle r(t) | \mathbf{A} | r'(t) \rangle |r(0)\rangle \langle r'(0)| \\ &= \sum_{rr'} \sum_n e^{+i(\epsilon_r - \epsilon_{r'})t} A_{rr',n} e^{+i\Omega n t} |r(0)\rangle \langle r'(0)| . \end{aligned} \quad (5.11)$$

Likewise, the reverse transform back from the Heisenberg picture can be achieved by acting with  $U(t, 0)[\dots]U^\dagger(t, 0)$ . Unfortunately, solving Eq. (5.6) in the first place is generally notoriously difficult and will in most cases have to be performed perturbatively or numerically.

### 5.1.2 Example: Circularly driven two-level system

An example where everything can be obtained analytically are circularly driven two-level systems

$$H(t) = \frac{\omega}{2} \sigma^z + P \sigma^+ e^{-i\Omega t} + P^* \sigma^- e^{+i\Omega t} , \quad (5.12)$$

where  $\sigma^\pm = \frac{1}{2}[\sigma^x \pm i\sigma^y]$  and  $P$  denotes the amplitude of the driving. We can use the rotation

$$V(t) = e^{-i\Omega/2\sigma^z t} \quad (5.13)$$

on the complete Hamiltonian to move into a different frame, where the Hamiltonian is time-independent. For this, we get

$$V^\dagger(t)\sigma^z V(t) = \sigma^z, \quad V^\dagger(t)\sigma^\pm V(t) = \sigma^\pm e^{\pm i\Omega t}. \quad (5.14)$$

Therefore, applying this to the Schrödinger equation  $|\Psi\rangle = V(t) \left| \tilde{\Psi} \right\rangle$  transforms it into

$$-i\frac{\Omega}{2}\sigma^z V(t) \left| \tilde{\Psi} \right\rangle + V(t) \left| \dot{\tilde{\Psi}} \right\rangle = -iHV(t) \left| \tilde{\Psi} \right\rangle, \quad (5.15)$$

which we can rewrite as

$$\left| \dot{\tilde{\Psi}} \right\rangle = \left[ -iV^\dagger(t)HV(t) + i\frac{\Omega}{2}\sigma^z \right] \left| \tilde{\Psi} \right\rangle = -i \left[ \left( \frac{\omega - \Omega}{2} \right) \sigma^z + P\sigma^+ + P^*\sigma^- \right] \left| \tilde{\Psi} \right\rangle. \quad (5.16)$$

In this frame, the Hamiltonian is time-independent, and by exponentiating it we obtain the corresponding time evolution operator in this frame. Inserting the original transformation, therefore time evolution operator in the original frame is given by

$$U(t) = e^{-i\frac{\Omega}{2}\sigma^z t} e^{-i \left[ \left( \frac{\omega - \Omega}{2} \right) \sigma^z + P\sigma^+ + P^*\sigma^- \right] t}. \quad (5.17)$$

This is not yet the desired decomposition, since the first operator does not have the period of the driving. Looking at the time evolution operator over one period, we get

$$\begin{aligned} U(T) &= \exp \{ -i\pi\sigma^z \} \exp \left\{ -i \left[ \left( \frac{\omega - \Omega}{2} \right) \sigma^z + P\sigma^+ + P^*\sigma^- \right] \frac{2\pi}{\Omega} \right\} \\ &= -\exp \left\{ -i \left[ \left( \frac{\omega - \Omega}{2} \right) \sigma^z + P\sigma^+ + P^*\sigma^- \right] \frac{2\pi}{\Omega} \right\} \\ &= \exp \left\{ -i \left[ \left( \frac{\omega - \Omega}{2} \right) \sigma^z + P\sigma^+ + P^*\sigma^- \right] \frac{2\pi}{\Omega} + i\pi\mathbf{1} \right\} \\ &= \exp \left\{ -i \left[ \left( \frac{\omega - \Omega}{2} \right) \sigma^z + P\sigma^+ + P^*\sigma^- - \frac{\Omega}{2}\mathbf{1} \right] \frac{2\pi}{\Omega} \right\}. \end{aligned} \quad (5.18)$$

From this, we can directly read off the Floquet Hamiltonian

$$\bar{H} = \left( \frac{\omega - \Omega}{2} \right) \sigma^z + P\sigma^+ + P^*\sigma^- - \frac{\Omega}{2}\mathbf{1}. \quad (5.19)$$

Clearly, this is not the conventional average rotating-wave Hamiltonian (which would not have terms proportional to  $P$  and  $P^*$ ). To find the kick operator, we proceed with this result

$$U(t) = V(t) e^{-i\frac{\Omega t}{2}\mathbf{1}} e^{-i\bar{H}t} = e^{-i\Omega t/2(\sigma^z + \mathbf{1})} e^{-i\bar{H}t}, \quad (5.20)$$

which leaves us with

$$U_{\text{kick}}(t) = e^{-i\Omega t/2(\sigma^z + \mathbf{1})} = \begin{pmatrix} e^{-i\Omega t} & 0 \\ 0 & 1 \end{pmatrix}, \quad (5.21)$$

from which we can clearly see the periodicity. The eigenstates of the Floquet Hamiltonian are the initial Floquet states, and by acting on them with the kick operator, we get the time-dependent Floquet states  $|r(t)\rangle = U_{\text{kick}}(t) |r(0)\rangle$ . Note that with this decomposition, the eigenvalues of the Floquet Hamiltonian still have to be mapped into the first Brillouin zone.

An analogous discussion can be applied for a circularly driven harmonic oscillator model.

### 5.1.3 Extended space decomposition

Any periodic state  $|u(t)\rangle = |u(t+T)\rangle$  will always have a Fourier decomposition

$$|u(t)\rangle = \sum_{n=-\infty}^{+\infty} |u_n\rangle e^{in\Omega t}, \quad |u_n\rangle = \frac{1}{T} \int_0^T |u(t)\rangle e^{-in\Omega t} dt, \quad (5.22)$$

where the sum ranges over all integers.

First, we define an **extended space**, within which we can represent all periodic states

$$|u(t)\rangle \Leftrightarrow |u\rangle_E = \sum_n |n\rangle \otimes |u_n\rangle. \quad (5.23)$$

Obviously, any periodic state can be represented in the extended space, and given the extended space representation, we can get back to the periodic state.

Second, since a periodic operator  $O(t) = O(t+T) = \sum_n O_n e^{in\Omega t}$  with the same period maps a periodic state to another periodic state with the same period, we have to see how periodic operators can be represented in the extended space

$$|v(t)\rangle = O(t)|u(t)\rangle = \sum_k \left[ \sum_n O_n |u_{k-n}\rangle \right] e^{ik\Omega t} \Leftrightarrow |v\rangle_E = \sum_k |k\rangle \otimes \left[ \sum_n O_n |u_{k-n}\rangle \right]. \quad (5.24)$$

If this should make any sense, we demand  $O_E |u\rangle_E = |v\rangle_E$ . This allows us to identify

$$O(t) \Leftrightarrow O_E = \sum_n F_n \otimes O_n \quad : \quad F_n |k\rangle \equiv |k+n\rangle. \quad (5.25)$$

Insertion indeed shows that

$$\begin{aligned} O_E |u\rangle_E &= \sum_{nm} F_n |m\rangle \otimes O_n |u_m\rangle = \sum_{nm} |m+n\rangle \otimes O_n |u_m\rangle \\ &= \sum_{nk} |k\rangle \otimes O_n |u_{k-n}\rangle = \sum_k |k\rangle \otimes \left[ \sum_n O_n |u_{k-n}\rangle \right]. \end{aligned} \quad (5.26)$$

Third, we repeat the previous argument for the time derivative. Since the time-derivative of a periodic function is just another periodic function, we get

$$-i\partial_t |u(t)\rangle = \sum_n \Omega n |u_n\rangle e^{in\Omega t} \Leftrightarrow \Omega \sum_n (n |n\rangle) \otimes |u_n\rangle \equiv \Omega \sum_n (F^z |n\rangle) \otimes |u_n\rangle, \quad (5.27)$$

which implies the relation

$$-i\partial_t \Leftrightarrow \Omega F^z \otimes \mathbf{1} \quad : \quad F^z |n\rangle \equiv n |n\rangle. \quad (5.28)$$

Now, we can represent Eq. (5.6) in the extended space

$$\left[ \sum_k F_k \otimes H_k + \Omega F^z \otimes \mathbf{1} \right] |r\rangle_E = \epsilon_r |r\rangle_E. \quad (5.29)$$

From the action of  $F_k$  and  $F^z$  on  $|r\rangle_E = \sum_n |n\rangle \otimes |r_n\rangle$  one can see that the matrix on the l.h.s. has a block-banded structure

$$H_E = \begin{pmatrix} \ddots & & & & & & \\ \ddots & H_0 - 1 \cdot \Omega \cdot \mathbf{1} & H_{-1} & H_{-2} & \dots & & \\ \ddots & H_{+1} & H_0 + 0 \cdot \Omega \cdot \mathbf{1} & H_{-1} & \ddots & & \\ \dots & H_{+2} & H_{+1} & H_0 + 1 \cdot \Omega \cdot \mathbf{1} & \ddots & & \\ & \vdots & & & \ddots & \ddots & \\ & & & & & \ddots & \ddots \end{pmatrix}, \quad (5.30)$$

where the  $H_k$  are blocks given by the Fourier components of the Hamiltonian and  $\Omega$  is the frequency of the driving. We can introduce a cutoff in Floquet space and consider only the lowest few Fourier components, leading to a finite-dimensional matrix, of which the eigenvalues are approximations to the quasienergies and the eigenvectors are approximations to the Floquet states in the extended space. Transferring them back to the original space allows one to approximate the exact solution. For simple drivings such as  $\cos(\Omega t)$ , one will only have the Fourier components close to the diagonal  $H_{\pm 1}$ . Then, for large  $\Omega$ , the blocks will be well separated and convergence will be good with already few Floquet modes considered.

To get e.g. the Floquet Hamiltonian  $\bar{H}$ , we have to determine the quasienergies  $\epsilon_r$  and also the Floquet states  $|r(0)\rangle = \sum_n |r_n\rangle$ . From the extended space eigenvectors  $|r\rangle_E = \sum_n |r_n\rangle \otimes |n\rangle$ , this can be reconstructed.

#### 5.1.4 Example: Driven two-level system

As a simple example, we consider a driven two-level system

$$H(t) = \frac{\omega}{2} \sigma^z + \lambda \cos(\Omega t) \sigma^x. \quad (5.31)$$

The driving chosen here is not of the circular form, such that a simple analytic solution is not available.

We can numerically integrate the time-dependent Schrödinger equation with some solver, which serves as a benchmark.

Alternatively, we can approximately calculate the time evolution operator either by computing only a finite number of Floquet states in extended space, or by performing transformations to interaction pictures, within which we can perform a RWA. The result is shown in Fig. 5.1

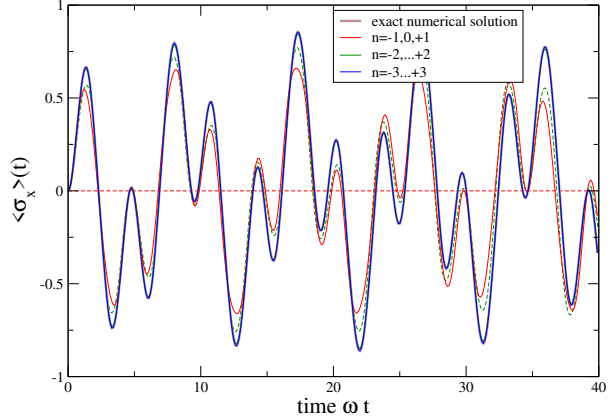
#### Extended space diagonalization

Alternatively, we can diagonalize the Hamiltonian representation in extended space

$$H_E = \left( \begin{array}{c|cc|c} \ddots & & & \\ \hline \ddots & \frac{\omega}{2} \sigma^z - \Omega \mathbf{1} & \frac{\lambda}{2} \sigma^x & \mathbf{0} \\ & \frac{\lambda}{2} \sigma^x & \frac{\omega}{2} \sigma^z & \frac{\lambda}{2} \sigma^x \\ \hline & \mathbf{0} & \frac{\lambda}{2} \sigma^x & \frac{\omega}{2} \sigma^z + \Omega \mathbf{1} & \ddots \\ & & & & \ddots & \ddots \end{array} \right), \quad (5.32)$$

take only the quasienergies and eigenvectors from the first Brillouin zone and transfer them back in the time domain. In the above equation, the lines symbolize a cutoff for  $n \in \{-1, 0, +1\}$ .

Figure 5.1: Plot of the time-dependent expectation value of some observable according to the exact numerical integration (gray) and from reconstruction from diagonalization in the extended space (solid colored). Convergence is already achieved with very few Floquet modes considered. The convergence for the generalized RWA (thin dashed) by contrast is significantly worse. Whereas the naive RWA and the first order RWA (dashed red) corresponding to Eq. (5.33) and Eq. (5.36) do not show any time dependence, the next best RWA solution from Eq. (5.40) (dashed green) shows some sufficient approximation, but the extended space diagonalization appears superior, at least for the considered parameters. Parameters:  $\Omega = 2\omega$ ,  $\lambda = \omega$ ,  $\langle \sigma^z \rangle_0 = +1$ .



### Generalized RWA method

The naive RWA applied to the Hamiltonian reads

$$H_{RWA} = \frac{\omega}{2}\sigma^z \quad : \quad U_{RWA,0} = e^{-i\frac{\omega t}{2}\sigma^z}. \quad (5.33)$$

As in our example, we start in an eigenstate of  $\sigma^z$ , this will not evolve at all under this effective time evolution operator.

Alternatively, we could treat the driving term as strong and the constant term as perturbation. Transforming with  $U_1(t) = e^{-i\lambda/\Omega \sin(\Omega t)\sigma^x}$  into an interaction picture and performing the RWA in that picture eventually already provides a useful improvement. In the transformed picture, the full Hamiltonian becomes

$$\tilde{H}(t) = \frac{\omega}{2}U_1^\dagger(t)\sigma^z U_1(t) = \frac{\omega}{2} \cos\left[\frac{2\lambda}{\Omega} \sin(\Omega t)\right] \sigma^z + \frac{\omega}{2} \sin\left[\frac{2\lambda}{\Omega} \sin(\Omega t)\right] \sigma^y. \quad (5.34)$$

The rotating wave approximation in this frame yields

$$\tilde{H}_{RWA} = \frac{\omega}{2} \mathcal{J}_0\left(\frac{2\lambda}{\Omega}\right) \sigma^z, \quad (5.35)$$

where  $\mathcal{J}_n(x)$  denotes a Bessel function, such that the time evolution operator in the original frame reads

$$U(t) \approx U_{RWA,1}(t) = U_1(t) \underbrace{e^{-i\mathcal{J}_0\left(\frac{2\lambda}{\Omega}\right)\frac{\omega t}{2}\sigma^z}}_{U_{\text{kick}}(t)} = \underbrace{e^{-i\lambda/\Omega \sin(\Omega t)\sigma^x}}_{U_{\text{kick}}(t)} \underbrace{e^{-i\mathcal{J}_0\left(\frac{2\lambda}{\Omega}\right)\frac{\omega t}{2}\sigma^z}}_{e^{-i\tilde{H}t}}. \quad (5.36)$$

Still, starting in an eigenstate of  $\sigma^z$  one will have some evolution, but the expectation value of  $\sigma^x$  will remain constant also under this effective time evolution operator.

We can in principle apply this recursively by transforming again to yet another picture. Writing the Fourier components

$$\begin{aligned}\tilde{H}(t) &= \frac{\omega}{2} \mathcal{J}_0\left(\frac{2\lambda}{\Omega}\right) \sigma^z + \frac{\omega}{2} \mathcal{J}_1\left(\frac{2\lambda}{\Omega}\right) (-ie^{+i\Omega t} + ie^{-i\Omega t}) \sigma^y + \dots \\ &= \frac{\omega}{2} \mathcal{J}_0\left(\frac{2\lambda}{\Omega}\right) \sigma^z + \omega \mathcal{J}_1\left(\frac{2\lambda}{\Omega}\right) \sin(\Omega t) \sigma^y + \dots,\end{aligned}\quad (5.37)$$

we use yet another unitary  $U_2(t) = \exp\{-i\frac{\omega}{\Omega} \mathcal{J}_1\left(\frac{2\lambda}{\Omega}\right) [1 - \cos(\Omega t)] \sigma^y\}$ . In the resulting picture, we obtain

$$\tilde{\tilde{H}}(t) \approx \frac{\omega}{2} \mathcal{J}_0\left(\frac{2\lambda}{\Omega}\right) U_2^\dagger(t) \sigma^z U_2(t), \quad (5.38)$$

which allows to perform the RWA

$$\begin{aligned}\tilde{\tilde{H}}_{RWA} &\approx \frac{\omega}{2} \mathcal{J}_0\left(\frac{2\lambda}{\Omega}\right) \mathcal{J}_0\left(\frac{2\omega}{\Omega} \mathcal{J}_1\left(\frac{2\lambda}{\Omega}\right)\right) \cos\left[\frac{2\omega}{\Omega} \mathcal{J}_1\left(\frac{2\lambda}{\Omega}\right)\right] \sigma^z \\ &\quad - \frac{\omega}{2} \mathcal{J}_0\left(\frac{2\lambda}{\Omega}\right) \mathcal{J}_0\left(\frac{2\omega}{\Omega} \mathcal{J}_1\left(\frac{2\lambda}{\Omega}\right)\right) \sin\left[\frac{2\omega}{\Omega} \mathcal{J}_1\left(\frac{2\lambda}{\Omega}\right)\right] \sigma^x,\end{aligned}\quad (5.39)$$

which allows to write the time evolution operator in the original frame as

$$U(t) \approx U_{RWA,2} = \underbrace{U_1(t)U_2(t)}_{U_{\text{kick}}(t)} \underbrace{e^{-i\tilde{\tilde{H}}_{RWA}t}}_{e^{-i\tilde{H}t}}. \quad (5.40)$$

Thereby, we obtain approximate but analytic expressions for the Floquet Hamiltonian and the kick operator that become valid for fast driving.

## 5.2 Open systems

### 5.2.1 Secular and Nonsecular master equation

We use that the time evolution operator of the system alone can be written as

$$U(t) = \sum_r e^{-i\epsilon_r t} |r(t)\rangle \langle r(0)|. \quad (5.41)$$

Having performed the Born- and Markov approximations in the interaction picture, the nonsecular master equation (1.62) reads

$$\begin{aligned}\dot{\rho} &= - \int_0^\infty \text{Tr}_B \{ [\mathbf{H}_I(t), [\mathbf{H}_I(t - \tau), \rho(t) \otimes \bar{\rho}_B]] \} d\tau \\ &= \sum_{\alpha\beta} \int_0^\infty d\tau \{ [\mathbf{A}_\alpha(t), \rho(t) \mathbf{A}_\beta(t - \tau)] C_{\beta\alpha}(-\tau) - [\mathbf{A}_\alpha(t), \mathbf{A}_\beta(t - \tau) \rho(t)] C_{\alpha\beta}(+\tau) \}.\end{aligned}\quad (5.42)$$

Here, boldface operators denote the usual interaction picture, which due to the time-dependence of the system Hamiltonian becomes non-trivial  $\mathbf{A}_\alpha(\mathbf{t}) = U^\dagger(t) A_\alpha U(t)$ . This master equation is in general not of Lindblad form.

To perform the secular approximation, we use the representation of the time evolution operator

$$\begin{aligned}
\mathbf{A}_\alpha(\mathbf{t}) &= \sum_{rr'} e^{+i(\epsilon_r - \epsilon_{r'})t} \langle r(t) | A_\alpha | r'(t) \rangle |r(0)\rangle \langle r'(0)|, \\
&= \sum_{rr'} \sum_n e^{+i(\epsilon_r - \epsilon_{r'})t} A_{\alpha,rr'}^n e^{+in\Omega t} |r(0)\rangle \langle r'(0)| \\
\mathbf{A}_\beta(\mathbf{t} - \boldsymbol{\tau}) &= \sum_{ss'} e^{+i(\epsilon_s - \epsilon_{s'})(t-\tau)} \langle s(t-\tau) | A_\beta | s'(t-\tau) \rangle |s(0)\rangle \langle s'(0)| \\
&= \sum_{ss'} \sum_m e^{+i(\epsilon_s - \epsilon_{s'})(t-\tau)} A_{\beta,ss'}^m e^{+im\Omega(t-\tau)} |s(0)\rangle \langle s'(0)|.
\end{aligned} \tag{5.43}$$

Technically, the **secular approximation** can now be performed as follows: Since the Floquet energies are by construction chosen in the first Brillouin zone  $-\Omega/2 < \epsilon_r \leq +\Omega/2$ , any difference of them is at most given by the driving frequency  $|\epsilon_r - \epsilon_{r'}| < \Omega$ . Therefore, we require fast driving as a necessary (but not sufficient) condition to perform the secular approximation. For fast driving, the terms oscillatory in time  $t$  can only cancel of the separately meet the resonance conditions

$$m = -n, \quad \epsilon_s - \epsilon_{s'} = -(\epsilon_r - \epsilon_{r'}), \tag{5.44}$$

leading to the secular version of the master equation

$$\begin{aligned}
\dot{\boldsymbol{\rho}} &= \sum_{\alpha\beta} \sum_n \sum_{rr's's'} \int_0^\infty d\tau e^{+i(\epsilon_r - \epsilon_{r'})\tau} e^{+in\Omega\tau} \delta_{\epsilon_r - \epsilon_{r'}, \epsilon_{s'} - \epsilon_s} A_{\alpha,rr'}^n A_{\beta,ss'}^{-n} \times \\
&\quad \{ [|r(0)\rangle \langle r'(0)|, \boldsymbol{\rho}(\mathbf{t}) |s(0)\rangle \langle s'(0)|] C_{\beta\alpha}(-\tau) - [|r(0)\rangle \langle r'(0)|, |s(0)\rangle \langle s'(0)| \boldsymbol{\rho}(\mathbf{t})] C_{\alpha\beta}(+\tau) \}.
\end{aligned} \tag{5.45}$$

This equation is of Lindblad form and has time-independent coefficients in the interaction picture and will therefore also have a stationary solution in the interaction picture. However, one should note that with increasing system Hilbert space dimension, it will become increasingly difficult to justify the validity of the secular approximation: Since for an  $N$ -dimensional system Hilbert space, we will have  $N$  quasienergies in the first Brillouin zone, the spacing between them will generically become small when  $N$  is large.

As known for the secular master equation, when we additionally assume that the quasienergies in the first Brillouin zone are non-degenerate  $\delta_{\epsilon_r, \epsilon_s} = \delta_{rs}$ , this actually leads to a decoupling of populations and coherences in the Floquet basis. With defining  $\rho_{qq'} = \langle q(0) | \boldsymbol{\rho} | q'(0) \rangle$  we get for

coherences ( $q \neq q'$  and  $\epsilon_q \neq \epsilon_{q'}$ ) the equation

$$\begin{aligned}
\dot{\rho}_{qq'} &= \sum_{\alpha\beta} \sum_n \int_0^\infty d\tau e^{in\Omega\tau} A_{\alpha,qq}^{+n} A_{\beta,q'q'}^{-n} C_{\beta\alpha}(-\tau) \rho_{qq'} \\
&\quad - \sum_{\alpha\beta} \sum_n \sum_s \int_0^\infty d\tau e^{i(\epsilon_s - \epsilon_{q'})\tau} e^{in\Omega\tau} A_{\alpha,sq'}^{+n} A_{\beta,q's}^{-n} C_{\beta\alpha}(-\tau) \rho_{qq'} \\
&\quad - \sum_{\alpha\beta} \sum_n \sum_s \int_0^\infty d\tau e^{i(\epsilon_q - \epsilon_s)\tau} e^{in\Omega\tau} A_{\alpha,qs}^{+n} A_{\beta,sq}^{-n} C_{\alpha\beta}(+\tau) \rho_{qq'} \\
&\quad + \sum_{\alpha\beta} \sum_n \int_0^\infty d\tau e^{in\Omega\tau} A_{\alpha,q'q'}^{+n} A_{\beta,qq}^{-n} C_{\alpha\beta}(+\tau) \rho_{qq'} \\
&= \sum_{\alpha\beta} \sum_n \gamma_{\alpha\beta}(n\Omega\tau) A_{\alpha,q'q'}^{+n} A_{\beta,qq}^{-n} \rho_{qq'} \\
&\quad - \sum_{\alpha\beta} \sum_n \sum_s \left[ \int_0^\infty d\tau e^{i(\epsilon_q - \epsilon_s)\tau} e^{in\Omega\tau} C_{\alpha\beta}(+\tau) \right] A_{\alpha,qs}^{+n} A_{\beta,sq}^{-n} \rho_{qq'} \\
&\quad - \sum_{\alpha\beta} \sum_n \sum_s \left[ \int_0^\infty d\tau e^{i(\epsilon_s - \epsilon_{q'})\tau} e^{-in\Omega\tau} C_{\alpha\beta}(-\tau) \right] A_{\beta,sq'}^{-n} A_{\alpha,q's}^{+n} \rho_{qq'}. \tag{5.46}
\end{aligned}$$

Separating the  $s = q$  or  $s = q'$  terms in the respective summations we see that the positive contribution from the first line is actually cancelled. The remaining terms can be expressed by even and odd FTs of the CFs, which can be used to show that the coherences in the Floquet basis will actually decay.

Similarly, we find that the populations in the Floquet basis decouple from the coherences

$$\begin{aligned}
\dot{\rho}_{qq} &= + \sum_{\alpha\beta} \sum_s \sum_n \int_0^\infty d\tau e^{+i(\epsilon_q - \epsilon_s)\tau} e^{+in\Omega\tau} A_{\alpha,qs}^{+n} A_{\beta,qs}^{-n} C_{\beta\alpha}(-\tau) \rho_{ss} \\
&\quad - \sum_{\alpha\beta} \sum_s \sum_n \int_0^\infty d\tau e^{+i(\epsilon_s - \epsilon_q)\tau} e^{+in\Omega\tau} A_{\alpha,qs}^{+n} A_{\beta,qs}^{-n} C_{\beta\alpha}(-\tau) \rho_{qq} \\
&\quad - \sum_{\alpha\beta} \sum_s \sum_n \int_0^\infty d\tau e^{+i(\epsilon_q - \epsilon_s)\tau} e^{+in\Omega\tau} A_{\alpha,qs}^{+n} A_{\beta,qs}^{-n} C_{\alpha\beta}(+\tau) \rho_{qq} \\
&\quad + \sum_{\alpha\beta} \sum_s \sum_n \int_0^\infty d\tau e^{+i(\epsilon_s - \epsilon_q)\tau} e^{+in\Omega\tau} A_{\alpha,qs}^{+n} A_{\beta,qs}^{-n} C_{\alpha\beta}(+\tau) \rho_{ss} \\
&= + \sum_{\alpha\beta} \sum_s \sum_n \int_0^\infty d\tau e^{+i(\epsilon_q - \epsilon_s)\tau} e^{-in\Omega\tau} A_{\beta,qs}^{-n} A_{\alpha,qs}^{+n} C_{\alpha\beta}(-\tau) \rho_{ss} \\
&\quad - \sum_{\alpha\beta} \sum_s \sum_n \int_0^\infty d\tau e^{+i(\epsilon_s - \epsilon_q)\tau} e^{-in\Omega\tau} A_{\beta,qs}^{-n} A_{\alpha,qs}^{+n} C_{\alpha\beta}(-\tau) \rho_{qq} \\
&\quad - \sum_{\alpha\beta} \sum_s \sum_n \int_0^\infty d\tau e^{+i(\epsilon_q - \epsilon_s)\tau} e^{+in\Omega\tau} A_{\alpha,qs}^{+n} A_{\beta,qs}^{-n} C_{\alpha\beta}(+\tau) \rho_{qq} \\
&\quad + \sum_{\alpha\beta} \sum_s \sum_n \int_0^\infty d\tau e^{+i(\epsilon_s - \epsilon_q)\tau} e^{+in\Omega\tau} A_{\alpha,qs}^{+n} A_{\beta,qs}^{-n} C_{\alpha\beta}(+\tau) \rho_{ss} \\
&= \sum_s \left[ \sum_{\alpha\beta} \sum_n \gamma_{\alpha\beta}(\epsilon_s - \epsilon_q + n\Omega) A_{\alpha,qs}^{+n} A_{\beta,qs}^{-n} \right] \rho_{ss} - \left[ \sum_s \sum_{\alpha\beta} \sum_n \gamma_{\alpha\beta}(\epsilon_q - \epsilon_s + n\Omega) A_{\alpha,qs}^{+n} A_{\beta,qs}^{-n} \right] \rho_{qq}.
\end{aligned} \tag{5.47}$$

This has the form of a standard rate equation, but now in the Floquet basis.

**Def. 21** (Floquet rate equation). *In the Floquet basis, the secular master equation appears as a rate equation*

$$\dot{\rho}_{qq} = \sum_s W_{qs}(\xi) \rho_{ss} - \sum_s W_{sq}(0) \rho_{qq} \tag{5.48}$$

with transition rates

$$W_{qs}(\xi) = \sum_{\alpha\beta} \sum_{n=-\infty}^{+\infty} \gamma_{\alpha\beta}(\epsilon_s - \epsilon_q + n\Omega) e^{+i\xi(\epsilon_s - \epsilon_q + n\Omega)} A_{\beta,qs}^{-n} A_{\alpha,qs}^{+n} \tag{5.49}$$

given by the FT of the correlation function  $\gamma_{\alpha\beta}(\omega)$  and  $A_{\alpha,qs}^n = \frac{1}{T} \int_0^T \langle s(t) | A_\alpha | q(t) \rangle e^{-in\Omega t} dt$ .

- This expression is analogous to the rate equation (1.83) for undriven systems. We further observe that the transition rates are invariant with respect to the Brillouin zone ambiguity. Specifically, under the transformations  $\epsilon_q \rightarrow \epsilon_q + m_q\Omega$  as well as  $|q(t)\rangle \rightarrow e^{+im_q\Omega t} |q(t)\rangle$  (and

similar for  $\epsilon_s$  and  $|s(t)\rangle$ , respectively), the transition rates are invariant

$$\begin{aligned}
A_{\alpha,sq}^{+n} &\rightarrow A_{\alpha,sq}^{n-m_q+m_s}, & A_{\beta,qs}^{-n} &\rightarrow A_{\beta,qs}^{-n+m_q-m_s}, \\
W_{qs}(\xi) &\rightarrow \sum_{\alpha\beta} \sum_n \gamma_{\alpha\beta}(\epsilon_s - \epsilon_q + (n + m_s - m_q)\Omega) e^{i\xi(\epsilon_s - \epsilon_q + (n+m_s-m_q)\Omega)} A_{\beta,qs}^{-n+m_q-m_s} A_{\alpha,sq}^{n-m_q+m_s} \\
&= \sum_{\alpha\beta} \sum_m \gamma_{\alpha\beta}(\epsilon_s - \epsilon_q + m\Omega) e^{i\xi(\epsilon_s - \epsilon_q + m\Omega)} A_{\beta,qs}^{-m} A_{\alpha,sq}^{+m} = W_{qs}(\xi),
\end{aligned} \tag{5.50}$$

where we have used  $m = n + m_s - m_q$ .

- In general, counting fields may now occur on the diagonal of the rate matrix.
- The ratio of two transition rates becomes

$$\begin{aligned}
\frac{W_{qs}}{W_{sq}} &= \frac{\sum_{\alpha\beta} \sum_n \gamma_{\alpha\beta}(\epsilon_s - \epsilon_q + n\Omega) A_{\alpha,sq}^{+n} A_{\beta,qs}^{-n}}{\sum_{\alpha\beta} \sum_n \gamma_{\alpha\beta}(\epsilon_q - \epsilon_s + n\Omega) A_{\alpha,qs}^{+n} A_{\beta,sq}^{-n}} = \frac{\sum_{\alpha\beta} \sum_n \gamma_{\alpha\beta}(\epsilon_s - \epsilon_q + n\Omega) A_{\alpha,sq}^{+n} A_{\beta,qs}^{-n}}{\sum_{\alpha\beta} \sum_n \gamma_{\beta\alpha}(\epsilon_q - \epsilon_s - n\Omega) A_{\beta,qs}^{-n} A_{\alpha,sq}^{+n}} \\
&= \frac{\sum_{\alpha\beta} \sum_n \gamma_{\alpha\beta}(\epsilon_s - \epsilon_q + n\Omega) A_{\alpha,sq}^{+n} A_{\beta,qs}^{-n}}{\sum_{\alpha\beta} \sum_n e^{\beta(\epsilon_q - \epsilon_s - n\Omega)} \gamma_{\alpha\beta}(\epsilon_s - \epsilon_q + n\Omega) A_{\beta,qs}^{-n} A_{\alpha,sq}^{+n}},
\end{aligned} \tag{5.51}$$

where we have used the KMS relation. We note that in general it breaks detailed balance due to the  $n\Omega$  term, and will therefore in general not imply thermalization in the Floquet basis [36, 37].

- Two limiting cases however are of interest, where the detailed balance condition is restored and where one therefore finds thermalization in the respective Floquet basis. First, the case of very fast driving: Since in general the FTs of the correlation functions will decay at large arguments, for large  $\Omega$  only the  $n = 0$  term in the sum remains, yielding

$$\frac{W_{qs}}{W_{sq}} \approx \frac{\sum_{\alpha\beta} \gamma_{\alpha\beta}(\epsilon_s - \epsilon_q) A_{\alpha,sq}^0 A_{\beta,qs}^0}{\sum_{\alpha\beta} e^{\beta(\epsilon_q - \epsilon_s)} \gamma_{\alpha\beta}(\epsilon_s - \epsilon_q) A_{\beta,qs}^0 A_{\alpha,sq}^0} = e^{-\beta(\epsilon_q - \epsilon_s)}, \tag{5.52}$$

and we thermalize in the Floquet basis where only the  $n = 0$  coefficients contribute. This however just describes the thermalization for a model where a naive rotating wave approximation has been performed on  $H_S$ .

Second, there is the case of very slow driving: Quite often, the dependence of the Fourier coefficients  $A_{\alpha,sq}^n = \frac{1}{T} \int_0^T \langle s(t) | A_\alpha | q(t) \rangle e^{-in\Omega t} dt$  will be such that  $A_{\alpha,sq}^n \approx 0$  for  $n > N_{\text{cut}}$ . When then  $N_{\text{cut}}\Omega$  is still small or the FT of the correlation function is sufficiently flat, we may drop the frequency in the argument of the FTs of the CFs

$$\frac{W_{qs}}{W_{sq}} \approx \frac{\sum_{\alpha\beta} \gamma_{\alpha\beta}(\epsilon_s - \epsilon_q) \sum_n A_{\alpha,sq}^{+n} A_{\beta,qs}^{-n}}{\sum_{\alpha\beta} e^{\beta(\epsilon_q - \epsilon_s)} \gamma_{\alpha\beta}(\epsilon_s - \epsilon_q) \sum_n A_{\beta,qs}^{-n} A_{\alpha,sq}^{+n}} = e^{-\beta(\epsilon_q - \epsilon_s)}. \tag{5.53}$$

Again we achieve thermalization in the Floquet eigenbasis. From the adiabatic theorem we would expect thermalization in the time-dependent energy eigenbasis, and the arguments of Sec. 2.3 apply. However, it should be noted that the limit is in conflict with the previously used fast-driving assumption.

- When we transform the rate equation back into the Schrödinger picture, we can use

$$U |r(0)\rangle \langle r'(0)| U^\dagger = e^{-i(\epsilon_r - \epsilon_{r'})t} |r(t)\rangle \langle r'(t)| \quad (5.54)$$

to show that – when coherences in the Floquet basis have already decayed – the rate equation does not change at all. Instead of the initial Floquet states, it then only describes the transitions between time-dependent Floquet states, and we can represent the density matrix as

$$\rho(t) = \sum_s \rho_{ss}(t) |s(t)\rangle \langle s(t)| \rightarrow \sum_s \bar{\rho}_{ss} |s(t)\rangle \langle s(t)|, \quad (5.55)$$

Note that only after some transient relaxation  $\rho(t)$  will have the same period as the driving.

### 5.2.2 Example: open two-level system for circular driving

When we additionally couple our example from Sec. 5.1.2 to a reservoir of bosonic oscillators

$$H(t) = \frac{\omega}{2} \sigma^z + P \sigma^+ e^{-i\Omega t} + P^* \sigma^- e^{+i\Omega t} + \sigma^x \sum_k (h_k b_k + h_k^* b_k^\dagger) + \sum_k \omega_k b_k^\dagger b_k, \quad (5.56)$$

we can essentially use the results for the closed system to determine everything. We had derived a Floquet Hamiltonian and kick operator before

$$\begin{aligned} \bar{H} &= \left( \frac{\omega - \Omega}{2} \right) \sigma^z + P \sigma^+ + P^* \sigma^- - \frac{\Omega}{2} \mathbf{1}, \\ U_{\text{kick}}(t) &= e^{-i\Omega t/2(\sigma^z + \mathbf{1})}. \end{aligned} \quad (5.57)$$

Accordingly, the quasi-energies are

$$\epsilon_{\pm} = +\frac{1}{2} \left[ -\Omega \pm \sqrt{(\omega - \Omega)^2 + 4|P|^2} \right], \quad (5.58)$$

and since the rates are invariant, we can omit the folding into the first Brillouin zone. Then, we get for the corresponding matrix elements

$$\begin{aligned} A_{sq}^n &= \frac{1}{T} \int_0^T \langle s(t) | \sigma^x | q(t) \rangle e^{-in\Omega t} dt \\ &= \frac{1}{T} \int_0^T \langle s(0) | U_{\text{kick}}^\dagger(t) \sigma^x U_{\text{kick}}(t) | q(0) \rangle e^{-in\Omega t} dt \\ &= \frac{1}{T} \int_0^T \langle s(0) | \begin{pmatrix} 0 & e^{+i\Omega t} \\ e^{-i\Omega t} & 0 \end{pmatrix} | q(0) \rangle e^{-in\Omega t} dt \\ &= \delta_{n,+1} \langle s(0) | \sigma^+ | q(0) \rangle + \delta_{n,-1} \langle s(0) | \sigma^- | q(0) \rangle \end{aligned} \quad (5.59)$$

analytically. Specifically, one finds that there will generally be only contributions with  $n \in \{-1, +1\}$ .

Thereby, we can formulate the rate equation between Floquet states as outlined in Def. 21. Furthermore, by using the energy counting field  $\xi$ , we may also track the energy transferred

into/from the reservoir. With the bosonic correlation function FT  $\gamma(\omega) = J(\omega)[1 + n_B(\omega)]$  with  $J(\omega) = -J(-\omega)$ , the rates become

$$W_{qs}(\xi) \rightarrow \gamma(\epsilon_s - \epsilon_q - \Omega) |\langle s(0) | \sigma^- | q(0) \rangle|^2 e^{+i(\epsilon_s - \epsilon_q - \Omega)\xi} + \gamma(\epsilon_s - \epsilon_q + \Omega) |\langle s(0) | \sigma^+ | q(0) \rangle|^2 e^{+i(\epsilon_s - \epsilon_q + \Omega)\xi}, \quad (5.60)$$

where the counting fields may actually show up on the diagonal entries of the rate matrix.

First, we see that to evaluate the time-dependent energy current via the current formula  $I(t) = -i\text{Tr} \{ \mathcal{L}'(0) \rho(t) \}$ , we may equivalently use the interaction picture. There, neglecting coherences between Floquet states, this becomes

$$\begin{aligned} I_E(t) &= \sum_{qs} (-i) W'_{qs}(0) P_{ss}(t) \\ &= \sum_{qs} \left[ (\epsilon_s - \epsilon_q - \Omega) \gamma(\epsilon_s - \epsilon_q - \Omega) |\langle s(0) | \sigma^- | q(0) \rangle|^2 \right. \\ &\quad \left. + (\epsilon_s - \epsilon_q + \Omega) \gamma(\epsilon_s - \epsilon_q + \Omega) |\langle s(0) | \sigma^+ | q(0) \rangle|^2 \right] P_{ss}(t), \end{aligned} \quad (5.61)$$

where the energy differences of the Floquet Hamiltonian are additionally shifted by multiples of the driving frequency (here just  $\pm\Omega$ ). This shows that a microscopic treatment of the counting field derivation is necessary here. Furthermore invoking the stationary limit  $P_{ss}(t) \rightarrow \bar{P}_{ss}$ , the current becomes stationary. Such a stationary current is an artifact of the secular approximation, in reality we can expect the current to behave oscillatory as well.

Clearly, also for a single thermal reservoir, the stationary energy current will not vanish, as the work done on the system by driving must eventually be dissipated into the reservoirs as heat.

### 5.2.3 Upgrade: Two-terminal driven Two-Level system

We can also couple our driven system to two reservoirs  $\nu \in \{L, R\}$

$$H(t) = \frac{\omega}{2} \sigma^z + P \sigma^+ e^{-i\Omega t} + P^* \sigma^- e^{+i\Omega t} + \sigma^x \sum_{k\nu} (h_{k\nu} b_{k\nu} + h_{k\nu}^* b_{k\nu}^\dagger) + \sum_{k\nu} \omega_{k\nu} b_{k\nu}^\dagger b_{k\nu}. \quad (5.62)$$

All previous calculations go through, we just get additive rates

$$W_{qs}(\xi) \rightarrow W_{qs}^L(\xi_L) + W_{qs}^R(\xi_R). \quad (5.63)$$

The currents entering the system from the individual reservoirs are also not conserved. Instead, the first law allows to express the power applied to the system at steady state by the heat currents

$$\dot{W} = -I_E^{(L)} - I_E^{(R)}. \quad (5.64)$$

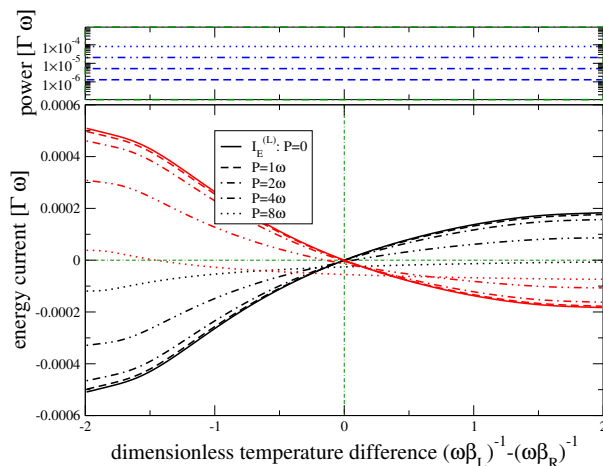
In contrast, without driving, the energy currents would approach

$$\bar{I}_E^{(L)} = -\bar{I}_E^{(R)} = \frac{\Gamma_L(\omega) \Gamma_R(\omega)}{\Gamma_L(\omega)[1 + 2n_L(\omega)] + \Gamma_R(\omega)[1 + 2n_R(\omega)]} \omega [n_L(\omega) - n_R(\omega)]. \quad (5.65)$$

This is illustrated in Fig. 5.2, exemplified for a spectral coupling density of the form

$$\Gamma_\nu(\omega) = \frac{4\Gamma_\nu \omega \delta_\nu^2 \epsilon_\nu}{\omega^4 + 2\omega^2(\delta_\nu - \epsilon_\nu)(\delta_\nu + \epsilon_\nu) + (\delta_\nu^2 + \epsilon_\nu^2)^2} = -\Gamma_\nu(-\omega). \quad (5.66)$$

Figure 5.2: Plot of the energy currents entering the system from the left (black) and right (red) reservoirs for different values of the driving amplitude  $P$  (legend). Without driving ( $P = 0$ , solid), the currents reproduce Eq. (5.65), and their sum cancels. For finite driving, the observed mismatch  $\dot{W} = -I_E^{(L)} - I_E^{(R)}$  denotes the work rate (top panel). Parameters:  $\Gamma_\nu = \Gamma$ ,  $(\beta_L\omega)^{-1} + (\beta_R\omega)^{-1} = 2$ ,  $\epsilon_L = 10\omega$ ,  $\epsilon_R = 20\omega$ ,  $\delta_L = \delta_R = \omega$ ,  $\Omega = 100\omega$ .



Here, on the right the left reservoir is hotter than the right one and vice versa. For small driving amplitudes (dashed) essentially the result of the undriven system (solid) is reproduced. As the driving amplitude becomes larger (legend), the curves shift asymmetrically due to the asymmetric spectral density. Finally, for very large driving amplitude (dotted), the invested mechanical power is dissipated as heat into both reservoirs, such that both heat currents become negative over a wide range of parameters.

Cooling of the colder reservoir (i.e., positive black curves on the left or positive red curves on the right) is not observed anywhere, due to similar arguments as put forward in Sec. 2.8 for two-level systems. Consistently, the power injected into the system is always positive, such that no useful thermodynamic function is performed. To perform useful thermodynamic functions, we require a more complex system. Such systems however arise naturally by employing a reaction-coordinate mapping as discussed in Sec. 4.3, i.e., if one goes beyond the weak-coupling approximation. For example, by using a reaction-coordinate for the cold reservoir only (this is numerically more favorable to avoid the modelling of large occupation numbers), one can demonstrate heat engine and refrigerator operational modes [38].

# Chapter 6

## Feedback control

The time dependence in previous treatments just followed an open-loop control protocol, i.e., the time dependence of the driving was known from the beginning and did not depend on any measurement outcome obtained during the course of the evolution. The idea of feedback control is to measure during the evolution (possibly continuously), and afterwards to alter parameters e.g. in the Hamiltonian conditioned on the measurement outcome to achieve a certain goal. Such goals could for example be the stabilization of certain quantum states in presence of a disturbing environment or the sorting of particles against the usual flow as is done by a Maxwell demon. To achieve a theory describing these effects, we will review the measurement postulate of quantum mechanics. In reality, there will be a delay in this dynamics, either due to a finite duration of the measurement or due to a processing lag between the measurement and the control action. To describe this is notoriously difficult, and we will therefore put the delay aspect aside in our treatment. Then, under some assumptions, a simplified Markovian description is still possible.

### 6.1 Measurement

#### 6.1.1 Projective measurements

The measurement postulate typically taught in quantum mechanics states that a measurement of some observable

$$\hat{O} = \sum_{\ell} O_{\ell} |\ell\rangle \langle \ell| = \sum_{\ell} O_{\ell} P_{\ell} \quad (6.1)$$

can yield only the eigenvalues of the observable  $O_{\ell}$ . This happens with probabilities  $p(\ell)$  that depend on the state  $|\Psi_0\rangle$  right before the measurement

$$p(\ell) = \langle \Psi_0 | P_{\ell} | \Psi_0 \rangle = |\langle \Psi_0 | \ell \rangle|^2, \quad (6.2)$$

and the state right after the measurement is the eigenstate of the observable corresponding to the outcome  $\ell$

$$|\Psi^{(\ell)}\rangle = \frac{P_{\ell} |\Psi_0\rangle}{\sqrt{p(\ell)}} = \frac{P_{\ell} |\Psi_0\rangle}{\|P_{\ell} |\Psi_0\rangle\|}. \quad (6.3)$$

Any initial (prior to the measurement) density matrix can be decomposed into a set of orthonormal states (spectral decomposition). Applying the above measurement postulate to each of

these states and afterwards averaging the outcome over the weights must yield the same result as the measurement recipe applied to the density matrix. The only possible choice is then, that the probability of the outcome  $\ell$  is given by

$$p(\ell) = \text{Tr} \{P_\ell \rho\} = \langle \ell | \rho | \ell \rangle , \quad (6.4)$$

and that after the measurement, the density matrix becomes

$$\rho^{(\ell)} = \frac{P_\ell \rho P_\ell}{\text{Tr} \{P_\ell \rho P_\ell\}} = \frac{P_\ell \rho P_\ell}{p(\ell)} . \quad (6.5)$$

It is clear that this is a very formal and effective description of a measurement, exemplified by some objections:

- It contains no mentioning of the properties of the detector: How should it be coupled to the system, how should it be read out etc.
- It does not describe measurement errors.
- When measuring the same observable again (without allowing for intermediate dynamics), one will obtain the same result with certainty. This follows from the projector property  $P_\ell^2 = P_\ell$ . A prominent consequence is that if such projective measurements are continuously performed, quantum systems are pinned to the initial outcome, a phenomenon known as **quantum Zeno effect**.
- The measurement does not take any time.

Below, we will introduce generalized (weak) measurements in an attempt to address some of these objections.

### 6.1.2 Weak measurements

By including the dynamics of a detector into the description and then applying the projective measurement postulate on the detector only, one obtains the dynamics of the reduced system, which on average corresponds to a Kraus map. We will first state the generalized measurement recipe [13] and then consider an example.

**Def. 22** (POVM measurements). *General quantum measurements are described by positive operator-valued measures (POVMs), which consist of a set of measurement operators  $\{M_m\}$  which obey*

$$\sum_m M_m^\dagger M_m = \mathbf{1} , \quad (6.6)$$

*and where  $m$  labels a particular outcome that occurs with probability*

$$p(m) = \text{Tr} \{M_m^\dagger M_m \rho\} , \quad (6.7)$$

*and leads to the conditional post-measurement density matrix*

$$\rho^{(m)} = \frac{M_m \rho M_m^\dagger}{p(m)} . \quad (6.8)$$

Obviously, when the measurement operators become projectors  $M_m \rightarrow P_m = |m\rangle\langle m|$ , we recover the previous measurement postulate.

The measurement recipe above can be understood fully by projective measurements, but in a joint Hilbert space composed of system and detector

$$H(t) = H_S + H_D + g(t)H_{SD} \quad (6.9)$$

with a dimensionless envelope function  $g(t)$  as follows:

- Before the measurement, system and detector are uncoupled  $g(t < 0) = 0$ , and the detector is in a defined state.
- The measurement begins with letting system and detector interact (ideally unitarily) for a duration  $\tau$  within which we have  $g(0 < t < \tau) \neq 0$ . During this stage, correlations (e.g. entanglement) can develop between system and detector.
- The measurement period is ended by a projective measurement on the Hilbert space of the detector, and afterwards system and detector are again decoupled  $g(t > \tau) = 0$ . The projective measurement of the detector only will have some effect on the system, which we want to formalize.

We will further simplify this scheme by assuming that the measurement process takes zero time (this can be lifted and is just done for simplicity). To achieve any effect then, this requires that the envelope function must diverge during the measurement, such that the effects of  $H_S$  and  $H_d$  during the correlation phase can be neglected

$$U_c \rightarrow e^{-i \int_0^\tau g(t) dt H_{sd}} = e^{-i\lambda H_{sd}}, \quad (6.10)$$

where the parameter  $\lambda$  describes the strength of the measurement.

As an example, we consider a qubit as the system and a harmonic oscillator as the detector, coupled by the interaction

$$H_{SD} = \frac{1}{2} [\mathbf{1} - \sigma^z] \otimes (a + a^\dagger). \quad (6.11)$$

The idea behind this coupling is that the detector should remain in its initial state when the system is initially in state  $|\uparrow\rangle$  and should be distributed all over its phase space when the system is initially in state  $|\downarrow\rangle$ . Here, we use the notation  $\sigma^z |\uparrow\rangle = +|\uparrow\rangle$  and  $\sigma^z |\downarrow\rangle = -|\downarrow\rangle$ . Thereby, by measuring the detector projectively, we also obtain information on the system. We prepare the detector prior to the measurement in its ground state

$$\rho(0^-) = \rho_S^0 \otimes |0\rangle\langle 0| \quad (6.12)$$

with  $a^\dagger a |0\rangle = 0$ . Under the assumptions of an instantaneous measurement as outlined before, the correlating unitary becomes

$$\begin{aligned} U_c &= e^{-i\lambda H_{sd}} = \mathbf{1} \otimes \mathbf{1} + \frac{1}{2} [\mathbf{1} - \sigma^z] \otimes \left( e^{-i\lambda(a+a^\dagger)} - \mathbf{1} \right) = \frac{1}{2} [\mathbf{1} + \sigma^z] \otimes \mathbf{1} + \frac{1}{2} [\mathbf{1} - \sigma^z] e^{-i\lambda(a+a^\dagger)} \\ &= |\uparrow\rangle\langle\uparrow| \otimes \mathbf{1} + |\downarrow\rangle\langle\downarrow| \otimes e^{-i\lambda(a+a^\dagger)}. \end{aligned} \quad (6.13)$$

After the correlation operation, the joint density matrix becomes

$$\begin{aligned}\rho(0^+) &= U_c \rho(0^-) U_c^\dagger \\ &= |\uparrow\rangle \langle \uparrow| \rho_S^0 |\uparrow\rangle \langle \uparrow| \otimes |0\rangle \langle 0| + |\downarrow\rangle \langle \downarrow| \rho_S^0 |\downarrow\rangle \langle \downarrow| \otimes e^{-i\lambda(a+a^\dagger)} |0\rangle \langle 0| e^{+i\lambda(a+a^\dagger)} \\ &\quad + |\uparrow\rangle \langle \uparrow| \rho_S^0 |\downarrow\rangle \langle \downarrow| \otimes |0\rangle \langle 0| e^{+i\lambda(a+a^\dagger)} + |\downarrow\rangle \langle \downarrow| \rho_S^0 |\uparrow\rangle \langle \uparrow| \otimes e^{-i\lambda(a+a^\dagger)} |0\rangle \langle 0|. \end{aligned} \quad (6.14)$$

Now, we can have many different measurement outcomes if we measure the number operator of the harmonic oscillator  $a^\dagger a = \sum_{n=0}^{\infty} n |n\rangle \langle n|$ . We get

$$\begin{aligned}M_0 \rho_S M_0^\dagger &= \text{Tr}_D \{ |0\rangle \langle 0| \rho(0^+) |0\rangle \langle 0| \} = \langle 0| \rho(0^+) |0\rangle \\ &= |\uparrow\rangle \langle \uparrow| \rho_S^0 |\uparrow\rangle \langle \uparrow| + |\downarrow\rangle \langle \downarrow| \rho_S^0 |\downarrow\rangle \langle \downarrow| e^{-\lambda^2} + |\uparrow\rangle \langle \uparrow| \rho_S^0 |\downarrow\rangle \langle \downarrow| e^{-\lambda^2/2} + |\downarrow\rangle \langle \downarrow| \rho_S^0 |\uparrow\rangle \langle \uparrow| e^{-\lambda^2/2}, \end{aligned} \quad (6.15)$$

where we have used that  $\langle 0| e^{i\lambda(a+a^\dagger)} |0\rangle = \langle 0| e^{i\lambda(a^\dagger+a)} |0\rangle = \langle 0| e^{+i\lambda a^\dagger} e^{+i\lambda a} e^{-1/2[i\lambda a^\dagger, i\lambda a]} |0\rangle = e^{-\lambda^2/2}$  and similar for  $\lambda \rightarrow -\lambda$ . With an analogous argument, we have

$$M_{n \geq 1} \rho_S M_{n \geq 1}^\dagger = \langle n| \rho(0^+) |n\rangle = |\downarrow\rangle \langle \downarrow| \rho_S^0 |\downarrow\rangle \langle \downarrow| \frac{\lambda^{2n} e^{-\lambda^2}}{n!}. \quad (6.16)$$

We can thereby identify the measurement operators

$$M_0 = |\uparrow\rangle \langle \uparrow| + e^{-\lambda^2/2} |\downarrow\rangle \langle \downarrow|, \quad M_{n \geq 1} = \frac{\lambda^n e^{-\lambda^2/2}}{\sqrt{n!}} |\downarrow\rangle \langle \downarrow|. \quad (6.17)$$

- Measuring outcome  $n \geq 1$ , the renormalized system density matrix is afterwards in state  $|\downarrow\rangle$ . The probability for this outcome is

$$p(n \geq 1) = \frac{\lambda^{2n} e^{-\lambda^2}}{n!} \langle \downarrow| \rho_S^0 |\downarrow\rangle, \quad (6.18)$$

which shows that this outcome can only occur if the initial state actually has a  $\downarrow$  component.

- In contrast, measuring  $n = 0$ , we might conclude that the initial state was  $|\uparrow\rangle$ , but this is not exact. There is an  $e^{-\lambda^2}$  probability that a subsequent direct measurement would actually yield the other result. The probability of this outcome is

$$p(0) = \langle \uparrow| \rho_S^0 |\uparrow\rangle + \langle \downarrow| \rho_S^0 |\downarrow\rangle e^{-\lambda^2} \quad (6.19)$$

Clearly, for  $\lambda \rightarrow \infty$  the erroneous contribution vanishes, and then this measurement outcome can occur only if the initial state has an  $\uparrow$  component.

Clearly, the measurement operators are not projectors. This implies that two subsequent measurements may yield different outcomes. Note also that one can explicitly show that

$$M_0^\dagger M_0 + \sum_{n \geq 1} M_n^\dagger M_n = |\uparrow\rangle \langle \uparrow| + |\downarrow\rangle \langle \downarrow| = \mathbf{1}. \quad (6.20)$$

## 6.2 External piecewise-constant feedback

Control means that in dependence of the particular measurement outcome  $m$ , we change some parameter of the system, which can be done in a variety of ways. Even if the original dynamics (without feedback) was Markovian, this will generally yield non-Markovian equations. Only in particular limits, another effectively Markovian description arises. We will here

- neglect a delay between measurement and control (this assumes that the processing of the measurement results is much faster than the internal system dynamics) and
- assume that control operations can be performed infinitely fast.

### 6.2.1 Repeated feedback operations

Closed-loop (or feedback) control means that the system is monitored (either continuously or at certain times) and that the result of these measurements is fed back by changing some parameter of the total system. Under measurement with outcome  $m$  (an index characterizing the possible outcomes), the density matrix transforms as

$$\rho \xrightarrow{m} \frac{M_m \rho M_m^\dagger}{\text{Tr} \{M_m^\dagger M_m \rho\}}, \quad (6.21)$$

and the probability at which this outcome occurs is given by  $p(m) = \text{Tr} \{M_m^\dagger M_m \rho\} = \text{Tr} \{M_m \rho M_m^\dagger\}$ . This can also be written in superoperator notation ( $\mathcal{M}_m \rho \hat{=} M_m \rho M_m^\dagger$ )

$$\rho \xrightarrow{m} \frac{\mathcal{M}_m \rho}{\text{Tr} \{\mathcal{M}_m \rho\}}. \quad (6.22)$$

Let us assume that conditioned on the measurement result  $m$  at time  $t$ , we apply a conditional Lindblad propagator  $\mathcal{L}_m$  for the time interval  $\Delta t$ . Then, a measurement result  $m$  at time  $t$  provided, the density matrix at time  $t + \Delta t$  will be given by

$$\rho^{(m)}(t + \Delta t) = e^{\mathcal{L}^{(m)} \Delta t} \frac{\mathcal{M}_m \rho}{\text{Tr} \{\mathcal{M}_m \rho(t)\}}. \quad (6.23)$$

However, to obtain an effective description of the density matrix evolution, we have to average over all measurement outcomes – where we have to weight each outcome by the corresponding probability

$$\rho(t + \Delta t) = \sum_m \text{Tr} \{\mathcal{M}_m \rho(t)\} e^{\mathcal{L}^{(m)} \Delta t} \frac{\mathcal{M}_m \rho(t)}{\text{Tr} \{\mathcal{M}_m \rho(t)\}} = \sum_m e^{\mathcal{L}^{(m)} \Delta t} \mathcal{M}_m \rho(t). \quad (6.24)$$

Note that this is an iteration scheme and not a conventional master equation. More generally – not constraining the conditioned dynamics to Lindblad evolutions – one could also write

$$\rho(t + \Delta t) = \sum_m \mathcal{K}^{(m)}(\Delta t) \mathcal{M}_m \rho(t), \quad (6.25)$$

where  $\mathcal{K}^{(m)}(\Delta t) \rho \hat{=} \sum_\alpha K_\alpha^{(m)}(\Delta t) \rho K_\alpha^{(m)\dagger}(\Delta t)$  with  $\sum_\alpha K_\alpha^{(m)\dagger} K_\alpha^{(m)} = \mathbf{1}$  is a conditioned Kraus map. Furthermore, the conditioned Liouvillian  $\mathcal{L}^{(m)}$  or the Kraus map  $\mathcal{K}^{(m)}$  may well depend on the time  $t$  (at which the measurement is performed) and on the width of the time interval  $\Delta t$ .

### 6.2.2 Continuous feedback limit

Expanding now the exponential of the Liouvillian in the limit of a continuous feedback control scheme  $\Delta t \rightarrow 0$ , we obtain

$$\rho(t + \Delta t) = \sum_m \mathcal{M}_m \rho(t) + \Delta t \sum_m \mathcal{L}_m \mathcal{M}_m \rho(t). \quad (6.26)$$

The problem is that in this expression – although  $\sum_m M_m^\dagger M_m = \mathbf{1}$  – we cannot simplify the first term on the r.h.s. since in general  $\sum_m \mathcal{M}_m \neq \mathbf{1}$ . Physically, this results from the fact that a quantum measurement always has an effect on the system – independent of whether conditioned control actions or not take place. Thereby, in general an effective Liouvillian under continuous feedback control does not exist, and the evolution is described rather by an iteration of the form (6.24) or (6.25). However, for projective measurements a weaker condition can be fulfilled, namely that the measurement superoperators have projector properties

$$\mathcal{M}_m \mathcal{M}_n = \mathcal{M}_m \delta_{mn}. \quad (6.27)$$

Acting with  $\sum_m \mathcal{M}_m$  from the left on Eq. (6.26), we can conclude that

$$\frac{\sum_m \mathcal{M}_m \rho(t + \Delta t) - \sum_m \mathcal{M}_m \rho(t)}{\Delta t} = \sum_{nm} \mathcal{M}_n \mathcal{L}_m \mathcal{M}_m \rho(t) = \sum_{nmk} \mathcal{M}_n \mathcal{L}_m \mathcal{M}_m \mathcal{M}_k \rho(t), \quad (6.28)$$

which we can turn into a master equation for the projected part of the density matrix

$$\dot{\tilde{\rho}}(t) = \sum_m \mathcal{M}_m \rho(t). \quad (6.29)$$

This defines an effective feedback master equation for projective measurements.

**Def. 23** (Feedback Liouvillian for projective measurements). *For projective measurements  $\mathcal{M}_m \mathcal{M}_n = \mathcal{M}_m \delta_{mn}$ , the projected density matrix  $\tilde{\rho} = \sum_n \mathcal{M}_n \rho$  obeys the feedback master equation*

$$\dot{\tilde{\rho}} = \mathcal{L}_{\text{fb}} \tilde{\rho}, \quad \mathcal{L}_{\text{fb}} = \sum_n \mathcal{M}_n \sum_m \mathcal{L}_m \mathcal{M}_m. \quad (6.30)$$

We note that  $\mathcal{L}_{\text{fb}}$  typically only acts in a particular subspace. When considered for the full system, it will formally become multistable. For example, expressing the measurements as  $\mathcal{M}_m \rho \hat{=} |m\rangle \langle m| \rho |m\rangle \langle m|$ , and one particular stationary state  $\mathcal{L}_{\text{fb}} \bar{\rho} = 0$ , we see that we can add arbitrary coherences  $\bar{\rho}' = \bar{\rho} + \sum_{n \neq m} \alpha_{nm} |n\rangle \langle m|$ , and will obtain another stationary state  $\mathcal{L}_{\text{fb}} \bar{\rho}' = 0$ , since these additional terms will vanish under the projective measurements. This distinction is formal, since after the first application of the effective feedback Liouvillian, the coherences will be gone, but needs to be taken into account when solving for stationary states.

### 6.2.3 Example: Feedback control of the SET

Quantum point contacts yield information on the occupation of nearby quantum dots. Idealizing this interaction as a projective measurement, we have

$$M_0 = |0\rangle \langle 0|, \quad M_1 = |1\rangle \langle 1|, \quad (6.31)$$

and when we vectorize the density matrix as  $(\rho_{00}, \rho_{11}, \rho_{01}, \rho_{10})^T$ , we obtain

$$\begin{aligned} \text{vec}(M_0 \rho M_0^\dagger) &= \mathcal{M}_0 \text{vec}(\rho) = \begin{pmatrix} 1 & 0 & 0 & 0 \\ 0 & 0 & 0 & 0 \\ 0 & 0 & 0 & 0 \\ 0 & 0 & 0 & 0 \end{pmatrix} \text{vec}(\rho), \\ \text{vec}(M_1 \rho M_1^\dagger) &= \mathcal{M}_1 \text{vec}(\rho) = \begin{pmatrix} 0 & 0 & 0 & 0 \\ 0 & 1 & 0 & 0 \\ 0 & 0 & 0 & 0 \\ 0 & 0 & 0 & 0 \end{pmatrix} \text{vec}(\rho), \end{aligned} \quad (6.32)$$

from which one can directly see that  $\mathcal{M}_0 + \mathcal{M}_1 \neq \mathbf{1}$ . However, for the single dot coherences are not relevant anyways, such that if we restrict ourselves as commonly done to the subspace of populations in the system energy eigenbasis, we recover a Markovian equation. The conditional generators for the SET are

$$\begin{aligned} \mathcal{L}_0 &= \left( \begin{array}{cc|cc} -\Gamma_L^0 f_L^0 - \Gamma_R^0 f_R^0 & +\Gamma_L^0(1-f_L^0) + \Gamma_R^0(1-f_R^0) & 0 & 0 \\ +\Gamma_L^0 f_L^0 + \Gamma_R^0 f_R^0 & -\Gamma_L^0(1-f_L^0) - \Gamma_R^0(1-f_R^0) & 0 & 0 \\ \hline 0 & 0 & \eta & 0 \\ 0 & 0 & 0 & \eta^* \end{array} \right), \\ \mathcal{L}_1 &= \left( \begin{array}{cc|cc} -\Gamma_L^1 f_L^1 - \Gamma_R^1 f_R^1 & +\Gamma_L^1(1-f_L^1) + \Gamma_R^1(1-f_R^1) & 0 & 0 \\ +\Gamma_L^1 f_L^1 + \Gamma_R^1 f_R^1 & -\Gamma_L^1(1-f_L^1) - \Gamma_R^1(1-f_R^1) & 0 & 0 \\ \hline 0 & 0 & \eta & 0 \\ 0 & 0 & 0 & \eta^* \end{array} \right), \end{aligned} \quad (6.33)$$

where the upper index denotes a conditional change of the tunnel rate or the dot level entering the Fermi function. Then, the definition 23 of the feedback Liouvillian yields

$$\mathcal{L}_{\text{fb}} = \left( \begin{array}{cc|cc} -\Gamma_L^0 f_L^0 - \Gamma_R^0 f_R^0 & +\Gamma_L^1(1-f_L^1) + \Gamma_R^1(1-f_R^1) & 0 & 0 \\ +\Gamma_L^0 f_L^0 + \Gamma_R^0 f_R^0 & -\Gamma_L^1(1-f_L^1) - \Gamma_R^1(1-f_R^1) & 0 & 0 \\ \hline 0 & 0 & 0 & 0 \\ 0 & 0 & 0 & 0 \end{array} \right), \quad (6.34)$$

i.e., as before populations and coherences evolve in a decoupled fashion – since measurement and dissipation both point to the system energy eigenbasis. Note that the population part

$$\mathcal{L}_{\text{fb}} = \begin{pmatrix} -\Gamma_L^0 f_L^0 - \Gamma_R^0 f_R^0 & +\Gamma_L^1(1-f_L^1) + \Gamma_R^1(1-f_R^1) \\ +\Gamma_L^0 f_L^0 + \Gamma_R^0 f_R^0 & -\Gamma_L^1(1-f_L^1) - \Gamma_R^1(1-f_R^1) \end{pmatrix} \quad (6.35)$$

does no longer obey detailed balance, which can lead to interesting consequences such as an apparent violation of the second law.

## 6.3 Wiseman-Milburn feedback

### 6.3.1 Dissipative control loops

A special case of the weak measurement feedback discussed before arises when we consider bipartite systems, composed of subsystems  $A$  and  $B$ , where we perform strong projective measurements only

on the subsystem  $B$ . From the perspective of the total system, such measurements will not be fully projective and will therefore appear as weak measurements. Let us therefore denote the density matrix of the compound system by

$$\sigma(t) = \sum_{nm} \rho^{(nm)}(t) \otimes |n\rangle \langle m|, \quad (6.36)$$

where the  $|n\rangle$  label a particular basis in the Hilbert space of subsystem  $B$ , and correspondingly,  $\rho^{(nm)}(t)$  is a conditional (not normalized) density matrix in subsystem  $A$ . Furthermore, we will assume that the diagonal conditional density matrices  $\rho^{(n)}(t) \equiv \rho^{(nn)}(t)$  follow a conditional master equation

$$\dot{\rho}^{(n)}(t) = \mathcal{L}_0 \rho^{(n)}(t) + \mathcal{L}_+ \rho^{(n-1)}(t) + \mathcal{L}_- \rho^{(n+1)}(t), \quad (6.37)$$

which occurs, for example, quite naturally in problems of Full Counting Statistics, cf. Sec. 3. In this case,  $n$  actually denotes the excitations counted in a detector, which may be, for example, the number of photons emitted by a cavity or the number of electrons that have passed through a quantum dot system or a QPC. We recall that given a decomposition in terms of counting fields, such an  $n$ -resolved master equation may be obtained by performing an inverse Fourier transform

$$\rho^{(n)}(t) = \frac{1}{2\pi} \int_{-\pi}^{+\pi} \rho(\chi, t) e^{-in\chi} d\chi, \quad (6.38)$$

and by tracing over the ancilla (detector) states we recover the density matrix of the system

$$\rho(t) = \text{Tr}_D \{ \sigma(t) \} = \sum_n \rho^{(n)}(t) = \rho(\chi, t)|_{\chi=0}. \quad (6.39)$$

Now, we take  $t$  as the initial time, and setting initially the detector to the defined state  $|0\rangle$ , we can write the initial total density matrix as  $\sigma(t) = \rho(t) \otimes |0\rangle \langle 0|$ , i.e., initially  $\rho^{(nm)}(t) = \delta_{n0} \delta_{m0} \rho(t)$ , which simply means that we have to reset our counting variable to zero after each measurement or that we use a new ancilla variable after every measurement. Then, we write the total density matrix at time  $t + \Delta t$  as (neglecting terms of order  $\Delta t^2$ )

$$\begin{aligned} \sigma(t + \Delta t) &= \sigma(t) + \Delta t \sum_{nm} \dot{\rho}^{(nm)}(t) \otimes |n\rangle \langle m| \\ &= \rho(t) \otimes |0\rangle \langle 0| + \Delta t \sum_n \dot{\rho}^{(n)}(t) \otimes |n\rangle \langle n| + \Delta t \sum_{n \neq m} \dot{\rho}^{(nm)}(t) \otimes |n\rangle \langle m| \\ &= \rho(t) \otimes |0\rangle \langle 0| + \Delta t \sum_n [\mathcal{L}_0 \rho^{(n)}(t) + \mathcal{L}_+ \rho^{(n-1)}(t) + \mathcal{L}_- \rho^{(n+1)}(t)] \otimes |n\rangle \langle n| \\ &\quad + \Delta t \sum_{n \neq m} \dot{\rho}^{(nm)}(t) \otimes |n\rangle \langle m| \\ &= \rho(t) \otimes |0\rangle \langle 0| + \Delta t [\mathcal{L}_0 \rho(t) \otimes |0\rangle \langle 0| + \mathcal{L}_+ \rho(t) \otimes | +1\rangle \langle +1| + \mathcal{L}_- \rho(t) \otimes | -1\rangle \langle -1|] \\ &\quad + \Delta t \sum_{n \neq m} \dot{\rho}^{(nm)}(t) \otimes |n\rangle \langle m|. \end{aligned} \quad (6.40)$$

Here, the neglect of higher-order terms means that we consider times  $\Delta t$  that are so short that at most a single particle can be detected in the detector. Now, we perform a projective measurement

of the ancilla (the particles counted by the detector) and compute the effective action of this process (dissipation plus subsequent measurement) on the reduced density matrix

$$\begin{aligned}\mathcal{M}_0(\Delta t)\rho(t) &\equiv \text{Tr}_D \{ |0\rangle \langle 0| \sigma(t + \Delta t) |0\rangle \langle 0| \} = [\mathbf{1} + \mathcal{L}_0 \Delta t] \rho(t), \\ \mathcal{M}_{-1}(\Delta t)\rho(t) &\equiv \text{Tr}_D \{ |-1\rangle \langle -1| \sigma(t + \Delta t) |-1\rangle \langle -1| \} = \mathcal{L}_- \Delta t \rho(t), \\ \mathcal{M}_{+1}(\Delta t)\rho(t) &\equiv \text{Tr}_D \{ |+1\rangle \langle +1| \sigma(t + \Delta t) |+1\rangle \langle +1| \} = \mathcal{L}_+ \Delta t \rho(t).\end{aligned}\quad (6.41)$$

We see that the effective propagation superoperators to lowest order indeed add up to the identity, regardless of the jump type. Here, this occurs as they also contain effects of dissipation.

The basic idea of Wiseman-Milburn feedback is now to perform an instantaneous unitary rotation right after the measurement outcome  $\pm$ :

$$\mathcal{U}_\pm \text{vec}(\rho) = \text{vec}(U_\pm \rho U_\pm^\dagger), \quad (6.42)$$

which can be implemented as a  $\delta$ -kick on the Hamiltonian  $U = e^{-iV}$ , just as with our discussion of the correlating unitary in measurements. Upon not measuring any change of the ancilla variable (the particle detector), no control action is performed. Consequently, the feedback iteration for the density matrix becomes

$$\begin{aligned}\rho(t + \Delta t) &= [\mathcal{M}_0(\Delta t) + \mathcal{U}_- \mathcal{M}_-(\Delta t) + \mathcal{U}_+ \mathcal{M}_+(\Delta t)] \rho(t) \\ &= [\mathbf{1} + \Delta t (\mathcal{L}_0 + \mathcal{U}_+ \mathcal{L}_+ + \mathcal{U}_- \mathcal{L}_-)] \rho(t),\end{aligned}\quad (6.43)$$

which yields the Wiseman-Milburn feedback Liouvillian [6].

**Def. 24** (Wisemen-Milburn feedback Liouvillian). *For a Lindblad Liouvillian decomposable as  $\mathcal{L} = \mathcal{L}_+ + \mathcal{L}_- + \mathcal{L}_0$ , the Wiseman-Milburn Liouvillian reads*

$$\mathcal{L}_{\text{fb}} = \mathcal{L}_0 + \mathcal{U}_+ \mathcal{L}_+ + \mathcal{U}_- \mathcal{L}_-, \quad (6.44)$$

where  $\mathcal{U}_\pm \rho \hat{=} U_\pm \rho U_\pm^\dagger$  denotes the unitary control action and  $\mathcal{L}_\pm$  the jump terms associated with particle increase (+) or decrease (-) in the detector.

The major difference in the derivation in comparison to the previous section was that we assumed that the measurement could take finite time to complete. During this time, dissipation acts on the measured system even in absence of any control actions.

A potential application of this scheme lies in the stabilization of pure states. Whereas a conventional Lindbladian evolution

$$\dot{\rho} = -i[H, \rho] + \sum_\alpha \gamma_\alpha \left[ L_\alpha \rho L_\alpha^\dagger - \frac{1}{2} \{ L_\alpha^\dagger L_\alpha, \rho \} \right] \quad (6.45)$$

will normally lead to a highly mixed stationary state  $\bar{\rho}^2 \neq \bar{\rho}$ , a feedback-controlled Lindbladian evolution is described by

$$\begin{aligned}\dot{\rho} &= -i[H, \rho] + \sum_\alpha \gamma_\alpha \left[ U_\alpha L_\alpha \rho L_\alpha^\dagger U_\alpha^\dagger - \frac{1}{2} \{ L_\alpha^\dagger L_\alpha, \rho \} \right] \\ &= -i \underbrace{\left[ H - i \sum_\alpha \frac{\gamma_\alpha}{2} L_\alpha^\dagger L_\alpha \right]}_{H_{\text{eff}}} \rho + i \rho \underbrace{\left[ H + i \sum_\alpha \frac{\gamma_\alpha}{2} L_\alpha^\dagger L_\alpha \right]}_{H_{\text{eff}}^\dagger} + \sum_\alpha \gamma_\alpha U_\alpha L_\alpha \rho L_\alpha^\dagger U_\alpha^\dagger,\end{aligned}\quad (6.46)$$

where in the last line we have defined an effective non-hermitian Hamiltonian. This rewriting has the advantage that we can now aim to find unitary control operations  $U_\alpha$  that may stabilize the particular eigenstates of  $H_{\text{eff}} |\Psi\rangle = \epsilon |\Psi\rangle$  with  $\epsilon \in \mathbb{C}$ , such that the stationary state becomes  $\bar{\rho} = |\Psi\rangle \langle \Psi|$ . Inserting this pure state yields the condition

$$0 = -i\epsilon |\Psi\rangle \langle \Psi| + i\epsilon^* |\Psi\rangle \langle \Psi| + \sum_{\alpha} \gamma_{\alpha} U_{\alpha} L_{\alpha} |\Psi\rangle \langle \Psi| L_{\alpha}^{\dagger} U_{\alpha}^{\dagger}. \quad (6.47)$$

The unitary control can now be chosen such that  $U_{\alpha} L_{\alpha} |\Psi\rangle = \sigma_{\alpha} |\Psi\rangle$  with some complex number  $\sigma_{\alpha}$ , and the condition for stabilization then becomes  $2\Im(\epsilon) + \sum_{\alpha} \gamma_{\alpha} |\sigma_{\alpha}|^2 = 0$ .

### 6.3.2 Application: Stabilization of Fock states

We start from the master equation of a cavity coupled to a thermal bath

$$\begin{aligned} \dot{\rho} = & -i [\Omega a^{\dagger} a, \rho] \\ & + \Gamma(1 + n_B) \left[ e^{+i\chi} a \rho a^{\dagger} - \frac{1}{2} \{a^{\dagger} a, \rho\} \right] + \Gamma n_B \left[ e^{-i\chi} a^{\dagger} \rho a - \frac{1}{2} \{a a^{\dagger}, \rho\} \right], \end{aligned} \quad (6.48)$$

which we have already presented in Sec. 1.2.2, and which is here just equipped with an additional counting field  $\chi$  for the number of emitted or absorbed photons. Without any measurements and feedback, the stationary state of this master equation is just a statistical mixture of energy eigenstates. In particular at large temperatures, this is not a pure state but highly mixed.

Now, acting with different unitary operations whenever a photon is emitted  $U_+$  (simple detection with a click of a photo-detector) or absorbed from the system (this is more difficult, we would need to shine light on the system and then infer the absorption from the absence of a click in a photodetector placed on the other side), we would obtain the effective feedback master equation

$$\begin{aligned} \dot{\rho} = & -i [\Omega a^{\dagger} a, \rho] \\ & + \Gamma(1 + n_B) \left[ U_+ a \rho a^{\dagger} U_+^{\dagger} - \frac{1}{2} \{a^{\dagger} a, \rho\} \right] + \Gamma n_B \left[ U_- a^{\dagger} \rho a U_-^{\dagger} - \frac{1}{2} \{a a^{\dagger}, \rho\} \right] \\ = & -i H_{\text{eff}} \rho + i \rho H_{\text{eff}}^{\dagger} + \Gamma(1 + n_B) U_+ a \rho a^{\dagger} U_+^{\dagger} + \Gamma n_B U_- a^{\dagger} \rho a U_-^{\dagger}, \end{aligned} \quad (6.49)$$

where we have defined the effective **non-Hermitian Hamiltonian**

$$H_{\text{eff}} = \Omega a^{\dagger} a - i \frac{\Gamma}{2} (1 + n_B) a^{\dagger} a - i \frac{\Gamma}{2} n_B a a^{\dagger}. \quad (6.50)$$

Clearly, the Fock states are eigenstates of  $H_{\text{eff}}$

$$\begin{aligned} H_{\text{eff}} |m\rangle & = \left[ \Omega m - i \frac{\Gamma}{2} (1 + n_B) m - i \frac{\Gamma}{2} n_B (1 + m) \right] |m\rangle = \epsilon_m |m\rangle, \\ \langle m| H_{\text{eff}}^{\dagger} & = \langle m| \left[ \Omega m + i \frac{\Gamma}{2} (1 + n_B) m + i \frac{\Gamma}{2} n_B (1 + m) \right] = \epsilon_m^* \langle m|. \end{aligned} \quad (6.51)$$

We can now ask what unitary operations one needs to apply to stabilize a particular particle number eigenstate  $\bar{\rho} = |m\rangle \langle m|$ . Inserting this in the master equation yields the condition

$$\begin{aligned} 0 = & [-\Gamma(1 + n_B) m - \Gamma n_B (1 + m)] |m\rangle \langle m| \\ & + \Gamma(1 + n_B) m U_+ |m-1\rangle \langle m-1| U_+^{\dagger} + \Gamma n_B (m+1) U_- |m+1\rangle \langle m+1| U_-^{\dagger}, \end{aligned} \quad (6.52)$$

which can be fulfilled by unitary control operations obeying

$$U_+ |m - 1\rangle = |m\rangle , \quad U_- |m + 1\rangle = |m\rangle . \quad (6.53)$$

There are many unitaries fulfilling this condition, but their actual implementation may be hard, in particular if only a selected Fock state is to be stabilized. Generally, the decomposition into an effective non-hermitian Hamiltonian and its eigenstates may be helpful to find suitable control actions for obtaining pure stationary states [39].



# Chapter 7

## Selected applications

### 7.1 An electronic Maxwell demon: External feedback

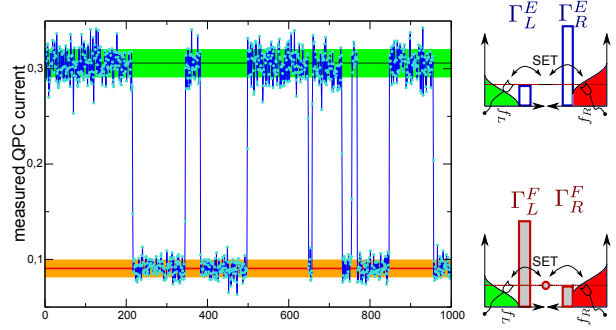
Maxwell invented his famous demon as a thought experiment to demonstrate that thermodynamics is a macroscopic effective theory: An intelligent being (the demon) living in a box is measuring the speed of molecules of some gas in the box. An initial thermal distribution of molecules implies that the molecules have different velocities. The demon measures the velocities and inserts an impermeable wall whenever the the molecule is too fast or lets it pass into another part of the box when it is slow. As time progresses, this would lead to a sorting of hot and cold molecules, and the temperature difference could be exploited to perform work.

This is nothing but a feedback (closed-loop) control scheme: The demon performs a measurement (is the molecule slow or fast) and then uses the information to perform an appropriate control action on the system (inserting a wall or not). Classically, the insertion of a wall requires in the idealized case no work, such that only information is used to create a temperature gradient. However, the Landauer principle states that with each bit of information erased, heat of at least  $k_B T \ln(2)$  is dissipated into the environment. To remain functionable, the demon must at some point start to delete the information, which leads to the dissipation of heat. The dissipated heat will exceed the energy obtainable from the thermal gradient.

#### 7.1.1 Phenomenology of an electronic setup

An analog of a Maxwell demon may be implemented in an electronic context: There, an experimentalist takes the role of the demon. The box is replaced by the SET (including the contacts), on which by a nearby QPC a measurement of the dot state (simply empty or filled) is performed. Depending on the measurement outcome, the tunneling rates are modified in time in a piecewise constant manner: When there is no electron on the dot, the left tunneling rate  $\Gamma_L$  is increased (low barrier) and the right tunneling rate  $\Gamma_R$  is decreased (high barrier). The opposite is done when there is an electron on the dot, see Fig. 7.1. Thus, the only difference in comparison to the previous chapter is that now **information of the system state is used to modify the tunneling rates**. Very simple considerations already demonstrate that with this scheme, it will be possible to transport electrons against an existing bias only with time-dependent tunneling rates. When one junction is completely decoupled  $\Gamma_{L/R}^{\min} \rightarrow 0$ , this will completely rectify the transport from left to right also against the bias (if the bias is finite). In the following, we will address the statistics of this device.

Figure 7.1: Sketch of the feedback scheme: For a filled dot (low QPC current), the left tunneling rate is minimal and the right tunneling rate is maximal and vice-versa for an empty dot. The dot level itself is not changed.



We have already derived the effective master equation under continuous feedback control in Eq. (6.35). Taking only the populations of the monitored dot into account, the effective Liouvillian under feedback has the first column from the Liouvillian conditioned on an empty dot and the second column from the Liouvillian conditioned on the filled dot

$$\mathcal{L}_{\text{eff}}(\chi_L, \chi_R) = \begin{pmatrix} -\Gamma_L^E f_L - \Gamma_R^E f_R & +\Gamma_L^F(1-f_L)e^{+i\chi_L} + \Gamma_R^F(1-f_R)e^{+i\chi_R} \\ +\Gamma_L^E f_L e^{-i\chi_L} + \Gamma_R^E f_R e^{-i\chi_R} & -\Gamma_L^F(1-f_L) - \Gamma_R^F(1-f_R) \end{pmatrix}. \quad (7.1)$$

Evidently, it still obeys trace conservation but now the tunneling rates in the two columns are different ones.

**Exercise 34** (Current at zero bias). (1 points)

Calculate the feedback-current at zero bias  $f_L = f_R = f$  in dependence on  $f$ . What happens at zero temperatures, where  $f \rightarrow \{0, 1\}$ ?

The effective Liouvillian describes the average evolution of trajectories under continuous monitoring and feedback. The validity of the effective description can be easily checked by calculating Monte-Carlo solutions as follows:

Starting e.g. with a filled dot, the probability to jump out e.g. to the right lead during the small time interval  $\Delta t$  reads  $P_{\text{out,R}}^{(F)} = \Gamma_R^F(1-f_R)\Delta t$ . Similarly, we can write down the probabilities to jump out to the left lead and also the probabilities to jump onto an empty dot from either the left or right contact

$$\begin{aligned} P_{\text{out,R}}^{(F)} &= \Gamma_R^F(1-f_R)\Delta t, & P_{\text{out,L}}^{(F)} &= \Gamma_L^F(1-f_L)\Delta t, \\ P_{\text{in,R}}^{(E)} &= \Gamma_R^E f_R \Delta t, & P_{\text{in,L}}^{(E)} &= \Gamma_L^E f_L \Delta t. \end{aligned} \quad (7.2)$$

Naturally, these jump probabilities also uniquely determine the change of the particle number on either contact. The remaining probability is simply the one that no jump occurs during  $\Delta t$ . A Monte-Carlo simulation is obtained by randomly drawing one out of three possible outcomes with the appropriate probabilities. For example, when the dot is empty, we can jump in from left contact, from the right contact, or remain empty. Alternatively, when the dot is filled, we can jump out to the left contact, to the right contact, or remain filled. Updating the dot state and the left and right particle numbers accordingly then by repeating the procedure several times yields a single trajectory for  $n(t)$ ,  $n_L(t)$ , and  $n_R(t)$ . The ensemble average of many such trajectories agrees

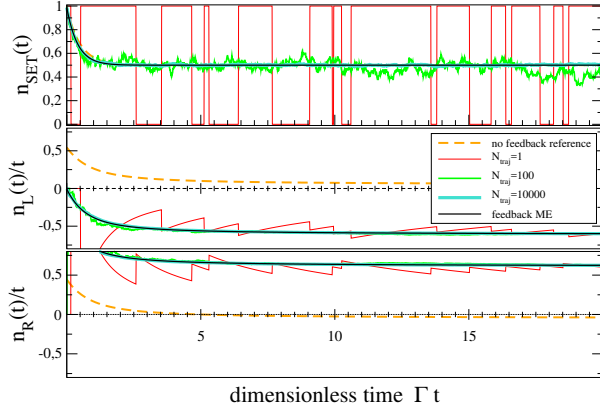


Figure 7.2: Comparison of a single (thin red curve with jumps, same realization in all panels) and the average of 100 (medium thickness, green) and 10000 (bold smooth curve, turquoise) trajectories with the solution from the effective feedback master equation (thin black) for the dot occupation (top), the number of particles on the left (middle), and the number of particles on the right (bottom). The average of the trajectories converges to the effective feedback master equation result. The reference curve without feedback (dashed orange) may be obtained by using vanishing feedback parameters and demonstrates that the direction of the current may actually be reversed via sufficiently strong feedback. Parameters:  $\Gamma_L = \Gamma_R \equiv \Gamma$ ,  $f_L = 0.45$ ,  $f_R = 0.55$ ,  $\delta_L^E = \delta_R^F = 1.0$ ,  $\delta_R^E = \delta_L^F = -10.0$ , and  $\Gamma\Delta t = 0.01$ .

perfectly with the solution of the effective feedback master equation

$$\begin{aligned}
 \langle n \rangle_t &= \text{Tr} \{ d^\dagger d e^{\mathcal{L}_{\text{eff}}(0,0)t} \rho_0 \}, \\
 \langle n_L \rangle_t &= (-i\partial_\chi) \text{Tr} \{ e^{\mathcal{L}_{\text{eff}}(\chi,0)t} \rho_0 \} \Big|_{\chi=0}, \\
 \langle n_R \rangle_t &= (-i\partial_\chi) \text{Tr} \{ e^{\mathcal{L}_{\text{eff}}(0,\chi)t} \rho_0 \} \Big|_{\chi=0},
 \end{aligned} \tag{7.3}$$

see Fig. 7.2. To compare with the case without feedback, we parametrize the change of tunneling rates by dimensionless constants

$$\Gamma_L^E = e^{\delta_L^E} \Gamma_L, \quad \Gamma_R^E = e^{\delta_R^E} \Gamma_R, \quad \Gamma_L^F = e^{\delta_L^F} \Gamma_L, \quad \Gamma_R^F = e^{\delta_R^F} \Gamma_R, \tag{7.4}$$

where  $\delta_\alpha^\beta \rightarrow 0$  reproduces the case without feedback and  $\delta_\alpha^\beta > 0 (< 0)$  increases (decreases) the tunneling rate to contact  $\alpha$  conditioned on dot state  $\beta$ . The general current can directly be calculated as

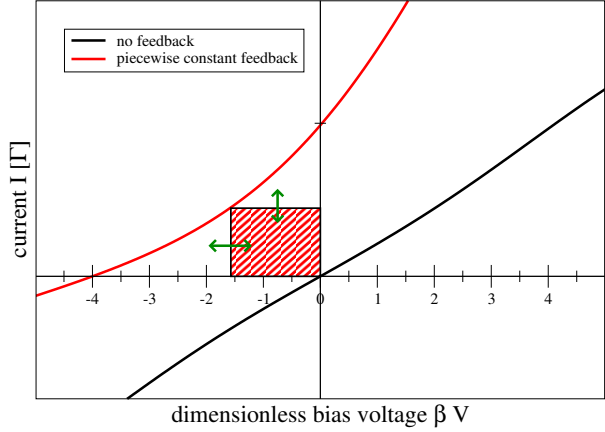
$$I = \frac{f_L(1-f_R)\Gamma_L^E\Gamma_R^F - (1-f_L)f_R\Gamma_L^F\Gamma_R^E}{\Gamma_L^E f_L + \Gamma_L^F(1-f_L) + \Gamma_R^E f_R + \Gamma_R^F(1-f_R)}, \tag{7.5}$$

which reduces to the conventional current (2.41) without feedback when  $\Gamma_\alpha^\beta \rightarrow \Gamma_\alpha$ . For finite feedback strength however, this will generally induce a non-vanishing current at zero bias, see Fig. 7.3. In our idealized setup, this current is only generated by the information on whether the dot is occupied or empty – hence the interpretation as a Maxwell demon. When the contacts are held at equal temperatures  $\beta_L = \beta_R = \beta$ , this raises the question for the maximum power

$$P = -IV = -I(\mu_L - \mu_R) \tag{7.6}$$

generated by the device.

Figure 7.3: Current voltage characteristics for finite feedback strength  $\delta = 1$  (red curve) and without feedback  $\delta = 0$  (black curve). For finite feedback, the current may point in the other direction than the voltage leading to a positive power  $P = -IV$  (shaded region) generated by the device.



In what follows, we will consider symmetric feedback characterized by a single parameter

$$\delta_L^E = \delta_R^F = -\delta_L^F = -\delta_R^E = +\delta, \quad (7.7)$$

where  $\delta > 0$  favors transport from left to right and  $\delta < 0$  transport from right to left and also symmetric bare tunneling rates  $\Gamma = \Gamma_L = \Gamma_R$ . With these assumptions, it is easy to see that for large feedback strengths  $\delta \gg 1$ , the current simply becomes

$$I \rightarrow \Gamma e^\delta \frac{f_L(1-f_R)}{f_L + (1-f_R)}. \quad (7.8)$$

To determine the maximum power, we would have to maximize with respect to left and right chemical potentials  $\mu_L$  and  $\mu_R$ , the lead temperature  $\beta$  and the dot level  $\epsilon$ . However, as these parameters only enter implicitly in the Fermi functions, it is more favorable to use that for equal temperatures

$$\beta(\mu_L - \mu_R) = \beta V = \ln \left[ \frac{f_L(1-f_R)}{(1-f_L)f_R} \right], \quad (7.9)$$

such that we can equally maximize

$$P = -IV = \frac{1}{\beta}(-I\beta V) \rightarrow \frac{\Gamma e^\delta}{\beta} \left[ -\frac{f_L(1-f_R)}{f_L + (1-f_R)} \ln \left( \frac{f_L(1-f_R)}{(1-f_L)f_R} \right) \right]. \quad (7.10)$$

The term in square brackets can now be maximized numerically with respect to the parameters  $f_L$  and  $f_R$  in the range  $0 \leq f_{L/R} \leq 1$ , such that one obtains for the maximum power at strong feedback

$$P \leq k_B T \Gamma e^\delta 0.2785 \quad \text{at} \quad f_L = 0.2178 \quad f_R = 0.7822. \quad (7.11)$$

The average work extracted from the SET circuit between two QPC measurement points at  $t$  and  $t + \Delta t$  is therefore given by

$$\langle W \rangle \leq k_B T \Gamma e^\delta \Delta t 0.2785. \quad (7.12)$$

We can contrast this with the heat dissipated in the QPC circuit to perform the measurement. Naively, to perform feedback efficiently, it is required that the QPC sampling rate is fast enough

that all state changes of the SET are faithfully detected (no tunneling charges are missed). This requires that  $\Gamma e^\delta \Delta t < 1$ . Therefore, we can refine the upper bound for the average work

$$W \leq k_B T 0.2785. \quad (7.13)$$

This has to be contrasted with the Landauer principle, which states that for each deleted bit in the demon's brain (each QPC data point encoding high current or low current) heat of

$$Q \geq k_B T \ln(2) \approx k_B T 0.6931 \quad (7.14)$$

is dissipated. These rough estimates indicate that the second law does not appear to be violated.

Finally, we use our knowledge of Full Counting Statistics to investigate the fluctuation theorem. The conventional fluctuation theorem for the SET at equal temperatures

$$\frac{P_{+n}(t)}{P_{-n}(t)} = e^{n\beta V} \quad (7.15)$$

is modified in presence of feedback. Since the Liouvillian still contains the counting fields in the conventional way, simply the factor in the exponential, but not the dependence on the number of tunneled electrons  $n$  is changed. To evaluate the FT, we identify symmetries in the cumulant-generating function (or alternatively the eigenvalues of the Liouvillian)

$$\begin{aligned} \lambda(-\chi) &= \lambda \left( +\chi + i \ln \left[ \frac{\Gamma_L^E \Gamma_R^F f_L (1 - f_R)}{\Gamma_L^F \Gamma_R^E (1 - f_L) f_R} \right] \right) \\ &= \lambda \left( +\chi + i \ln \left[ e^{+4\delta} \frac{f_L (1 - f_R)}{(1 - f_L) f_R} \right] \right) = \lambda \left( +\chi + i \ln [e^{+4\delta} e^{\beta V}] \right) \\ &= \lambda(+\chi + i(4\delta + \beta V)). \end{aligned} \quad (7.16)$$

**Exercise 35** (Fluctuation theorem under feedback). *Show the validity of this equation.*

From this symmetry of the cumulant-generating function we obtain for the fluctuation theorem under feedback

$$\lim_{t \rightarrow \infty} \frac{P_{+n}(t)}{P_{-n}(t)} = e^{n(\beta V + 4\delta)} = e^{n\beta(V - V^*)}, \quad (7.17)$$

where  $V^* = -4\delta/\beta$  denotes the voltage at which the current (under feedback) vanishes.

If our previous investigations we had found that the fluctuation theorems are related to the entropy production. Now, in addition to the expected entropy production  $\Delta_i S = n\beta V$  we find an additional contribution, which one could – lacking a microscopic description of the feedback mechanism – interpret as an information term modifying the entropy balance of the system in presence of feedback.

**Exercise 36** (Vanishing feedback current). *(1 points)*

*Show for equal temperatures that the feedback current vanishes when  $V = V^* = -4\delta/\beta$ .*

The fact that the estimates concerning the second law are rather vague result from the missing physical implementation of the control loop. In our model, it could be anything, even represented by a human being pressing a button whenever the QPC current changes. The entropy produced by such a humanoid implementation of the control loop would by far exceed the local entropy reduction manifested by a current running against the bias. Below, we will therefore investigate these questions in greater detail.

### 7.1.2 Conventional entropy production in rate equations

In this section, we will mathematically treat rate equations of the form

$$\dot{P}_a = \sum_{\nu} \sum_b W_{ab}^{(\nu)} P_b, \quad (7.18)$$

where for  $a \neq b$  the quantity  $W_{ab}^{(\nu)}$  is the transition rate from state  $b$  to state  $a$  and  $\nu$  denotes a reservoir which triggers the particular transition. Naturally, conservation of probabilities implies that  $\sum_a W_{ab}^{(\nu)} = 0$  for all  $a$  and for each reservoir  $\nu$ , such that the diagonal elements are fixed via

$$W_{aa}^{(\nu)} = - \sum_{b \neq a} W_{ba}^{(\nu)}. \quad (7.19)$$

Having in mind that each reservoir is kept at a local equilibrium state, we also postulate the existence of a local detailed balance condition for each reservoir. This implies that the ratio of forward and backward transition rates between states  $i$  and  $j$  that are triggered by reservoir  $\nu$  obey

$$\frac{W_{ji}^{(\nu)}}{W_{ij}^{(\nu)}} = e^{-\beta_{\nu}[(E_j - E_i) - \mu_{\nu}(N_j - N_i)]}, \quad (7.20)$$

where  $\beta_{\nu}$  and  $\mu_{\nu}$  denote inverse temperature and chemical potential of the corresponding reservoir, and  $E_i$  and  $N_i$  denote energy and particle number of the state  $i$ , respectively. The above relation follows naturally from the extension of the KMS condition to systems with chemical potentials and is – as we have seen – automatically fulfilled for a large number of microscopically derived models.

Then, the Shannon entropy of the system

$$S(t) = - \sum_i P_i(t) \ln P_i(t) \quad (7.21)$$

obeys the balance equation

$$\begin{aligned} \dot{S} &= - \frac{d}{dt} \sum_i P_i \ln P_i = - \sum_i \dot{P}_i \ln P_i \\ &= - \sum_{ij} \sum_{\nu} W_{ij}^{(\nu)} P_j \ln \left( P_i \frac{W_{ji}^{(\nu)}}{P_j W_{ij}^{(\nu)}} \frac{P_j W_{ij}^{(\nu)}}{W_{ji}^{(\nu)}} \right) \\ &= + \sum_{ij} \sum_{\nu} W_{ij}^{(\nu)} P_j \ln \left( \frac{W_{ij}^{(\nu)} P_j}{W_{ji}^{(\nu)} P_i} \right) + \sum_{ij} \sum_{\nu} W_{ij}^{(\nu)} P_j \ln \left( \frac{W_{ji}^{(\nu)}}{W_{ij}^{(\nu)}} \frac{1}{P_j} \right) \\ &= + \underbrace{\sum_{ij} \sum_{\nu} W_{ij}^{(\nu)} P_j \ln \left( \frac{W_{ij}^{(\nu)} P_j}{W_{ji}^{(\nu)} P_i} \right)}_{\geq 0} + \sum_{ij} \sum_{\nu} W_{ij}^{(\nu)} P_j \underbrace{\ln \left( \frac{W_{ji}^{(\nu)}}{W_{ij}^{(\nu)}} \right)}_{-\beta_{\nu}[(E_j - E_i) - \mu_{\nu}(N_j - N_i)]}. \end{aligned} \quad (7.22)$$

In the above lines, we have simply used trace conservation  $\sum_i W_{ij}^{(\nu)} = 0$  and finally the local detailed balance property (7.20). This property enables us to identify in the long-term limit the second term as energy and matter currents. When multiplied by the inverse temperature of the corresponding reservoir, they would combine to an entropy flow, which motivates the definition below.

**Def. 25** (Entropy Flow). *For a rate equation satisfying detailed balance, the entropy flow from reservoir  $\nu$  is defined as*

$$\begin{aligned} \dot{S}_e^{(\nu)} &= \sum_{ij} W_{ij}^{(\nu)} P_j \ln \frac{W_{ji}^{(\nu)}}{W_{ij}^{(\nu)}} = + \sum_{ij} W_{ij}^{(\nu)} P_j [-\beta_\nu [(E_j - E_i) - \mu_\nu (N_j - N_i)]] \\ &= \beta_\nu \left( I_E^{(\nu)} - \mu_\nu I_M^{(\nu)} \right), \end{aligned} \quad (7.23)$$

where energy currents  $I_E^{(\nu)}$  and matter currents  $I_M^{(\nu)}$  associated to reservoir  $\nu$  count positive when entering the system.

The remaining contribution corresponds to a production term [40]. We note that it is always positive, which can be deduced from the formal similarity to the Kullback-Leibler divergence of two probability distributions or – more directly – using the Logarithmic Sum Inequality.

**Exercise 37** (Logarithmic Sum Inequality). *Show that for non-negative  $a_i$  and  $b_i$*

$$\sum_{i=1}^n a_i \ln \frac{a_i}{b_i} \geq a \ln \frac{a}{b}$$

with  $a = \sum_i a_i$  and  $b = \sum_i b_i$ .

Its positivity is perfectly consistent with the second law of thermodynamics, and we therefore identify the remaining contribution as entropy production.

**Def. 26** (Entropy Production). *For a rate equation, the irreversible entropy production is defined as*

$$\dot{S}_i = \sum_{ij} \sum_{\nu} W_{ij}^{(\nu)} P_j \ln \left( \frac{W_{ij}^{(\nu)} P_j}{W_{ji}^{(\nu)} P_i} \right) \geq 0. \quad (7.24)$$

*It is always positive and at steady state balanced by the entropy flow.*

Using the positivity of the entropy production rate, we obtain the global second law

$$\dot{S} - \sum_{\nu} \beta_\nu \left( I_E^{(\nu)} - \mu_\nu I_M^{(\nu)} \right) \geq 0. \quad (7.25)$$

From classical thermodynamics for a reservoir in equilibrium, we have

$$dU = TdS - pdV + \mu dN, \quad (7.26)$$

which for a reservoir with  $dV = 0$  can be solved for  $dS = \frac{1}{T}dU - \frac{1}{T}\mu dN = \beta dU - \beta\mu dN$ , where we have used that in our units  $k_B = 1$ . Applying this to every reservoir, we see that with the convention  $\frac{dU}{dt} \rightarrow -I_E^{(\nu)}$  and  $\frac{dN}{dt} \rightarrow -I_M^{(\nu)}$ , the second term is actually the total entropy produced in the reservoirs.

When the dimension of the system's Hilbert space is finite and the rate equation approaches a stationary state, its Shannon entropy will also approach a constant value  $\dot{S} = 0$ . Therefore, at steady state the entropy production in the system must be balanced by the entropy flow through its terminals

$$\dot{S}_i = -\dot{S}_e = -\sum_{\nu} \beta_{\nu} \left( I_E^{(\nu)} - \mu_{\nu} I_M^{(\nu)} \right). \quad (7.27)$$

The above formula conveniently relates the entropy production to energy and matter currents from the terminals into the system. Evidently, the entropy production is thus related to heat currents  $\dot{Q}^{(\nu)} = I_E^{(\nu)} - \mu_{\nu} I_M^{(\nu)}$ , which can be determined from a master equation by means of the Full Counting Statistics.

Below, we will show that the above definitions are consistent with what we had before when the Liouville superoperators  $\mathcal{L}^{(\nu)}$  have a block structure separating the evolution of coherences and populations, i.e., when in the energy eigenbasis we have

$$H|i\rangle = E_i|i\rangle, \quad N|i\rangle = N_i|i\rangle, \quad \langle i|\mathcal{L}^{(\nu)}\rho|i\rangle = \sum_j W_{ij}^{(\nu)} \langle j|\rho|j\rangle. \quad (7.28)$$

For this, it is helpful to note that the trace of a product of two matrices can be written as terms only arising from products of the diagonal terms and terms composed of products from off-diagonal terms

$$\text{Tr}\{AB\} = \sum_{i,j} A_{ij}B_{ji} = \sum_i A_{ii}B_{ii} + \sum_{i \neq j} A_{ij}B_{ji}, \quad (7.29)$$

which also implies that traces of products of a diagonal matrix  $A$  and an off-diagonal matrix  $B$  will always vanish.

For a full Lindblad master equation we defined the energy current entering the system in Eq. (2.14). It can be written as (we drop for simplicity all time dependencies)

$$\begin{aligned} I_E^{(\nu)} &= \text{Tr}\{H(\mathcal{L}^{(\nu)}\rho)\} = \sum_i E_i(\mathcal{L}^{(\nu)}\rho)_{ii} = \sum_{ij} E_i W_{ij}^{(\nu)} \rho_{jj} \\ &= \sum_{i \neq j} E_i W_{ij}^{(\nu)} \rho_{jj} - \sum_{i \neq j} E_i W_{ji}^{(\nu)} \rho_{ii} = \sum_{ij} (E_i - E_j) W_{ij}^{(\nu)} \rho_{jj}, \end{aligned} \quad (7.30)$$

which is the same as the energy current based on the rate equation when we identify  $P_j = \rho_{jj}$ . In complete analogy, we find for the matter current defined in Eq. (2.16)

$$I_M^{(\nu)} = \text{Tr}\{N(\mathcal{L}^{(\nu)}\rho)\} = \sum_{ij} (N_i - N_j) W_{ij}^{(\nu)} \rho_{jj}. \quad (7.31)$$

This proves that the definitions for the currents based on the rate equation and on the master equation coincide when the master equation assumes block form separating coherences and populations in the system energy eigenbasis, as is known for the BMS limit, cf. Def. 6.

Now, we consider the entropy production rate defined in Eq. (2.28)

$$\dot{S}_i^{\text{Sp}} = - \sum_{\nu} \text{Tr} \{ [\mathcal{L}^{(\nu)} \rho] [\ln \rho - \ln \bar{\rho}^{(\nu)}] \} = \sum_{\nu} \dot{S}_i^{\text{Sp}, \nu}. \quad (7.32)$$

For simplicity of notation, we introduce the projection to the diagonal elements of the matrix  $A$  in the system energy eigenbasis as a superoperator

$$\mathcal{P}A = \sum_i |i\rangle \langle i| A |i\rangle \langle i|. \quad (7.33)$$

From this, we can conclude that an individual reservoir-specific term in the Spohn entropy production rate  $\dot{S}_i^{\text{Sp}} \geq 0$  can be written as

$$\begin{aligned} \dot{S}_i^{\text{Sp}, \nu} &= -\text{Tr} \{ (\mathcal{P}\mathcal{L}^{(\nu)}\rho)\mathcal{P}[\ln \rho - \ln \bar{\rho}^{(\nu)}] \} - \text{Tr} \{ ((1 - \mathcal{P})\mathcal{L}^{(\nu)}\rho)(1 - \mathcal{P})[\ln \rho - \ln \bar{\rho}^{(\nu)}] \} \\ &= -\text{Tr} \{ (\mathcal{P}\mathcal{L}^{(\nu)}\rho)\mathcal{P}[\ln \rho - \ln \bar{\rho}^{(\nu)}] \} - \text{Tr} \{ ((1 - \mathcal{P})\mathcal{L}^{(\nu)}\rho)(1 - \mathcal{P}) \ln \rho \} \\ &= -\text{Tr} \{ (\mathcal{P}\mathcal{L}^{(\nu)}\rho)\mathcal{P}[\ln \mathcal{P}\rho - \ln \bar{\rho}^{(\nu)}] \} - \text{Tr} \{ ((1 - \mathcal{P})\mathcal{L}^{(\nu)}\rho)(1 - \mathcal{P}) \ln \rho \} \\ &\quad + \text{Tr} \{ (\mathcal{P}\mathcal{L}^{(\nu)}\rho)\mathcal{P}[\ln \mathcal{P}\rho - \ln \rho] \} \\ &= -\text{Tr} \{ (\mathcal{P}\mathcal{L}^{(\nu)}\rho)\mathcal{P}[\ln \mathcal{P}\rho - \ln \bar{\rho}^{(\nu)}] \} \\ &\quad + \text{Tr} \{ ((1 - \mathcal{P})\mathcal{L}^{(\nu)}\rho)(1 - \mathcal{P})[\ln \mathcal{P}\rho - \ln \rho] \} + \text{Tr} \{ (\mathcal{P}\mathcal{L}^{(\nu)}\rho)\mathcal{P}[\ln \mathcal{P}\rho - \ln \rho] \} \\ &= -\text{Tr} \{ (\mathcal{L}^{(\nu)}\mathcal{P}\rho)[\ln \mathcal{P}\rho - \ln \bar{\rho}^{(\nu)}] \} - \text{Tr} \{ (\mathcal{L}^{(\nu)}\rho)[\ln \rho - \ln \mathcal{P}\rho] \}, \end{aligned} \quad (7.34)$$

where in the second step we have used that  $\bar{\rho}^{(\nu)}$  (and its logarithm) is diagonal in the energy eigenbasis in which we evaluate the trace. In the last step, we have used again the previous decomposition into diagonal and off-diagonal contributions. Furthermore, we also used that  $\mathcal{P}\mathcal{L} = \mathcal{L}\mathcal{P}$  (block form of the Liouvillian). Therefore, we see that the entropy production additively splits into a part arising from the dynamics of the populations and another part coming from the dynamics of the coherences.

The first term for the populations can be written as

$$\begin{aligned} \dot{S}_i^{1, \nu} &= -\text{Tr} \{ (\mathcal{L}^{(\nu)}\mathcal{P}\rho)[\ln \mathcal{P}\rho - \ln \bar{\rho}^{(\nu)}] \} = - \sum_{ij} W_{ij}^{(\nu)} P_j \left[ \ln P_i - \ln \bar{P}_i^{(\nu)} \right] \\ &= - \sum_{ij} W_{ij}^{(\nu)} P_j \ln P_i + \sum_{ij} W_{ij}^{(\nu)} P_j \ln \bar{P}_i^{(\nu)} = + \sum_{ij} W_{ij}^{(\nu)} P_j \ln \frac{P_j}{P_i} + \sum_{ij} W_{ij}^{(\nu)} P_j \ln \frac{\bar{P}_i^{(\nu)}}{\bar{P}_j^{(\nu)}} \\ &= \sum_{ij} W_{ij}^{(\nu)} P_j \ln \frac{P_j \bar{P}_i^{(\nu)}}{P_i \bar{P}_j^{(\nu)}} = \sum_{ij} W_{ij}^{(\nu)} P_j \ln \frac{P_j W_{ij}^{(\nu)}}{P_i W_{ji}^{(\nu)}} \geq 0, \end{aligned} \quad (7.35)$$

where we have used that  $\sum_i W_{ij}^{(\nu)} = 0$  and eventually that  $\frac{\bar{P}_i^{(\nu)}}{\bar{P}_j^{(\nu)}} = \frac{W_{ij}^{(\nu)}}{W_{ji}^{(\nu)}}$ . We see that it exactly reproduces the entropy production rate for rate equation in Def. 26.

Finally, we discuss the coherences. From the contractivity of completely positive trace-preserving maps [11] we can show that

$$D(e^{\mathcal{L}\Delta t} \rho(t) | e^{\mathcal{L}\Delta t} \mathcal{P}\rho(t)) \leq D(\rho(t) | \mathcal{P}\rho(t)) \quad (7.36)$$

that one can as  $\Delta t \rightarrow 0$  obtain an inequality of the form

$$\dot{S}_i^{2,\nu} = -\text{Tr} \{ (\mathcal{L}^{(\nu)} \rho(t)) [\ln \rho(t) - \ln \mathcal{P} \rho(t)] \} \geq 0. \quad (7.37)$$

**Exercise 38** (Entropy production of coherent decay). *Show that under the assumptions discussed in this section, the above inequality holds. You may want to use that (why)  $\text{Tr} \{ (e^{\mathcal{L}\Delta t} \rho) \ln e^{\mathcal{L}\Delta t} \mathcal{P} \rho \} = \text{Tr} \{ (e^{\mathcal{L}\Delta t} \mathcal{P} \rho) \ln e^{\mathcal{L}\Delta t} \mathcal{P} \rho \}$ .*

This proves that for the standard quantum-optical master equation, the total master equation entropy production  $\dot{S}_i^{\text{Sp}} = \sum_{\nu} [\dot{S}_i^{1,\nu} + \dot{S}_i^{2,\nu}]$  decomposes into two separately positive terms, one describing the evolution of the populations only – with the usual entropy production for rate equations remaining in general finite at large times – and another transient term containing the entropic contributions stemming from the decay of the coherences.

### 7.1.3 Entropic analysis of rate equations with feedback

We will in this section discuss the necessary modifications in the entropy production rate in rate equations that are subject to feedback control actions. The control actions will be allowed to change both the tunneling rates [41] and the energies of the system [42].

We now consider a feedback conditioned on the system being in state  $j$ . Physically, this means that some external controller monitors the state of the system, and upon detecting the system in state  $j$ , it immediately changes the system properties accordingly: The energies of all levels  $i$  are **without delay** changed to  $E_i^{(j)}$  and also the transition rates due to reservoir  $\nu$  from  $j$  to other states are changed to  $W_{ij}^{(j,\nu)}$ . Then, the rate equation under feedback becomes

$$\dot{P}_i = \sum_{\alpha} \sum_j W_{ij}^{(j,\alpha)} P_j. \quad (7.38)$$

As we will see, one can distinguish between changes of bare tunneling rates and changes of the energy levels. Whereas the first type leaves the energetics of the system invariant but changes the entropy and is for this reason also called Maxwell demon feedback [41], changing the energy levels modifies both the energetic and entropic balances. It can therefore also not be considered a simple work source.

During a jump  $j \rightarrow i$  (where the system particle number changes according to  $\Delta N_{ij} = N_i - N_j$ ), the energy balance of the system becomes  $\Delta E_{ij} = (E_i^{(j)} - E_j^{(j)}) + (E_i^{(i)} - E_i^{(j)})$ , where the first contribution is exchanged with the reservoir and contributes to the heat via  $\Delta Q_{ij} = (E_i^{(j)} - E_j^{(j)}) - \mu(N_i - N_j)$ , and the second describes feedback energy  $\Delta E_{\text{fb}}$  injected into the system from the control action following immediately thereafter, see also Fig. 7.4 for an illustration. This enables us to write the energy and particle currents entering the system from reservoir  $\nu$  as

$$\begin{aligned} I_E^{(\nu)} &= \sum_{ij} (E_i^{(j)} - E_j^{(j)}) W_{ij}^{(j,\nu)} P_j, \\ I_M^{(\nu)} &= \sum_{ij} (N_i - N_j) W_{ij}^{(j,\nu)} P_j. \end{aligned} \quad (7.39)$$

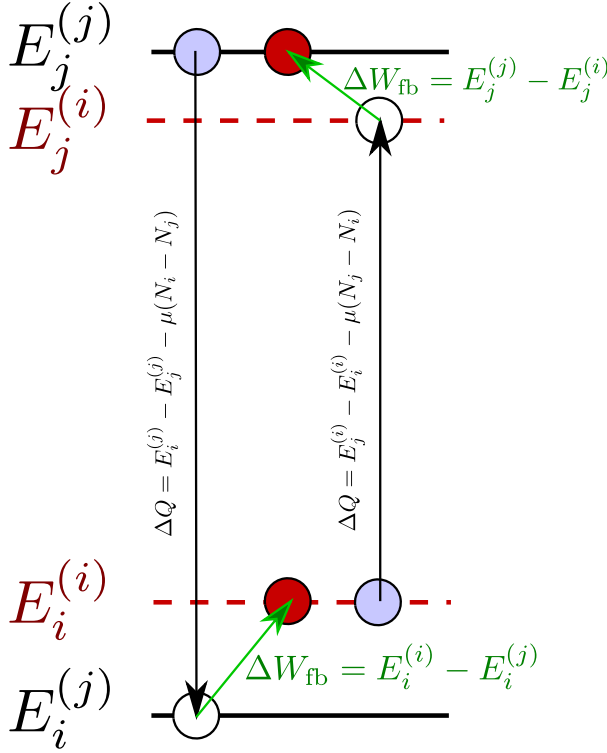


Figure 7.4: Sketch of the energetic balance for the transition from from state  $j \rightarrow i$  (left) and from state  $i \rightarrow j$  (right) subject to feedback control applied immediately thereafter. The initial transition (blue to hollow circles) leads to the exchange of heat between system and reservoir (vertical terms). Immediately thereafter, the control action changes the energy levels (hollow to filled red circles), thereby injecting energy into the system if the level is occupied.

The energy injected in the system with the feedback actions can be similarly computed

$$I_E^{\text{fb}} = \sum_{\nu} \sum_{ij} (E_i^{(i)} - E_i^{(j)}) W_{ij}^{(j,\nu)} P_j, \quad (7.40)$$

and together we find for the total change of the system energy  $E = \sum_i E_i^{(i)} P_i$

$$\begin{aligned} \dot{E} &= \sum_{ij} \sum_{\nu} E_i^{(i)} W_{ij}^{(j,\nu)} P_j \\ &= \sum_{\nu} \sum_{i \neq j} E_i^{(i)} W_{ij}^{(j,\nu)} P_j - \sum_{\nu} \sum_{i \neq j} E_i^{(i)} W_{ji}^{(i,\nu)} P_i \\ &= \sum_{\nu} \sum_{i,j} (E_i^{(i)} - E_j^{(j)}) W_{ij}^{(j,\nu)} P_j = \left( \sum_{\nu} I_E^{(\nu)} \right) + I_E^{\text{fb}} \\ &= \sum_{\nu} \mu_{\nu} I_M^{(\nu)} + I_E^{\text{fb}} + \sum_{\nu} (I_E^{(\nu)} - \mu_{\nu} I_M^{(\nu)}). \end{aligned} \quad (7.41)$$

This is the first law of thermodynamics, where in the last line we can identify the chemical work done on the system, the energy injected from the feedback, and the heat currents entering from the reservoirs.

We can also consider the evolution of the systems Shannon entropy  $S = -\sum_i P_i \ln P_i$ , where

we get from algebraic manipulations [7]

$$\begin{aligned}\dot{S} &= - \sum_i \dot{P}_i \ln P_i = \dot{S}_i + \dot{S}_e, \\ \dot{S}_i &= \sum_\nu \sum_{ij} W_{ij}^{(j,\nu)} P_j \ln \left( \frac{W_{ij}^{(j,\nu)} P_j}{W_{ji}^{(i,\nu)} P_i} \right) \geq 0, \\ \dot{S}_e &= \sum_\nu \sum_{ij} W_{ij}^{(j,\nu)} P_j \ln \left( \frac{W_{ji}^{(i,\nu)}}{W_{ij}^{(j,\nu)}} \right).\end{aligned}\quad (7.42)$$

Here, the positivity of the entropy production rate  $\dot{S}_i$  follows from mathematical terms (it has the form of a relative entropy), and the second term  $\dot{S}_e$  can from the conventional detailed balance relation (7.20) in absence of feedback be identified as the negative entropy change in the reservoirs. However, the feedback changes the detailed balance relation in a way which we phenomenologically parametrize as

$$\frac{W_{ji}^{(i,\nu)}}{W_{ij}^{(j,\nu)}} = e^{\beta_\nu [(E_i^{(j)} - E_j^{(j)}) - \mu_\nu (N_i - N_j)]} e^{-\Delta_{ij}^{(\nu)}} e^{-\sigma_{ij}^{(\nu)}}. \quad (7.43)$$

Here, the first term is associated with the entropy change of the reservoirs, indeed we can recover the heat flow from the reservoirs into the system from it. The second term  $\Delta_{ij}^{(\nu)}$  parametrizes changes of the transition rates that are not associated with energetic changes in the system. Consequently, it must not depend on the reservoir temperatures. Finally, the term  $\sigma_{ij}^{(\nu)}$  gathers all remaining influences of the feedback. By distinguishing between  $\Delta_{ij}^{(\nu)}$  and  $\sigma_{ij}^{(\nu)}$  we have presupposed that an unambiguous discrimination between these feedback effects is possible. Inserting this decomposition into the “entropy flow” term we obtain

$$\begin{aligned}\dot{S}_e &= \sum_\nu \beta_\nu \dot{Q}^{(\nu)} - \mathcal{I}_1 - \mathcal{I}_2, \\ \mathcal{I}_1 &= \sum_\nu \sum_{ij} W_{ij}^{(j,\nu)} P_j \Delta_{ij}^{(\nu)}, \\ \mathcal{I}_2 &= \sum_\nu \sum_{ij} W_{ij}^{(j,\nu)} P_j \sigma_{ij}^{(\nu)}.\end{aligned}\quad (7.44)$$

Solving for the entropy production, we can express it as

$$\dot{S}_i = \dot{S} - \sum_\nu \beta_\nu \dot{Q}^{(\nu)} + \mathcal{I}_1 + \mathcal{I}_2 \geq 0. \quad (7.45)$$

This is the second law of thermodynamics in presence of a non-equilibrium environment and feedback control.

At steady state,  $\dot{S} \rightarrow 0$ , and the usual inequality for the currents  $-\sum_\nu \beta_\nu \dot{Q}^{(\nu)} \geq 0$  is modified by two effective currents. The first one  $\mathcal{I}_1$  is associated with feedback actions that have no direct impact on the energetics, whereas the second one takes the energetic feedback actions into account. We note here that these information currents are just an effective description (for example, they can become negative), since we have not made the implementation of the feedback loop explicit in our treatment but remain at a phenomenologic level. If that is done for a microscopic treatment

of the detector [43], it is possible to link the effective information current with the time-derivative of the mutual information between controlled system and detector device [44, 45].

Depending on the regime, one may identify contributions to the total entropy production rate (7.45) which are negative. These always need to be compensated by the other, positive contributions, which enables one to define information-theoretic efficiencies that are upper-bounded by one.

### 7.1.4 Our example: Maxwell's demon

For error-free feedback the average feedback rate matrix becomes (for simplicity without counting fields)

$$\mathcal{L}_{\text{fb}} = \sum_{\nu} \begin{pmatrix} -\Gamma_{\nu}^E f_{\nu}^E & +\Gamma_{\nu}^F [1 - f_{\nu}^F] \\ +\Gamma_{\nu}^E f_{\nu}^E & -\Gamma_{\nu}^F [1 - f_{\nu}^F] \end{pmatrix}. \quad (7.46)$$

Here, the piecewise-constant driving leads to two possible values of the SET tunneling rates  $\Gamma_{\nu} \rightarrow \Gamma_{\nu}^{E/F}$  and also of the system Hamiltonian ( $\epsilon \rightarrow \epsilon^{E/F}$ ). Since the dot parameters in the description only enter implicitly, we described the latter by conditional Fermi functions  $f_{\nu} \rightarrow f_{\nu}^{E/F} = f_{\nu}(\epsilon^{E/F})$ . With such a feedback scheme, one will in general inject both energy and information into the system, which can be consistently treated on the local level.

Assuming the conditioned dot Hamiltonian as  $H_S = \epsilon_{E/F} d^{\dagger} d$ , the empty dot has energies  $E_0^{(0)} = 0$  and  $E_1^{(0)} = \epsilon_E$ , and when filled, the system has energies  $E_0^{(1)} = 0$  and  $E_1^{(1)} = \epsilon_F$ . Therefore, we can identify the heat entering the system from reservoir  $\nu$  during a jump out of the system as  $\Delta Q_{\text{out}}^{(\nu)} = E_0^{(1)} - E_1^{(1)} - \mu_{\nu}(N_0 - N_1) = -\epsilon_F + \mu$  and for a jump into the system as  $\Delta Q_{\text{in}}^{(\nu)} = E_1^{(0)} - E_0^{(0)} - \mu_{\nu}(N_1 - N_0) = +\epsilon_E - \mu$ , leading to an overall heat current of

$$\begin{aligned} \dot{Q}^{(\nu)} &= -(\epsilon_F - \mu_{\nu}) \mathcal{L}_{\text{fb}}^{01,\nu} P_1 + (\epsilon_E - \mu_{\nu}) \mathcal{L}_{\text{fb}}^{10,\nu} P_0 \\ &= I_E^{(\nu)} - \mu_{\nu} I_M^{(\nu)}, \end{aligned} \quad (7.47)$$

which also defines energy  $I_E^{(\nu)}$  and matter  $I_M^{(\nu)}$  currents entering the system from reservoir  $\nu$

$$\begin{aligned} I_E^{(\nu)} &= \epsilon_E \mathcal{L}_{\text{fb}}^{10,\nu} P_0 - \epsilon_F \mathcal{L}_{\text{fb}}^{01,\nu} P_1 = \epsilon_E \Gamma_{\nu}^E f_{\nu}^E P_0 - \epsilon_F \Gamma_{\nu}^F (1 - f_{\nu}^F) P_1, \\ I_M^{(\nu)} &= \mathcal{L}_{\text{fb}}^{10,\nu} P_0 - \mathcal{L}_{\text{fb}}^{01,\nu} P_1 = \Gamma_{\nu}^E f_{\nu}^E P_0 - \Gamma_{\nu}^F (1 - f_{\nu}^F) P_1, \end{aligned} \quad (7.48)$$

and we see that they are no longer tightly coupled. A similar result holds if also the energy of the empty state is changed by the feedback. We can show that the energy change of the system is balanced by the energy currents entering the system from both reservoirs and the energy current injected by the feedback

$$I_E^{\text{fb}} = (\epsilon_F - \epsilon_E) \sum_{\nu} \mathcal{L}_{\text{fb}}^{10,\nu} P_0. \quad (7.49)$$

The first law at steady state then simply reads  $I_E^{(L)} + I_E^{(R)} + I_E^{\text{fb}} = 0$ .

To discuss the entropic balance, we can with Eq. (7.46) write the ratio of backward- and forward rates for each reservoir as

$$\begin{aligned} \frac{\mathcal{L}_{\text{fb}}^{01,\nu}}{\mathcal{L}_{\text{fb}}^{10,\nu}} &= \frac{\Gamma_{\nu}^F (1 - f_{\nu}^F)}{\Gamma_{\nu}^E f_{\nu}^E} = \left( \frac{1 - f_{\nu}^E}{f_{\nu}^E} \right) \left[ \frac{\Gamma_{\nu}^F}{\Gamma_{\nu}^E} \right] \left\{ \frac{1 - f_{\nu}^F}{1 - f_{\nu}^E} \right\}, \\ \frac{\mathcal{L}_{\text{fb}}^{10,\nu}}{\mathcal{L}_{\text{fb}}^{01,\nu}} &= \frac{\Gamma_{\nu}^E f_{\nu}^E}{\Gamma_{\nu}^F (1 - f_{\nu}^F)} = \left( \frac{f_{\nu}^F}{1 - f_{\nu}^F} \right) \left[ \frac{\Gamma_{\nu}^E}{\Gamma_{\nu}^F} \right] \left\{ \frac{f_{\nu}^E}{f_{\nu}^F} \right\}, \end{aligned} \quad (7.50)$$

where we see from  $(1 - f_\nu^E)/f_\nu^E = e^{+\beta_\nu(\epsilon_E - \mu_\nu)}$  and  $f_\nu^F/(1 - f_\nu^F) = e^{-\beta_\nu(\epsilon_F - \mu_\nu)}$  that the terms in round parentheses (...) will when inserted in the “entropy flow” term

$$\dot{S}_e^{(\nu)} = \sum_{ij} W_{ij}^{(j,\nu)} P_j \ln \frac{W_{ji}^{(i,\nu)}}{W_{ij}^{(j,\nu)}} \quad (7.51)$$

compose the entropy change in the reservoirs  $-\beta_\nu \dot{Q}^{(\nu)}$ , compare Eq. (7.47). The terms in square brackets [...] are a pure Maxwell-demon contribution [41] in the sense that they only affect the entropic balance directly, and the terms in curly brackets {...} describe the influence on the feedback energy injection on the entropic balance. We therefore define the feedback parameters

$$\begin{aligned} \Delta_{01}^{(\nu)} &= \ln \frac{\Gamma_\nu^F}{\Gamma_\nu^E}, & \Delta_{10}^{(\nu)} &= \ln \frac{\Gamma_\nu^E}{\Gamma_\nu^F}, \\ \sigma_{01}^{(\nu)} &= \ln \frac{f_\nu^F}{f_\nu^E}, & \sigma_{10}^{(\nu)} &= \ln \frac{1 - f_\nu^E}{1 - f_\nu^F}, \end{aligned} \quad (7.52)$$

compare also Eq. (7.43). We see that the information contribution of the feedback obeys  $\Delta_{01}^{(\nu)} = -\Delta_{10}^{(\nu)}$  and the energetic contribution obeys  $\sigma_{01}^{(\nu)} \sigma_{10}^{(\nu)} = \beta_\nu(\epsilon_E - \epsilon_F)$ . With these, the “entropy flow” term becomes modified by information currents  $\dot{S}_e = \sum_\nu \beta_\nu \dot{Q}^{(\nu)} - \mathcal{I}_1 - \mathcal{I}_2$ , of which the first reads explicitly

$$\begin{aligned} \mathcal{I}_1 &= \sum_\nu [\mathcal{L}_{\text{fb}}^{01,\nu} P_1 - \mathcal{L}_{\text{fb}}^{10,\nu} P_0] \ln \frac{\Gamma_\nu^F}{\Gamma_\nu^E} = - \sum_\nu \ln \frac{\Gamma_\nu^F}{\Gamma_\nu^E} I_M^{(\nu)} \\ &\xrightarrow{t \rightarrow \infty} \left( \ln \frac{\Gamma_R^F}{\Gamma_R^E} - \ln \frac{\Gamma_L^F}{\Gamma_L^E} \right) I_M = I_M \ln \left[ \frac{\Gamma_L^E \Gamma_R^F}{\Gamma_L^F \Gamma_R^E} \right]. \end{aligned} \quad (7.53)$$

Above, it is visible that the individual contributions to the information current  $\mathcal{I}_1$  are tightly coupled to the matter current. At steady state, we have conservation of the matter currents  $I_M = I_M^{(L)} = -I_M^{(R)}$ , such that also the total information current is tightly coupled to the matter current.

Looking at the second information current we see that

$$\mathcal{I}_2 = \sum_\nu \left[ \mathcal{L}_{\text{fb}}^{01,\nu} P_1 \ln \frac{f_\nu^F}{f_\nu^E} + \mathcal{L}_{\text{fb}}^{10,\nu} P_0 \ln \frac{1 - f_\nu^E}{1 - f_\nu^F} \right]. \quad (7.54)$$

Inserting these in the steady-state entropy production rate  $\dot{S}_i = -\dot{S}_e$  we can use the first law at steady state  $I_E^{(L)} + I_E^{(R)} + I_E^{\text{fb}} = 0$  to find that at equal temperatures  $\beta = \beta_L = \beta_R$  the second law reads

$$\begin{aligned} \dot{S}_i &\xrightarrow{t \rightarrow \infty} -\beta(I_E^{(L)} - \mu_L I_M^{(L)} + I_E^{(R)} - \mu_R I_M^{(R)}) + \mathcal{I}_1 + \mathcal{I}_2 \\ &= \beta(\mu_L - \mu_R) I_M + \beta I_E^{\text{fb}} + \mathcal{I}_1 + \mathcal{I}_2 \geq 0. \end{aligned} \quad (7.55)$$

Here, the first term contains the produced electric power  $P = -(\mu_L - \mu_R) I_M$ , which without feedback would always be negative. The second term contains the purely informational contribution of the feedback to the entropic balance. The third term quantifies how the difference of left and right energy currents  $I_E^{(L)} + I_E^{(R)} = -I_E^{\text{fb}}$  affects the heat exchanged with the reservoirs. If the feedback does not affect the energy levels ( $\epsilon_E = \epsilon_F$ ), this term will naturally vanish. Finally, the

last term describes the effect of the feedback level driving on the entropic balance. Since the level driving also enters the entropic balance, we cannot interpret this simply as work on the system.

For simplicity, we can parametrize the tunneling rates using only a single parameter

$$\begin{aligned}\Gamma_L^F &= \Gamma e^{+\delta}, & \Gamma_R^F &= \Gamma e^{-\delta}, \\ \Gamma_L^E &= \Gamma e^{-\delta}, & \Gamma_R^E &= \Gamma e^{+\delta},\end{aligned}\tag{7.56}$$

which will for  $\delta > 0$  favor transport from right to left. This will not change the energetics, but the entropic balance is affected by the information current  $\mathcal{I}_1$ . When we similarly parametrize the changes of the dot level as

$$\epsilon_F = \epsilon e^{+\Delta}, \quad \epsilon_E = \epsilon e^{-\Delta},\tag{7.57}$$

this will for  $\Delta \neq 0$  inject energy into the system via feedback operations. This secondary type of feedback will not only modify the energy balance (first law), visible in an imbalance between left and right energy currents  $I_E^{(L)} \neq -I_E^{(R)}$ . In addition, it also affects the entropic balance via both a modification of the heat flow and the information current  $\mathcal{I}_2$ . These effects are illustrated in Fig. 7.5.

It is clearly visible that neglecting the feedback completely, one may observe an apparent violation of the second law (dashed and solid red curves). The unconscious injection of energy may lead to a significant increase of the overall produced power (solid red curve) but also implies an apparent violation of the second law under Maxwell-demon feedback (solid green curve). By contrast, the full entropy production rate (7.55) is always positive as expected (black curves).

Finally, we turn to the integral fluctuation theorem for entropy production. Formally, we get a fluctuation theorem for the probabilities of transferred particles from left to right, since the when we equip Eq. (7.46) with counting fields, we get

$$\mathcal{L}_{\text{fb}}(\chi) = \begin{pmatrix} -\Gamma_L^E f_L^E & +\Gamma_L^F [1 - f_L^F] e^{-i\chi} \\ +\Gamma_L^E f_L^E e^{+i\chi} & -\Gamma_L^F [1 - f_L^F] \end{pmatrix} + \begin{pmatrix} -\Gamma_R^E f_R^E & +\Gamma_R^F [1 - f_R^F] \\ +\Gamma_R^E f_R^E & -\Gamma_R^F [1 - f_R^F] \end{pmatrix}.\tag{7.58}$$

In the long-term cumulant-generating function we obtain the symmetry

$$C(-\chi, t) = C(+\chi + i\alpha, t), \quad \alpha = \ln \frac{f_L^E (1 - f_R^F) \Gamma_L^E \Gamma_R^F}{(1 - f_L^F) f_R^E \Gamma_L^F \Gamma_R^E},\tag{7.59}$$

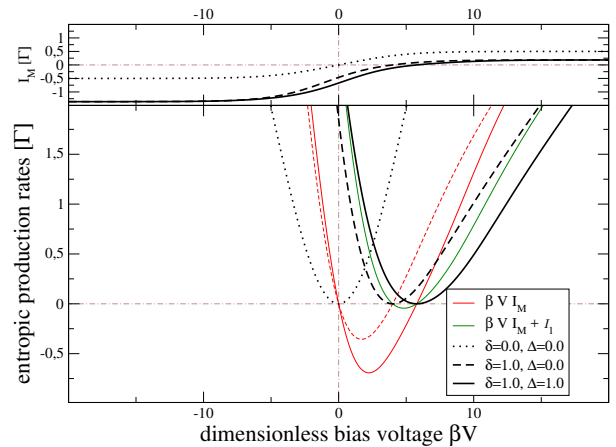
which leads to a fluctuation theorem of the form

$$\lim_{t \rightarrow \infty} \frac{P_{+n}(t)}{P_{-n}(t)} = e^{+n\alpha}.\tag{7.60}$$

When  $f_\nu^E = f_\nu^F$ , we indeed recover our previous fluctuation theorem (7.17). In this case, we have indeed the total entropy production in the exponent. However, when the feedback injects energy into the system  $f_\nu^E \neq f_\nu^F$ , we have already found that the average entropy production is no longer tightly coupled to the matter current and can therefore not be simply proportional to the total number of particles travelling through the system. The observed symmetry is then just a purely mathematical one – actually a fluctuation theorem is observed for any fluctuating two-level system, regardless of any detailed balance relation.

A corresponding experiment has recently been performed [46]. Beyond weak coupling, the analysis can also be performed with reaction-coordinates as discussed in Sec. 4.4, but becomes significantly more involved [47].

Figure 7.5: Plot of the matter current from left to right (top) and contributions to the total entropy production rate (7.55) (bottom) for situations without feedback  $\delta = \Delta = 0$  (dotted), with Maxwell-demon feedback  $\delta = +1.0$ ,  $\Delta = 0$  (dashed), and with energy-injecting feedback  $\delta = \Delta = +1.0$  (solid). With feedback active (dashed and solid), we see that the matter current at equilibrium  $V = 0$  becomes negative and remains negative for a small region  $0 < V < V^*$ , where the device produces positive power  $P = -VI_M$  either using only information ( $\Delta = 0$ ) or information and energy injection ( $\Delta \neq 0$ ). Red thin curves of similar style denote the naive entropy production rate  $\beta(\mu_L - \mu_R)I_M = -\beta P$  that one would conjecture in ignorance of any feedback actions taken. Green thin curves of similar style denote the naive entropy production rate  $-\beta(\mu_L - \mu_R)I_M + \mathcal{I}_1$  that one would conjecture when assuming that the feedback does not affect the energy levels. The black curves denote the true entropy production rate, which is positive in all parameter regimes. Dash-dotted lines just serve for orientation. Other parameters:  $\beta\epsilon = 1$ .



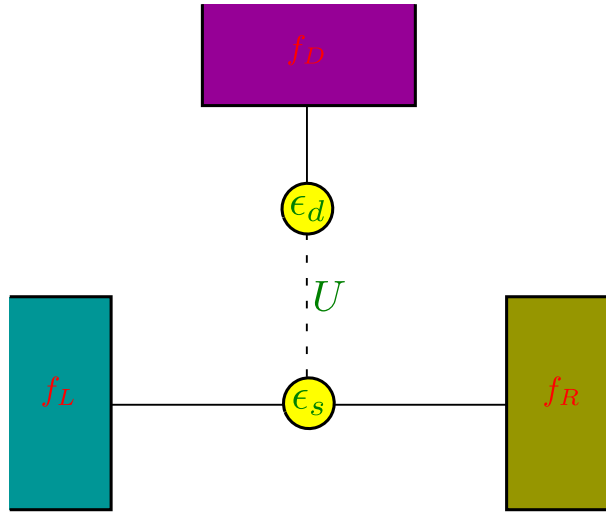


Figure 7.6: Sketch of an SET (bottom circuit) that is capacitively coupled via the Coulomb interaction  $U$  to another quantum dot. The additional quantum dot is tunnel-coupled to its own reservoir with Fermi function  $f_D$ . Since the associated stationary matter current vanishes, only energy can be transferred across this junction (dotted line).

## 7.2 An electronic Maxwell demon: Autonomous feedback

In contrast to external feedback loops, we can augment a quantum system by replacing the measurement, signal processing, and control actions by a single auxiliary system, which we add to the original quantum system. The controller and the original quantum systems are then treated in an all-inclusive fashion. Typically, such setups are less flexible, since the control protocol cannot just be changed by altering classical parts of the feedback loop. However, they offer more understanding on the thermodynamics as the complete feedback loop can be treated as part of the system.

### An autonomous version of a Maxwell demon

Consider a single-electron transistor as before now capacitively interacting with another quantum dot, which is coupled to its own reservoir as depicted in Fig. 7.6. The system Hamiltonian of this three-terminal system reads

$$H_S = \epsilon_d c_d^\dagger c_d + \epsilon_s c_s^\dagger c_s + U c_d^\dagger c_d c_s^\dagger c_s, \quad (7.61)$$

where  $\epsilon_s$  and  $\epsilon_d$  denote the on-site energies of the SET dot and the demon dot, respectively, whereas  $U$  denotes the Coulomb interaction between the two dots. The system dot is tunnel-coupled to left and right leads, whereas the demon dot is tunnel-coupled to its junction only

$$H_I = \sum_k \left( t_{kL} c_s c_{kL}^\dagger + t_{kL}^* c_{kL} c_s^\dagger \right) + \sum_k \left( t_{kR} c_s c_{kR}^\dagger + t_{kR}^* c_{kR} c_s^\dagger \right) + \sum_k \left( t_{kd} c_d c_{kd}^\dagger + t_{kd}^* c_{kd} c_d^\dagger \right). \quad (7.62)$$

Furthermore, all the junctions are modeled as non-interacting fermions

$$H_B = \sum_{\nu \in \{L, R, d\}} \sum_k \epsilon_{k\nu} c_{k\nu}^\dagger c_{k\nu}. \quad (7.63)$$

Treating the tunneling amplitudes perturbatively and fixing the reservoirs at thermal equilibrium states we derive the standard quantum-optical master equation, compare also Def. 6. Importantly, we do not apply the popular wide-band limit here (which would mean to approximate  $\Gamma_\nu(\omega) \approx \Gamma_\nu$ ). In the energy eigenbasis of  $H_S$  – further-on denoted by  $|\rho\sigma\rangle$  where  $\rho \in \{E, F\}$  describes the systems dot state and  $\sigma \in \{0, 1\}$  denotes the state of the demon dot (both either

empty or filled, respectively) – the populations obey a simple rate equation defined by Eq. (1.82). Denoting the populations by  $p_{\rho\sigma} = \langle \rho\sigma | \rho | \rho\sigma \rangle$ , the rate equation  $\dot{P} = \mathcal{L}P$  in the ordered basis  $P = (p_{0E}, p_{1E}, p_{0F}, p_{1F})^T$  decomposes into the contributions due to the different reservoirs  $\mathcal{L} = \mathcal{L}_D + \mathcal{L}_L + \mathcal{L}_R$ , which read

$$\mathcal{L}_D = \begin{pmatrix} -\Gamma_D f_D & +\Gamma_D(1-f_D) & 0 & 0 \\ +\Gamma_D f_D & -\Gamma_D(1-f_D) & 0 & 0 \\ 0 & 0 & -\Gamma_D^U f_D^U & +\Gamma_D^U(1-f_D^U) \\ 0 & 0 & +\Gamma_D^U f_D^U & -\Gamma_D^U(1-f_D^U) \end{pmatrix},$$

$$\mathcal{L}_\alpha = \begin{pmatrix} -\Gamma_\alpha f_\alpha & 0 & +\Gamma_\alpha(1-f_\alpha) & 0 \\ 0 & -\Gamma_\alpha^U f_\alpha^U & 0 & +\Gamma_\alpha^U(1-f_\alpha^U) \\ +\Gamma_\alpha f_\alpha & 0 & -\Gamma_\alpha(1-f_\alpha) & 0 \\ 0 & +\Gamma_\alpha^U f_\alpha^U & 0 & -\Gamma_\alpha^U(1-f_\alpha^U) \end{pmatrix}, \quad \alpha \in \{L, R\}, \quad (7.64)$$

where we have used the abbreviations  $\Gamma_\alpha = \Gamma_\alpha(\epsilon_s)$  and  $\Gamma_\alpha^U = \Gamma_\alpha(\epsilon_s + U)$  for  $\alpha \in \{L, R\}$  and  $\Gamma_D = \Gamma_D(\epsilon_d)$  and  $\Gamma_D^U = \Gamma_D(\epsilon_d + U)$  for the tunneling rates and similarly for the Fermi functions  $f_\alpha = f_\alpha(\epsilon_s)$ ,  $f_\alpha^U = f_\alpha(\epsilon_s + U)$ ,  $f_D = f_D(\epsilon_d)$ , and  $f_D^U = f_D(\epsilon_d + U)$ , respectively. We note that all contributions separately obey local-detailed balance relations. Closer inspection of the rates in Eq. (7.64) reveals that these rates could have been guessed without any microscopic derivation. For example, the transition rate from state  $|1E\rangle$  to state  $|0E\rangle$  is just given by the bare tunneling rate for the demon junction  $\Gamma_D$  multiplied by the probability to find a free space in the terminal at transition frequency  $\epsilon_d$ . Similarly, the transition rate from state  $|1F\rangle$  to state  $|0F\rangle$  corresponds to an electron jumping out of the demon dot to its junction, this time, however, transporting energy of  $\epsilon_d + U$ . We have ordered our basis such that the upper left block of  $\mathcal{L}_D$  describes the dynamics of the demon dot conditioned on an empty system dot, whereas the lower block accounts for the dynamics conditioned on a filled system.

As a whole, the system respects the second law of thermodynamics. We demonstrate this by analyzing the entropy production by means of the Full Counting Statistics. In order to avoid having to trace six counting fields, we note that the system obeys three conservation laws, since the two dots may only exchange energy but not matter

$$I_M^{(L)} + I_M^{(R)} = 0, \quad I_M^{(D)} = 0, \quad I_E^{(L)} + I_E^{(R)} + I_E^{(D)} = 0, \quad (7.65)$$

where  $I_E^{(\nu)}$  and  $I_M^{(\nu)}$  denote energy and matter currents to terminal  $\nu$ , respectively. Therefore, three counting fields should in general suffice to completely track the full entropy production in the long-term limit. For simplicity however, we compute the entropy production for the more realistic case of equal temperatures at the left and right SET junction  $\beta = \beta_L = \beta_R$ . Technically, this is conveniently performed by balancing with the entropy flow and using the conservation laws

$$\begin{aligned} \dot{S}_i &= -\dot{S}_e = -\sum_\nu \beta^{(\nu)} (I_E^{(\nu)} - \mu^{(\nu)} I_M^{(\nu)}) \\ &= -\beta (I_E^{(L)} - \mu_L I_M^{(L)} + I_E^{(R)} - \mu_R I_M^{(R)}) - \beta_D I_E^{(D)} \\ &= (\beta - \beta_D) I_E^{(D)} + \beta (\mu_L - \mu_R) I_M. \end{aligned} \quad (7.66)$$

Here,  $I_E^{(D)}$  is the energy current from the demon lead and  $I_M$  the matter current from left to right. Thus, we conclude that for equal temperatures left and right it should even suffice to track e.g. only the energy transferred from the demon junction and the particles transferred from left to

right through the SET. Therefore, we introduce counting fields for the energy transferred from the demon into the system ( $\xi$ ) and for the particles transferred from the system into the right junction ( $\chi$ ), and the counting-field dependent rate equation becomes

$$\begin{aligned} \mathcal{L}_D(\xi) &= \begin{pmatrix} -\Gamma_D f_D & +\Gamma_D(1-f_D)e^{-i\xi\epsilon_d} & 0 & 0 \\ +\Gamma_D f_D e^{+i\xi\epsilon_d} & -\Gamma_D(1-f_D) & 0 & 0 \\ 0 & 0 & -\Gamma_D^U f_D^U & +\Gamma_D^U(1-f_D^U)e^{-i\xi(\epsilon_d+U)} \\ 0 & 0 & +\Gamma_D^U f_D^U e^{+i\xi(\epsilon_d+U)} & -\Gamma_D^U(1-f_D^U) \end{pmatrix}, \\ \mathcal{L}_R(\chi) &= \begin{pmatrix} -\Gamma_R f_R & 0 & +\Gamma_R(1-f_R)e^{+i\chi} & 0 \\ 0 & -\Gamma_R^U f_R^U & 0 & +\Gamma_R^U(1-f_R^U)e^{+i\chi} \\ +\Gamma_R f_R e^{-i\chi} & 0 & -\Gamma_R(1-f_R) & 0 \\ 0 & +\Gamma_R^U f_R^U e^{-i\chi} & 0 & -\Gamma_R^U(1-f_R^U) \end{pmatrix}. \end{aligned} \quad (7.67)$$

These counting fields can now be used to reconstruct the statistics of energy and matter transfer. The currents can be obtained by performing suitable derivatives of the rate matrix. For example, the energy current to the demon is given by  $I_E^{(D)} = -i\text{Tr} \left\{ \partial_\xi \mathcal{L}(\xi, 0) |_{\xi=0} \bar{\rho} \right\}$ , where  $\bar{\rho}$  is the steady state  $\mathcal{L}(0, 0)\bar{\rho} = 0$ .

To test the fluctuation theorem, we note that the matrix elements of the full Liouvillian

$$L_{ij}(\chi, \xi) = (\mathcal{L}_D(\xi) + \mathcal{L}_L + \mathcal{L}_R(\chi))_{ij} \quad (7.68)$$

obey the symmetries

$$\begin{aligned} L_{13}(-\chi) &= \frac{1-f_L}{f_L} L_{31} \left( +\chi + i \ln \frac{f_L(1-f_R)}{(1-f_L)f_R} \right) = \frac{1-f_L}{f_L} L_{31} (+\chi + i\beta(\mu_L - \mu_R)), \\ L_{24}(-\chi) &= \frac{1-f_L^U}{f_L^U} L_{42} \left( +\chi + i \ln \frac{f_L^U(1-f_R^U)}{(1-f_L^U)f_R^U} \right) = \frac{1-f_L^U}{f_L^U} L_{42} (+\chi + i\beta(\mu_L - \mu_R)), \\ L_{12}(-\xi) &= L_{21} \left( +\xi + \frac{i}{\epsilon_d} \ln \frac{1-f_D}{f_D} \right) = L_{21} \left( +\xi + \frac{i}{\epsilon_d} \beta_D(\epsilon_d - \mu_D) \right), \\ L_{34}(-\xi) &= L_{43} \left( +\xi + \frac{i}{\epsilon_d + U} \ln \frac{1-f_D^U}{f_D^U} \right) = L_{43} \left( +\xi + \frac{i}{\epsilon_d + U} \beta_D(\epsilon_d + U - \mu_D) \right), \end{aligned} \quad (7.69)$$

which can be used to show that the long-term generating function (given by the dominant eigenvalue of the Liouvillian) obeys the symmetry

$$\mathcal{C}(-\xi, -\chi) = \mathcal{C}(\xi + i(\beta - \beta_D), \chi + i\beta(\mu_L - \mu_R)). \quad (7.70)$$

This symmetry implies – when monitoring the energy from the demon to the system  $e_D$  and the number of electrons transferred from left to right  $n_S$  – for the corresponding probability distribution the fluctuation theorem

$$\lim_{t \rightarrow \infty} \frac{P_{+\Delta n_S, +\Delta e_D}}{P_{-\Delta n_S, -\Delta e_D}} = e^{(\beta - \beta_D)\Delta e_D + \beta(\mu_L - \mu_R)\Delta n_S}. \quad (7.71)$$

Instead of determining the continuous energy emission distribution, we could alternatively have counted the discrete number of electrons entering the demon dot at energy  $\epsilon_D$  and leaving it at energy  $\epsilon_D + U$ . Since this process leads to a net energy extraction of energy  $U$  from the system, the corresponding matter current is tightly coupled to the energy current across the demon junction,

i.e., their number would be related to the energy via  $\Delta e_D = n_D U$ . Comparing the value in the exponent of Eq. (7.71) with the average expectation value of the entropy production in Eq. (7.66), we can also – roughly speaking – interpret the fluctuation theorem as the ratio of probabilities for trajectories with a positive and negative entropy production.

In addition, we identify  $P = (\mu_L - \mu_R)I_M^{(R)} = -(\mu_L - \mu_R)I_M^{(L)}$  as the power generated by the device, which – when the current flows against the bias – may yield a negative contribution  $\beta P$  to the overall entropy production. In these parameter regimes however, the negative contribution  $\beta(\mu_L - \mu_R)I_M^{(R)}$  must be over-balanced by the second term  $(\beta - \beta_D)I_E^{(D)}$ , which clearly requires – when the demon reservoir is colder than the SET reservoirs  $\beta_D > \beta_S$  – that the energy current flows out of the demon  $I_E^{(D)} < 0$ . As a whole, the system therefore just converts a thermal gradient between the two subsystems into power: A fraction of the heat coming from the hot SET leads is converted into power, and the remaining fraction is dissipated as heat at the cold demon junction. The corresponding efficiency for this conversion can be constructed from the output power  $P = -(\mu_L - \mu_R)I_M^{(L)}$  and the input heat  $\dot{Q}_L + \dot{Q}_R = -I_E^{(D)} - (\mu_L - \mu_R)I_M^{(L)} = \dot{Q}_{\text{diss}} + P$ , where  $\dot{Q}_{\text{diss}} = -I_E^{(D)}$  is the heat dissipated into the demon reservoir. Using that  $\dot{S}_i \geq 0$  we find that the efficiency – which of course is only useful in parameter regimes where the power is positive  $\beta(\mu_L - \mu_R)I_M^{(R)} > 0$  – is upper-bounded by Carnot efficiency

$$\eta = \frac{P}{\dot{Q}^{(L)} + \dot{Q}^{(R)}} = \frac{P}{\dot{Q}_{\text{diss}} + P} \leq 1 - \frac{T_D}{T} = \eta_{\text{Car}}. \quad (7.72)$$

For practical applications a large efficiency is not always sufficient. For example, a maximum efficiency at zero power output would be quite useless. Therefore, it has become common standard to first maximize the power output of the device and then compute the corresponding efficiency at maximum power. Due to the nonlinearity of the underlying equations, this may be a difficult numerical optimization problem. To reduce the number of parameters, we assume that  $f_D^U = 1 - f_D$  (which is the case when  $\epsilon_D = \mu_D - U/2$ ) and  $f_L^U = 1 - f_R$  as well as  $f_R^U = 1 - f_L$  (which for  $\beta_L = \beta_R = \beta$  is satisfied when  $\epsilon_S = 1/2(\mu_L + \mu_R) - U/2$ ), see also the left panel of Fig. 7.7. Furthermore, we parametrize the modification of the tunneling rates by a single parameter via

$$\begin{aligned} \Gamma_L &= \Gamma \frac{e^{+\delta}}{\cosh(\delta)}, & \Gamma_L^U &= \Gamma \frac{e^{-\delta}}{\cosh(\delta)} \\ \Gamma_R &= \Gamma \frac{e^{-\delta}}{\cosh(\delta)}, & \Gamma_R^U &= \Gamma \frac{e^{+\delta}}{\cosh(\delta)} \end{aligned} \quad (7.73)$$

to favor transport in a particular direction. We have inserted the normalization by  $\cosh(\delta)$  to keep the tunneling rates finite as the feedback strength  $\delta$  is increased. Trivially, at  $\delta = 0$  we recover symmetric unperturbed tunneling rates and when  $\delta \rightarrow \infty$ , transport will be completely rectified. The matter current from left to right in the limit where the demon dot is much faster than the SET ( $\Gamma_D \rightarrow \infty$  and  $\Gamma_D^U \rightarrow \infty$ ) becomes

$$I_M^{(L)} = \frac{\Gamma}{2} [f_L - f_R + \tanh(\delta) (f_L + f_R - 2f_D)]. \quad (7.74)$$

Similarly, we obtain for the energy current to the demon

$$I_E^{(D)} = \frac{\Gamma U}{2} [f_L + f_R - 2f_D + (f_L - f_R) \tanh(\delta)], \quad (7.75)$$

which determines the dissipated heat. These can be converted into an efficiency solely expressed by Fermi functions when we use that

$$\begin{aligned}\beta(\mu_L - \mu_R) &= \ln \left( \frac{f_L(1-f_R)}{(1-f_L)f_R} \right), \\ \beta U &= \ln \left( \frac{f_R(1-f_R^U)}{(1-f_R)f_R^U} \right) \rightarrow \ln \left( \frac{f_R f_L}{(1-f_R)(1-f_L)} \right),\end{aligned}\quad (7.76)$$

which can be used to write the efficiency of heat to power conversion as

$$\eta = \frac{P}{\dot{Q}_{\text{diss}} + P} = \frac{1}{1 + \frac{\beta \dot{Q}_{\text{diss}}}{\beta P}} = \frac{1}{1 + \frac{\ln \left( \frac{f_R f_L}{(1-f_R)(1-f_L)} \right) (f_L + f_R - 2f_D + (f_L - f_R) \tanh(\delta))}{\ln \left( \frac{f_L(1-f_R)}{(1-f_L)f_R} \right) (f_L - f_R + (f_L + f_R - 2f_D) \tanh(\delta))}}, \quad (7.77)$$

which is also illustrated in Fig. 7.7.

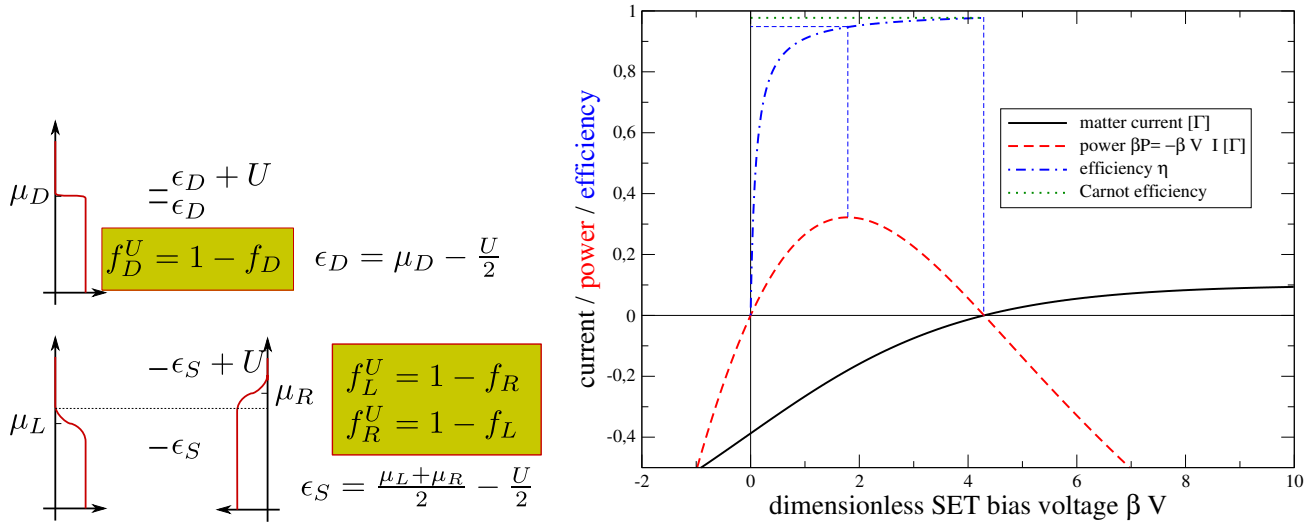


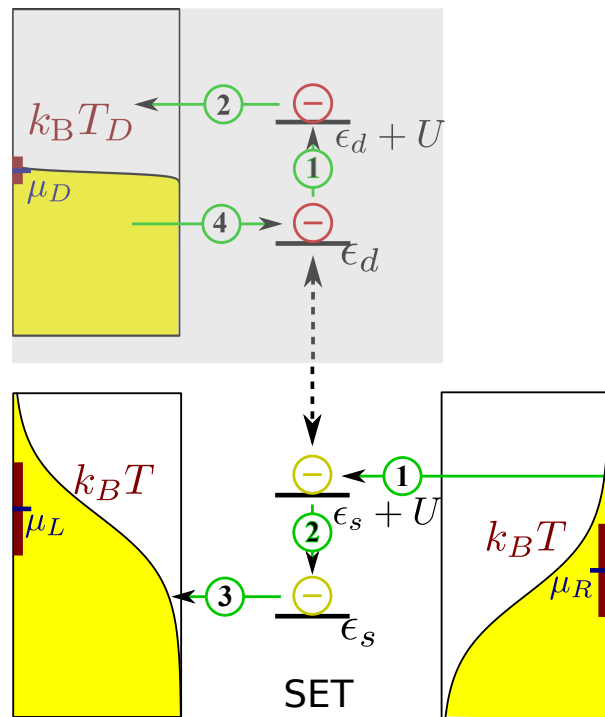
Figure 7.7:

**Left:** Sketch of the assumed configurations of chemical potentials, which imply at  $\beta_L = \beta_R$  relations between the Fermi functions.

**Right:** Plot of current (solid black, in units of  $\Gamma$ ), dimensionless power  $\beta VI$  (dashed red, in units of  $\Gamma$ ), and efficiency  $\eta$  (dash-dotted blue) versus dimensionless bias voltage. At equilibrated bias (origin), the efficiency vanishes by construction, whereas it reaches Carnot efficiency (dotted green) at the new equilibrium, i.e., at zero power. At maximum power however, the efficiency still closely approaches the Carnot efficiency. Parameters:  $\delta = 100$ , tunneling rates parametrized as in Eq. (7.73),  $f_D = 0.9 = 1 - f_D^U$ ,  $\beta \epsilon_S = -0.05 = -\beta(\epsilon_S + U)$ , such that the Carnot efficiency becomes  $\eta_{\text{Carnot}} = 1 - (\beta U)/(\beta_D U) \approx 0.977244$ .

Beyond these average considerations, the qualitative action of the device may also be understood at the level of single trajectories, see Fig. 7.8. It should be noted that at the trajectory level, all possible trajectories are still allowed, even though ones with positive total entropy production must on average dominate. As a whole, the system thereby merely converts a temperature gradient (cold demon, hot system) into useful power (current times voltage).

Figure 7.8: Level sketch of the setup. Shaded yellow regions represent occupied levels in the leads with chemical potentials and temperatures indicated. Central horizontal lines represent transition energies of system and demon dot, respectively. When the other dot is occupied, the bare transition frequency of every system is shifted by the Coulomb interaction  $U$ . The shown trajectory then becomes likely in the suggested Maxwell-demon mode: Initially, the SET is empty and the demon dot is filled. When  $\Gamma_R^U \gg \Gamma_L^U$ , the SET dot is most likely first filled from the left lead, which shifts the transition frequency of the demon (1). When the bare tunneling rates of the demon are much larger than that of the SET, the demon dot will rapidly equilibrate by expelling the electron to its associated reservoir (2) before a further electronic jump at the SET may occur. At the new transition frequency, the SET electron is more likely to escape first to the left than to the right when  $\Gamma_L \gg \Gamma_R$  (3). Now, the demon dot will equilibrate again by filling with an electron (4) thus restoring the initial state. In essence, an electron is transferred against the bias through the SET circuit while in the demon system an electron enters at energy  $\epsilon_d$  and leaves at energy  $\epsilon_d + U$  leading to a net transfer of  $U$  from the demon into its reservoir.



### Local View: A Feedback-Controlled Device

An experimentalist having access only to the SET circuit would measure a positive generated power, conserved particle currents  $I_M^{(L)} + I_M^{(R)} = 0$ , but possibly a slight mismatch of left and right energy currents  $I_E^{(L)} + I_E^{(R)} = -I_E^{(D)} \neq 0$ . This mismatch could not fully account for the generated power, since for any efficiency  $\eta > 1/2$  in Fig. 7.8 we have  $|I_E^{(D)}| < P$ . Therefore, the experimentalist would conclude that his description of the system by energy and matter flows is not complete and he might suspect Maxwell's demon at work. Here, we will make the reduced dynamics of the SET dot alone more explicit by deriving a reduced rate equation.

We can evidently write the rate equation defined by Eqs. (7.64) as  $\dot{P}_\alpha = \mathcal{L}_{\alpha\alpha'} P_{\alpha'}$ . Here,  $\alpha \in \{E0, E1, F0, F1\}$  labels the energy eigenstates of the total system composed by the single dot and the demon dot. Resolving these two degrees of freedom  $\alpha = (ij)$ , where  $i \in \{E, F\}$  and  $j \in \{0, 1\}$ , we can equivalently write  $\dot{P}_{ij} = \mathcal{L}_{ij, i'j'} P_{i'j'}$ , where  $i$  and  $j$  label the system ( $i$ ) and detector/demon ( $j$ ) degrees of freedom, respectively. If we discard the dynamics of the demon dot by tracing over its degrees of freedom  $P_i = \sum_j P_{ij}$ , we formally arrive at a non-Markovian evolution equation for the populations of the SET dot.

$$\dot{P}_i = \sum_{i'} \sum_{jj'} \mathcal{L}_{ij, i'j'} P_{i'j'} = \sum_{i'} \left[ \sum_{jj'} \mathcal{L}_{ij, i'j'} \frac{P_{i'j'}}{P_{i'}} \right] P_{i'} = \mathcal{L}_{ii'}(t) P_{i'}. \quad (7.78)$$

This equation is non-Markovian, since to solve for the time-dependent rates  $\mathcal{L}_{ii'}$  we would need to integrate over the solution of the full rate equation, which implies that they depend on the values of the system of the past. However, we may identify  $\frac{P_{i'j'}}{P_{i'}}$  as the conditional probability of the demon being in state  $j'$  provided the system is in state  $i'$ .

Then, the argument is similar to that put forward in Sec. 3.1.7: Direct inspection of the rates suggests that when we assume the limit where the bare rates of the demon system are much larger than the SET tunneling rates, these conditional probabilities will assume their conditioned stationary values much faster than the SET dynamics. In this limit, the dynamics is mainly dominated by transitions between just two mesostates instead of the original four states. These mesostates are associated to either a filled or an empty system quantum dot, respectively. We may hence arrive again at a Markovian description by approximating

$$P_{j'|i} = \frac{P_{i'j'}}{P_{i'}} \rightarrow \frac{\bar{P}_{i'j'}}{\bar{P}_{i'}}, \quad (7.79)$$

which yields the coarse-grained rate matrix

$$\mathcal{L}_{ii'} = \sum_{jj'} \mathcal{L}_{ij, i'j'} \frac{\bar{P}_{i'j'}}{\bar{P}_{i'}}. \quad (7.80)$$

For the model at hand, the stationary conditional probabilities become in the limit where  $\Gamma_D^{(U)} \gg \Gamma_{L/R}^{(U)}$

$$\begin{aligned} P_{0|E} &= \frac{\bar{P}_{E0}}{\bar{P}_E} = 1 - f_D, & P_{1|E} &= \frac{\bar{P}_{E1}}{\bar{P}_E} = f_D, \\ P_{0|F} &= \frac{\bar{P}_{F0}}{\bar{P}_F} = 1 - f_D^U, & P_{1|F} &= \frac{\bar{P}_{F1}}{\bar{P}_F} = f_D^U, \end{aligned} \quad (7.81)$$

and just describe the fact that – due to the time-scale separation – the demon dot immediately reaches a thermal stationary state that depends on the occupation of the SET dot. The temperature and chemical potential of the demon reservoir determine if and how well the demon dot – which can be envisaged as the demon’s memory capable of storing just one bit – captures the actual state of the system dot. For example, for high demon temperatures it will be roughly independent on the system dots occupation as  $f_D \approx f_D^U \approx 1/2$ . At very low demon temperatures however, and if the chemical potential of the demon dot is adjusted such that  $\epsilon_d - \mu_D < 0$  and  $\epsilon_d + U - \mu_D > 0$ , the demon dot will nearly accurately (more formally when  $\beta_D U \gg 1$ ) track the system occupation, since  $f_D \rightarrow 1$  and  $f_D^U \rightarrow 0$ . Then, the demon dot will immediately fill when the SET dot is emptied and its electron will leave when the SET dot is filled. It thereby faithfully detects the state of the SET. In the presented model, the demon temperature thereby acts as a source of error in the demon’s measurement of the system’s state. In addition, the model at hand allows to investigate the detector backaction on the probed system, which is often neglected. Here, this backaction is essential, and we will now investigate it by analyzing the reduced dynamics in detail.

The coarse-grained probabilities  $P_E$  and  $P_F$  of finding the SET dot empty or filled, respectively, obey the rate equation dynamics

$$\mathcal{L} = \begin{pmatrix} -L_{FE} & +L_{EF} \\ +L_{FE} & -L_{EF} \end{pmatrix} \quad (7.82)$$

with the coarse-grained rates

$$\begin{aligned} L_{EF} &= L_{E0,F0} \frac{\bar{P}_{F0}}{\bar{P}_F} + L_{E1,F1} \frac{\bar{P}_{F1}}{\bar{P}_F} \\ &= [\Gamma_L(1 - f_L) + \Gamma_R(1 - f_R)](1 - f_D^U) + [\Gamma_L^U(1 - f_L^U) + \Gamma_R^U(1 - f_R^U)] f_D^U, \\ L_{FE} &= L_{F0,E0} \frac{\bar{P}_{E0}}{\bar{P}_E} + L_{F1,E1} \frac{\bar{P}_{E1}}{\bar{P}_E} \\ &= [\Gamma_L f_L + \Gamma_R f_R](1 - f_D) + [\Gamma_L^U f_L^U + \Gamma_R^U f_R^U] f_D. \end{aligned} \quad (7.83)$$

We note that a naive experimenter – not aware of the demon interacting with the SET circuit – would attribute the rates in the coarse-grained dynamics to just two reservoirs:  $\mathcal{L} = \mathcal{L}_L + \mathcal{L}_R$  with the rates  $\mathcal{L}_{EF}^{(\alpha)} = (1 - f_D^U)\Gamma_\alpha(1 - f_\alpha) + f_D^U\Gamma_\alpha^U(1 - f_\alpha^U)$  and  $\mathcal{L}_{FE}^{(\alpha)} = (1 - f_D)\Gamma_\alpha f_\alpha + f_D\Gamma_\alpha^U f_\alpha^U$ . Thus, when the SET is not sensitive to the demon state  $\Gamma_{L/R}^U \approx \Gamma_{L/R}$  and  $f_{L/R}^U \approx f_{L/R}$ , local detailed balance is restored, and we recover the conventional SET rate equation.

We note that the matter current

$$I_M^{(\nu)} = L_{EF}^{(\nu)} \bar{P}_F - \mathcal{L}_{FE}^{(\nu)} \bar{P}_E \quad (7.84)$$

is conserved  $I_M^{(L)} = -I_M^{(R)}$ , such that the entropy production becomes

$$\begin{aligned} \dot{S}_i &= \sum_{\nu \in \{L,R\}} L_{EF}^{(\nu)} \bar{P}_F \ln \left( \frac{\mathcal{L}_{EF}^{(\nu)} \bar{P}_F}{\mathcal{L}_{FE}^{(\nu)} \bar{P}_E} \right) + \mathcal{L}_{FE}^{(\nu)} \bar{P}_E \ln \left( \frac{\mathcal{L}_{FE}^{(\nu)} \bar{P}_E}{\mathcal{L}_{EF}^{(\nu)} \bar{P}_F} \right) \\ &= \sum_{\nu \in \{L,R\}} \left( L_{EF}^{(\nu)} \bar{P}_F - \mathcal{L}_{FE}^{(\nu)} \bar{P}_E \right) \ln \left( \frac{\mathcal{L}_{EF}^{(\nu)} \bar{P}_F}{\mathcal{L}_{FE}^{(\nu)} \bar{P}_E} \right) \\ &= I_M^{(L)} \ln \left( \frac{\mathcal{L}_{EF}^{(L)} \mathcal{L}_{FE}^{(R)}}{\mathcal{L}_{FE}^{(L)} \mathcal{L}_{EF}^{(R)}} \right) = I_M^{(L)} \mathcal{A}, \end{aligned} \quad (7.85)$$

and is thus representable in a simple flux-affinity form. Similarly, we note that if we would count particle transfers from the left to the right reservoir, the following fluctuation theorem would hold

$$\frac{P_{+n}}{P_{-n}} = e^{n\mathcal{A}}, \quad (7.86)$$

and the fact that these fluctuations could in principle be resolved demonstrates that the affinity in the entropy production is a meaningful and measurable quantity. Without the demon dot, the conventional affinity of the SET would simply be given by

$$\mathcal{A}_0 = \ln \left( \frac{(1-f_L)f_R}{f_L(1-f_R)} \right) = \beta_L(\epsilon - \mu_L) - \beta_R(\epsilon - \mu_R), \quad (7.87)$$

and ignoring the physical implementation of the demon, we can interpret the modification of the entropy production due to the demon as an additional information current that is tightly coupled to the particle current

$$\dot{S}_i = I_M^{(L)} \mathcal{A}_0 + I_M^{(L)} (\mathcal{A} - \mathcal{A}_0) = \dot{S}_i^{(0)} + \mathcal{I}. \quad (7.88)$$

When the demon temperature is lowered such that  $\beta_D U \gg 1$  and its chemical potential is adjusted such that  $f_D \rightarrow 1$  and  $f_D^U \rightarrow 0$ , the affinity becomes

$$\mathcal{A} = \ln \left( \frac{\Gamma_L(1-f_L)\Gamma_R^U f_R^U}{\Gamma_L^U f_L^U \Gamma_R(1-f_R)} \right) = \ln \left( \frac{\Gamma_L \Gamma_R^U}{\Gamma_L^U \Gamma_R} \right) + \ln \left( \frac{f_L f_R^U}{f_L^U f_R} \right) + \mathcal{A}_0. \quad (7.89)$$

The last term on the right-hand side is simply the affinity without the demon dot. The first two terms quantify the modification of the affinity. The pure limit of a Maxwell demon is reached, when the energetic backaction of the demon on the SET is negligible, i.e., when  $f_L^U \approx f_L$  and  $f_R^U \approx f_R$ , which requires comparably large SET temperatures  $\beta_{L/R} U \ll 1$ . Of course, to obtain any nontrivial effect, it is still necessary to keep non-flat tunneling rates  $\Gamma_{L/R}^U \neq \Gamma_{L/R}$ , and in this case one recovers the case discussed in the previous section – identifying  $\Gamma_\alpha^E$  with  $\Gamma_\alpha$  and  $\Gamma_\alpha^F$  with  $\Gamma_\alpha^U$ .

A similar experiment has been performed in Ref. [48]. As with the external feedback loop, a discussion beyond the lowest order master equation is possible with reaction-coordinate mappings as discussed in Sec. 4.4 but significantly more involved [49].

## 7.3 Charge detectors

Charge detectors are an important tool which we have used multiple times. Here, we will try to understand their effect on the system better and to link their presence with an effective description of quantum measurements. We will start from the point contact Hamiltonian

$$\begin{aligned} H_{\text{QPC}} = & \sum_k \epsilon_{kL} \gamma_{kL}^\dagger \gamma_{kL} + \sum_k \epsilon_{kR} \gamma_{kR}^\dagger \gamma_{kR} \\ & + (1 - \delta d^\dagger d) \sum_{kk'} t_{kk'} \gamma_{kL} \gamma_{k'R}^\dagger + (1 - \delta d^\dagger d) \sum_{kk'} t_{kk'}^* \gamma_{k'R} \gamma_{kL}^\dagger, \end{aligned} \quad (7.90)$$

where  $t_{kk'}$  denotes the tunneling amplitude from mode  $k$  of the left QPC lead to mode  $k'$  of the right QPC lead. The prefactor  $1 - \delta d^\dagger d$  reduces (we consider only  $0 \leq \delta \leq 1$ ) the magnitude of

these amplitudes when a nearby charge (we will specify it later) is present. For  $\delta = 0$ , the QPC is insensitive to the nearby dot occupation, and  $\delta \rightarrow 1$  means that transport through the QPC is completely blocked when the monitored dot is occupied. We label our system coupling operator as  $A = \mathbf{1} - \delta d^\dagger d$  and for our reservoir we have  $B = \sum_{kk'} [t_{kk'} \gamma_{kL} \gamma_{k'R}^\dagger + \text{h.c.}]$ .

According to Eq. (3.93), the coarse-graining dissipator for a single coupling operator can be written as

$$\begin{aligned}
\dot{\rho}_{\mathbf{S}} &= -i \left[ \frac{1}{2i\tau} \int_0^\tau dt_1 \int_0^\tau dt_2 C^0(t_1 - t_2) \text{sgn}(t_1 - t_2) \mathbf{A}(t_1) \mathbf{A}(t_2), \rho_{\mathbf{S}} \right] \\
&\quad + \frac{1}{\tau} \int_0^\tau dt_1 \int_0^\tau dt_2 \left[ C^\chi(t_1 - t_2) \mathbf{A}(t_2) \rho_{\mathbf{S}} \mathbf{A}(t_1) - \frac{C^0(t_1 - t_2)}{2} \{ \mathbf{A}(t_1) \mathbf{A}(t_2), \rho_{\mathbf{S}} \} \right] \\
&= -i \left[ \frac{1}{2i2\pi\tau} \int_0^\tau dt_1 \int_0^\tau dt_2 \int d\omega \sigma^0(\omega) e^{-i\omega(t_1 - t_2)} \mathbf{A}(t_1) \mathbf{A}(t_2), \rho_{\mathbf{S}} \right] \\
&\quad + \frac{1}{2\pi\tau} \int_0^\tau dt_1 \int_0^\tau dt_2 \int d\omega e^{-i\omega(t_1 - t_2)} \left[ \gamma^\chi(\omega) \mathbf{A}(t_2) \rho_{\mathbf{S}} \mathbf{A}(t_1) - \frac{\gamma^0(\omega)}{2} \{ \mathbf{A}(t_1) \mathbf{A}(t_2), \rho_{\mathbf{S}} \} \right].
\end{aligned} \tag{7.91}$$

For later notation, we also split the correlation function into right- (21) and left-moving (12) components

$$\gamma^\chi(\omega) = e^{+i\chi} \gamma_{21}(\omega) + e^{-i\chi} \gamma_{12}(\omega). \tag{7.92}$$

Continuous measurements can be modeled by repeated pointwise measurements conducted in time intervals  $\Delta t$ . Following this assumption, the coarse-graining time  $\tau$  should actually be chosen to coincide with the measurement period  $\tau = \Delta t$ . Then, two important limits are relevant.

- When the measurement period  $\Delta t$  than the time scales of the coupling operators, we can neglect the time-dependence of the coupling operators completely. Then,  $\mathbf{A}(t) \rightarrow A$ , and the dissipator assumes a local form. Sometimes, this approach is known as **singular coupling limit**. For example, when we are measuring so frequent that all time dependencies can be neglected, the dissipator becomes with  $\tau = \Delta t$  as

$$\dot{\rho}_{\mathbf{S}} = + \frac{\Delta t}{2\pi} \int d\omega \left[ \gamma^\chi(\omega) A \rho_{\mathbf{S}} A - \frac{\gamma^0(\omega)}{2} \{ A^2, \rho_{\mathbf{S}} \} \right]. \tag{7.93}$$

Here, we have neglected also the Lamb-shift.

- In the opposite limit where the measurement period is much larger than the timescale of the QPC correlation functions, we can extend  $\tau = \Delta t \rightarrow \infty$ , which effectively implements a secular approximation. Then, the time-dependence of the coupling operator  $\mathbf{A}(t)$  is essential to determine the form of the dissipator.

For a realistic measurement device, the appropriate choice will be in between these extreme limits.

### 7.3.1 Single quantum dot

When the QPC couples only to a single quantum dot (SQD)

$$H_S = \epsilon d^\dagger d, \quad (7.94)$$

we see that the interaction commutes with the dot Hamiltonian, such that to lowest order (the dot may itself have further leads) no energy is exchanged between the QPC and the dot. For a single dot, the interaction picture dynamics is trivial  $\mathbf{A}(t) = 1 - \delta d^\dagger d$ . In Sec. 3.4.2, we have already computed the correlation functions for such a QPC model, including a counting field for the number of charges that enter the right QPC lead. We had calculated the Fourier transforms of the reservoir correlation function in Eqns. (3.116)

$$\gamma^x(\omega) = \frac{T}{2\pi} \frac{e^{-i\chi}(\omega - V)}{1 - e^{-\beta(\omega - V)}} + \frac{T}{2\pi} \frac{e^{+i\chi}(\omega + V)}{1 - e^{-\beta(\omega + V)}} = \gamma_{21}(\omega)e^{+i\chi} + \gamma_{12}(\omega)e^{-i\chi}, \quad (7.95)$$

where  $T > 0$  is the baseline transmission of the QPC,  $\beta$  its ambient temperature, and  $V$  the QPC bias voltage. Furthermore, when the time between two measurements  $\Delta t$  of the particles transferred through the QPC is large in comparison to the decay time of the correlation function, we may safely extend the coarse-graining time  $\tau \rightarrow \infty$ , such that the dissipator becomes

$$\begin{aligned} \dot{\rho}_{\mathbf{S}} = & -i \left[ \frac{1}{2i} (\sigma_{12}(0) + \sigma_{21}(0)) (1 - \delta d^\dagger d)^2, \rho_{\mathbf{S}} \right] \\ & + \gamma_{12}(0) \left[ e^{-i\chi} (1 - \delta d^\dagger d) \rho_{\mathbf{S}} (1 - \delta d^\dagger d) - \frac{1}{2} \{ (1 - \delta d^\dagger d)^2, \rho_{\mathbf{S}} \} \right] \\ & + \gamma_{21}(0) \left[ e^{+i\chi} (1 - \delta d^\dagger d) \rho_{\mathbf{S}} (1 - \delta d^\dagger d) - \frac{1}{2} \{ (1 - \delta d^\dagger d)^2, \rho_{\mathbf{S}} \} \right]. \end{aligned} \quad (7.96)$$

As superpositions of states with different charge are not allowed for the SQD, the most general density matrix of a single dot can be written as  $\rho_{\mathbf{S}}(t) = P_0(t) |0\rangle\langle 0| + P_1(t) |1\rangle\langle 1|$ , which obey the generalized master equation

$$\frac{d}{dt} \begin{pmatrix} P_0(t) \\ P_1(t) \end{pmatrix} = (\gamma_{21}(e^{+i\chi} - 1) + \gamma_{12}(e^{-i\chi} - 1)) \begin{pmatrix} 1 & 0 \\ 0 & (1 - \delta)^2 \end{pmatrix} \begin{pmatrix} P_0(t) \\ P_1(t) \end{pmatrix}. \quad (7.97)$$

Here, we have used the abbreviations

$$\gamma_{21} = \gamma_{21}(0) = \frac{TV}{1 - e^{-\beta V}}, \quad \gamma_{12} = \gamma_{12}(0) = \frac{TV}{e^{+\beta V} - 1}. \quad (7.98)$$

At vanishing counting field, the effect of the QPC vanishes completely. Writing the probabilities in a vector  $\rho = (P_0, P_1)^T$ , we can write this as

$$\dot{\rho} = \mathcal{L}_{\text{dt}}(\chi)\rho, \quad \mathcal{L}_{\text{dt}}(\chi) = (\gamma_{21}(e^{+i\chi} - 1) + \gamma_{12}(e^{-i\chi} - 1)) \begin{pmatrix} 1 & 0 \\ 0 & (1 - \delta)^2 \end{pmatrix}. \quad (7.99)$$

If no further leads change the occupation of the SQD, the prefactor directly encodes the cumulant-generating function of the QPC statistics, and we would get the two currents

$$I_E = \gamma_{21} - \gamma_{12} = TV, \quad I_F = (1 - \delta)^2 (\gamma_{21} - \gamma_{12}) = (1 - \delta)^2 TV, \quad (7.100)$$

depending on whether the dot is initially filled or empty, respectively. Similarly, we can compute the zero-frequency noise from the second derivative with respect to the counting field

$$S_E = \gamma_{21} + \gamma_{12} = TV \coth \left[ \frac{\beta V}{2} \right], \quad S_F = (1 - \delta)^2 (\gamma_{21} + \gamma_{12}) = (1 - \delta)^2 TV \coth \left[ \frac{\beta V}{2} \right]. \quad (7.101)$$

For large bias voltage, we can approximate this by  $\coth \left[ \frac{\beta V}{2} \right] \rightarrow 1$ , and the width of the current is just controlled by the bias voltage as well, such that transport becomes Poissonian. In contrast, for small bias voltage, the noise becomes  $S_E \rightarrow 2T/\beta$  and  $S_F \rightarrow (1 - \delta)^2 S_E$ , which is just linear in the temperature.

The Fano factor  $F = S/|I|$  is therefore just given by

$$F_E = F_F = \coth \left[ \frac{\beta V}{2} \right], \quad (7.102)$$

and it is not dependent on the dot occupation. In particular, it reaches 1 (Poissonian transport, shot noise) when  $V \rightarrow \infty$  and diverges as  $2/(\beta V)$  for small bias voltage. To use the point contact as a detector, we require that ideally, during the measurement time  $\Delta t$ , the system does not change due to other processes. Using a factoring initial state  $\rho(t) = \rho(t) \otimes |0\rangle \langle 0|$  corresponding to initially zero particles counted in the detector, the most general joint system-detector density matrix at time  $t + \Delta t$  is given by

$$\sigma(t + \Delta t) = \sum_{nm} \rho^{(nm)}(t + \Delta t) \otimes |n\rangle \langle m|. \quad (7.103)$$

Here,  $\rho^{(nm)}(t + \Delta t) = \langle n | \sigma(t + \Delta t) | m \rangle$ . Now, by performing a projective measurement with the measurement operators  $M_n = |n\rangle \langle n|$  we see that

$$M_n \sigma(t + \Delta t) M_n^\dagger = \rho^{(nn)}(t + \Delta t) \otimes |n\rangle \langle n|. \quad (7.104)$$

Then, the detector value is reset to zero (or equivalently, we use another detector), and the whole procedure is repeated. To infer how a projective measurement of the detector charges affects the system density matrix, we consider its  $n$ -resolved version

$$\rho^{(n)}(t + \Delta t) = \frac{1}{2\pi} \int_{-\pi}^{+\pi} e^{\mathcal{L}(\chi)\Delta t} e^{-in\chi} d\chi \rho(t) = \mathcal{K}_n(\Delta t) \rho(t). \quad (7.105)$$

When the bias voltage is large, transport becomes unidirectional, and we can simplify

$$\mathcal{L}_{\text{dt}}(\chi) \rightarrow \gamma_{21} (e^{+i\chi} - 1) \begin{pmatrix} 1 & 0 \\ 0 & (1 - \delta)^2 \end{pmatrix}, \quad (7.106)$$

which enables us to compute all integrals explicitly

$$\rho^{(n)}(t + \Delta t) = \begin{pmatrix} \frac{\gamma_{21}^n \Delta t^n}{n!} e^{-\gamma_{21} \Delta t} & 0 \\ 0 & \frac{(1-\delta)^{2n} \gamma_{21}^n \Delta t^n}{n!} e^{-(1-\delta)^2 \gamma_{21} \Delta t} \end{pmatrix} \rho(t) = \mathcal{K}_n(\Delta t) \rho(t). \quad (7.107)$$

These are just two Poissonian distributions moving at different pace: A fast one with cumulants  $\gamma_{21} \Delta t$  for the empty dot and a slow one with cumulants  $(1 - \delta)^2 \gamma_{21} \Delta t$ . The propagator  $\mathcal{K}_n(\Delta t)$  describes the effective action of measurement and interaction with the measurement device during  $\Delta t$ . Due to the normalization of the Poissonian distributions, we have  $\sum_n \mathcal{K}_n = \mathbf{1}$ , such that upon neglecting all measurement results, the measurement on the SQD has no effect. Starting with an arbitrary initial state  $\rho(0)$ , a trajectory can now be simulated as follows:

- Compute the probabilities of observing  $n$  particles transferred through the QPC during  $[t, t + \Delta t]$

$$P_n(\Delta t) = \frac{1}{2\pi} \int_{-\pi}^{+\pi} \text{Tr} \{ e^{\mathcal{L}(\chi)\Delta t} \rho(t) \} e^{-in\chi} d\chi \quad : \quad -\infty < n < +\infty. \quad (7.108)$$

In reality, it suffices to consider only values for  $n$  that are not much larger than  $TV\Delta t$ , since the probabilities for higher values will be negligible.

- Randomly select one particular outcome  $\bar{n}$  according to the given probability distribution. Technically, this can be achieved by ordering the intervals  $\{[\sum_{k<n} P_k, \sum_{k<n} P_k + P_n]\}$  and then drawing a random number that is uniformly distributed in  $[0, 1]$ . The interval  $[\sum_{k<\bar{n}} P_k, \sum_{k<\bar{n}} P_k + P_{\bar{n}}]$  into which the random number falls then defines selected measurement outcome  $\bar{n}$ . The time-resolved current through the QPC is given by

$$I_{\bar{n}} = \frac{\bar{n}}{\Delta t} \quad (7.109)$$

and other time-resolved observables can be computed as usual via  $O(t) = \text{Tr} \{ \hat{O}\rho(t) \}$ .

- Project the generalized density matrix on the chosen outcome (essential!) via

$$\rho(t + \Delta t) = \frac{1}{2\pi P_{\bar{n}}} \int_{-\pi}^{+\pi} e^{\mathcal{L}(\chi)\Delta t} \rho(t) e^{-i\bar{n}\chi} d\chi. \quad (7.110)$$

The result then serves as the initial state for the next iteration.

A corresponding trajectory is for a fast detector monitoring an SET quantum dot  $\mathcal{L}(\chi) = \mathcal{L}_{\text{dt}}(\chi) + \mathcal{L}_{\text{SET}}$  shown in Fig. 7.9. The projection onto the outcome of the charge measurement is essential for the observed temporal correlation: Having observe a large current, it is more likely to again observed a large current in the next measurement again (and vice versa).

For sufficiently large  $\Delta t$ , we can define a reasonable threshold such that  $(1 - \delta)^2 \gamma_{21} \Delta t < n_{\text{th}} < \gamma_{21} \Delta t$ . We can calculate it analytically by solving for the  $n$  where Poissonian distributions are identical

$$\frac{(1 - \delta)^{(2n)} (\gamma_{21} \Delta t)^n}{n!} e^{-(1-\delta)^2 \gamma_{21} \Delta t} = \frac{(\gamma_{21} \Delta t)^n}{n!} e^{-\gamma_{21} \Delta t}, \quad (7.111)$$

which eventually yields

$$n_{\text{th}} = \frac{-\delta(1 - \delta/2)\gamma\Delta t}{\ln(1 - \delta)}. \quad (7.112)$$

Now, by absorbing all measurement outcomes below the threshold into the outcome of a filled dot and the outcomes above the threshold into the outcome of an empty dot we get two measurement superoperators, which have a simple parametrization

$$\mathcal{K}_E = \sum_{n \geq n_{\text{th}}} \mathcal{K}_n(\Delta t) = \begin{pmatrix} 1 - P_{\text{err}}^0 & 0 \\ 0 & P_{\text{err}}^1 \end{pmatrix}, \quad \mathcal{K}_F = \sum_{n < n_{\text{th}}} \mathcal{K}_n(\Delta t) = \begin{pmatrix} P_{\text{err}}^0 & 0 \\ 0 & 1 - P_{\text{err}}^1 \end{pmatrix}, \quad (7.113)$$

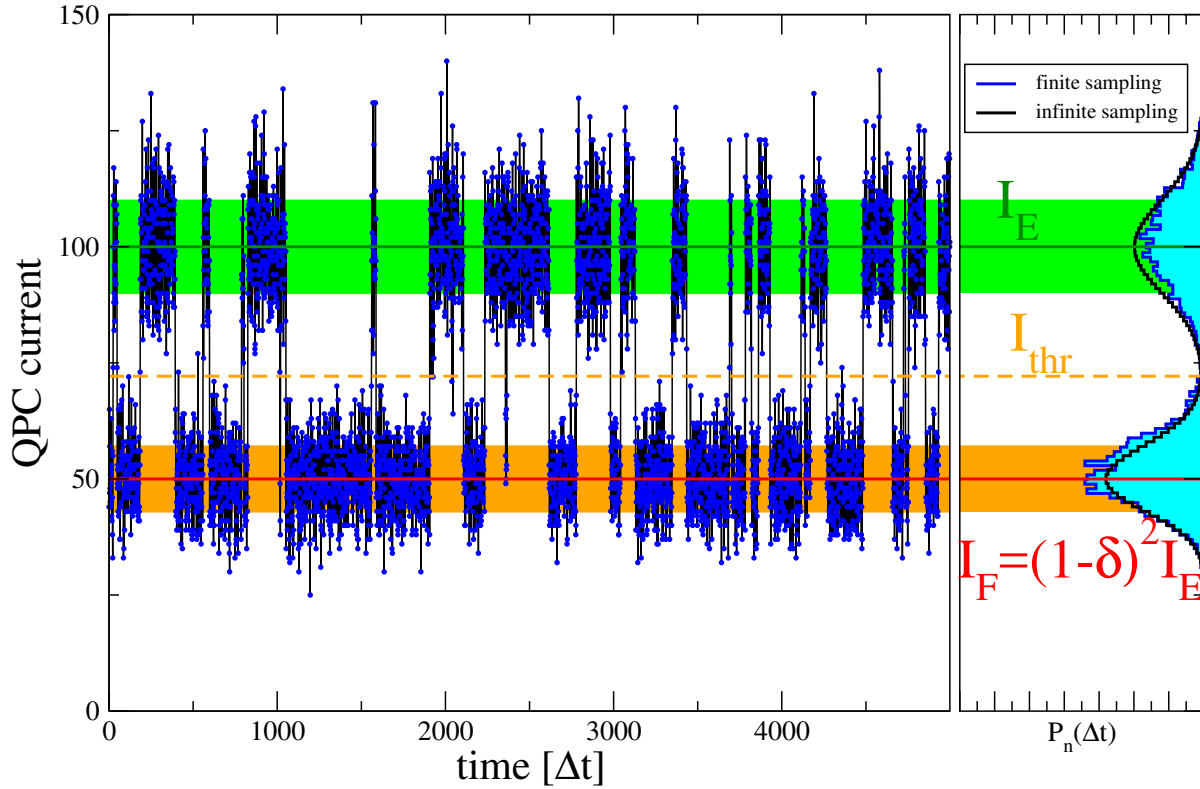


Figure 7.9: Left: Simulated QPC current (7.109) – adapted from Fig. 3.8 – when the dot is allowed to experience slow occupation changes. Solid lines and shaded regions correspond to mean current  $I_{E/F}$  (7.100) and noise  $\sqrt{S_{E/F}}$  (7.101), respectively. To use the device as a detector discriminating empty and filled dot, a discrimination threshold (orange) needs to be chosen suitably. Right: Sampling of the trajectory on the left into a histogram (light color). The black curve would result for infinite sampling. By collecting all measurement outcomes above the threshold into the outcome empty (E) and all measurement outcomes below the threshold as corresponding to the outcome filled (F), one automatically implements a weak measurement on the system (allowing e.g. for the possibility of errors). Parameters as in Fig. 3.8.

with  $P_{\text{err}}^{0(1)}$  the probability of erroneously measuring the empty (filled) state. For suitably chosen  $n_{\text{th}}$ , these indeed approach projectors onto the empty or the filled state as for  $\gamma\Delta t \rightarrow \infty$  we have  $P_{\text{err}} \rightarrow 0$ .

We just note here that for the evolution of an isolated SQD, it does not lead to qualitatively different results whether we consider the limit of infinite coarse-graining times  $\tau \rightarrow \infty$  or the opposite limit  $\tau \rightarrow 0$ . In both treatments, the effect of the detector on the dynamics of the dot occupation vanishes on average.

### 7.3.2 Double quantum dot: Least-invasive measurement

Now, we consider a double quantum dot (DQD)

$$H_S = \epsilon(d_L^\dagger d_L + d_R^\dagger d_R) + T_c(d_L^\dagger d_R + d_R^\dagger d_L) + U d_L^\dagger d_L d_R^\dagger d_R, \quad (7.114)$$

with symmetric on-site energies  $\epsilon$ , Coulomb interaction  $U$ , and tunneling amplitude  $T_c$  (generalizations are of course possible). The transformation into the interaction picture may proceed via the calculation of eigenvalues and eigenvectors of the system Hamiltonian.

If we only measure the left site occupation with the QPC (measuring on the right site is of course also possible), the system coupling operator in the Schrödinger picture becomes  $A = \mathbf{1} - \delta d_L^\dagger d_L$ . However, in contrast to the SQD, the transformation into the interaction picture is less trivial

$$\begin{aligned} \mathbf{A}(t) &= \mathbf{1} - \delta e^{+iH_S t} d_L^\dagger d_L e^{-iH_S t} \\ &= \mathbf{1} - \frac{\delta}{2} \left( d_L^\dagger d_L + d_R^\dagger d_R \right) - \frac{\delta}{4} e^{+2iT_c t} \left[ d_L^\dagger d_L - d_R^\dagger d_R - d_L^\dagger d_R + d_R^\dagger d_L \right] \\ &\quad - \frac{\delta}{4} e^{-2iT_c t} \left[ d_L^\dagger d_L - d_R^\dagger d_R - d_R^\dagger d_L + d_L^\dagger d_R \right] \\ &\equiv A_0 + A_+ e^{+2iT_c t} + A_- e^{-2iT_c t}, \end{aligned} \quad (7.115)$$

where we note that it does only depend on the internal DQD tunneling amplitude  $T_c$ . We can insert this in the coarse-graining dissipator, which under neglect of the Lamb-shift  $\sigma(\omega) \rightarrow 0$  and in the unidirectional QPC transport limit  $\gamma_{12}(\omega) \rightarrow 0$  becomes

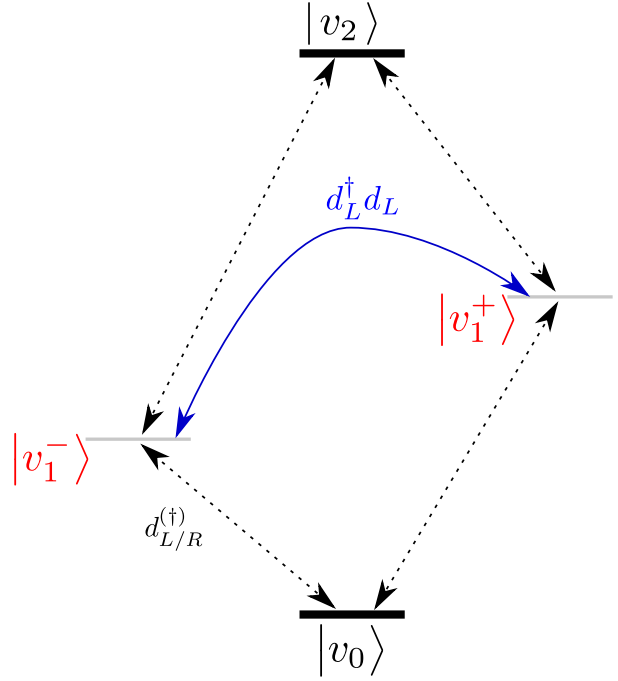
$$\dot{\rho}_{\mathbf{S}} = \frac{1}{2\pi\tau} \int_0^\tau dt_1 dt_2 \int d\omega e^{-i\omega(t_1-t_2)} \gamma_{21}(\omega) \left[ e^{+i\chi} \mathbf{A}(t_2) \rho_{\mathbf{S}} \mathbf{A}(t_1) - \frac{1}{2} \{ \mathbf{A}(t_1) \mathbf{A}(t_2), \rho_{\mathbf{S}} \} \right]. \quad (7.116)$$

Out of the many contributions that arise when inserting the actual time-dependence of the system operator, we only keep those that survive in the limit  $\tau \rightarrow \infty$ , yielding

$$\begin{aligned} \dot{\rho}_{\mathbf{S}} &= \gamma_{21}(+2T) \left[ e^{+i\chi} A_- \rho_{\mathbf{S}} A_+ - \frac{1}{2} \{ A_+ A_-, \rho_{\mathbf{S}} \} \right] + \gamma_{21}(-2T) \left[ e^{+i\chi} A_+ \rho_{\mathbf{S}} A_- - \frac{1}{2} \{ A_- A_+, \rho_{\mathbf{S}} \} \right] \\ &\quad + \gamma_{21}(0) \left[ e^{+i\chi} A_0 \rho_{\mathbf{S}} A_0 - \frac{1}{2} \{ A_0 A_0, \rho_{\mathbf{S}} \} \right]. \end{aligned} \quad (7.117)$$

This dissipator looks quite different from the SQD dissipator: A local coupling in the Hamiltonian leads to a non-local coupling in the dissipator. Phenomenologically, it can move charges between left and right dot and thereby change the charge configuration just by the physical back-action of the measurement. It induces dephasing in the energy eigenbasis of the system but also acts dissipatively, since it can exchange energy with the system, compare Fig. 7.10. The simplest case

Figure 7.10: Sketch of the energy levels of the DQD, which for the chosen simple parameters are at  $E_0 = 0$ ,  $E_{1\pm} = \epsilon \pm T_c$  and  $E_2 = 2\epsilon + U$ . Tunnel-couplings to further DQD leads via  $d_L$  and  $d_R$  from left and right dots may induce the dotted transitions (changing the DQD charge), whereas the coupling to the QPC may only induce transition between the singly-charged states (solid blue) with energy difference  $\Delta E = 2T_c$ .



arises when we consider QPC transmissions that would not allow for energy exchange, which could e.g. be achieved by choosing a narrow transmission function for the QPC, leading to a peaked QPC correlation function. Then, we have

$$\gamma_{21}(+2T_c) \approx 0, \quad \gamma_{21}(-2T_c) \approx 0, \quad \gamma_{21}(0) \neq 0. \quad (7.118)$$

By keeping only the contribution arising from  $A_0$ , we effectively forbid the detector to exchange energy with the system, as can be seen by realizing that  $[H_S, A_0] = 0$ . Then, the dissipator further simplifies

$$\dot{\rho}_{\mathbf{S}} = +\gamma_{21}(0) \left[ e^{+i\chi} A_0 \rho_{\mathbf{S}} A_0 - \frac{1}{2} \{A_0 A_0, \rho_{\mathbf{S}}\} \right] = (e^{+i\chi} \mathcal{J} + \mathcal{L}_0) \rho_{\mathbf{S}}, \quad (7.119)$$

Evaluating this in the energy eigenbasis, this yields with  $A_0 = \mathbf{1} - \delta/2 d_L^\dagger d_L - \delta/2 d_R^\dagger d_R$  the coupled equations (we abbreviate  $\gamma = \gamma_{21}(0)$ )

$$\begin{aligned} \dot{\rho}_{00} &= \gamma(e^{+i\chi} - 1)\rho_{00}, \\ \dot{\rho}_{--} &= \gamma(1 - \delta/2)^2(e^{+i\chi} - 1)\rho_{--}, \\ \dot{\rho}_{++} &= \gamma(1 - \delta/2)^2(e^{+i\chi} - 1)\rho_{++}, \\ \dot{\rho}_{22} &= \gamma(1 - \delta)^2(e^{+i\chi} - 1)\rho_{22}, \\ \dot{\rho}_{-+} &= \gamma(1 - \delta/2)^2(e^{+i\chi} - 1)\rho_{-+}, \\ \dot{\rho}_{+-} &= \gamma(1 - \delta/2)^2(e^{+i\chi} - 1)\rho_{+-}. \end{aligned} \quad (7.120)$$

This means that the measurement damps the coherences in the energy eigenbasis – but leaves the coherences in the local (site-) basis. Without counting ( $\chi \rightarrow 0$ ), there would be no effect of the measurement, not even dephasing. With counting, we have an additional dephasing in the energy eigenbasis due to the measurement. In this limit, the QPC makes no difference between an electron situated on the left or right dot, since it couples to the hybridized states. Consequently,

in its cumulant-generating function we only see three different currents:  $I_0 = \gamma$  for the empty DQD,  $I_1 = \gamma(1 - \delta/2)^2$  for the singly-charged DQD (coherences also contribute to this sector), and  $I_2 = \gamma(1 - \delta)^2$  for the doubly charged DQD. When the DQD is in addition coupled to electronic leads that lead to slow occupation changes, the allowed coherences  $\rho_{-+}$  and  $\rho_{+-}$  will be damped away, and the QPC will only switch between the three allowed current values, not at all resolving the location of the electron in the singly-charged sector. The switching between these currents is dictated by the rates which we have previously calculated for the DQD coupled to two leads, compare Eq. (2.49). When we use four additional counting fields for the DQD leads  $\boldsymbol{\chi} = (\chi_L, \chi_R)$  and  $\boldsymbol{\xi} = (\xi_L, \xi_R)$  for transferred particles and energy, respectively, the total Liouvillian can be written as

$$\mathcal{L}(\boldsymbol{\chi}, \boldsymbol{\xi}, \chi) = \mathcal{L}_{\text{DQD}}(\boldsymbol{\chi}, \boldsymbol{\xi}) + \mathcal{L}_{\text{dt}}(\chi), \quad (7.121)$$

where  $\mathcal{L}_{\text{DQD}}(\boldsymbol{\chi}, \boldsymbol{\xi})$  denotes the DQD Liouvillian with counting fields describing the matter and energy transfers to left and right DQD leads, and where  $\mathcal{L}_{\text{dt}}(\chi)$  is defined by Eq. (7.120). The fact that the measurement is hardly invasive is also exemplified by the fact that the fluctuation theorem for the DQD, exemplified by an existing symmetry of the form, compare Eq. (3.152),

$$\mathcal{L}_{\text{DQD}}^T(-\boldsymbol{\chi} - \mathbf{iA}, -\boldsymbol{\xi} - \mathbf{iB}) = \mathcal{L}_{\text{DQD}}(\boldsymbol{\chi}, \boldsymbol{\xi}), \quad \mathbf{A} = (-\mu_L\beta_L, -\mu_R\beta_R), \quad \mathbf{B} = (\beta_L, \beta_R), \quad (7.122)$$

is under the assumption (7.119) not changed by the presence of the detector

$$\mathcal{L}^T(-\boldsymbol{\chi} - \mathbf{iA}, -\boldsymbol{\xi} - \mathbf{iB}, \chi) = \mathcal{L}(\boldsymbol{\chi}, \boldsymbol{\xi}, \chi), \quad (7.123)$$

since the counting field of the latter only occurs on the diagonal in this limit. By contrast, if TQD and QPC detector are allowed to exchange energy, a fluctuation theorem involving only the monitored system does no longer hold. For this, also the entropy produced in the detector leads then need to be considered. To interpret the outcome of the detector, we consider Fig. 7.11.

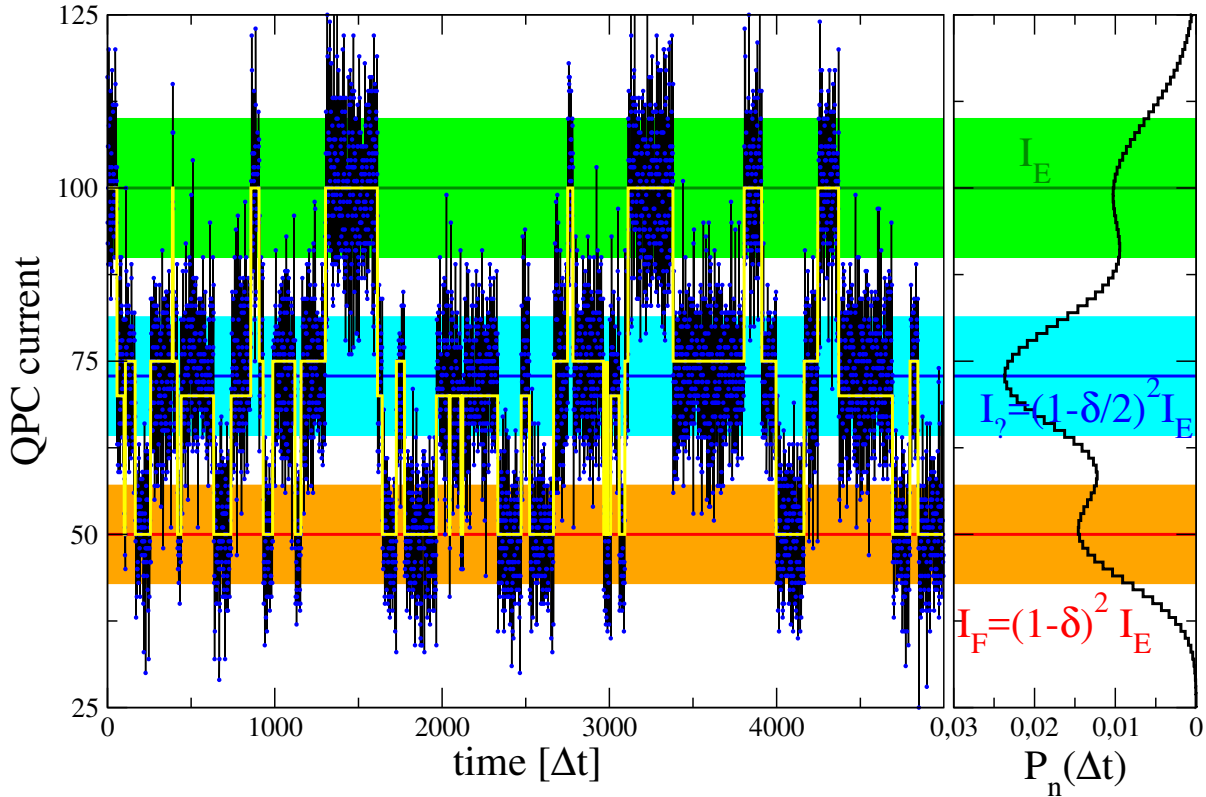


Figure 7.11: Left: Simulated QPC current when the DQD is allowed to experience slow occupation changes. Solid lines and shaded regions correspond to mean current and noise, respectively. The yellow curve depicts the actual state of the system, ordered from top to bottom values as  $|v_0\rangle$ ,  $|v_-\rangle$ ,  $|v_+\rangle$ , and  $|v_2\rangle$ , respectively. Right: Corresponding histogram for infinitely long sampling of the trajectory – calculated by computing the weighted average (for the chosen parameters we have  $P_0 = P_- = P_+ = P_2 = 1/4$ ) of Poissonian distributions for the respective QPC currents. In contrast to Fig. 7.9, there are now three QPC currents observed, and two thresholds can be defined. By collecting all measurement outcomes above the upper threshold into the outcome empty (E) and all measurement outcomes below the lower threshold as corresponding to the outcome filled (F), we can implement the measurement superoperators as before. However, in addition there is now a third outcome (inconclusive). When measuring the medium current, the probability for the left dot to be occupied or empty is  $1/2$ . Other parameters as in Fig. 3.8.

There, one can observe three currents, where the lowest one corresponds to a doubly filled DQD, and the highest one to an empty DQD. The intermediate current corresponds to a singly-charged DQD, where however due to the high symmetry we cannot resolve the location of the charge at all. Therefore, upon measuring this intermediate current, the probability to find the monitored empty or filled is just one half, respectively. Since the original intention of the detector model was to measure the charge of the left dot, this outcome should be termed inconclusive. Thereby, we have designed a measurement that does not perturb the system state, a so-called quantum-non-demolition measurement or **QND-measurement**. Technically, this requires a low-bandwidth detector not inducing any transitions between energy eigenstates but only dephasing. The price to pay for this is an inconclusive measurement outcome.

The Liouvillian superoperators obey due to our special choice of operators  $[\mathcal{J}, \mathcal{L}_0] = 0$ . In this

case, we can compute the effective measurement propagator exactly

$$\mathcal{K}_n(\Delta t) = \frac{1}{2\pi} \int_{-\pi}^{+\pi} e^{e^{+ix}\mathcal{J}\Delta t + \mathcal{L}_0\Delta t - in\chi} d\chi = \frac{\mathcal{J}^n \Delta t^n}{n!} e^{\mathcal{L}_0\Delta t}, \quad (7.124)$$

and by defining the thresholds  $n_1 < n_2$ , we can define the measurement superoperators in the same way as we did before

$$\mathcal{K}_E = \sum_{n \geq n_2} \mathcal{K}_n(\Delta t), \quad \mathcal{K}_? = \sum_{n_1 < n < n_2} \mathcal{K}_n(\Delta t), \quad \mathcal{K}_F = \sum_{n \leq n_1} \mathcal{K}_n(\Delta t). \quad (7.125)$$

In contrast to the single quantum dot however, the measurement – when performed on a singly-charged state – does not resolve the site of the electron. Furthermore, not considering the counting statistics of the QPC at all ( $\chi \rightarrow 0$ ), we see that the associated Liouvillian vanishes. From this we can also show that

$$\mathcal{K}_E + \mathcal{K}_? + \mathcal{K}_F = \mathbf{1}. \quad (7.126)$$

Note that the equations would be more complicated if we allowed the QPC to exchange energy with the DQD system (e.g. finite  $\gamma_{21}(\pm 2T)$ , such that e.g. the blue transition in Fig. 7.10 would be allowed) or if we would make the DQD more asymmetric  $\epsilon_L \neq \epsilon_R$ . Then also the original fluctuation theorem would be modified or would have to be generalized by including the QPC counting field, and depending on the system configuration one may also observe four different currents instead of three, allowing for the possibility to approximately locate the electron.

### 7.3.3 Triple quantum dot: Least invasive measurement

Motivated by experimental setups of tunable triple quantum dots [50] we now we consider a serial double quantum dot (TQD), which for simplicity we choose highly symmetric and in addition without Coulomb interaction

$$H_S = \epsilon(d_L^\dagger d_L + d_C^\dagger d_C + d_R^\dagger d_R) + T_L(d_L^\dagger d_C + d_C^\dagger d_L) + T_R(d_C^\dagger d_R + d_R^\dagger d_C). \quad (7.127)$$

The spectrum of the TQD can in this simple case also be obtained analytically

$$\begin{aligned}
|v_0\rangle &= |000\rangle, & E_0 &= 0, \\
|v_1^-\rangle &= \frac{1}{\sqrt{2 + 2\frac{T_R^2}{T_L^2}}} |100\rangle - \frac{1}{\sqrt{2}} |010\rangle + \frac{1}{\sqrt{2 + 2\frac{T_L^2}{T_R^2}}} |001\rangle, & E_1^- &= \epsilon - \sqrt{T_L^2 + T_R^2}, \\
|v_1^0\rangle &= -\sqrt{\frac{T_R^2}{T_L^2 + T_R^2}} |100\rangle + \frac{1}{\sqrt{1 + \frac{T_R^2}{T_L^2}}} |001\rangle, & E_1^0 &= \epsilon, \\
|v_1^+\rangle &= \frac{1}{\sqrt{2 + 2\frac{T_R^2}{T_L^2}}} |100\rangle + \frac{1}{\sqrt{2}} |010\rangle + \frac{1}{\sqrt{2 + 2\frac{T_L^2}{T_R^2}}} |001\rangle, & E_1^+ &= \epsilon + \sqrt{T_L^2 + T_R^2}, \\
|v_2^-\rangle &= \frac{1}{\sqrt{2 + 2\frac{T_L^2}{T_R^2}}} |110\rangle - \frac{1}{\sqrt{2}} |101\rangle + \frac{1}{\sqrt{2 + 2\frac{T_R^2}{T_L^2}}} |011\rangle, & E_2^- &= 2\epsilon - \sqrt{T_L^2 + T_R^2}, \\
|v_2^0\rangle &= -\sqrt{\frac{T_L^2}{T_L^2 + T_R^2}} |110\rangle + \frac{1}{\sqrt{1 + \frac{T_L^2}{T_R^2}}} |011\rangle, & E_2^0 &= 2\epsilon, \\
|v_2^+\rangle &= \frac{1}{\sqrt{2 + 2\frac{T_L^2}{T_R^2}}} |110\rangle + \frac{1}{\sqrt{2}} |101\rangle + \frac{1}{\sqrt{2 + 2\frac{T_R^2}{T_L^2}}} |011\rangle, & E_2^+ &= 2\epsilon + \sqrt{T_L^2 + T_R^2}, \\
|v_3\rangle &= |111\rangle, & E_3 &= 3\epsilon.
\end{aligned} \tag{7.128}$$

We see that the splitting between states of equal charge that have a non-vanishing matrix element with the operator  $d_C^\dagger d_C$  is  $\Delta E = 2\sqrt{T_L^2 + T_R^2}$ .

When the point contact measures the central dot, i.e.,  $A = \mathbf{1} - \delta d_C^\dagger d_C$ , the transformation into the interaction picture becomes

$$\mathbf{A}(t) = A_0 + A_- e^{-2it\sqrt{T_L^2 + T_R^2}} + A_+ e^{+2it\sqrt{T_L^2 + T_R^2}}. \tag{7.129}$$

Here, we have specifically

$$A_0 = \mathbf{1} - \frac{\delta}{2} \left[ \frac{T_R^2}{T_L^2 + T_R^2} d_R^\dagger d_R + \frac{T_L^2}{T_L^2 + T_R^2} d_L^\dagger d_L + d_C^\dagger d_C + \frac{T_L T_R}{T_L^2 + T_R^2} (d_L^\dagger d_R + d_R^\dagger d_L) \right]. \tag{7.130}$$

The dissipator then becomes in the unidirectional transport limit (under neglect of Lamb-shift and taking  $\tau \rightarrow \infty$ )

$$\begin{aligned}
\dot{\rho}_{\mathbf{s}} &= \gamma_{21} (+2\sqrt{T_L^2 + T_R^2}) \left[ e^{+ix} A_- \rho_{\mathbf{s}} A_+ - \frac{1}{2} \{A_+ A_-, \rho_{\mathbf{s}}\} \right] \\
&\quad + \gamma_{21} (-2\sqrt{T_L^2 + T_R^2}) \left[ e^{+ix} A_+ \rho_{\mathbf{s}} A_- - \frac{1}{2} \{A_- A_+, \rho_{\mathbf{s}}\} \right] \\
&\quad + \gamma_{21}(0) \left[ e^{+ix} A_0 \rho_{\mathbf{s}} A_0 - \frac{1}{2} \{A_0 A_0, \rho_{\mathbf{s}}\} \right].
\end{aligned} \tag{7.131}$$

The presence of the detector may again in principle induce transitions between eigenstates of the same charge, Fig. 7.12. However, to obtain the least invasive detector we consider a limit where

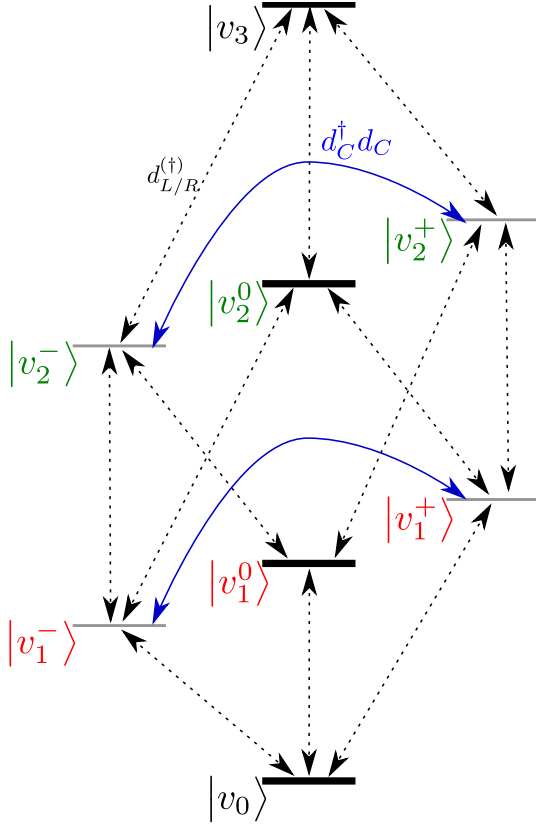


Figure 7.12: Sketch of the energy levels of the TQD. Only the eigenstates marked bold have either an always filled or and always empty central dot. In principle, the leads of the TQD may induce transitions between states with total particle difference  $\pm 1$  (dotted), whereas the QPD may induce only transitions between states of equal charge (blue). However, due to the high symmetry in the model ( $\epsilon_L = \epsilon_C = \epsilon_R = \epsilon$  and  $U = 0$ ), only particular transitions are allowed. In the QND limit, even the QPC-induced transition between the equally-charged states (solid blue) with energy difference  $\Delta E = 2\sqrt{T_L^2 + T_R^2}$  is forbidden.

the detector does not inject energy, by considering the limit  $\gamma_{21}(\pm 2\sqrt{T_L^2 + T_R^2}) \rightarrow 0$ , i.e.,

$$\dot{\rho}_{\mathbf{S}} = \gamma_{21}(0) \left[ e^{+i\chi} A_0 \rho_{\mathbf{S}} A_0 - \frac{1}{2} \{A_0 A_0, \rho_{\mathbf{S}}\} \right]. \quad (7.132)$$

That in this case the detector does not inject energy is also exemplified by the relation  $[H_S, A_0] = 0$ . However, now even in absence of counting  $\chi \rightarrow 0$ , the effect of the detector is non-trivial. In contrast to the DQD, the dissipator  $\mathcal{L}(0)$  does not vanish. This is essentially due to the fact that the system energy eigenstates with a different occupation of the central dot have different energies, compare  $|v_1^0\rangle$  with  $|v_1^\pm\rangle$  and  $|v_2^0\rangle$  with  $|v_2^\pm\rangle$ .

By sandwiching the dissipator, we get the following equations for the diagonal entries (for simplicity, we only state these as we assume that the coherences are damped away in the long-term limit by additional leads attached to the TQD left and right)

$$\begin{aligned} \dot{\rho}_0 &= \gamma(e^{+i\chi} - 1)\rho_0, \\ \dot{\rho}_{10} &= \gamma(e^{+i\chi} - 1)\rho_{10}, \\ \dot{\rho}_{1-} &= \gamma(1 - \delta/2)^2(e^{+i\chi} - 1)\rho_{1-}, \\ \dot{\rho}_{1+} &= \gamma(1 - \delta/2)^2(e^{+i\chi} - 1)\rho_{1+}, \\ \dot{\rho}_{2-} &= \gamma(1 - \delta/2)^2(e^{+i\chi} - 1)\rho_{2-}, \\ \dot{\rho}_{2+} &= \gamma(1 - \delta/2)^2(e^{+i\chi} - 1)\rho_{2+}, \\ \dot{\rho}_{20} &= \gamma(1 - \delta)^2(e^{+i\chi} - 1)\rho_{20}, \\ \dot{\rho}_3 &= \gamma(1 - \delta)^2(e^{+i\chi} - 1)\rho_3. \end{aligned} \quad (7.133)$$

The equations for the 12 allowed coherences are similar with one exception (not shown): As  $\chi \rightarrow 0$ , the QPC has a non-vanishing effect on some of the coherences. As with the DQD, we can identify three currents:  $I_E = \gamma$ , when the central dot is empty with certainty,  $I_1 = \gamma(1 - \delta/2)$ , when the central dot is empty with probability 1/2, and  $I_F = \gamma(1 - \delta)^2$ , when the central dot is filled with certainty. We can readily set up the BMS rate equation in the energy eigenbasis of the TQD

$$\dot{\rho}_{aa} = \sum_b \gamma_{ab,ab} \rho_{bb} - \sum_b \gamma_{ba,ba} \rho_{aa}, \quad \gamma_{ab} = \sum_{\alpha\beta} \gamma_{\alpha\beta} (E_b - E_a) \langle a | A_\beta | b \rangle \langle a | A_\alpha^\dagger | b \rangle^*, \quad (7.134)$$

which for brevity we do not show explicitly here. Fig. 7.12 may serve as a guidance here, for example, the rate to relax from  $|v_1^0\rangle$  to  $|v_0\rangle$  is given by

$$R_{0,10} = \Gamma_L [1 - f_L(\epsilon)] \frac{T_R^2}{T_L^2 + T_R^2} + \Gamma_R [1 - f_R(\epsilon)] \frac{T_L^2}{T_L^2 + T_R^2}. \quad (7.135)$$

We can set up the full master equation as before, and, as the QPC counting field only enters on the diagonal, the same arguments as before apply, such that the TQD fluctuation theorem is not modified in this limit. In a similar fashion as for the DQD, we can also generate trajectories for the QPC current. The result (not shown) looks just as the curve with symbols in Fig. 7.11, and again the possibility of an inconclusive measurement result occurs. However, even when one measures e.g. a high current with sufficient confidence, one is not sure whether the TQD is actually in the state  $|v_0\rangle$  or in the state  $|v_1^0\rangle$ . This limitation of measurement is something fundamental and related to the uncertainty relation.

From the results of the last two sections, we see that a minimally invasive detector (leading only to dephasing in the system energy eigenbasis) does not completely fulfil the purpose for which it was constructed: It measures populations of energy eigenstates instead of populations of sites, which need not always coincide and therefore induces an inconclusive outcome. Below, we will discuss a variant of the detector that measures the local occupation.

### 7.3.4 Projective QPC limit

So far, we have explored the limit where the QPC correlation functions decayed much faster than the dynamics of the system, enabling the coarse-graining time to be sent to infinity (i.e., the secular master equation) even though we actually used finite measurement intervals. Now, we consider the limit where the internal dynamics of the system can be neglected, which can happen for a number of reasons

- the system Hamiltonian is weak comparable to the interaction and the bath  $|H_S| \ll |H_I| \ll |H_B|$ , such that the interaction picture dynamics is negligible,
- the system dynamics in the interaction picture is much slower than the decay of the correlation functions, such that for small measurement intervals  $\tau = \Delta t$ , the dominant variation in the integrand is generated by the correlation functions
- the coupling operators commute with the system Hamiltonian, such that they remain time-independent throughout,
- the measurement duration is so small that neither the decay of the correlation function nor the dynamics of the system coupling operators matters.



Since for this dissipator we have  $[\mathcal{J}, \mathcal{J}_0] = \mathbf{0}$ , we can calculate the quantities for detection analytically

$$\mathcal{K}_n(\Delta t) = \frac{1}{2\pi} \int_{-\pi}^{+\pi} e^{\mathcal{L}_{\text{dt}}(\chi)\Delta t - in\chi} d\chi = \frac{\mathcal{J}^n \Delta t^n}{n!} e^{-\mathcal{J}_0 \Delta t}. \quad (7.140)$$

In particular, we use the identity

$$(\mathbf{1} - \delta d^\dagger d)^n = [dd^\dagger + (1 - \delta)d^\dagger d]^n = dd^\dagger + (1 - \delta)^n d^\dagger d. \quad (7.141)$$

to compute

$$\begin{aligned} \mathcal{J}^n \rho &= \gamma^n [dd^\dagger + (1 - \delta)^n d^\dagger d] \rho [dd^\dagger + (1 - \delta)^n d^\dagger d], \\ e^{-\mathcal{J}_0 \Delta t} \rho &= \sum_{n=0}^{\infty} \frac{(-1)^n \gamma^n \Delta t^n}{2^n n!} [1 - \delta d^\dagger d]^{2n} \rho \sum_{m=0}^{\infty} \frac{(-1)^m \gamma^m \Delta t^m}{2^m m!} [1 - \delta d^\dagger d]^{2m} \\ &= \sum_{n=0}^{\infty} \frac{(-1)^n \gamma^n \Delta t^n}{2^n n!} [dd^\dagger + (1 - \delta)^{2n} d^\dagger d] \rho \sum_{m=0}^{\infty} \frac{(-1)^m \gamma^m \Delta t^m}{2^m m!} [dd^\dagger + (1 - \delta)^{2m} d^\dagger d]^m \\ &= [e^{-\gamma/2\Delta t} dd^\dagger + e^{-\gamma/2\Delta t(1-\delta)^2} d^\dagger d] \rho [e^{-\gamma/2\Delta t} dd^\dagger + e^{-\gamma/2\Delta t(1-\delta)^2} d^\dagger d] \\ &= e^{-\gamma\Delta t} dd^\dagger \rho dd^\dagger + e^{-\gamma(1-\delta)^2\Delta t} d^\dagger \rho d^\dagger d + e^{-\gamma(1-\delta+\delta^2/2)\Delta t} (dd^\dagger \rho d^\dagger d + d^\dagger \rho dd^\dagger), \\ e^{+\mathcal{J}e^{+ix}\Delta t} \rho &= \sum_{n=0}^{\infty} \frac{\gamma^n \Delta t^n e^{+inx}}{n!} [dd^\dagger + (1 - \delta)^n d^\dagger d] \rho [dd^\dagger + (1 - \delta)^n d^\dagger d] \\ &= \sum_{n=0}^{\infty} \frac{\gamma^n \Delta t^n e^{inx}}{n!} [dd^\dagger \rho dd^\dagger + (1 - \delta)^{2n} d^\dagger \rho d^\dagger d + (1 - \delta)^n (dd^\dagger \rho d^\dagger d + d^\dagger \rho dd^\dagger)] \\ &= e^{+\gamma\Delta t e^{+ix}} dd^\dagger \rho dd^\dagger + e^{+\gamma\Delta t(1-\delta)^2 e^{+ix}} d^\dagger \rho d^\dagger d + e^{+\gamma\Delta t(1-\delta) e^{+ix}} (dd^\dagger \rho d^\dagger d + d^\dagger \rho dd^\dagger). \end{aligned} \quad (7.142)$$

In particular, from combining the last two identities we obtain for the action of the full dissipator

$$e^{\mathcal{L}_{\text{dt}}(0)\Delta t} \rho = dd^\dagger \rho dd^\dagger + d^\dagger \rho d^\dagger d + e^{-\gamma\Delta t \delta^2/2} (dd^\dagger \rho d^\dagger d + d^\dagger \rho dd^\dagger). \quad (7.143)$$

From this, we obtain that the exponential of this particular dissipator has a very similar action than the dissipator itself

$$(e^{\mathcal{L}_{\text{dt}}(0)\Delta t} - \mathbf{1}) \rho = (e^{-\gamma\Delta t \delta^2/2} - 1) (dd^\dagger \rho d^\dagger d + d^\dagger \rho dd^\dagger) = \frac{1 - e^{-\gamma\Delta t \delta^2/2}}{\gamma\delta^2/2} \mathcal{L}_{\text{dt}}(0) \rho. \quad (7.144)$$

This can be helpful to evaluate the energy change of the system during such a measurement of duration  $\Delta t$

$$\Delta E = \text{Tr} \{ H_S (e^{\mathcal{L}_{\text{dt}}(0)\Delta t} - \mathbf{1}) \rho \} = \frac{1 - e^{-\gamma\Delta t \delta^2/2}}{\gamma\delta^2/2} \text{Tr} \{ H_S (\mathcal{L}_{\text{dt}}(0) \rho) \}, \quad (7.145)$$

which enables to define a current

$$I_E^{\text{ms}} = \frac{\Delta E}{\Delta t} = \frac{1 - e^{-\alpha}}{\alpha} \text{Tr} \{ H_S (\mathcal{L}_{\text{dt}}(0) \rho) \}, \quad \alpha = \frac{\gamma\Delta t \delta^2}{2}. \quad (7.146)$$

For small  $\alpha$ , this corresponds to the usual phenomenologically defined current, whereas for large  $\alpha$ , this tends to zero. We also note that the prefactor is always smaller than one.

We can be more specific and ask for the system energy change for a specific measurement outcome

$$\Delta E_n = \text{Tr} \left\{ H_S \left( \frac{\mathcal{K}_n(\Delta t)\rho}{\text{Tr} \{ \mathcal{K}_n(\Delta t)\rho \}} - \rho \right) \right\}, \quad (7.147)$$

or – after having defined a suitable threshold to separate between just two outcomes (empty and filled) – for the average system energy change under measuring the outcome empty (E) or filled (F), respectively

$$\Delta E_E = \frac{1}{P_E} \text{Tr} \{ H_S(\mathcal{K}_E(\Delta t) - P_E)\rho \}, \quad \Delta E_F = \frac{1}{P_F} \text{Tr} \{ H_S(\mathcal{K}_F(\Delta t) - P_F)\rho \}, \quad (7.148)$$

where  $P_E = \text{Tr} \{ \mathcal{K}_E(\Delta t)\rho \}$  and  $P_F = \text{Tr} \{ \mathcal{K}_F(\Delta t)\rho \}$ , respectively. For these questions it is helpful to compute

$$\begin{aligned} \mathcal{K}_n(\Delta t)\rho &= \frac{(\gamma\Delta t)^n}{n!} e^{-\gamma\Delta t} dd^\dagger pdd^\dagger + \frac{(\gamma\Delta t(1-\delta)^2)^n}{n!} e^{-\gamma\Delta t(1-\delta)^2} d^\dagger d\rho d^\dagger d \\ &\quad + \frac{(\gamma\Delta t(1-\delta))^n}{n!} e^{-\gamma\Delta t(1-\delta)} e^{-\gamma\Delta t\delta^2/2} (dd^\dagger \rho d^\dagger d + d^\dagger d\rho dd^\dagger). \end{aligned} \quad (7.149)$$

It may be convenient to parametrize such a measurement by just two dimensionless numbers  $0 \ll y \ll x$

$$x = \gamma\Delta t, \quad y = \gamma\Delta t(1-\delta)^2. \quad (7.150)$$

Then, we have

$$\sqrt{xy} = \gamma\Delta t(1-\delta), \quad \frac{\gamma\Delta t\delta^2}{2} = \frac{(\sqrt{x} - \sqrt{y})^2}{2}, \quad (7.151)$$

which completely defines the measurement superoperators. The measurement becomes strong (in the sense that it deletes coherences) when  $x$  and  $y$  are very different, and it also becomes error-free (projective) when both  $x$  and  $y$  are very large but different. It becomes completely non-invasive (after normalization), when  $x = y$ .

From summing up all outcomes up to a threshold  $n_{\text{th}}$ , we get the propagator for the coarse-grained measurement result *filled*

$$\begin{aligned} \mathcal{K}_F\rho &= \frac{\Gamma(n_{\text{th}} + 1, \gamma\Delta t)}{\Gamma(n_{\text{th}} + 1)} dd^\dagger pdd^\dagger + \frac{\Gamma(n_{\text{th}} + 1, \gamma\Delta t(1-\delta)^2)}{\Gamma(n_{\text{th}} + 1)} d^\dagger d\rho d^\dagger d \\ &\quad + \frac{\Gamma(n_{\text{th}} + 1, \gamma\Delta t(1-\delta))}{\Gamma(n_{\text{th}} + 1)} e^{-\gamma\Delta t\delta^2/2} (dd^\dagger \rho d^\dagger d + d^\dagger d\rho dd^\dagger), \end{aligned} \quad (7.152)$$

and from  $\mathcal{K}_E + \mathcal{K}_F = e^{\mathcal{L}_{\text{dt}}\Delta t}$  we conclude for the result *empty*

$$\begin{aligned} \mathcal{K}_E\rho &= \left( 1 - \frac{\Gamma(n_{\text{th}} + 1, \gamma\Delta t)}{\Gamma(n_{\text{th}} + 1)} \right) dd^\dagger pdd^\dagger + \left( 1 - \frac{\Gamma(n_{\text{th}} + 1, \gamma\Delta t(1-\delta)^2)}{\Gamma(n_{\text{th}} + 1)} \right) d^\dagger d\rho d^\dagger d \\ &\quad + \left( 1 - \frac{\Gamma(n_{\text{th}} + 1, \gamma\Delta t(1-\delta))}{\Gamma(n_{\text{th}} + 1)} \right) e^{-\gamma\Delta t\delta^2/2} (dd^\dagger \rho d^\dagger d + d^\dagger d\rho dd^\dagger). \end{aligned} \quad (7.153)$$

The function  $f(n_{\text{th}}, x) \equiv \frac{\Gamma(n_{\text{th}}+1, x)}{\Gamma(n_{\text{th}}+1)}$  behaves similar to a Fermi function as a function of  $x$ , it is always between 0 and 1, in particular it is 1 when  $x \ll n_{\text{th}}$  and it is zero when  $x \gg n_{\text{th}}$ . Its steepest descent is found at  $x^* = n_{\text{th}}$ , for which an optimal value can also be expressed in terms of  $x$  and  $y$

$$n_{\text{th}} = \frac{x - y}{\ln \frac{x}{y}}. \quad (7.154)$$

With the additional suppression of coherences, these measurement superoperators indeed approach ideal projectors onto the empty or filled state, respectively. Furthermore, being the exponential of Lindblad evolutions, they preserve the density matrix properties (after normalization), i.e., they automatically implement a weak measurement of the occupation, with the limit  $\gamma \Delta t \delta^2 / 2 \rightarrow \infty$  limit of a strong measurement (deleting the coherences).

We now consider a series of infinitesimally short measurements, parametrized only by  $x$  and  $y$  and performed at timesteps of  $\Delta\tau > 0$ , in between which the Liouvillian  $\mathcal{L}_{\text{TQD}}$  of a triple quantum dot shall be acting. The density matrix at time  $t + \Delta\tau$  can then be iteratively obtained

$$\rho(t + \Delta\tau) = \frac{1}{P_n(x, y)} e^{\mathcal{L}_{\text{TQD}} \Delta\tau} \mathcal{K}_n(x, y) \rho(t), \quad P_n(x, y) = \text{Tr} \{ \mathcal{K}_n(x, y) \rho(t) \}, \quad (7.155)$$

where  $P_n(x, y)$  denotes the probability to measure  $n$  particles. We can now check how different measurement schemes affect the subsequent evolution [6], see Fig. 7.13. In the first three panels of Fig. 7.13 we consider a measurement in the site basis, derived within the singular-coupling limit, described by the exponential of Eq. (7.137). In the last (bottom right) panel we consider a non-invasive quantum non-demolition (QND) measurement, described by the exponential of Eq. (7.132).

First, when  $x = y$  (or  $\delta = 0$ , top left), the detector (here measuring in the local basis) is not sensitive at all to the system and it does not influence its dynamics. For unidirectional transport, the detector statistics is then just Poissonian and the system behaves as if it was not monitored, i.e., the dot occupation simply evolves according to the SET master equation until it reaches a stationary value.

Second, when the detector measures in the local basis (top right) and is sensitive to the system occupation, the repeated application of the measurement leads to the superposition of two Poissonian processes for the detector statistics, and projects the system density matrix, suppressing coherences. The occupation of the central dot is clearly correlated with the measurement result, although the correlation is not perfect due to measurement errors.

Third, an even more frequent application of the measurement (bottom left) leads for an invasive detector to the suppression of coherences, quantum-Zeno trapping the population of the central dot, independent of the initial condition (blue and magenta). Significantly less jumps are observed, and the error rate of the measurement drops.

Finally, when implementing a QND-measurement in the energy eigenbasis (bottom right), a third, inconclusive, outcome is introduced in the detector statistics, during which the system evolves coherently as if it was decoupled from the leads. This coherent dynamics is the intrinsic evolution of the TQD energy eigenstates, generated only by  $H_{\text{TQD}}$ . Thus, if for example decoupled the TQD from its reservoirs  $\Gamma_L = \Gamma_R = 0$  and initialize the system in one of the pure states  $|v_{1/2}^\pm\rangle$ , such a non-invasive detector would not have any effect.

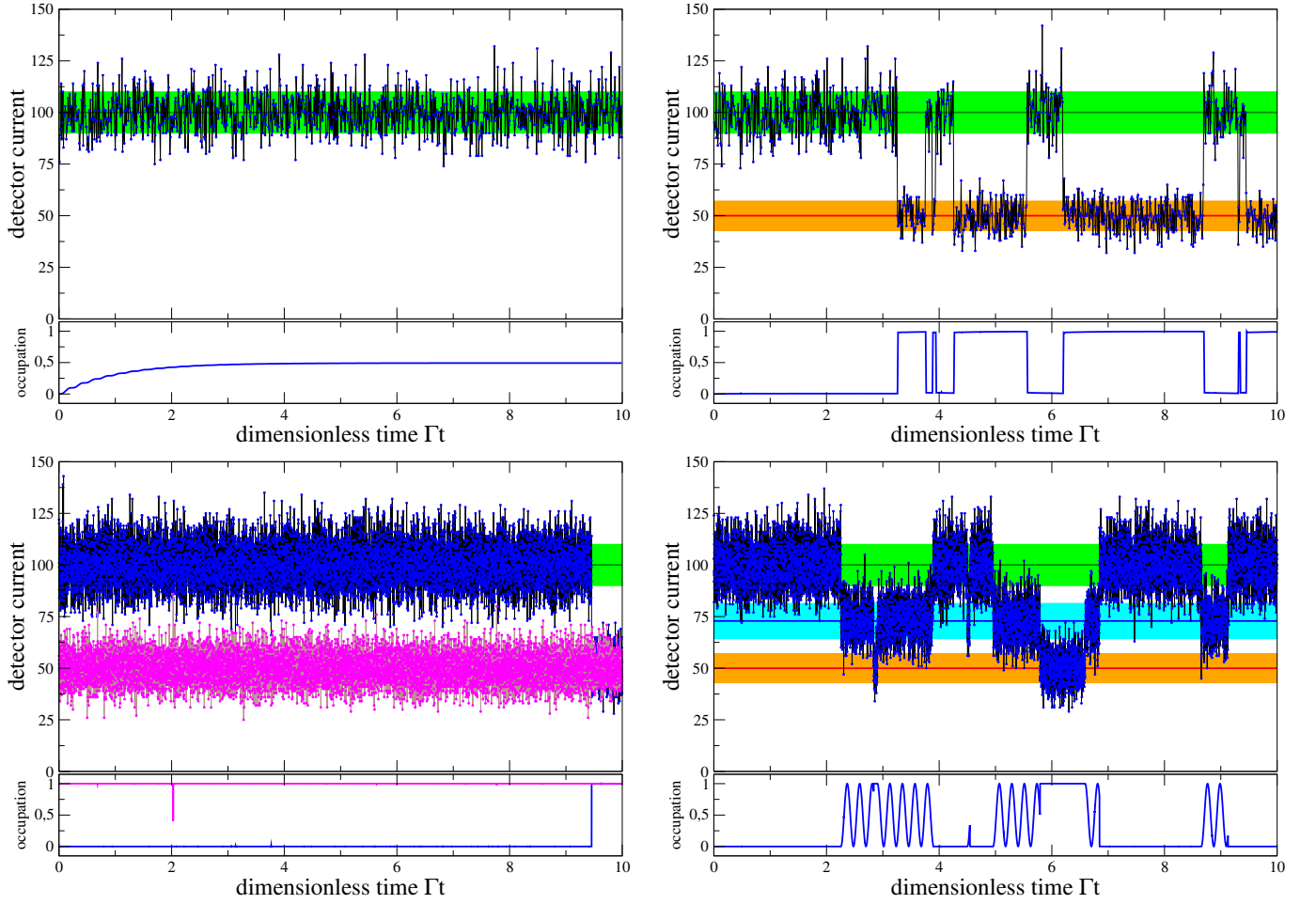


Figure 7.13: Plot of detector current trajectories (symbols) and system occupations (curves) for a completely insensitive detector (top left), an invasive detector (top right), an invasive detector which measures 10 times more frequently (bottom left, for different initial conditions) and a non-invasive QND detector which measures also very frequently but in the energy eigenbasis (bottom right). Parameters:  $\Gamma_L = \Gamma_R = \Gamma$ ,  $\beta_L = \beta_R = \beta$ ,  $T_L = T_R = T$ ,  $\beta\Gamma = 0.01$ ,  $\beta T = 0.1$ ,  $\beta\mu_L = +5 = -\beta\mu_R$ ,  $\beta\epsilon = 1$ ,  $x = 100$ ,  $y = 50$  (top left:  $y = 100$ ),  $\Gamma\Delta t = 0.01$  (top panels),  $\Gamma\Delta t = 0.001$  (bottom panels).

## 7.4 A non-perturbative form for entropy production

A recent paper by M. Esposito nicely discusses general properties of entropy production that hold independent of the used master equation approaches [51]. We start from a setting where both system and interaction Hamiltonians are allowed to be time-dependent

$$H(t) = H_S(t) + \sum_{\nu} H_I^{(\nu)}(t) + \sum_{\nu} H_B^{(\nu)}. \quad (7.156)$$

Initially, we assume that the system and reservoirs are uncorrelated, and that the reservoirs are initially at thermal equilibrium states

$$\rho(0) = \rho_S(0) \bigotimes_{\nu} \bar{\rho}_{\nu}, \quad \bar{\rho}_{\nu} = \frac{e^{-\beta_{\nu}(H_B^{(\nu)} - \mu_{\nu} N_B^{(\nu)})}}{Z_{\nu}}, \quad (7.157)$$

where  $Z_\nu$  and  $N_B^{(\nu)}$  denote partition function and reservoir particle number of reservoir  $\nu$ , respectively. We will only assume this at the initial time, but not for  $t > 0$ . In fact, the treatment is so general that the reservoirs can be arbitrarily small, they can even consist of single qubits and they can move arbitrarily far away from any product state during the evolution. The only formal requirement is that they are initially represented as a thermal equilibrium state.

Since the evolution of the total universe is unitary, its total entropy is a constant of motion, yielding the relation

$$\Sigma(t) = -\text{Tr} \{ \rho(t) \ln \rho(t) \} = -\text{Tr} \{ \rho(0) \ln \rho(0) \} = -\text{Tr}_S \{ \rho_S(0) \ln \rho_S(0) \} - \sum_\nu \text{Tr}_\nu \{ \bar{\rho}_\nu \ln \bar{\rho}_\nu \} , \quad (7.158)$$

where we have used that for an initial product state it is additive in system and reservoir contributions. Now, we introduce the exact (i.e., without any master equation approximation) local reduced density matrices of system and reservoirs

$$\rho_S(t) = \text{Tr}_{\{\nu\}} \{ \rho(t) \} , \quad \rho_\nu(t) = \text{Tr}_{S, \nu' \neq \nu} \{ \rho(t) \} , \quad (7.159)$$

and turn to the entropy of the system

$$S(t) = -\text{Tr}_S \{ \rho_S(t) \ln \rho_S(t) \} . \quad (7.160)$$

We see that its initial value is related to the full entropy of the universe via

$$S(0) = \Sigma(0) + \sum_\nu \text{Tr}_\nu \{ \bar{\rho}_\nu \ln \bar{\rho}_\nu \} . \quad (7.161)$$

Its change can therefore be written as

$$\begin{aligned} \Delta S(t) &= S(t) - S(0) \\ &= -\text{Tr}_S \{ \rho_S(t) \ln \rho_S(t) \} + \text{Tr} \{ \rho(t) \ln \rho(t) \} - \sum_\nu \text{Tr}_\nu \{ \bar{\rho}_\nu \ln \bar{\rho}_\nu \} \\ &= -\text{Tr} \{ \rho(t) \ln \rho_S(t) \} + \text{Tr} \{ \rho(t) \ln \rho(t) \} - \sum_\nu \text{Tr}_\nu \{ \bar{\rho}_\nu \ln \bar{\rho}_\nu \} \\ &= -\text{Tr} \left\{ \rho(t) \ln \left[ \rho_S(t) \otimes_\nu \bar{\rho}_\nu \right] \right\} + \text{Tr} \{ \rho(t) \ln \rho(t) \} + \sum_\nu \text{Tr}_\nu \{ [\rho_\nu(t) - \bar{\rho}_\nu] \ln \bar{\rho}_\nu \} \\ &= D \left( \rho(t) \left\| \rho_S(t) \otimes_\nu \bar{\rho}_\nu \right. \right) - \sum_\nu \beta_\nu \text{Tr}_\nu \left\{ [\rho_\nu(t) - \bar{\rho}_\nu] \left[ H_B^{(\nu)} - \mu_\nu N_B^{(\nu)} \right] \right\} , \end{aligned} \quad (7.162)$$

where the first term is nothing but the distance – expressed in terms of the quantum relative entropy, compare Eq. (1.104) – between the actual exact density matrix of the full universe  $\rho(t)$  and the product state of the exact reduced system density matrix and the reservoir states. The first term is thus positive and vanishes if and only if the system and bath density matrices are not correlated, it will be denoted as the **entropy production**

$$\Delta_i S(t) = D \left( \rho(t) \left\| \rho_S(t) \otimes_\nu \bar{\rho}_\nu \right. \right) \geq 0 . \quad (7.163)$$

We see that the entropy production is large when the distance between the actual state and the product state is large, such that it can be seen as quantifying the correlations between system and reservoir. For finite-size reservoirs, recurrences can occur, and the entropy production can behave periodically. We therefore note that its production rate need not be positive. In particular, for periodically evolving universes we must observe times where  $\frac{d}{dt}\Delta_i S(t) < 0$ .

By contrast, the second term in (7.162) can be expressed by the heat leaving the reservoirs (analogous to entropy flow)

$$\begin{aligned}\Delta_e S(t) &= - \sum_{\nu} \beta_{\nu} \text{Tr}_{\nu} \left\{ [\rho_{\nu}(t) - \bar{\rho}_{\nu}] \left[ H_B^{(\nu)} - \mu_{\nu} N_B^{(\nu)} \right] \right\} \\ &= \sum_{\nu} \beta_{\nu} \Delta Q_{\nu}(t),\end{aligned}\tag{7.164}$$

where the the heat flowing out of the reservoir  $\nu$  is defined as

$$\Delta Q_{\nu}(t) = \left\langle H_B^{(\nu)} - \mu_{\nu} N_B^{(\nu)} \right\rangle_0 - \left\langle H_B^{(\nu)} - \mu_{\nu} N_B^{(\nu)} \right\rangle_t.\tag{7.165}$$

Summarizing, the second law can be written in standard form

$$\Delta S(t) = \Delta_i S(t) + \sum_{\nu} \beta_{\nu} \Delta Q_{\nu}(t),\tag{7.166}$$

or equivalently as  $\Delta_i S(t) = \Delta S(t) - \sum_{\nu} \beta_{\nu} \Delta Q_{\nu}(t) \geq 0$ , where only the definition of the heat has to be adapted. A few notes are in order.

- By performing the operation  $\lim_{t \rightarrow \infty} \frac{1}{t} [\dots]$  on Eq. (7.166), we find for a finite-sized system and a constant global Hamiltonian

$$- \sum_{\nu} \beta_{\nu} \lim_{t \rightarrow \infty} \frac{\langle H_{\nu} - \mu_{\nu} N_{\nu} \rangle_0 - \langle H_{\nu} - \mu_{\nu} N_{\nu} \rangle_t}{t} = \lim_{t \rightarrow \infty} \frac{\Delta_i S(t)}{t} \geq 0.\tag{7.167}$$

Now, if the currents leaving the reservoirs assume steady state values in the long-time limit (this is an assumption)

$$\lim_{t \rightarrow \infty} \frac{d}{dt} \langle H_{\nu} \rangle_t = -\bar{I}_E^{\nu}, \quad \lim_{t \rightarrow \infty} \frac{d}{dt} \langle N_{\nu} \rangle_t = -\bar{I}_M^{\nu},\tag{7.168}$$

we can invoke the rule of l'Hospital to evaluate the limit, yielding

$$- \sum_{\nu} \beta_{\nu} (\bar{I}_E^{\nu} - \mu_{\nu} \bar{I}_M^{\nu}) \geq 0.\tag{7.169}$$

This shows that under the assumption of stationary currents, the conventional form of the second law at steady state also holds beyond weak coupling and also if interactions are present inside the system, thus confirming and generalizing our considerations based on the Landauer formula in Sec. 4.1.4.

- In general (for  $t > 0$ ) the total entropy is not just the sum of system entropy (7.160) and reservoir entropies

$$S_{\nu}(t) = -\text{Tr} \{ \rho_{\nu}(t) \ln \rho_{\nu}(t) \}.\tag{7.170}$$

Instead, it is modified by the correlations between system and reservoir (e.g. entanglement). The **correlation entropy** is therefore defined as

$$S_c(t) = \Sigma(t) - S(t) - \sum_{\nu} S_{\nu}(t). \quad (7.171)$$

Due to the assumption of an initial product state we have  $S_c(0) = 0$ , and therefore with  $\Sigma(t) = \Sigma(0)$  the relation

$$S_c(t) = S_c(t) - S_c(0) = -\Delta S(t) - \sum_{\nu} \Delta S_{\nu}(t) \quad (7.172)$$

However, by construction we also have

$$\begin{aligned} D\left(\rho(t) \parallel \rho_S(t) \otimes_{\nu} \rho_{\nu}(t)\right) &= \text{Tr}\{\rho(t) \ln \rho(t)\} - \text{Tr}\left\{\rho(t) \left[\ln \rho_S(t) + \sum_{\nu} \ln \rho_{\nu}(t)\right]\right\} \\ &= -\Sigma(t) - \text{Tr}_S\{\rho_S(t) \ln \rho_S(t)\} - \sum_{\nu} \text{Tr}_{\nu}\{\rho_{\nu}(t) \ln \rho_{\nu}(t)\} \\ &= -\Sigma(t) + S(t) + \sum_{\nu} S_{\nu}(t) = -S_c(t) \geq 0. \end{aligned} \quad (7.173)$$

The correlation entropy is thereby always negative. Now, since the sum of entropy production and correlation entropy

$$\Delta_i S(t) + S_c(t) = -\sum_{\nu} \beta_{\nu} \Delta Q_{\nu}(t) - \sum_{\nu} \Delta S_{\nu}(t) = \sum_{\nu} D(\rho_{\nu}(t) \parallel \bar{\rho}_{\nu}) \geq 0 \quad (7.174)$$

is still positive, we get the hierarchy

$$\Delta_i S(t) \geq -S_c(t) \geq 0. \quad (7.175)$$

- We can solve Eq. (7.162) for the entropy production

$$\Delta_i S(t) = S(t) - S(0) - \sum_{\nu} \beta_{\nu} \Delta Q_{\nu}(t). \quad (7.176)$$

Performing a time derivative on both sides yields

$$\frac{d}{dt} \Delta_i S(t) = \dot{S}(t) - \sum_{\nu} \beta_{\nu} \Delta \dot{Q}_{\nu}(t), \quad (7.177)$$

where  $\dot{Q}_{\nu}(t)$  now denotes the heat current entering the system from reservoir  $\nu$ . In general, this quantity will not be positive. However, assuming evolution under a Lindblad form, we know that also the entropy production rate  $\frac{d}{dt} \Delta_i S(t) \rightarrow \dot{S}_i \geq 0$  is positive, compare Sec. 2.3. Indeed, negative entropy production rates are sometimes used as a marker for a non-Markovian evolution [52].

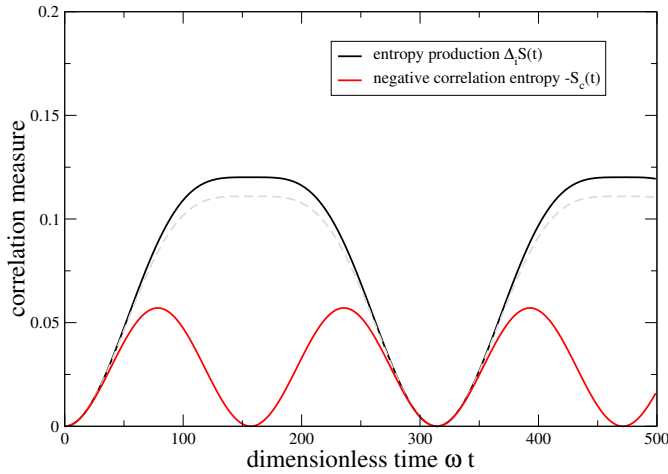


Figure 7.14: Plot of the correlation measures entropy production (7.182) and negative correlation entropy (7.183) for a system composed of two interacting qubits. The entropy production (black) is always greater than the negative correlation entropy (red), and both quantities are positive. The dashed grey curve shows the entropy production when the roles of system and bath are exchanged (for which  $S_c(t)$  remains invariant). For  $\lambda \rightarrow 0$ , both quantities vanish. Parameters:  $\omega_1 = \omega_2 = \omega$ ,  $\lambda = 0.01\omega$ ,  $\beta_1\omega_1 = 0$ ,  $\beta_2\omega_2 = 1.0$ .

### 7.4.1 Example: Two coupled qubits

To begin with something simple, we can test the above relations with just two qubits

$$H = \frac{\omega_1}{2}\sigma_1^z + \frac{\omega_2}{2}\sigma_2^z + \lambda\sigma_1^x\sigma_2^x, \quad (7.178)$$

where  $\lambda$  parametrizes the coupling strength between them. The first qubit can be considered as the system, whereas the second mimics the "reservoir". We consider the initial state

$$\rho(0) = \rho_1^0 \otimes \bar{\rho}_2 = \frac{e^{-\beta_1\omega_1/2\sigma^z}}{Z_1} \otimes \frac{e^{-\beta_2\omega_2/2\sigma^z}}{Z_2}, \quad (7.179)$$

where we have for simplicity also considered the first qubit in a thermal state (although this could also be a pure state). Then, we compute the exact solution via

$$\rho(t) = e^{-iHt}\rho(0)e^{+iHt}. \quad (7.180)$$

From this, we can compute the reduced density matrices

$$\rho_1(t) = \text{Tr}_2\{\rho(t)\}, \quad \rho_2(t) = \text{Tr}_1\{\rho(t)\}. \quad (7.181)$$

and the entropy production

$$\Delta_i S(t) = D(\rho(t)||\rho_1(t) \otimes \bar{\rho}_2) \quad (7.182)$$

and the negative correlation entropy

$$-S_c(t) = D(\rho(t)||\rho_1(t) \otimes \rho_2(t)). \quad (7.183)$$

The result is shown in Fig. 7.14 and confirms relation (7.175).

### 7.4.2 Example: Transient entropy production for pure-dephasing

We had solved the pure dephasing version of the spin-boson model

$$H = \Omega\sigma^z + \lambda\sigma^z \otimes \sum_k \left( h_k b_k + h_k^* b_k^\dagger \right) + \sum_k \omega_k b_k^\dagger b_k. \quad (7.184)$$

before. For the system, we would in the eigenbasis of  $\sigma^z$  simply obtain stationary populations and decaying coherences

$$|\rho_{01}|(t) = e^{-f(t)} |\rho_{01}^0|, \quad f(t) = \frac{4}{\pi} \int_0^\infty \Gamma(\omega) \frac{\sin^2(\omega t/2)}{\omega^2} \coth\left(\frac{\beta\omega}{2}\right) d\omega, \quad (7.185)$$

compare Eq. (1.148). To benchmark our master equation approaches we had also calculated the change of the reservoir energy

$$\Delta E(t) = \frac{2}{\pi} \int_0^\infty \frac{\Gamma(\omega)}{\omega} \sin^2\left(\frac{\omega t}{2}\right) d\omega \quad (7.186)$$

see Eq. (3.130), and the change of the reservoir particle number, which can be calculated in complete analogy

$$\Delta N(t) = \frac{2}{\pi} \int_0^\infty \frac{\Gamma(\omega)}{\omega^2} \sin^2\left(\frac{\omega t}{2}\right) d\omega. \quad (7.187)$$

For a single reservoir, Eq. (7.162) becomes

$$\Delta_i S(t) = S(t) - S(0) + \beta [\Delta E(t) - \mu \Delta N(t)]. \quad (7.188)$$

Using that  $\Delta E(t) > 0$ ,  $\Delta N(t) > 0$ , and for bosons  $\mu \leq 0$  (actually, we would normally drop it for photons), we can already conclude that the second term is separately positive. Also, if we would let  $t \rightarrow \infty$ , the final density matrix of the system would be diagonal, such that we can conclude that  $S(\infty) - S(0) > 0$ , but does this hold for all times? Parametrizing the density matrix by the occupation  $\rho_{11}$  and the time-dependent coherence  $\rho_{01}(t)$ , its von-Neumann entropy becomes

$$S(t) = -\frac{1}{2} \left[ 1 - \sqrt{(1 - 2\rho_{11})^2 + 4|\rho_{01}(t)|^2} \right] \ln \frac{1}{2} \left[ 1 - \sqrt{(1 - 2\rho_{11})^2 + 4|\rho_{01}(t)|^2} \right] \\ - \frac{1}{2} \left[ 1 + \sqrt{(1 - 2\rho_{11})^2 + 4|\rho_{01}(t)|^2} \right] \ln \frac{1}{2} \left[ 1 + \sqrt{(1 - 2\rho_{11})^2 + 4|\rho_{01}(t)|^2} \right]. \quad (7.189)$$

Using that as time increases, the coherences become smaller  $|\rho_{01}(t)|^2 = e^{-2f(t)} |\rho_{01}^0|^2$ , we find (in the regime  $0 \leq (1 - 2\rho_{11})^2 + 4|\rho_{01}(t)|^2 \leq 1$  that is allowed for a valid density matrix), that  $S(t) = -\frac{(1-x)/2 \ln(1-x)/2 - (1+x)/2 \ln(1+x)/2}{\sqrt{(1-2\rho_{11})^2 + 4|\rho_{01}(t)|^2} = x \in [0, 1]}$  is a monotonously decaying function when

$$\Delta_i S(t) = S(t) - S(0) + \beta [\Delta E(t) - \mu \Delta N(t)] \geq 0, \quad (7.190)$$

confirming the validity of the second law or – depending on the perspective – the validity of our exact solution.

### 7.4.3 Conclusion: Entropy production for periodic driving

We assume that a periodically driven system coupled to many reservoirs settles to an asymptotically periodic steady state for some large time  $t^*$  such that we can safely assume  $S(t^*+T) = S(t^*)$ . In addition, we assume that the initial state complies with the product state assumption or that possibly

present initial correlations do not play a role. Then, by performing the operation  $\frac{1}{T} \int_{t^*}^{t^*+T} \frac{d}{dt} [\dots] dt$  on Eq. (7.166) for some large initial time  $t^* \gg 0$  and period  $T > 0$ , we find

$$0 = \lim_{t^* \rightarrow \infty} \frac{\Delta_i S(t^* + T) - \Delta_i S(t^*)}{T} + \sum_{\nu} \beta_{\nu} [\langle I_E^{\nu} \rangle - \mu_{\nu} \langle I_M^{\nu} \rangle], \quad (7.191)$$

where  $\langle I_E^{\nu} \rangle$  and  $\langle I_M^{\nu} \rangle$  denote the period-averaged long-term energy and matter currents, respectively. Clearly, we also suppose these to exist. We can therefore write for large  $t^*$ :

$$\Delta_i S(t^* + T) = \Delta_i S(t^*) + \langle \sigma \rangle T, \quad \langle \sigma \rangle = - \sum_{\nu} \beta_{\nu} [\langle I_E^{\nu} \rangle - \mu_{\nu} \langle I_M^{\nu} \rangle]. \quad (7.192)$$

Here,  $\langle \sigma \rangle$  is a constant (at least for large times  $t^*$ ). Now, if we had  $\langle \sigma \rangle < 0$ , it would follow by recursive application of the above relation that positivity of  $\Delta_i S(t^* + nT)$  could not be maintained in the long-term limit, leading to a contradiction with its definition. We therefore conclude that the thus defined period-averaged entropy production rate must be positive

$$\langle \sigma \rangle = - \sum_{\nu} \beta_{\nu} [\langle I_E^{\nu} \rangle - \mu_{\nu} \langle I_M^{\nu} \rangle] \geq 0. \quad (7.193)$$

A similar argument (for a single reservoir and without particle exchange) is put forward in Ref. [53].



# Bibliography

- [1] H.-P. Breuer and F. Petruccione. *The Theory of Open Quantum Systems*. Oxford University Press, Oxford, 2002.
- [2] Marlan O. Scully and M. Suhail Zubairy. *Quantum Optics*. Cambridge University Press, 1997.
- [3] Leonard Mandel and Emil Wolf. *Optical coherence and quantum optics*. Cambridge University Press, 1995.
- [4] N. G. van Kampen. *Stochastic processes in physics and chemistry*. Elsevier, 1981.
- [5] M. Schlosshauer. *Decoherence and the Quantum-To-Classical Transition*. Springer-Verlag Berlin Heidelberg, 2007.
- [6] H. M. Wiseman and G. J. Milburn. *Quantum Measurement and Control*. Cambridge University Press, Cambridge, 2010.
- [7] G. Schaller. *Open Quantum Systems Far from Equilibrium*, volume 881 of *Lecture Notes in Physics*. Springer, Cham, 2014.
- [8] G. Lindblad. On the generators of quantum dynamical semigroups. *Communications in Mathematical Physics*, 48:119–130, 1976.
- [9] V. Gorini, A. Kossakowski, and E. C. G. Sudarshan. Completely positive dynamical semigroups of  $n$ -level systems. *Journal of Mathematical Physics*, 17:821, 1976.
- [10] Gregory Bulnes Cuetara, Massimiliano Esposito, and Gernot Schaller. Quantum thermodynamics with degenerate eigenstate coherences. *Entropy*, 18(12):447, 2016.
- [11] Göran Lindblad. Completely positive maps and entropy inequalities. *Communications in Mathematical Physics*, 40:147, 1975.
- [12] Herbert Spohn. Entropy production for quantum dynamical semigroups. *Journal of Mathematical Physics*, 19:1227, 1978.
- [13] Michael A. Nielsen and Isaac L. Chuang. *Quantum Computation and Quantum Information*. Cambridge University Press, Cambridge, 2000.
- [14] Tobias Brandes. Waiting times and noise in single particle transport. *Annalen der Physik (Berlin)*, 17:477, 2008.
- [15] M. Esposito, U. Harbola, and S. Mukamel. Nonequilibrium fluctuations, fluctuation theorems, and counting statistics in quantum systems. *Reviews of Modern Physics*, 81:1665–1702, 2009.

- [16] K. Schönhammer. Full counting statistics for noninteracting fermions: Exact results and the Levitov-Lesovik formula. *Phys. Rev. B*, 75:205329, May 2007.
- [17] Gavin E. Crooks. Entropy production fluctuation theorem and the nonequilibrium work relation for free energy differences. *Physical Review E*, 60:2721–2726, Sep 1999.
- [18] H. Haug and A.-P. Jauho. *Quantum Kinetics in Transport and Optics of Semiconductors*. Springer, 2008.
- [19] G. Schaller, P. Zedler, and T. Brandes. Systematic perturbation theory for dynamical coarse-graining. *Physical Review A*, 79:032110, 2009.
- [20] A. Dhar, K. Saito, and P. Hänggi. Nonequilibrium density-matrix description of steady-state quantum transport. *Physical Review E*, 85:011126, 2012.
- [21] Li-Ping Yang, C. Y. Cai, D. Z. Xu, Wei-Min Zhang, and C. P. Sun. Master equation and dispersive probing of a non-markovian process. *Physical Review A*, 87:012110, 2013.
- [22] G. B. Arfken and H. J. Weber. *Mathematical Methods For Physicists*. Elsevier LTD, Oxford, 2005.
- [23] P. Zedler, G. Schaller, G. Kießlich, C. Emary, and T. Brandes. Weak coupling approximations in non-Markovian transport. *Physical Review B*, 80:045309, 2009.
- [24] U. Kleinekathöfer. Non-Markovian theories based on a decomposition of the spectral density. *The Journal of Chemical Physics*, 121:2505, 2004.
- [25] Gheorghe Nenciu. Independent electron model for open quantum systems: Landauer-Büttiker formula and strict positivity of the entropy production. *Journal of Mathematical Physics*, 48:033302, 2007.
- [26] G. Schaller, T. Krause, T. Brandes, and M. Esposito. Single-electron transistor strongly coupled to vibrations: counting statistics and fluctuation theorem. *New Journal of Physics*, 15:033032, 2013.
- [27] J. Koch and F. von Oppen. Franck-condon blockade and giant Fano factors in transport through single molecules. *Physical Review Letters*, 94:206804, 2005.
- [28] G. D. Mahan. *Many-Particle Physics*. Springer Netherlands, 2000.
- [29] T. Brandes. Coherent and collective quantum optical effects in mesoscopic systems. *Physics Reports*, 408:315–474, 2005.
- [30] Milton Abramowitz and Irene A. Stegun, editors. *Handbook of Mathematical Functions*. National Bureau of Standards, 1970.
- [31] A. Nazir and G. Schaller. The reaction coordinate mapping in quantum thermodynamics. In F. Binder, L. A. Correa, C. Gogolin, J. Anders, and G. Adesso, editors, *Thermodynamics in the quantum regime – Recent progress and outlook*, Fundamental Theories of Physics. Springer, Cham, 2019.

- [32] M. P. Woods, R. Groux, A. W. Chin, S. F. Huelga, and M. B. Plenio. Mappings of open quantum systems onto chain representations and markovian embeddings. *Journal of Mathematical Physics*, 55:032101, 2014.
- [33] Patrick P. Hofer, Martí Perarnau-Llobet, L. David, M. Miranda, Géraldine Haack, Ralph Silva, Jonatan Bohr Brask, and Nicolas Brunner. Markovian master equations for quantum thermal machines: local versus global approach. *New Journal of Physics*, 19:123037, 2017.
- [34] Sebastian Restrepo, Sina Böhling, Javier Cerrillo, and Gernot Schaller. Electron pumping in the strong coupling and non-Markovian regime: A reaction coordinate mapping approach. *Phys. Rev. B*, 100:035109, Jul 2019.
- [35] Thomas Dittrich, Peter Hänggi, Gert-Ludwig Ingold, Bernhard Kramer, Gerd Schön, and Wilhelm Zwerger. *Quantum Transport and Dissipation*. Wiley-VCH, Weinheim, 1998.
- [36] T. Shirai, T. Mori, and S. Miyashita. Condition for emergence of the Floquet-Gibbs state in periodically driven open systems. *Physical Review E*, 91:030101, Mar 2015.
- [37] Tatsuhiko Shirai, Juzar Thingna, Takashi Mori, Sergey Denisov, Peter Hänggi, and Seiji Miyashita. Effective Floquet-Gibbs states for dissipative quantum systems. *New Journal of Physics*, 18:053008, 2016.
- [38] S. Restrepo, J. Cerrillo, P. Strasberg, and G. Schaller. From quantum heat engines to laser cooling: Floquet theory beyond the Born-Markov approximation. *New Journal of Physics*, 20:053063, 2018.
- [39] G. Kießlich, C. Emary, G. Schaller, and T. Brandes. Reverse quantum state engineering using electronic feedback loops. *New Journal of Physics*, 14:123036, 2012.
- [40] M. Esposito, K. Lindenberg, and C. Van den Broeck. Universality of efficiency at maximum power. *Physical Review Letters*, 102:130602, 2009.
- [41] Massimiliano Esposito and Gernot Schaller. Stochastic thermodynamics for "Maxwell demon" feedbacks. *Europhysics Letters*, 99:30003, 2012.
- [42] Gernot Schaller. Feedback-charging a metallic island. *Phys. Status Solidi B*, 254:1600549, 2017.
- [43] Philipp Strasberg, Gernot Schaller, Tobias Brandes, and Massimiliano Esposito. Thermodynamics of a physical model implementing a Maxwell demon. *Physical Review Letters*, 110:040601, 2013.
- [44] Andre C. Barato, David Hartich, and Udo Seifert. Rate of mutual information between coarse-grained non-Markovian variables. *Journal of Statistical Physics*, 153:460, 2013.
- [45] Jordan M. Horowitz and Massimiliano Esposito. Thermodynamics with continuous information flow. *Physical Review X*, 4:031015, Jul 2014.
- [46] Kensaku Chida, Samarth Desai, Katsuhiko Nishiguchi, and Akira Fujiwara. Power generator driven by Maxwell's demon. *Nature Communications*, 8:15310, 2017.

- [47] Gernot Schaller, Javier Cerrillo, Georg Engelhardt, and Philipp Strasberg. Electronic Maxwell demon in the coherent strong-coupling regime. *Phys. Rev. B*, 97:195104, May 2018.
- [48] J. V. Koski, A. Kutvonen, I. M. Khaymovich, T. Ala-Nissila, and J. P. Pekola. On-chip Maxwell's demon as an information-powered refrigerator. *Physical Review Letters*, 115:260602, Dec 2015.
- [49] Philipp Strasberg, Gernot Schaller, Thomas L. Schmidt, and Massimiliano Esposito. Fermionic reaction coordinates and their application to an autonomous Maxwell demon in the strong-coupling regime. *Phys. Rev. B*, 97:205405, May 2018.
- [50] Lukas Fricke, Michael Wulf, Bernd Kaestner, Frank Hohls, Philipp Mirovsky, Brigitte Mackrodt, Ralf Dolata, Thomas Weimann, Klaus Pierz, Uwe Siegner, and Hans W. Schumacher. Self-referenced single-electron quantized current source. *Phys. Rev. Lett.*, 112:226803, Jun 2014.
- [51] M. Esposito, K. Lindenberg, and C. Van den Broeck. Entropy production as correlation between system and reservoir. *New Journal of Physics*, 12:013013, 2010.
- [52] Philipp Strasberg and Massimiliano Esposito. Non-markovianity and negative entropy production rates. *Phys. Rev. E*, 99:012120, Jan 2019.
- [53] Akihito Kato and Yoshitaka Tanimura. Quantum heat current under non-perturbative and non-Markovian conditions: Applications to heat machines. *Journal of Chemical Physics*, 145:224105, 2016.

# Index

- bath correlation function, 24
- Bogoliubov transform, 130
- Bohr-frequencies, 26
- Born-Redfield equation, 25
- Bose-Einstein distribution, 10
- bosonic ladder operators, 9
  
- canonical equilibrium state, 8
- Carnot efficiency, 62
- Cauchy transform of an odd function, 135
- chemical work rate, 60
- coefficient of performance, 63
- conditional density matrix, 89
- correlation entropy, 218
- correlation function with counting fields, 92
- counting field, 80
- cumulant-generating function, 82
- current operator, 113
  
- density matrix, 7
  
- efficiency, 62
- energy counting field, 87
- energy current for rate equations, 59
- entropy production, 216
- extended space, 150
  
- Fermi-Dirac distribution, 10
- fermionic ladder operators, 10
- Fermis Golden Rule, 30
- Floquet states, 147
- Floquet theorem, 147
- Fock states, 9
- free propagator, 77
  
- generalized density matrix, 83
- grand-canonical equilibrium state, 8
  
- Hadamard lemma, 116
- Hamiltonian of mean force, 146
- heat current, 60
  
- infinite bias regime, 84
- interaction Hamiltonian with counting field, 91
- irreversible entropy production rate, 61
  
- Jordan-Wigner-transform, 47
  
- Kraus map, 12
- Kronecker product, 52
  
- Lamb-shift, 30, 33
- Landauer formula, 97, 114
- Lindblad form, 13
- Liouvillian superoperator, 51
- local Lindblad, 145
  
- matrix exponential, 8
- matter current for rate equations, 59
- mean of a distribution, 80
- mechanical work rate, 60
- mixed, 7
  
- non-Hermitian Hamiltonian, 170
- non-Markovian master equation, 24
  
- partial trace, 19
- partition function, 55
- Pauli matrices, 9
- phonon mapping, 135
- polaron transform, 116
- polaron transformation, 43
- projective measurement, 8
- pure, 7
  
- QND-measurement, 206
- quantum Zeno effect, 162
- quasienergies, 147
  
- rate equation, 30
- reaction coordinate, 132
- Redfield equation, 25
- residual reservoir, 132
- Rubin spectral density, 136

secular approximation, [26](#), [154](#)  
singular coupling limit, [198](#)  
spectral density, [31](#), [111](#), [131](#), [132](#)  
spectral representation, [7](#)  
spin valve, [104](#)

tensor products, [9](#)  
thermoelectric generator, [62](#)  
time evolution operator, [8](#)  
time evolution operator with counting field, [91](#)  
transmission, [96](#), [114](#)  
transport window, [57](#)  
tunnel rate, [111](#)

vacuum state, [9](#)  
von-Neumann, [8](#)  
von-Neumann entropy, [8](#)

waiting time distribution, [88](#)  
wide-band limit, [111](#)  
width of a distribution, [80](#)